



Université
de Toulouse

THÈSE

En vue de l'obtention du

DOCTORAT DE L'UNIVERSITÉ DE TOULOUSE

Délivré par :

Université Toulouse 3 Paul Sabatier (UT3, Paul Sabatier)

Présentée et soutenue par :

Diana RAMIREZ-GARCES

Titre :

Analyses of CRN effectors (Crinkler and Necrosis) of the oomycete *Aphanomyces euteiches*

Ecole Doctorale SEVAB: Interaction Plantes-Microorganismes

Unité de recherche :

Laboratoire de Recherche en Sciences Végétales (LRSV, UMR 5546)

Directeur(s) de Thèse :

Dr. Elodie GAULIN, Maître de Conférences, UT3 Paul Sabatier, HDR

Rapporteurs :

Dr. Marie DUFRESNE, Maître de Conférences, Université Paris-Sud Orsay

Dr. Franck PANABIERES, DR2 INRA Sophia-Antipolis

Dr. Sylvain JEANDROZ Professeur, AgroSup Dijon

Autres membre du JURY

Dr. Christophe ROUX, Professeur Université Paul Sabatier, Toulouse

Acknowledgments

This work has been fruitful thanks to the support of many people that participated directly or distantly, motivating this four-year journey with their good energy, laughs and dancing-and-chanting moods.

Je remercie tout d'abord ma directrice de thèse, Elodie Gaulin et le chef de l'équipe Bernard Dumas. Merci de m'avoir accueilli dans l'équipe et de m'avoir accordé l'espace, le temps et la confiance pour réaliser mon travail et accomplir cet objectif personnel.

Je remercie Sylvain Jeandroz, Franck Panabières et Marie Dufresne d'avoir accepté d'évaluer mon travail.

Laurent Camborde, le courage avec lequel tu as affronté 50000 femelles d'amphibiens est sans précédents. Et tout ça pour sauver les grenouilles colombiennes des Pyrénées. J'ai beaucoup aimé travailler avec toi. Tu as été une source de bonne humeur et énergie dans les moments de ralenti.

Une partie importante de ce travail a été possible grâce à Yves Martinez, Alain Jauneau, Aurélie Leru et Cécile Pouzet. Je vous remercie de votre disponibilité, grâce à laquelle j'ai pu apprendre et développer les techniques de microscopie. Je garde à l'esprit votre professionnalisme, votre polyvalence scientifique et surtout votre enthousiasme.

Aude Cerutti, merci de m'avoir accompagné durant une partie de ce travail. Une jolie expérience que je n'oublierai pas.

Je pense avec joie et une certaine nostalgie aux anciens membres de l'équipe : Thomas Rey, Mathieu Larroque, Olivier André, Amaury Nars et Yacine avec lesquels j'ai pu partager des moments très agréables. Elo, Sophie, merci pour votre compagnie et votre précieuse aide.

A mis hermanas del alma, Vanessa y Valentina: gracias por llegar a mi vida y acompañarme en este ciclo. Hubo momentos en los que solo deseábamos parar este mundo y bajarnos, pero ahora entendimos que el movimiento es indispensable y que la vida lleva su propio ritmo.

A mi familia, a los que están y también a los que se han ido. Esto es para ustedes.

.

Summary

The oomycete *Aphanomyces euteiches* is an important pathogen infecting roots of legumes (pea, alfalfa...) and the model legume *Medicago truncatula*. Oomycetes and other microbial eukaryotic pathogens secrete and deliver effector molecules into host intracellular compartments (intracellular/cytoplasmic effectors) to manipulate plant functions and promote infection. CRN (Cringling and Necrosis) proteins are a wide class of intracellular, nuclear-localized effectors commonly found in oomycetes and recently described in true fungi whose host targets, virulence roles, secretion and host-delivery mechanisms are poorly understood. We addressed the functional characterization of CRN proteins AeCRN5 and AeCRN13 of *A. euteiches* and AeCRN13's homolog of the chytrid fungal pathogen of amphibians *Batrachochytrium dendrobatidis*, BdCRN13. Gene and protein expression studies showed that AeCRN5 and AeCRN13 are expressed during infection of *M. truncatula*'s roots. Preliminary immunolocalization studies on AeCRN13 in infected roots indicated that the protein is secreted and translocated into root cells, depicting for the first time CRN secretion and translocation into the host during infection. The heterologous ectopic expression of AeCRNs and BdCRN13 in plant and amphibian cells indicated that these proteins target host nuclei and lead to the perturbation of host physiology. By developing an *in vivo* FRET-FLIM-based assay, we revealed that these CRNs target host nucleic acids: AeCRN5 targets plant RNA while AeCRN13 and BdCRN13 target DNA. Both CRN13 exhibit a HNH-like motif commonly found in endonucleases and we further demonstrated that both CRN13 display a nuclease activity *in vivo* inducing double-stranded DNA cleavage. This work reveals a new mode of action of intracellular eukaryotic effectors and brings new aspects for the comprehension of CRN's activities not only in oomycetes but, for the first time, also in true fungi.

Keywords: CRN, oomycetes, nucleus, effector, secretion, FRET-FLIM, *Aphanomyces euteiches*

Résumé

L'oomycète *Aphanomyces euteiches* est un pathogène racinaire de légumineuses cultivées (pois, luzerne ...) et de la plante modèle *Medicago truncatula*. Les oomycètes, comme d'autres microorganismes pathogènes eucaryotes, secrètent et transloquent des molécules à l'intérieur des cellules de l'hôte (effecteurs intracellulaires/cytoplasmiques) dans le but de manipuler les fonctions de la plante et de faciliter l'infection. Les protéines CRN (Crinkling and Necrosis) constituent une famille d'effecteurs nucléaires largement répandue chez les oomycètes et récemment décrites chez des espèces fongiques. Leurs cibles et rôle dans la virulence ainsi que leurs mécanismes de sécrétion et de translocation sont encore mal compris. Nous avons entrepris la caractérisation fonctionnelle des protéines AeCRN5 et AeCRN13 d'*A. euteiches* ainsi que de l'homologue d'AeCRN13 du champignon pathogène d'amphibien *Batrachochytrium dendrobatidis*, BdCRN13. Les analyses d'expression génique et protéique ont permis de montrer que AeCRN5 et AeCRN13 sont exprimés durant l'infection des racines de *M. truncatula*. Des résultats préliminaires d'immunolocalisation d'AeCRN13 ont révélé, pour la première fois, la sécrétion et translocation d'un CRN durant l'infection. Leur expression hétérologue, à la fois dans les cellules de plantes et d'amphibiens, a montré que ces protéines se localisent dans les noyaux où leurs activités conduisent à la perturbation de la physiologie de l'hôte. En développant un système *in vivo* basé sur la technique de FRET-FLIM, nous avons démontré que ces CRN ciblent les acides nucléiques: AeCRN5 cible l'ARN des plantes tandis qu'AeCRN13 et BdCRN13 lient l'ADN. Ces deux effecteurs CRN13 exhibent un motif de type HNH, lequel est typiquement retrouvé dans des endonucleases. Nous avons démontré que les CRN13 présentent une activité nuclease *in vivo* conduisant à la génération de coupures double brin de l'ADN. Ce travail a permis de mettre en évidence un nouvel mécanisme d'action des effecteurs de microorganismes eucaryotes et apporte des nouveaux aspects pour la compréhension de l'activité des protéines CRN d'oomycète mais aussi, pour la première fois, de champignon.

Mots clés : CRN, oomycète, noyau, effecteur, sécrétion, FRET-FLIM, *Aphanomyces euteiches*

List of abbreviations

Ae	<i>Aphanomyces euteiches</i>
AM	Arbuscular Mycorrhiza
AT	Adenosine Tyrosine
Avr	Avirulence
Bd	<i>Batrachochytrium dendrobatidis</i>
BFA	Brefeldin A
BIC	Biotrophic Interfacial Complex
CBEL	Cellulose Binding ELicitor
CD	Cell-Death
CN	Cyst Nematode
CRN	Crinkling and Necrosis
CSEPs	Candidate Secreted Effector Proteins
CWDEs	Cell Wall Degrading Enzymes
DBD	DNA Binding Domain
EIHM	ExtraInvasive Hyphal Membrane
ER	Endoplasmic Reticulum
ESTs	Expressed Sequence Tags
ETI	Effector-Triggered Immunity
FLIM	Fluorescence Life Image Measure
FRET	Fluorescence Resonance Energy Transfer
GFP	Green Fluorescent Protein
GWAS	Genome Wide Association Study
HATs	Histone AcetylTransferases
HDACs	Histone DeAcetylases
HIGS	Host-Induced Gene Silencing
HMTs	Histone MethylTransferases

JA	Jasmoninc Acid
MAMP	Microbe-Associated Molecular Pattern
MTFs	MAD-box Transcription Factors
NE	Nuclear Envelop
NES	Nuclear Export Signal
NLS	Nuclear Localization Signal
NPCs	Nuclear Pore Complex
NTR	Nuclear Transport Receptor
PAMP	Pathogen-Associated Molecular Pattern
PBS	Phosphate-Buffered Saline
PCW	Plant Cell Wall
PI(3)P	PhosphoInositol-3-Phosphate
PR	Pathogenesis Related
PTI	PAMP-Triggered Immunity
PVX	Potato Virus X
QTL	Quantitative Trait Loci
R	Resistance
RBPs	RNA Binding Protein
rDNA	ribosomal DNA
RKNs	Root Knot Nematodes
RLKs	Receptor Like Kinases
RLPs	Receptor Like Proteins
ROS	Reactive Oxygen Species
RRM	RNA Recognition Motif
RZE	Repeated Zoospore Emergence
SA	Salicylic Acid
SDS	Sodium Dodecyl Sulfate

SIX	Secreted In Xylem
SNPs	Single Nucleotide Polymorphism
SylA	SyringoLin A
T2SS	Type 2 Secretion System
T3E	Type 3 Effector
T3SS	Type 3 Secretion System
T4SS	Type 4 Secretion System
TALE	Transcription Activator-Like Effector
TBS	Tris-Buffered Saline
TE	Transposable Element
TFs	Transcription Factors
TIR	Toll Interleukin Receptor NB-LRR
TMV	Tomato Mosaic Virus
Tris	Tris (hydroxymethyl)-aminomethane
Ub	Ubiquitin
UBCEPs	Ubiquitin Cterminal Extension Proteins
WGA	Wheat Germ Agglutinin
Y2H	Yeast-2-Hybrid

Table of contents

General introduction	11
Oomycetes: plant and animal disease agents.....	13
Oomycetes are distinct from fungi.....	13
Oomycetes: diverse microorganisms and notorious plant pathogens.....	14
Phylogenetic distribution of oomycetes	15
Aphanomyces genus	16
An ancestral genus harboring diverse species	16
<i>A. euteiches</i> and the root rot disease of legumes	17
<i>A.euteiches</i> and <i>M. trunctatula</i> pathosystem.....	18
Molecular interplay between pathogen effectors and plant immunity	19
Plant immunity and effectors	19
Effector identification	22
Functional characterization of effectors	25
Effector delivery and localization.....	27
Function of effectors	30
The plant nucleus as a common field for microbial effectors.	32
The plant nucleus at the center of plant immunity.	32
Nuclear localized effectors and their activities.....	35
Bacterial effectors	36
Nematode effectors.....	38
Phytoplasma effectors.....	40
Fungal effectors.....	41
Oomycete effectors.....	42
RxLR effectors.....	42
CRN effectors.....	44
Chapter 1: Functional characterization of AeCRN13 of <i>A. euteiches</i> and its ortholog BdCRN13 of <i>B. dendrobatidis</i>	51
Complementary results.....	89

Materials and methods of complementary experiments.....	91
Chapter 2: Functional characterization of AeCRN5 of <i>A. euteiches</i>.....	93
Complementary results.....	119
Materials and methods of complementary experiments	121
General discussion and perspectives	122
References	131

General introduction

General introduction

The emergence of agriculture took place 10,000 years ago in eastern China, Mesopotamia, and MesoAmerica (Purugganan and Fuller, 2009) and was a crucial step for human survey and the blowing of civilizations. The cultivation of plants, rather than their gathering from nature, permitted humans to control when and how much food plants were grown and by this way ensure their food supply. This practice resulted in the domestication of wild plant species and conducted progressively to the appearance of plants presenting advantageous traits for humans (as rapid growth, bigger fruits...) and to modern crops. First agro-systems initiated, thus, with the beginning of plant domestication and, ever since their emergence, infectious plant diseases have manifested as a threat for food production and other human activities that depend on it.

Plant-pathogen microorganism associations are as old as 315 Ma, as evidenced in plant fossil records documenting the first pathogenic oomycetes in vascular plants (Strullu-Derrien et al., 2011). Human awareness of plant diseases date back to 3500 BC in Greek civilization and first descriptive reports were brought by Théophraste (370-286 BC). Plant diseases caused by microorganisms posed problems in ancient crop systems: japanese literature of the 600 century AC makes allusion to infectious diseases (blast disease on rice) that resulted in serious famines back in the days (Akai, 1974). But one can only speculate about their causative agents since it was only till principles in biology were cemented that plant pathology and etiology of plant diseases established their biotic origin.

From the beginning of our modern times, serious episodes of plant infectious diseases have taken place on various important crops. An emblematic example of how plant diseases affect humans is the potato blight disease caused by the oomycete *P. infestans*, responsible for the “Great Irish Famine” in the 1840s that led to important demographic and cultural changes in Ireland. Another oomycete, *P. viticola*, caused considerable losses for the European grape industry in the beginnings of the 20th century, reaching up to 70% loss in 1915 in France (Gessler et al., 2011).

Today the problem persists. Actually, it has been estimated that only infectious diseases, are responsible for 10% of all crop losses (Strange and Scott, 2005) and recent studies have raised the alarm on novel infectious diseases that are emerging and spreading, putting at risk plant health and thereby food security (Fisher et al., 2012). For instance, the black stem of wheat caused by the strain Ug99 of the fungus *P. graminis* *sf. tritici*, which has being threatening wheat cultures since 1998, is having a calamitous impact in the Middle East

and West Asia and other wheat-growing countries (Flood, 2010; Pennisi, 2010). Another example is the fungus *Magnaporthe oryzae* (the rice blast disease agent) aggressively infecting rice as well as other grass species including wheat. Only on rice, estimations indicate that harvest losses per year could feed 60 million people (Pennisi, 2010). Hence, it is urgent to provide means to avoid or to better manage these infections. To address this challenge it is crucial to better comprehend plant-pathogen interactions at the molecular level.

Among all microorganisms responsible for the contemporary menaces, the filamentous eukaryotic fungi and oomycetes stand as the most serious (Fisher et al., 2012; Flood, 2010; Pennisi, 2010). Indeed, oomycetes stand as notorious plant pathogens causing dramatic losses on crops, estimated at \$ 6.7 billion for *P. infestans* on tomato and potato (Haas et al., 2009) and from \$1 to \$2 billion for *P. sojae* on soybean (Tyler, 2007). In addition to crop systems, oomycetes can severely affect semi-natural and natural ecosystems, like in the case of *P. ramorum*, responsible for the sudden-oak-death disease (Grünwald et al., 2012). Despite the relevance of these diseases, means to avoid and control oomycete are scarce and often unsuccessful. Oomycete control recommendations include continuous spraying of complex fungicidal mixtures and prophylactic measures (Blum et al., 2010; Hobbelen et al., 2011). Fungicides extensively used for the control of fungal diseases often become ineffective because of the rapid appearance of insensitivity and long standing resistance (Judelson and Senthil, 2006; Pang et al., 2013). In addition, these can be inefficient because the metabolic pathways and key components that they target in fungi can be absent in oomycetes. Studies on the molecular basis governing pathogenicity and plant susceptibility can provide answers of why plants are susceptible to certain pathogens and identify the mechanisms through which pathogens infect successfully their hosts.

The general introduction of the manuscript is divided in different sections. First section is devoted to a general presentation of the current knowledge of the biology of oomycetes with a particular focus on the legume root rot pathogen agent *Aphanomyces euteiches*. Next section presents main concepts of molecular plant-microbe interactions and the emerging role of the plant nucleus in this context, followed by a description of microbial effectors that target this organelle. Lastly, the objectives of the PhD work are presented.

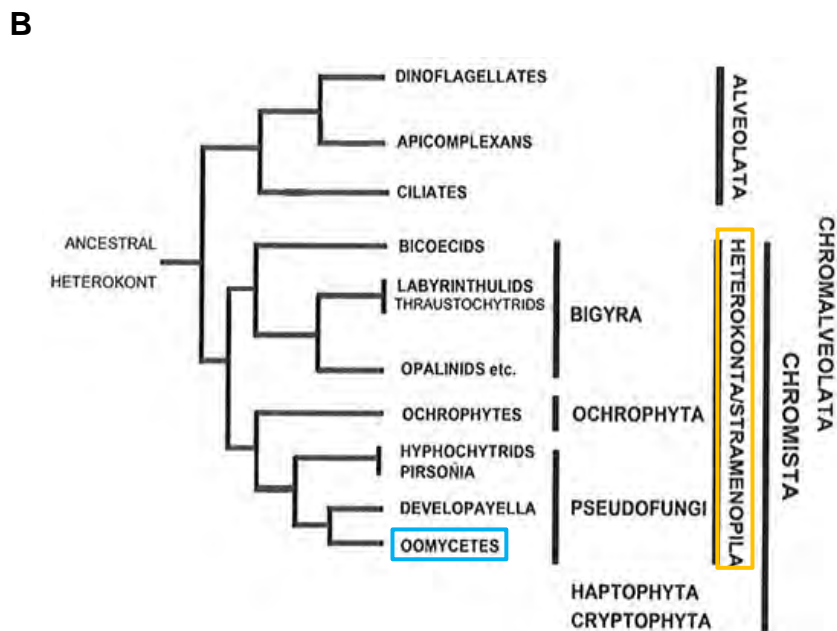
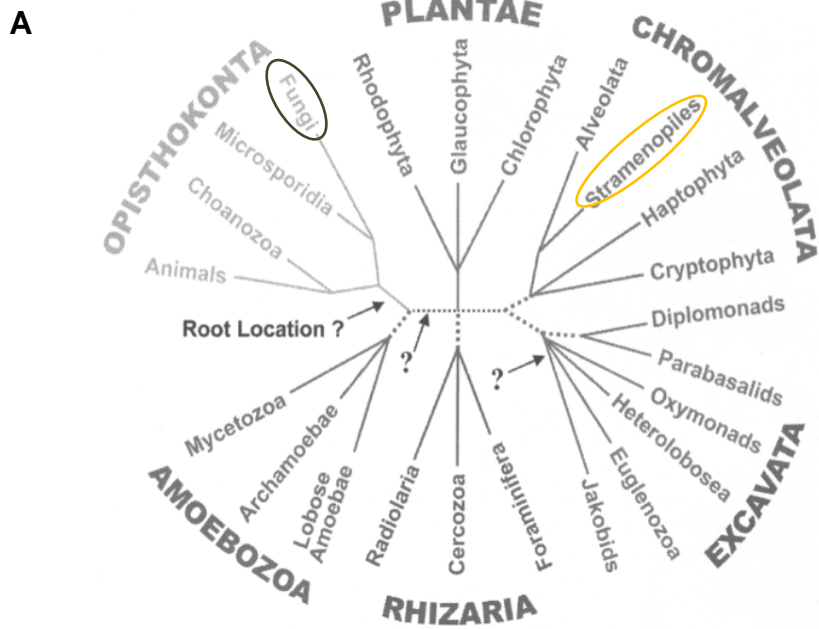


Figure 1. Schematic representations of the likely phylogeny of eukaryotes and the relationships of main phyla and classes of the Chromalveolata ensemble. A. Scheme of the current consensus of eukaryotic phylogeny showing the six super-ensembles: Opisthokonta, Plantae, Chromalveolata, Excavata, Rhizaria and Amoebozoa. Stramenopiles (within Heterokonts) are high-lighted in yellow. Adapted from Brinkmann and Phillippe (2007). **B.** Summary of the phylogenetic relationships of oomycetes (blue squared) within Stramenopiles (yellow squared) and their closest related groups. Adapted from Beakes and Sekimoto (2009).

Oomycetes: plant and animal disease agents.

Oomycetes are distinct from fungi

Oomycetes (commonly referred to as water moulds) are eukaryotic microorganisms regrouped in the Stramenipila kingdom (Brinkmann and Philippe, 2007; Beakes et al., 2012). They are heterotrophic organisms acquiring nutrients by absorption (osmotrophs) thanks to the transport into cells of nutrients produced by secreted depolymerizing enzymes on extracellular complex biological material. They present a hyphal tip-growth development that leads to the formation of complex branched mycelia. Because of these characteristics, oomycetes were thought to be related to fungi. It is known, now, that is not the case and that many traits shared with fungi are the result of convergent evolution. In fact, molecular phylogenetic studies based on the mitochondrial *cox2* gene (Thines et al., 2008), SSU and LSU rDNA genes (Voglmayr and Riethmüller, 2006) have replaced oomycetes in the super ensemble Chromalveolata (and within it, in Stramenopiles) far distant from true fungi (Opisthokonta) (figure 1 A). Oomycetes appear closely related to brown algae and diatoms and quite close to Apicomplexans (figure 1 B). The relatedness to brown algae together with the fact that the most ancestral oomycetes known today (*Eurychasma dicksonii* and *Haptoglossa spp*) are marine habitants, supports a marine origin of oomycetes (Beakes et al., 2012).

Cytological and biochemical studies corroborate the lack of relatedness to fungi and highlight main differences distinguishing them. Oomycetes present a coenocytic thallus which remains diploid throughout its vegetative stage (only formation of haploid nuclei occurs through meiosis for gamete formation). In contrast, fungal thalli are septate and carry haploid nuclei during vegetative stages. Additionally, their cell-wall polysaccharide composition is different. While chitin, N-acetylglucosamine residus 1,4-linked (1,4-GlcNac), remains largely the primary structural component of fungal cell-walls, oomycetes present a more diverse polymer composition. Cellulose and β -glucans remain the principle structural cell-wall constituents of late-divergent oomycetes (like *P. infestans*), whereas early-divergent species like *Saprolegnia spp* and *A. euteiches* present, in addition to cellulose, different levels of chitin (Badreddine et al., 2008; Guerriero et al., 2010). Recently, the cell-wall analysis of *A. euteiches* evidenced the presence of original polymers found for the first time in eukaryotes: 1,6-linked GlcNac residus in association to β -1,6 glucans (Mélida et al., 2013; Nars et al., 2013). Another major trait resides in the absence of biosynthetic pathways implicated in the synthesis of sterols in a large majority of oomycetes, compounds that oomycetes acquire from hosts by the secretion of sterol-carrier proteins during infection

(Mikes et al., 1998).

Oomycetes: diverse microorganisms and notorious plant pathogens

Between 600 and 1500 species are counted in the oomycetes lineage and, within Stramenopiles, they define a solely branch of highly diverse microorganisms. This is reflected, in a first instance, by the variety of their ecological niches since they occupy fresh-water, marine and terrestrial environments ubiquitously throughout the globe (Thines and Kamoun, 2010). In these environments, they present different life styles: as free-living organisms able to acquire nutrients from complex dead organic matter (saprophytes) and/or in association with other organisms. These symbioses are very often parasitic and ensure the derivation of all or part of their nutrition from the living host. When taking place, they are in a large extent pathogenic as they lead to the establishment of disease and mortality of hosts. It is worth to note that, to date, no mutualistic symbiotic oomycete has been described and that the earliest divergent oomycete, *Eurychasma dicksonii*, is an obligate pathogen of brown sea weeds (Grenville-Briggs et al., 2011). Thus, the capacity of parasitism seems to have appeared early in the history of oomycetes as well as their pathogenic behaviour which is a hallmark of this lineage.

Pathogenic oomycetes are highly diverse themselves, presenting a wide range of hosts which can be animals (like crustaceans, fishes, mammals including humans, nematodes) as well as algae and plants (Thines & Kamoun, 2010). Their impact can be seriously detrimental for natural ecosystems with important ecological consequences. For example, the plant pathogen oomycete *Phytophthora ramorum* (the agent of the sudden oak death disease) is destroying entire native North American forests and leading to a decrease of the woody species diversity as well as to changes on carbon and soil nitrogen cycling (Cobb et al., 2013). Another example is the crayfish plague caused by *Aphanomyces astaci* (listed as a notifiable disease of the World Organisation for Animal Health (<http://www.oie.int/en/animal-health-in-> causing the disappearance of entire species populations (Filipova et al., 2013; Vrålstad et al., 2011). Pathogenic oomycetes also constitute a serious threat to agricultural systems and therefore to food security (Fisher et al., 2012; Phillips et al., 2008). In this regard, phytopathogenic oomycetes merit considerable attention. It is estimated that 60% of oomycete species known today are plant pathogens (Thines & Kamoun, 2010). Among these, several stand as the most deadly pathogens of important cultivated plants. As already mentioned, the “plant destroyer” *Phytophthora infestans*, has been and continues to be a threat to potato and tomato representing an economical and societal problem worldwide (Nowicki et al., 2012). Other cultivated plants

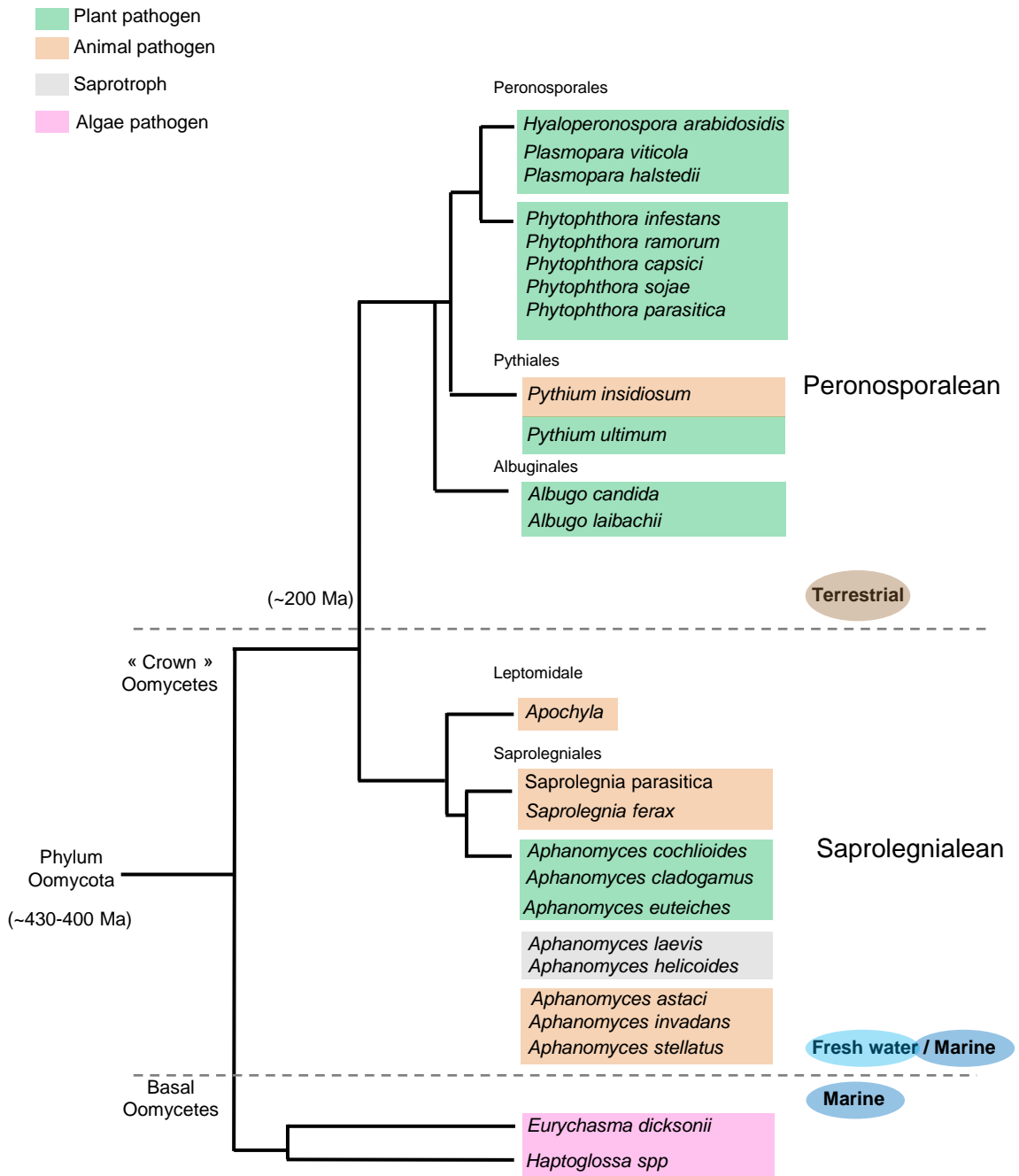


Figure 2. Summary scheme showing the phylogenetic relationships of main taxa groups of oomycetes, their environmental prevalence and lifestyles. Estimations place the origin of oomycete between ~430 and 400 million years ago (Ma). Late divergent « Crown » oomycetes are regrouped into two mayor ensembles: the Peronospolean lineage and the Saprolegnialean lineage, having separated ~200 million years ago (Ma). Representative species and their lifestyles are given. The scheme was generated based on information provided by Beakes and Sekimoto (2012), Dieguez-Uribeondo *et al* (2009) and Matari *et al* (2014).

like soybean, grape, broccoli, lettuce and sugar beet endure important diseases hosting species like *Phytophthora sojae*, *Plasmopara viticola*, *Peronospora parasitica*, *Bremia lactucea* and *Aphanomyces cochlidioides*, respectively.

Phylogenetic distribution of oomycetes

Oomycetes appeared 430-400 million years ago (Matari and Blair, 2014) and are grouped in two major taxonomic groups/lineages that encompass the most late-diverging groups of oomycetes or “crown oomycetes” (to exclude early-diverged basal lineages) as termed by Beakes and Sekimoto (2009): the Saprolegnialean and the Peronosporalean lineages (figure 2). The latter groups have been estimated to split 200 million year ago in the history of oomycetes and have, thus, different evolutionary histories which can be evidenced by biochemical features as for example the ability to synthesize sterols, a trait found only in Saprolegniales and in their closest relatives, the brown algae (Gaulin et al., 2010). Another distinctive trait concerns their ecological prevalence. Saprolegniales are predominantly found in aquatic environments (fresh water and estuarine) while Peronosporales occupy mainly terrestrial environments. The water-dependence of Saprolegniales is considered an ancestral trait and the tendency to have a lesser dependence on water is thought to be an evolutionary trend in oomycetes (Beakes and Sekimoto 2009).

Phytopathogenic oomycetes species are found in both lineages (figure 2) with a majority in the Peronosporalean lineage which stands as a phytopathogenic line. Species ascribed to genera *Phytophthora* (over 100 species, Kroon et al., 2012), *Albugo* and *Hyaloperonospora* as well as *Pythium* are phytopathogenic. Main exceptions are restricted to *Pythium* species since among the 150 plant pathogenic species some are animal pathogens like *P. insidiosum* (infecting mammals, Uzuhashi et al., 2010).

In contrast, the Saprolegnialean lineage is more heterogeneous since in addition to a large number of exclusively saprophytic species the group harbors zoopathogenic and phytopathogenic facultative species. Animal pathogens species of the genus *Saprolegnia* (i.e: *S. parasitica*) infect freshwater fishes, insects and amphibians (Sarowar et al., 2013). In *Aphanomyces* genus, species *A. invadans* and *A. astaci* develop on fishes and crayfishes species with elevated economic and ecological impacts (Phillips et al., 2008). Few plant pathogens species have been identified in Saprolegniales and are all included in the genus *Aphanomyces*.

- Plant pathogen lineage
- Saprotroph/opportunistic lineage
- Animal pathogen lineage

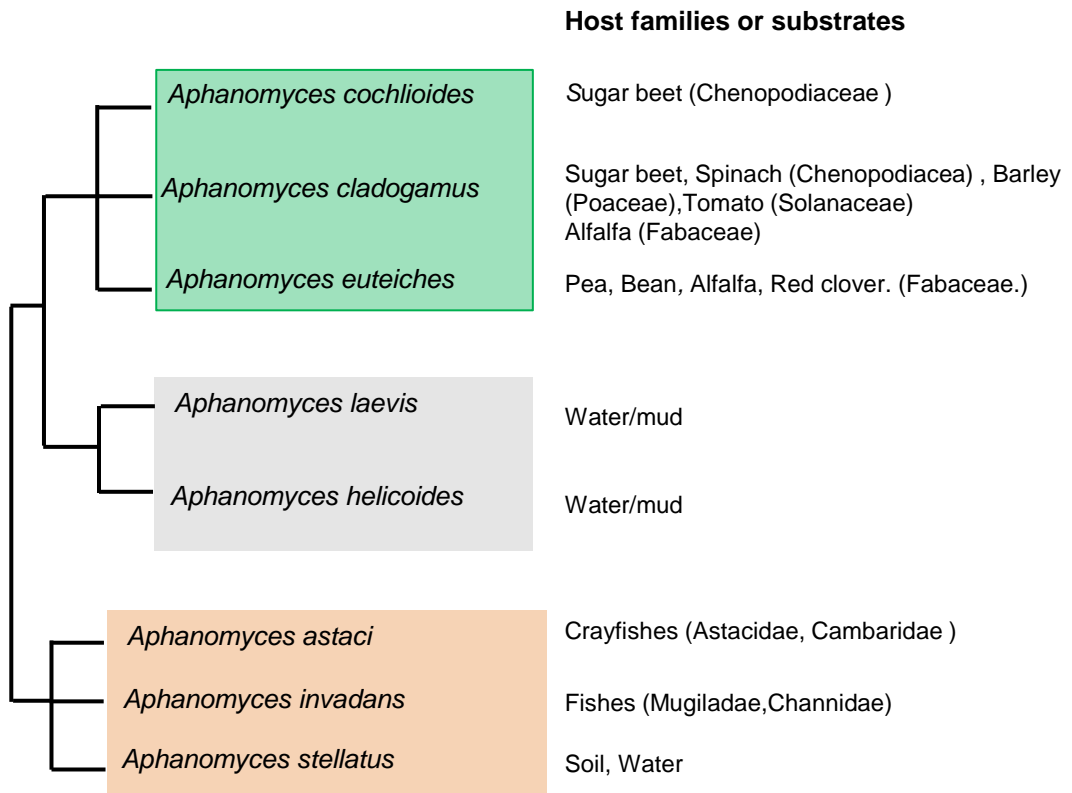


Figure 3. Close up summary scheme on *Aphanomyces* phylogeny, lifestyle and principal hosts or substrates.

The phylogenetic relationships were established by analysis of ITS sequences of nuclear rDNA of the principal *Aphanomyces spp* identified till date. Lives styles displayed by these species correlates to their phylogenetic regrouping defining three independent lineages: a plant pathogen lineage, a saprophytic/ oportunistc lineage and animal pathogenic lineage. Species *A. laevis* and *A. helicoides* are generally assigned as saprotrophs but isolated studies have documented their development on animals (insects). *A. stellatus* has been found as a free-living species but its ITS sequence analysis assigned it to the zoopathogenic lineage. The scheme was performed based on Dieguez-Uribeondo *et al.*, (2009).

Aphanomyces genus

An ancestral genus harboring diverse species

Aphanomyces genus regroups about 40 species (Diéguez-Uribeondo et al., 2009). This is an approximate number because their proper identification is difficult due to the reticence of some species to be isolated and maintained in pure cultures. Hence, its taxonomy is still in progress. Nevertheless, studies converge to the conclusion that *Aphanomyces* is an ancestral Saprolegniale group (Petersen and Rosendahl, 2000).

In an overall view, most species have prevalence for aquatic niches (fresh water and marine, mostly estuarine) with the exception of plant pathogens which occur in terrestrial wet environments. Phylogenetic studies of *Aphanomyces* genus regroup species in three independent lineages globally correlated to their life-styles (figure 3). A first line comprises plant pathogenic species, which in the Saprolegnialean line are only restricted to *Aphanomyces* genus. Within, species like *A. cladogamus* have a broad range of hosts of different families as Fabaceae (*Phaseolus vulgaris*, common bean), Poaceae (*Hordeum vulgare*, barley), Solanaceae (*Lycopersicon esculentum*, tomato) and Chenopodiaceae (*Spinacia oleacera*, spinach). *A. euteiches* displays a quite marked specialization for Fabaceae species while *A. cochlioides* is a host-narrow species reported so far only on sugar beet (*Beta vulgaris*) (Diéguez-Uribeondo et al., 2009). A second lineage harbors species with prevalence for saprophytism as *A. laevis* and *A. helicoides* which can exhibit opportunistic parasitism. Lastly, the zoopathogenic lineage regroups *A. astaci* (infecting freshwater crayfishes, Filipova et al., 2013) or *A. invadans* (responsible for the epizootic ulcerative syndrome of various species of estuarine fishes, (Boys et al., 2012) as well as *A. stellatus*, which, consensually defined as a saprotroph, has been found to develop on crustaceans (Royo et al., 2004).

The diversity of life styles and hosts of *Aphanomyces* species (animal/ plant pathogens and saprobe species) gives to this genus a special taxonomic position among Saprolegniales and towards Peronosporales.

Aphanomyces life cycle presents sexual and asexual stages. Sexual reproduction leads to the formation of oospores as the result of the fertilization of oogonia (female reproductive structures carrying the female haploid nuclei) by antheridia (male reproductive structures delivering haploid male nuclei). Oospores are long-resting structures which germinate to produce biflagellate motile zoospores (the primary infection entity). Such zoospores can also be produced as the result of asexual reproduction by live mycelium in roots via specialized hyphae (sporangium). As zoospores reach host surfaces, they encyst and

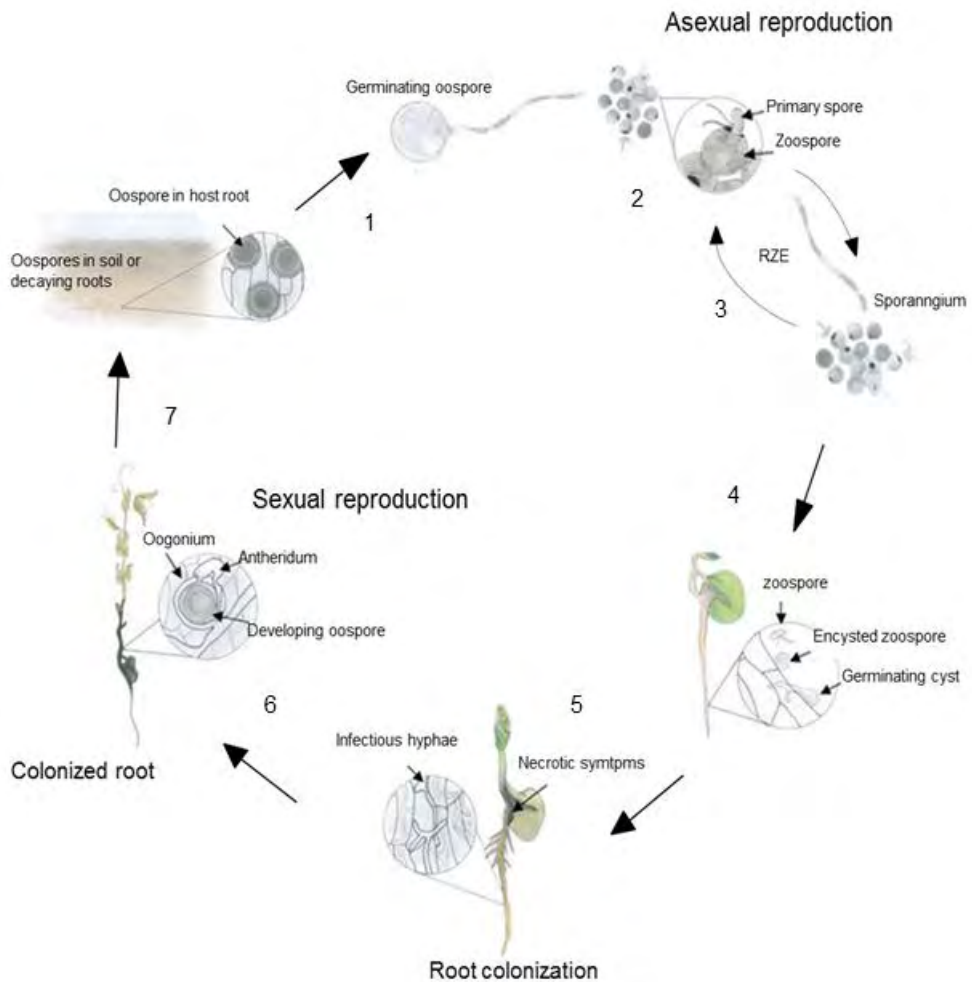


Figure 4. Infection life cycle of *A. euteiches* (Saprolegniales). Oospores present in soil germinate producing a sporangium (1). Primary spores (2N) are formed in the apex of the sporangium and release zoospores (asexual, biflagellate spores) through a pore of their cell wall (2). Zoospores can encyst and germinate to produce a novel sporangium giving rise to a second generation of primary spores and zoospores (3) a phenomenon called Repeated Zoospore Emergence (RZE). Zoospores that reach the host rhizoplane encyst and germinate producing an hyphae that directly penetrates host tissues (4). Infectious hyphae develops intercellularly (5) to completely colonize the root system and subsequently progress to hypocotyls (6). Within roots, sexual reproduction is assured by the differentiation of hyphae into antheridia and oogonia, carrying haploid nuclei (1N) and whose fusion results in the formation of oospores (2N). During the decomposition of dead plant tissue, oospore are then released in soils where they can remain dormant for up to 10 years (7). Adapted from the American Phytopathological Society (APS) <https://www.apsnet.org/>

germinate to penetrate host surfaces (figure 4). It is worth to note that some physiological and developmental behaviours are linked to the parasitic life style. Parasitic species present the capacity of Repeated Zoospore Emergence (RZE). This refers to the ability of a motile zoospore to encyst and to produce a second generation of zoospore rather than directly infect the host. It is believed that RZE allows to extend the duration of the infective stage and so the chances to come upon a suitable host. Also, plant parasitic species usually present both sexual and asexual stages whereas in animal pathogens the sexual stage is often absent or rare (Diéguez-Uribeondo et al., 2009).

A. *euteiches* and the root rot disease of legumes

Aphanomyces euteiches was first described by Dreschler in 1925 from infected pea (*Pisum sativum*) in the United States. It is a soil borne pathogen infecting roots of legumes as well as a facultative pathogen which means that it is able to grow as a saprobe outside the host (Papavizas and Davey, 1960). This renders its axenic culture possible. Its developmental cycle includes sexual and asexual stages. The species is homothallic (self-fertile) and presents sexual reproduction typically achieved by the formation of diploid oospores capable to subsist up to 10 years in soils on harsh conditions (Gaulin et al., 2007).

The disease caused by *A. euteiches* is commonly known as the root rot of legumes. Legumes affected include pea (*Pisum sativum*), alfalfa (*Medicago sativa*), snap and red kidney bean (*Phaseolus vulgaris*), faba bean (*Vicia faba*), red clover (*Trifolium pratense*) and white clover (*Trifolium repens*). Thus, *A. euteiches* has a relative large range of hosts within Fabaceae. Nevertheless its occurrence and degree of pathogenicity can differ from one host to another. Its characterization on pea and alfalfa has defined pathotypes: pea-infecting strains and alfalfa infecting strains from the USA and from France (Malvick and Grau 2001; Moussart et al., 2007; Wicker and Rouxel, 2001).

Infection takes place in roots as zoospores, chemo-attracted by root compounds (Sekizaki et al., 1993), encyst in the rhizoplane and germinate to penetrate root cortex tissues. Total colonization of roots is followed by the spread of the pathogen to stem (hypocotyls, epicotyls). Typically, its development provokes the disintegration of cortex tissues denoted by the appearance of softened and water-soaked areas of roots which become orange-brown or blackish-brown at later times of pathogen development. Symptoms can advance to stems and become evident by the necrosis of epicotyls and hypocotyls, and chlorosis of cotyledons followed by total discoloration (death) or foliage milting. Completion of infection is marked by the formation of oospores that ensure the dissemination. When

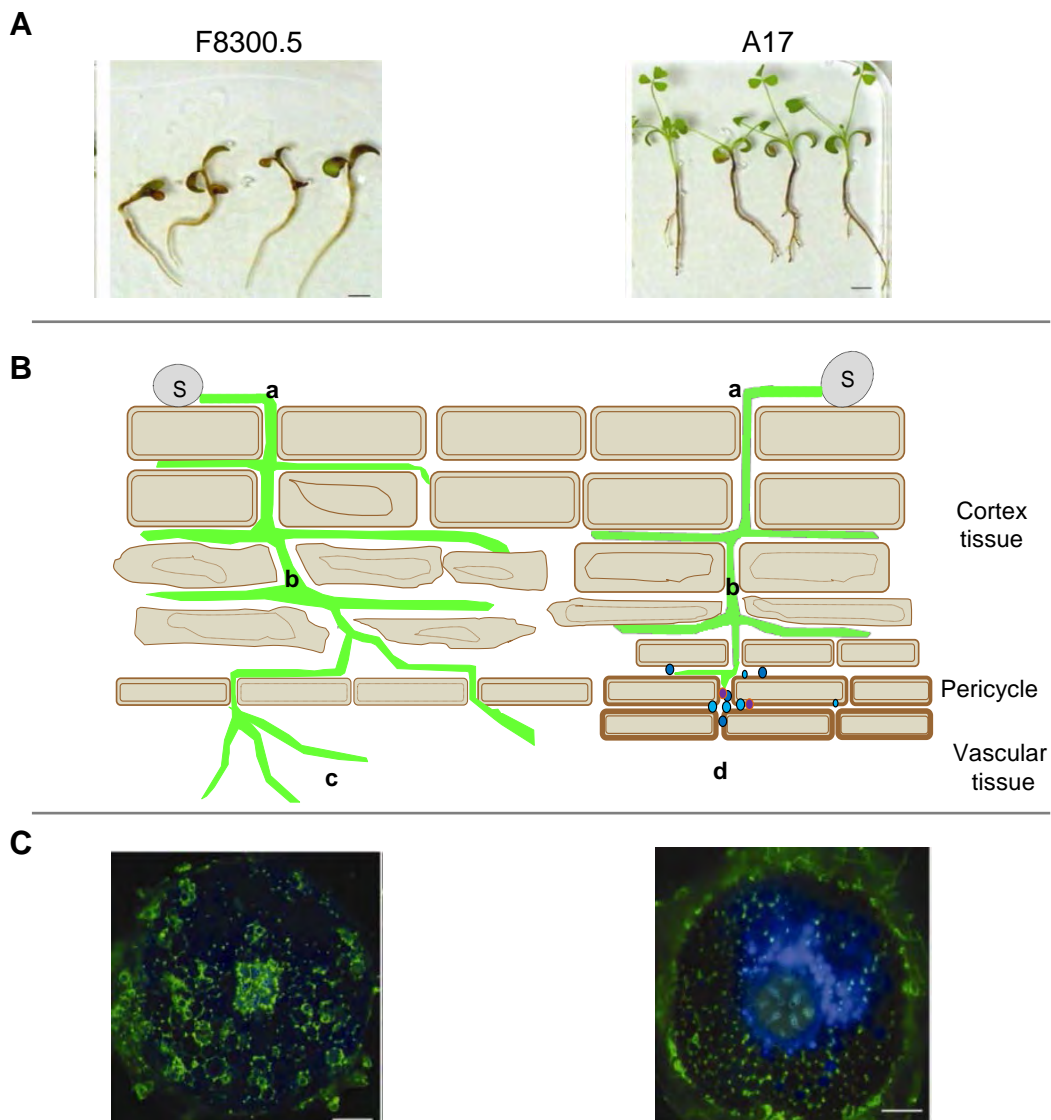


Figure 5. Infection model in the *Medicago truncatula/ Aphanomyces euteiches* pathosystem. **A.** Macroscopic symptoms displayed by *M. truncatula* F83005.5 (highly susceptible) and ecotypes A17 (partially resistant) infected with *A. euteiches* *in vitro* conditions (Djéballi *et al.*,2009). **B.** Scheme of a transversal section of a root infected by *A. euteiches* (green). On the left side, the scheme describes infection in F83005.5 where an asexual spore (S) has landed on the rhizoplane and germinated to produce a germ tube giving rise to an infectious hyphae that directly penetrates root cortex tissues (a). Hyphae develops between root cells of cortex which becomes completely colonized 6 days post inoculation. Cortical cells died as *A. euteiches* develops leading to root disassembly and water-soaked symptoms typical of root rot disease (b). The pathogen reaches the vascular cylinder before completion of its cycle (not shown) (c). On the right side, the infection is depicted in the tolerant host (A17) where the plant produces supplementary pericycle cell layers with higher levels of lignin in their cell-walls, reinforcing the root stele. In addition to this mechanical barrier, cells produce antimicrobial compounds (d). These cytological responses restrain the advance of the pathogen to the vascular cylinder. **C.** Cross-sections of infected roots showing full invasion (F83005.5) and partial invasion (A17) by *A. euteiches* (green) and the production of antimicrobial compounds by A17 (bleu) in the root stele, 15 days post inoculation (Djéballi *et al.*,2009).

conditions are appropriate, oospores germinate in the vicinity of hosts to produce zoosporangia.

Root rot disease occurs wherever host species are grown. Specially, it is a problem for pea and alfalfa-growing regions in North American and European countries. In France, it affects primary forage pea in northern regions (Gaulin et al., 2007). No effective control exists once *A. euteiches* is installed in soils. In addition, no fully resistant line of pea or alfalfa is available. Only prophylactic measures and crop rotation are preconized to prevent crop losses. Currently, improvement of crop resistance is done via the characterization of broad range resistance and identification of QTLs, which is the only type of resistance towards this pathogen (Djébali et al., 2009; Hamon et al., 2013; Bonhomme et al., 2014).

***A.euteiches* and *M. truncatula* pathosystem**

The legume *Medicago truncatula* is a close relative of the cultivated alfalfa (*M. sativa*) that has become a largely used model plant (Cook, 1999). Protocols suited for laboratory research have been established and a wide collection of mutants and natural genotypes are at disposition for the scientific community. Genomic resources include sequences of over 288 accessions (Stanton-Geddes et al., 2013). More interestingly, it is a host of *A. euteiches* showing great variability of susceptibility to this pathogen (Moussart et al., 2008).

A. euteiches/*M. truncatula* pathosystem has been developed and exploited in our research group to understand the molecular aspects behind the susceptible variability of the plant. The pathosystem makes use of a pea isolate of *A. euteiches* (ATCC 201684) and different genotypes of *M. truncatula* that display different degrees of tolerance to this strain. Two accessions exemplifying the opposite resistance degrees are line A17 (partially resistance) and line F83005.5 (highly susceptible). Genetic approaches and the use of an *in vitro* infection assay coupled to the characterization of infection phenotypes have led to the identification of a QTL (Djébali et al., 2009). Recently, the variability of 176 *M. truncatula* genotypes towards *A. euteiches* has been correlated to gene sequence architecture through a Genome Wide Association Study (GWAS). Single Nucleotide Polymorphisms (SNPs) in the promoter and coding region of an F-box gene have been spotted out and linked to *M. truncatula*'s variability to *A. euteiches* (Bonhomme et al., 2014). Although no expression polymorphism between resistance and susceptible lines could be shown, the identified SNPs are preconized to lead to functional and non-functional forms of the F-box protein which are associated to susceptibility and resistance, respectively. In addition to the F-

box gene, and consistent with the quantitative type of resistance towards *A. euteiches*, other genes have also been identified through the GWAS. These latter are associated to hormone regulation, notably the biosynthesis of cytokinine and transcription factors associated to ethylene response as well as gibberillin and abscisic acid (Bonhomme et al., 2014).

Molecular and cytological approaches carried in lines A17 and F83005.5 have evidenced particular plant mechanisms that might be implicated in the contrasting tolerance to *A. euteiches*. In both lines, upon inoculation of roots with zoospores, *A. euteiches* penetrates and starts to develop between cells of the outer cortex tissue within 1 day. No specialized infectious hyphae structures as appressoria or haustoria have been evidenced. The pathogen presents an intercellular development and invades the whole cortex area within 3 to 6 days. But, while in F83005.5 total invasion of cortical tissues is followed by the progression of the pathogen to vascular system, in A17 roots the pathogen progression is mostly restrained to cortical tissues. This inability to progress into the vascular system is correlated to the capacity of A17 to deploy a whole set of defense mechanisms like the production of phenolic compounds, the reinforcement of cell walls and, more particularly, the formation of supplementary pericycle cell layers that might act as a physical barrier for the invading hyphae (figure 5). Intriguingly, partial resistance of A17 is accompanied by an increase of lateral roots (Djébali et al., 2009).

Molecular interplay between pathogen effectors and plant immunity

Plant pathogen microorganisms have acquired the ability to take profit of the nutrient-rich niche that may be provided by plants to develop and reproduce. Indeed plants represent a well lasting source of carbon, nitrogen and water as well as a physical protection (Zuluaga et al., 2013). This mode of living implies an intimate association with plants in order to exploit goods. Because the development of associated microorganisms affects host plant health, conducting eventually to plant disease and death, these associations are termed as pathogenic.

Plant immunity and effectors

As any other living organism exposed to a multitude of microorganisms, plants sense these external cues to respond in the best-adapted manner. To defend themselves against pathogens, plants possess constitutive defenses consisting in pre-existing physical or

Table 1. Pathogen Molecular Associated Patterns (PAMPs) of bacteria fungi and oomycetes and their cognate receptors in plants.

Organism	PAMP (name)	Plant Receptor	Reference
Bacteria	Flagellin (flg22)	FLS2 (<i>A.thaliana</i>)	Félix et al. , 1999 Gomez-Gomez et al., 2001
	Elongtion factor EF-Tu (elf18/26)	ERF (<i>A.thaliana</i>)	Kunze et al., 2004
	Cold shock protein (RNP)	Not identified	Félix and Boller, 2003
	Lipopolysaccharide	Not identified	Newman et al., 2005
	Peptidoglycan	Lym1, Lym2 (<i>A. thaliana</i>)	Erbs et al., 2008a Willmann et al., 2011
Fungi	chitin	CeBip, (rice) CERK1 (<i>A.thaliana</i>)	Kouzai et al., 2014 Petutschnig et al., 2010
	Xylanase (EIX)	EIX (tomato)	Ron and Avni, 2004
Oomycetes	CBEL	Not identified	Gaulin et al.,2006 Larroque et al., 2013
	Pep13	Not identified	Nürnbergger et al.,1994 Brunner et al., 2002
	B-hepta glucans	GEBP (putative, soybean)	Umemoto et al., 1997
	INF1	NbLRK1 (<i>N.benthamiana</i>)	Kanzaki et al., 2008

biochemical barriers (i.e. hydrophobic cuticles, surface antimicrobial compounds...) that act as a first level of protection to avoid and limit development of potential harmful microorganisms. In addition, they possess an inducible multi-layered immune system that allows them to perceive microorganisms and activate a whole set of modular defenses (figure 6 A) (Dodds and Rathjen, 2010).

The first level of plant immunity is activated by the direct perception of conserved epitopes in commonly occurring molecules of microbes (pathogen or non-pathogen) called “Pathogen/Microbial-Associated Molecular Patterns “P/MAMPs”. These molecular signatures can be of different nature (protein, oligosaccharides...), they identify a whole classe of microbes and are absent from plants (table 1). Their recognition involves Pattern Recognition Receptors (PRRs) associated to the plasma membrane that belong to the family of Receptor-Like-Kinases (RLKs) and Receptor-like Proteins (RLP) (Boller and Felix, 2009) (figure 6). Best characterized examples are the 22-peptide present in the bacteria flagellin protein (flg22) and peptides elf18/26 of the bacterial EF-Tu elongation factor protein perceived by the RLKs FLS2 and EFR, respectively (Boller & Felix, 2009). Fungal chitin is perceived in rice by CEBiP (Kouzai et al., 2014) and by CERK1 in *A. thaliana* via their LysM extracellular domains (Petutschnig et al., 2010). The activation of the defense signaling after PAMP perception requires the association of these receptors to a central RLK regulator, named BAK1 (Kim et al., 2013) (figure 6). The importance of BAK1 in mediating PAMP-defense signaling and activation is well known for the above mentioned bacterial and fungal PAMPs and has been recently established for defense against nematodes and insects (Peng and Kaloshian, 2014). Oomycete PAMPs that elicit defense in plants have been identified but their cognate receptors and mechanisms behind their recognition remain for the most unknown. These include the epitope pep13 of transglutaminases (Brunner et al., 2002), the heptaglucans of *P. sojae* which has been proposed to be perceived by the GEBP (soybean) (Umemoto et al., 1997), the cellulose-binding domain of the cell-wall protein CBEL of *Phytophthora parasitica* (Gaulin et al., 2006) for which its eliciting activity requires BAK1 (Larroque et al., 2013) and finally, the sterol-binding protein elicitor INF1 from *Phytophthora spp* (Kamoun et al., 1998) for which a RLK has been identified (Kanzaki et al., 2008) (table 1).

PAMP/MAMPs recognition triggers a level of immunity referred to as PAMP-Triggered Immunity (PTI) also called basal immunity given the broad spectrum of occurrence of PAMP/MAMPs, not specific to a given pathogen. PTI includes subsets of early responses like the production of ROS species and ion fluxes. More intermediate events include the activation of signaling cascades involving mitogen-activated protein kinases (MAPKs)

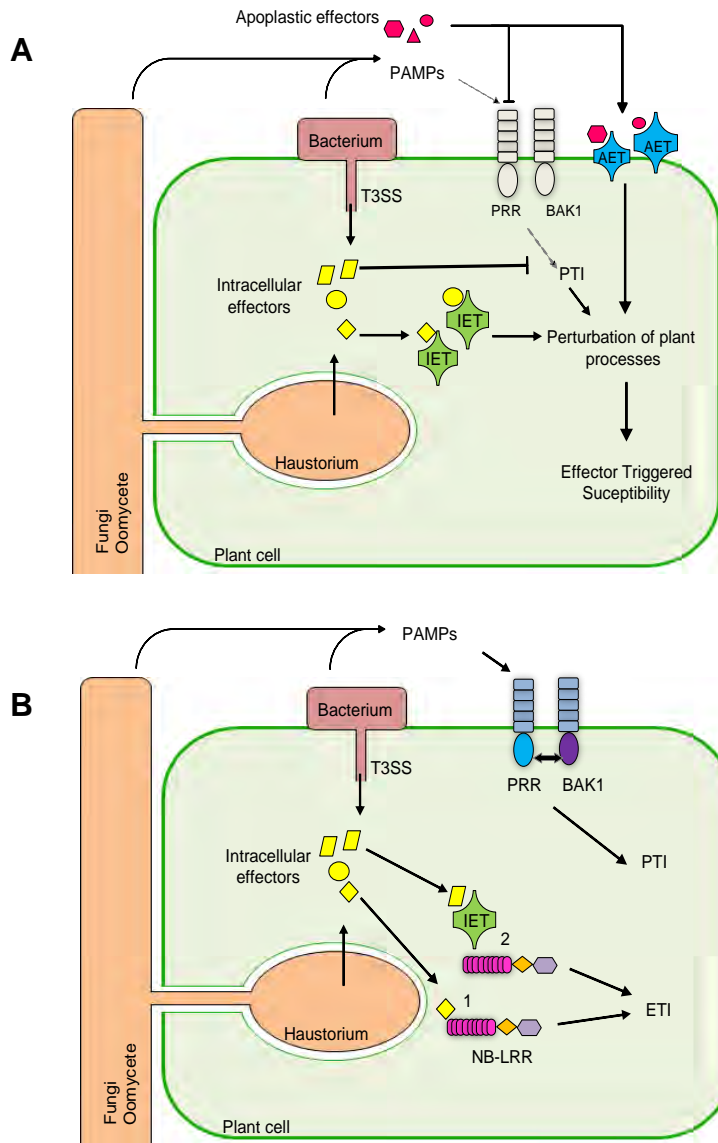


Figure 6. Global concepts of plant susceptibility triggered by microbial effectors (A) and plant immunity (B). **A.** Pathogens such as bacteria, fungi and oomycetes establish a close physical encounter with host cells. They secrete effectors into the apoplast (apoplastic effectors) of inside plant cells (intracellular effectors). Bacteria deliver them into host cells via the Type 3 secretion system (T3SS) and filamentous pathogens via infectious structures (haustoria). Apoplastic effectors interact with apoplastic effector targets (AET) and intracellular effectors with intracellular effector targets (IET). In susceptible plants (A), their interaction with targets perturb different plant processes that benefit the outcome of infection. Among these processes, PTI is an important target whose suppression is required for successful infection. **B.** Plant immunity activation resides on the perception of pathogens, which can be performed through two modes. A first mode, consists on the perception of PAMPs by PRRs (Patter Recognition Receptors) at the plasma membrane leading to the activation of PTI (PAMP-Triggered Immunity). Initiation of PTI signalling pathway requires the co-receptor BAK1. A second mode, relies on the direct perception of effectors (1) or on the perception of effector activities on plant targets (2) via intracellular nucleotide-binding receptors (NB-LRR), conducting to ETI (Effector-triggered Immunity). (Modified from Win et al., 2011)

(Pitzschke et al., 2009) that ultimately conduct to the activation of transcription factors (TFs) and expression of pathogenesis-related genes (PR) encoding antimicrobial compounds like chitinases and glucanases which directly degrade cell-wall structural components of pathogens (Dodds & Rathjen, 2010). Phytohormones like salicylic acid (SA) and jasmonic acid (JA) also play key roles in the signal transduction (Tsuda and Katagiri, 2010). All together, these defenses are generally sufficient to arrest pathogen infection and maintain plant health. Nevertheless, adapted pathogens have evolved means to break down or evade such defenses. These pathogens produce secreted molecules termed “effectors” which designates “all proteins and small molecules” produced and secreted by pathogens that “alter host-structure and function” and facilitate infection (Hogenhout et al., 2009). Effectors are secreted into the apoplast interface (apoplastic effectors) or are addressed inside host cells (intracellular effectors) to interact with plant targets. By doing so, effectors can suppress plant immunity and perturb other plant processes that conduct to host susceptibility or Effector-Triggered Susceptibility, a state benefiting the outcome of the infection (figure 6 A). Manipulation of PTI can be achieved by avoiding PAMP recognition or by directly suppressing PTI. For instance, the fungal LysM apoplastic effectors bind chitin, preventing its recognition by plants (Kombrink and Thomma, 2013). In oomycetes, several apoplastic-secreted protease inhibitors from *P. infestans* have been shown to directly bind plant apoplastic enzymes, suppressing directly their activities in this host space (Tian et al., 2005, 2007; Song et al., 2009).

Another type of defense relies on the recognition of specific effectors or effectors’ activities and is referred to as Effector-Triggered Immunity (ETI) (figure 6 B). This mechanism for pathogen recognition involves a particular class of receptors called R proteins (Resistance proteins) that are generally cytosolic. Effector recognition by R proteins leads to specific resistance and incompatible interactions, reason why in this context, recognized effectors are called Avirulence (Avr) proteins. This mechanism follows the gene-for-gene model conceptualized by Flor’s work (1971). ETI is similar in nature but is more rapid and strong than PTI (Tao et al., 2003; Tsuda and Katagiri, 2010) and is often accompanied with a cell-death or Hypersensitive Response (HR). Because it relies on the perception of effectors, it is a specific immunity.

R proteins are classified into two classes depending on the type of Nterminal domain: (Toll-like Receptor) TIR-NB-LRR or (coiled-coiled) CC-NB-LRR proteins. Two modes of effector recognition exist: (1) direct physical interaction of R proteins to effectors or (2) indirect interaction of R proteins. In this case, R proteins perceive modifications of plant proteins to which the R protein is associated and monitors (figure 6 B). These modified plant

proteins can be genuine virulence target of the effector (the guard model) or a mimic of one (the decoy model). It has been shown that activated R proteins interact with other proteins forming complexes mediating the signaling that conducts to defense response such signaling requires complexes to relocalize to specific subcellular compartments of plant cells (Dodds & Rathjen, 2010; Engelhardt et al., 2012; Qi and Innes, 2013).

In that instance, studies have recently demonstrated the importance of a nucleo-cytoplasmic trafficking of R proteins and other immune components for the activation of defense responses. The accepted model is that such relocalization is induced by pathogen perception and allows immune receptors to accumulate in the plant nucleus where they activate immune responses through transcriptional reprogramming (Qi and Innes, 2013).

Effector identification

Effector proteins were firstly identified thanks to their avirulence activity. In an ETI context, the effector behaves as an avirulent protein and the resultant incompatible interaction was of great aid to identify avirulence proteins in fungi, bacteria and oomycetes. Their cloning and molecular characterization pointed out the presence of secretion leaders either typical of the Type 3 Secretion System (T3SS, for bacteria Avr proteins) or canonical eukaryotic signal peptides (in oomycetal and fungal Avr proteins) (Armstrong et al., 2005; Staskawicz et al., 1984; van Kan et al., 1991). It was then suggested that such key factors were likely to be secreted by pathogens to reach host structures and compounds.

Effector identification has been possible by the use of transcriptomic, proteomic and genomic approaches coupled to functional screening systems based mostly on the capacity of effectors to modulate plant immunity. Transcriptomic studies have allowed to determine genes differentially expressed during infection and even specifically in particular infection stages and pathogen structures as haustoria (Godfrey et al., 2010; Hahn and Mendgen, 1997; Huang et al., 2004). Expressed Sequenced Tags (ESTs) obtained on cDNA libraries coupled with computational searches for secretion peptides provide putative effector secretomes and thus putative effector repertoires. By this means, 31 haustoria-specific *in planta*-induced genes from the rust fungus *Uromyces faba* were identified (Hahn and Mendgen, 1997) as well as 100 putative secreted proteins expressed predominantly in haustoria of *Blumeria graminis* (Godfrey et al., 2010). Moreover, *P. infestans* secretome analysis based on ESTs led to the identification of CRN proteins (Torto et al., 2003).

Proteomic approaches and/or biochemical purification of active secreted molecules have

proven to be successful on the characterization of key factors of infection. Mass spectrometry analysis of total proteins extracted from xylem sap of susceptible tomato infected with the vascular pathogen *Fusarium oxysporum* resulted on the identification of SIX (Secreted In Xylem) proteins of *F. oxysporum* specifically present during infection (Houterman et al., 2007). Further characterization of SIX1 and SIX2 proteins demonstrated their requirement for full virulence and as proteins recognized in tomato lines expressing I-3 and I-2 resistance proteins (Rep et al., 2004; Houterman et al., 2009). Proteomic approaches can be also useful when combined with predicted approaches. For instance, mining of *P. infestans*'s *in vivo* secretome has not only corroborated repertoires established *in silico* via gene model prediction on genomic data but has also extended the secretome repertoire (Meijer et al., 2014).

As numerous complete genomes are available, effector repertoires can be established directly on gene models and can be combined to transcriptomic and proteomic data to further support their effector role. *In silico* criteria to determine candidate secreted effector proteins (CSEPs) on genomic data are principally based on the presence of secretion leaders and the absence of transmembrane domains. For such criteria, sequence surveys make use of computational strategies developed to ensure accuracy of predictions (Bendtsen et al., 2004; Torto et al., 2003). Other criteria can be taken into account for the determination of CSEPs and have become widely used and accepted in the scientific community throughout observations made on some experimental data. As very often, the studied effector proteins display small sizes and a high content of cysteine, such characters are usually taken into account when defining potential candidates. These criteria have led to determine 929 proteins in the oomycete *Albugo candida* (Links et al., 2011) and 491 and 365 proteins from fungi *Blumeria graminis* and *Colletotrichum higginsianum*, respectively, have been proposed as putative effectors (Pedersen et al., 2012b; O'Connell et al., 2012). Genome survey on *Ustilago maydis* revealed 426 proteins potentially secreted (Mueller et al., 2008) and tissue-specific expressed, as revealed by transcriptome profiling (Gao et al., 2013).

Further amino acid sequence inspection of CSEPs repertoires has evidenced the presence of commonly occurring amino residues for some of them. These amino acids define motifs that serve as a basis for protein family classification and as a criterion when inspecting novel pathogen genomes (table 2). This was typically the case of oomycetes, for which sequence comparison of Avr proteins like ATR13 of *H. parasitica*, and Avr3a of *P. infestans* (Allen et al., 2004; Armstrong et al., 2005) led to determine a conserved Nterminal RxLR (Arginine, any amino acid, Leucine, Arginine) motif (Rehmany et al., 2005). Since evidenced as a sequence trait of Avr effectors, this motif has been used on genomic data of

Table 2. Conserved Nterminal motifs identified on Candidate Secreted Effectors Proteins (CSEPs) in fungi and oomycetes.

Motifs	Protein	Species	Reference
RxLR(dEER)	RxLR effectors	<i>Phytophthora spp</i> , <i>H. arabidopsidis</i> <i>A. Laibachii</i>	Rehmany et al., 2005; Haas et al., 2009; Baxter et al., 2010 Kemen et al., 2011
LSSLR(ILKS)L(KQ)SL	Ac-RXL	<i>A. candida</i>	Links et al. ,2011
LxLFLAK	CRN effectors	<i>Phytophthora spp</i> <i>H. arabidopsidis</i> , <i>A. euteiches</i>	Torto et al.,2003 ; Haas et al.,2009 ; Stam et al.,2013 Baxter et al.,2010
	CRN-like	<i>R. irregularis</i>	Lin et al., 2014
HVVVxxP	CRN effectors	<i>A. euteiches</i>	Gaulin et al.,2008 ; Gaulin et al., in preparation
LxLYLAR /K	CRN effectors	<i>P.ultimum</i>	Adhikari et al.,2013
CHxC	CHxC	<i>A. candida</i> , <i>A. laibachii</i> <i>P. infestans</i>	Pais et al., 2013 ; Kemen et al.,2011 ; Links et al., 2011
Y/F/WxC	Y/F/WxC	<i>B. graminis</i> <i>P. graminis</i> <i>M. lini</i>	Godfrey et al., 2010b ; Pedersen et al., 2012
			Saunders et al., 2012
			Duplessis et al. , 2011
RFYR	AvrL567	<i>M. lini</i>	Rafiqi et al.,2010
RGFLR, KFLK, RDLA	AvrM	<i>M. lini</i>	Rafiqi et al.,2010
RYWT, RTLK	AvrLm6	<i>L. maculans</i>	Kale et al. , 2010
RMLH and RIYER	Avr2	<i>F. oxysporum</i>	Kale et al., 2010
FYIQYLxNQPV and/or LVAA	CRN-like	<i>B. dendrobatidis</i>	Sun et al., 2011

all oomycetes and has led to the identification of a large number of RxLR proteins defining the RxLR class of oomycete effectors (563 coding genes in *P.infestans*, Haas et al., 2009, 134 in *H. parasitica*, and 396 in *P.sojae*, Baxter et al., 2010). The conservation of the Nterminal motif L/Q/FLAK has also allowed the identification and cataloguing of CRN effectors in oomycetes (Baxter et al., 2010; Haas et al., 2009; Stam et al., 2013a). Moreover, a CHXC motif has been recently proposed as a motif characterizing a third large class of effectors in oomycetes (Pais et al., 2013; Kemen et al., 2011; Links et al., 2011). In fungi, RxRL-like motifs (ie, RRLQ RGFLR... Rafiqi et al., 2010; Khang et al., 2010) have been proposed in Nterminal domains of CSEPs. In addition, a Nterminal Y/F/WxC motif, firstly found in the 100 haustoria-expressed CSEPs of *Blumeria graminis* (Godfrey et al., 2010; Pedersen et al., 2012) have also been reported in CSEPs of *Puccinia graminis* and *Melampsora larici-populina* (Duplessis et al., 2011; Saunders et al., 2012).

In addition to these criteria (presence of secretion signals, absence of transmembrane domains, small size, high content of cysteine residues), other sequence signatures like the signs of diversifying selection can pinpoint their potential effector role as this may infer that the protein in question is submitted to a counter selection by hosts. Indeed, this has been demonstrated for the carboxyl terminal domains of RxLR effector secretomes (Win et al., 2007).

With established effector repertoires in a considerable number of species, it is now possible to perform comparative genomics to provide clues explaining pathogen host-adaptation and particular infection strategies. For example, comparison of putative effectors of the closely related smut fungi *U. maydis* and *Sporisorium reilianum* (both infecting maize) have determined specific subsets of effectors in both species. These subsets could be at the basis of their different infection behaviours on maize and may also imply the targeting of distinct maize functions (Schirawski et al., 2010). Another example is the comparison made on seven pathogenic necrotrophic *Pythium* species that revealed the absence of RxLR effectors. Because RxLR proteins are present in the related hemibiotrophs *Phytophthora spp* and the obligate biotroph *H. arabidopsidis* and display *in planta* functions related to the suppression of host defenses, they have been generally attributed to the support of biotrophic lifestyles. The lack of RxLR effectors in *Pythium spp* could further support the latter idea as RxLR functions seem irrelevant for *Pythium* necrotrophic lifestyle (Adhikari et al., 2013). Genomic studies aiming to identify putative effectors can be directed on particular genomic environments. Actually, in *Leptosphaeria maculans*, putative effector coding genes are mainly found in AT-rich isochores and are often associated to transposable elements (TE) (Rouxel et al., 2011). These effector-TE associations have also been observed for *P. infestans*

RxLR and CRN genes (Haas et al., 2009). Therefore, identifying such genetic environments in species might be used as a strategy to spot out CSEPs.

Functional characterization of effectors

The different predictive approaches for effector identification can result in important number of candidates. Demonstrating their actual contribution to virulence, studying their effect and biochemical activities in plants as well as identifying their targets can be time consuming because of their number, because reverse genetic approaches may not lead to a phenotype and because, for some pathosystems, genetic manipulation of pathogens is not possible. Given this, rapid and efficient functional methods are required in order to screen and functionally characterize effectors.

For this purpose, and based on the concept that effectors are secreted molecules that act in plant cell interfaces, different systems have been developed to heterologously express effectors *in planta*, in order to test directly their cellular localization and any disturbance of plant physiology. Typically, effector proteins tagged with fluorescent proteins are overexpressed with or without their signal peptide (SP) to directly test their cellular localization by plant cell imaging (by means of confocal microscopy) (Caillaud et al., 2012; Stam et al., 2013a/b). Heterologous expression systems are also used to test the “pathogen-independent” host-delivery of effectors. As the presence of the SP is expected to drive the secretion of effectors into the plant apoplast, by expressing full length effector proteins (containing their SP), it is inferred that effectors localizing inside cells have re-entered the cytoplasm autonomously via intrinsic translocation signals in the protein. Based on this, it is then inferred that these effectors are likely to localize inside plant cells during infection (Rafiqi et al., 2010; Ribot et al., 2013).

N.benthamiana and *N.tabaccum* (Solanaceae) have become widely used for molecular plant-microbe interactions studies since they display different degrees of susceptibility to a variety of microorganisms as oomycetes (*P.capsici*, *P.infestans*), fungi (*Verticillium dahlia*, *Colletotrichum orbiculare*), bacteria (*P. syringae*), viruses (TMV, PVX...) and several cDNA libraries and molecular tools like microarrays are available (Goodin et al., 2008). Their foliar tissues are particularly amenable for genetic transformation via the bacteria *Agrobacterium tumefaciens*, compared to other plant model species like *A. thaliana* and crop species like barley. Infection with *A. tumefaciens* strains carrying an effector coding gene allows to, locally and transiently, transform plant cells and constitutes an easy way to express

efficiently an important number of effectors in plant cells. As an example, Caillaud and associates (2012) used this approach to screen the localization and cell-death activity of 49 intracellular RxLR effectors of *H. arabidopsidis*, evidencing the diversity of the subcellular compartments targeted by these proteins. Co-agroinfiltration of *N.benthamiana* leaves is also possible and has been validated, for example, for the study of Avr/R proteins resulting in the expected HR response (Van der Hoorn et al., 2000; Bos et al., 2006). Besides agroinfiltration, *Pseudomonas syringae* and its T3SS provide another strategy for delivering effector proteins directly in the cytosol of plant cells by translationally fusing T3 secretion leaders to the studied effectors. This strategy was used by Whisson and colleagues (2007) to demonstrate that the RxLR effector, Avr3a, is recognized by the R protein R3a in the cytoplasm of plant cells and thus that Avr3a is translocated inside plant cells during infection, proving for the first time that RxLR proteins are intracellular effector proteins (Whisson et al., 2007).

Cellular systems have also been developed for rapid and accurate functional studies. Methods based on protoplasts have been described and improved to transiently express effectors and/or reporter genes on various plant crop species like rice, maize, parsley, tomato...(Chen et al., 2006; Sheen, 2001). Such systems have been used to characterize molecular events linked to MAMP/PAMP perception, signal transduction of defense responses and effector activities (Brunner et al., 2014; Kansaki et al., 2014). Recently, a screen on 33 RxLR effectors using protoplasts of tomato and *A. thaliana* allowed to identify immune suppressive RxLR effectors and to correlate these activities to their cellular localization (Zheng et al., 2014). In addition, screening of 42 *in silico*-identified putative secreted effectors of *M. oryzae* permitted to identify 5 effectors capable of triggering cell-death on rice protoplast (Chen et al., 2013). Finally protoplasts can be also used to screen cDNA libraries for protein-protein interactions, analogously to Yeast-two Hybrid approaches (Y2H). This has been performed to identify plant protein partners of effectors of *A.tumefaciens* (Lee et al., 2012).

All together, these systems have rendered possible to bridge *in silico* identification to rapid validation of effector candidates and even their functional molecular dissection. Still, although providing a rapid way to initiate an effector characterization, experimental systems providing a natural host/microorganism context are required to accurately assess effector's functions.

Effector delivery and localization

Effectors are secreted to exert their functions either on the apoplast (apoplastic effectors) or inside host cells (intracellular/cytoplasmic effectors). In the case of gram negative bacteria, apoplastic effectors are secreted via the Type 2 Secretion System (T2SS) (Nivaskumar and Francetic, 2014) while apoplastic effectors from filamentous eukaryotic microorganisms are secreted via the classical endomembrane secretion pathway (Giraldo et al., 2013).

To reach host cytoplasm, intracellular effectors require passing across pathogen outer structures, the apoplastic space and outer structural components of host cells (cell-wall and plasma membrane). General concepts of secretion and host-delivery are schematized in figure 7. Delivery systems and mechanisms are well characterized for prokaryotic pathogens, which use the Type 3 and/or Type 4 Secretion System (T3SS/T4SS) to ensure the direct injection of effectors into the host cytosol (Büttner and Bonas, 2006). A total of 52 T3SS effector families have been identified in *Xanthomonas spp*, 58 in *Pseudomonas syringae* and 100 in *Ralstonia solanacearum* which display a great variability between strains (Baltrus et al., 2011; Peeters et al., 2013; Ryan et al., 2011). Intracellular effectors of nematodes are delivered into host cytoplasm via a protusible stylet that pierces plant cell-wall and mediates their injection across the host plasma membrane (Mitchum et al., 2013). For filamentous eukaryotic pathogens, secretion and delivery systems are less understood. In the case of fungi, it was very recently shown that intracellular effectors of the rice blast fungus *Magnaporthe oryzae* undergo an alternative secretion pathway different from the classical ER-Golgi secretory endomembrane pathway used for the secretion of apoplastic effectors (Giraldo et al., 2013). Such alternative secretion mechanisms result in the accumulation of effectors in particular zones of the infectious hyphae termed Biotrophic Interfacial Complex (BIC) (Giraldo et al., 2013; Khang et al., 2010).

In oomycetes, it is still not known whether intracellular effectors are secreted by particular secretion routes, but pioneer studies, using GFP-tagged effectors expressed by the pathogen, revealed their accumulation in located zones of haustoria, inferring that these structures ensure effector delivery into host cells. How fungal and oomycete effector proteins are secreted outside the pathogen plasma membrane and transported across the host-cell outer structures is a current topic of considerable interest and controversy.

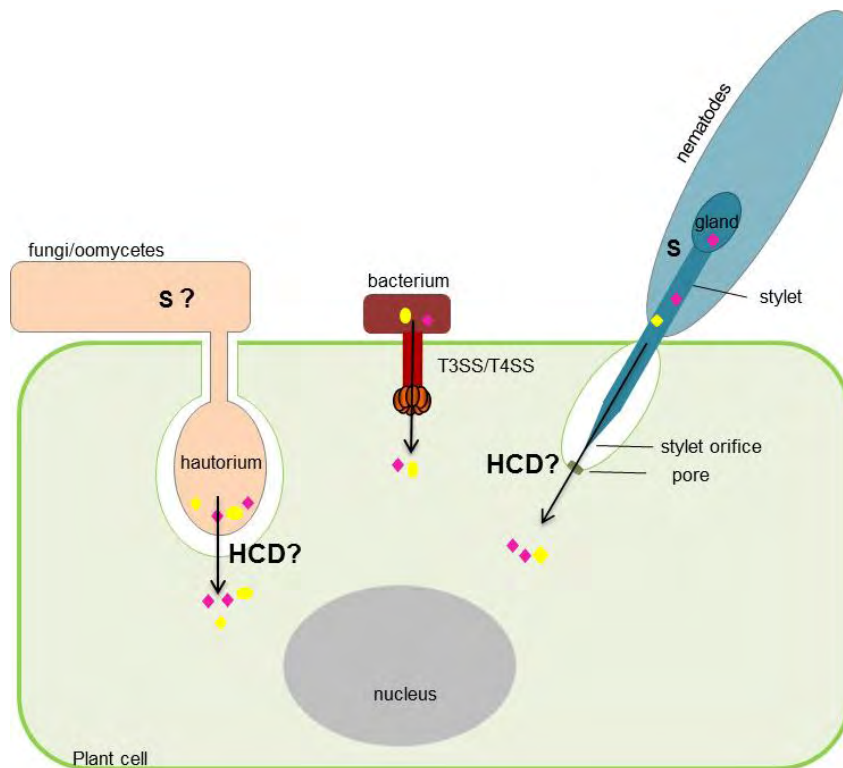


Figure 7. Schematic representation of the general concepts of secretion (S) and host-cell delivery (HCD) of intracellular effectors by phytopathogenic fungi, oomycetes, bacteria and nematodes.

Secretion and translocation of bacterial intracellular effectors to the interior of host cells is ensured by host-cell-contact-dependent secretion molecular systems (T3SS and T4SS).

Fungi and oomycetes intracellular effectors accumulate in infection structures as haustoria from which they translocate inside host cytoplasm. While it has been shown that intracellular effectors undergo ER-Golgi independent secretion pathways in the fungus *M. oryzae* (Giraldo et al., 2103) it is still not clear whether this can be a generality for other fungi and oomycete species.

Nematode intracellular effectors are produced in oesophageal gland cells and secreted via the ER-Golgi secretory network into secretory granules transported along the stylet and subsequently released into host cytoplasm via the stylet orifice. Structural analyses have depicted a small pore in the plasma membrane at the stylet orifice thought to allow direct delivery of effector proteins (Mitchum et al., 2013).

The studies on the translocation of fungal and oomycete effectors have shown that the N-terminal domains might carry the translocation signals. In oomycetes, amino terminal conserved motifs (downstream of their signal peptide sequences) like the RxLR motif (in RxLR effectors) and the L/Q/FLAK (in CRN effectors) characterize these regions and have been shown to act as signals for host delivery (Dou et al., 2008; Kale et al., 2010; Schornack et al., 2010; Whisson et al., 2007). In contrast, fungal amino terminal domains do not present an obvious conservation of residues. For some proteins, algorithm-based sequence surveys have suggested RxLR-like motifs.

Interestingly, the oomycete RxLR motif is highly similar and functionally equivalent to the RxLxE/D/Q (termed "Pexel") found in intracellular effectors of the human parasite *Plasmodium falciparum* (phylogenetically related to oomycetes) (Bhattacharjee et al., 2006; Hiller et al., 2004; Marti et al., 2004). The dissection of their export mechanisms has shown that, once addressed into the secretory pathway by secretion signals, these proteins interact with the lipid phosphatidylinositol 3-phosphate PI(3)P present in the endoplasmic reticulum (ER) membrane. In the ER lumen, the RxLxE/ D/Q is cleaved by the aspartic protease Plasmepsin V, a process that is thought to liberate the protein from the ER membrane to allow its subsequent vesicular ER-Golgi export. Once outside the plasma membrane, their actual translocation inside host cells has been proposed to be mediated by a *Plasmodium*-derived protein machinery or "translocon" (Bhattacharjee et al., 2012).

Functional translocation studies directed on the RxLRs motifs of *Phytophthora spp* have been based on recombinant proteins corresponding to tagged-Nterminal halves of RxLR effectors or tagged-full length proteins. First studies showed that the RxLR motif is sufficient to ensure the self-translocation of the fusion protein inside host cells without the need of pathogen-derived machinery, implying that translocation factors are provided by the host (Dou et al., 2008; Whisson et al., 2007). Kale and associates (2010) provided evidence that Nterminal moieties of oomycete RxLR effectors and RxLR-like fungal effectors bind PI(3)P via these motifs and that such binding is necessary for effector entry (Kale et al., 2010). They proposed an internalization model in which binding to PI(3)P present at the surface of the host cell would trigger endocytosis. Effectors would then be in host-derived plasma membrane vesicles and liberated thereafter, localizing freely in host cytoplasm (Kale et al., 2010). But at present, this model has been challenged as the same experiments have not been reproducible by other laboratories (Wawra et al., 2013). Latest studies, indicate that RxLR motifs are not sufficient to such binding and propose also the contribution of Cterminal domains. In addition to the cell entry, Cterminal binding to PI3P would also be required for the stability of the protein and for its virulence activity inside plant cells (Sun et al., 2013;

Yaeno et al., 2011). Such studies have included structural analyses that revealed that, despite the great variability of Cterminal domains between RxLR effectors in the scale of primary sequence, some Ctermini present similar protein folding where positively charged patches may explain their lipid binding properties (Yaeno et al., 2011).

The demonstration of the actual passage of effectors into host cytoplasm during infection has only been brought for fungal effectors like Uf-RTP1p from *U. fabae* and AvrM from *Melampsora lini* thanks to the use of specific antibodies (Kemen et al., 2005; Rafiqi et al., 2010) or by fluorescently tagged effectors expressed by the pathogen like in the case of PWL2, BAS1 and AVR1-CO39 of *M. oryzae* (Khang et al., 2010; Ribot et al., 2013). Deletion analysis of proteins indicates that signals in N-termini are responsible for translocation and that, as for RxLR proteins, the process can also be pathogen-independent (Rafiqi et al., 2010). As mentioned before, well conserved motifs are not apparent, but rather divergent RxLR-like motifs (i.e RRLQ RGFLR...) have been proposed. Structural analyses indicate that, when present, RxLR-like domains are structurally ordered regions which contrasts to the disordered structure of RxLR domains of oomycete effectors. This suggests that they might not be functionally equivalent and/or that both domains use different translocation mechanisms (Ve et al., 2013). Interestingly, in the case of AvrM (proposed as a RxLR-like protein), Nterminal regions necessary for host cell uptake do not bind PI3P (Gan et al., 2010; Ve et al., 2013) thus, it seems that cell uptake does not correlate with lipid binding for fungal effectors.

Once inside the host cell, intracellular effectors can be addressed to neighbor non- infected cells. A cell to cell movement of intracellular effectors has been observed for the PWL2 fungal effector (Khang et al., 2010). Plasmodesmata mediate the viral symplasmic movement (Tilsner et al., 2013) and is also suggested for blast fungal effectors and even the infectious hyphae itself (Kankanala et al., 2007). The trafficking of effectors to adjoining cells is thought to be part of a strategy aimed to prepare host cells for invasion. Various subcellular compartments and structures can be targeted by effectors. Chloroplasts, Golgi and tonoplast endomembranes are targeted by Type 3 effectors of bacteria (Jelenska et al., 2007; Nomura et al., 2011). In addition to these compartments, the plant nucleus is also targeted by intracellular effectors of bacteria, oomycetes (Canonne and Rivas, 2012; Caillaud et al., 2012; Stam et al., 2013b), as well as nematodes (Jaouannet et al., 2012) and fungi (Kemen et al., 2005). These different localizations can be explained by the presence of intrinsic addressing peptide signals (i.e: mitochondrial, plasma membrane, Golgi...). One prominent predictable signal detected in effectors accumulating in plant nuclei is the Nuclear Localization Signal

(NLS), indicating they might co-opt the nuclear trafficking machinery of hosts to access nuclei. This has been actually verified for some since the silencing of plants α -importins uncouples their nuclear accumulation (Kanneganti et al., 2007). The predictability of NLSs during systemic surveys of putative secreted effectors has rendered evident that a considerable number might target the host nucleus. For example, 14 putative effectors of *U. maydis* (Mueller et al., 2008) as well as 15 of the 265 putative effectors of *Heterodera glycines* nematode (Gao et al., 2003) contain NLSs and are, thus, likely to be translocated in nuclei of host cells after secretion. Hence, it seems that manipulation of nuclear functions might be a strategy benefiting pathogen infection.

Function of effectors

Molecular plant-microbe interactions can be seen as interacting networks of biochemical activities. This system biology concept proposed by Pritchard and Birch (2011) postulates that plant networks ensuring a cellular function (i.e, plant defense) are intricate relations of biochemical activities of plant components, each component accomplishing a function in the network. In this context, effectors target plant functions whose alterations lead to a different biochemical behaviour of host's networks and to a beneficial outcome for the pathogen. In such networks, certain functions are important "nodes" or hubs determining the biochemical behaviour of the network. Therefore, it is expected that microbial manipulation strategies converge to the targeting of these hubs.

The plant cell wall (PCW) is one of the first barriers encountered by any microbe tempting to enter plant tissues and represents a source of nutrients given its polysaccharidic nature. It needs to be broken down and/or softened by pathogens in order to establish them in host cells and to progress along host tissues (Cantu et al., 2008; Hématy et al., 2009). A first class of apoplastic effectors is cell-wall degrading enzymes (CWDEs) as pectinases, cellulases, arabinases... (Walton, 1994). Indeed, nematodes, fungi and oomycetes secrete CWDEs in the apoplast whose activities have been shown to be required for complete virulence (Bohlmann and Sobczak, 2014; Feng et al., 2014; Fu et al., 2013). These enzymes have been shown to act early during fungal infection, accompanying the mechanical pressure exerted by appressoria at penetration sites (Cantu et al., 2008), and intervene also all along the colonization of plant tissues macerating PCW to allow further advance of infectious hyphae. Their importance in the migratory stage of juvenile nematodes in plant roots has also been established (Bohlmann and Sobczak, 2014). Oomycetes and fungi display a large diversity of CWDEs (King et al., 2011; O'Connell et al., 2012; Ospina-Giraldo et al., 2010).

Although CWDEs of oomycetes remain globally poorly functionally characterized compared to fungi CDWEs, their cataloguing and studies point to their requirement during infection (Mingora et al., 2014; Zerillo et al., 2013). Fungal CWDEs have been shown to present a chronologically coordinated *in planta* expression. Their activities correlate to the constitution of host cell walls (King et al., 2011; O’Connell et al., 2012), depicting a strategy of adaptation to a specific host plant. For instance, during late stages of infection, *C. higginsianum* (infecting Brassicaceae species) relies on the activity of pectinases while *C. graminicola* (infecting maize) relies on cellulases and hemicellulases. This is consistent with the cell wall composition of their hosts as dicotyledonous present more pectin than monocotyledonous (containing more hemicellulose) (O’Connell et al., 2012). In addition, the broad host range necrotrophic fungi *Botrytis cinerea*, presents a particular endo-arabinase (BcAraA) necessary for its virulence in *A. thaliana* exhibiting a preferential expression in this host rather than in *N. benthamiana* (Nafisi et al., 2014). In the case of phytopathogenic bacteria, which penetrate plant tissues via natural opening (like stomata) or wounds, CWDEs (secreted via the T2SS) mediate the degradation of plant cell-wall carbohydrates and are thought to have, in a general way, a nutrient function (Nivaskumar and Francetic, 2014).

PCW alterations caused by CWDEs and PAMPs, exposed during this close encounter, can be perceived by plants to activate defenses (Hématy et al., 2009). In this context another class of apoplastic effectors is devoted to the manipulation of plant defenses. Best characterized examples in fungi, oomycetes and nematodes, have revealed that manipulation of plant immunity can be based on avoidance or direct suppression of plant defenses (Hewezi and Baum, 2013; Mueller et al., 2013). For instance, avoidance and/or deregulation of plant defenses activated by chitin perception is accomplished by LysM effectors of various fungal species. These effectors are characterized by the presence of LysM carbohydrate-binding domains that bind directly chitin with high affinity, interfering with the binding of chitin to their cognate plant PRR receptors (Kombrink & Thomma, 2013). The LysM Ecp6 from *C. fulvum* masks free chitin-derived fragments preventing their perception by LysM-containing PRR plant receptors. Others, like Avr4 (also from *C. fulvum*) and Mg1LysM from *M. graminicola* have been proposed to protect chitin from degradation by plant chitinases (Kombrink & Thomma, 2013).

Direct suppression of plant defenses can also rely on the inhibition of plant defense factors present in the apoplast and released upon infection. Several apoplastic effectors display protease inhibitory activities on host apoplastic proteases. For instance, the secreted effector Pit2 from *U. maydis* accumulates in the apoplast where it interacts with different

host cysteine proteases inhibiting their activities (Mueller et al., 2013). Effectors Avr2 of the fungus *Cladosporium fulvum* and EPIC1 and EPIC2B from the oomycete *P. infestans* interact with and inhibit the cysteine protease Rcr3 of tomato (Song et al., 2009). This plant protease is also targeted by the nematode effector VAP1 from *G. rostochiensis* (Lozano-Torres et al., 2012). Rcr3 is an example of a plant function targeted by different effectors of distinct pathogens protruding, therefore, as an important plant defense factor and illustrating the concept of hub proposed by Pritchard and Birch (2011). In addition to plant proteases other defense-related plant functions have been revealed as direct targets of effectors. The protein Pep1 of *U. maydis* has been demonstrated to inhibit the activity of the host peroxidase POX12 conducting to reduction of H₂O₂ levels, a strategy of crucial importance for *U. maydis* compatibility in maize (Hemetsberger et al., 2012).

Another class of apoplastic effectors seems to contribute in a different manner by displaying a cytotoxic/cell-killing activity. The Nep1-like protein (NLPs) family is widely distributed in bacteria, fungi and particularly in oomycetes (absent in plants and animals). These proteins induce cell-death, ethylene production and wilting in plants (Gijzen and Nürnberger, 2006). Genetic approaches have demonstrated their contribution to virulence and gene expression studies have shown that in hemibiotrophic fungi and oomycetes their pic of expression coincides with necrotrophic infection stages (Feng and Li, 2013; Gijzen & Nürnberger, 2006). Because of this, they are proposed to be secreted toxins facilitating cell-death required for the necrotrophic infection states. Still, their exact biochemical activities and plant targets remain unknown.

Regarding intracellular effectors, the identification and characterization of them in distinct microbial pathogens has shown that they can be addressed to diverse subcellular compartments.

The plant nucleus as a common field for microbial effectors.

The plant nucleus at the center of plant immunity.

Plant immunity resides on the perception of microorganisms either at the surface of cells (i.e, through plasma membrane receptors) or in the cytosol (i.e, via R proteins) and conducts to the activation of a defense program. Upon pathogen perception, robust changes of gene expression occur (Maleck et al., 2000; Tao et al., 2003). The information necessary for

such transcriptional reprogramming needs to be transduced from the cytosol to the nucleus. The signaling convergence towards the nucleus is mediated by defense integrators/activators and nuclear components whose dynamics are required during microbial infection.

A first aspect of these dynamics concerns the nuclear shuttling of activated R proteins and their signaling complexes, which is necessary for the proper induction of disease resistance (Qi and Innes, 2013). In the absence of pathogen, inactivated R proteins can be associated to the plasma membrane and endomembranes (like RPM1 and RPS4 of *A. thaliana*, respectively) or can display a nucleo-cytoplasmic distribution like the barley MLA10, the tobacco N protein and the *Arabidopsis* SNC1 protein (Caplan et al., 2008; Chang et al., 2013). Following recognition of their corresponding cognate effectors, the activated R protein pools can be detected in the nucleus. This has been seen for RPS4 upon activation by AvrRPS4 of *P. syringae* (Heidrich et al., 2011) and it has been shown that the nuclear levels of MLA10 R protein (recognizing Avr10 from the barley pathogen *Blumeria graminis f. sp. horde*) increase during infection (Chang et al., 2013) which is also the case for the tobacco N protein in the presence of the viral effector p50 (Caplan et al., 2008) and Pb1 from rice infected by *M. oryzae* (Inoue et al., 2013). The depletion of nuclear pools of activated R proteins by forced mislocalization to the cytoplasm uncouples full resistance. The nuclear exclusion of MLA10 conducts to the loss of growth arrest of *B. graminis* (Chang et al., 2013) and is also the case for Pb1mediating blast (*M. oryzae*) resistance (Inoue et al., 2013). Interestingly, it has been observed that the nuclear sequestration of activated RPS4 mediates bacterial growth inhibition without HR while its sequestration in cytosol impairs growth inhibition but not the HR (Heidrich et al., 2011). Because of these different outputs of defenses, it has been proposed that each pool of R proteins activate different signaling pathways and that the establishment of a nucleo-cytoplasmic distribution is imperative for the proper resistance (Qi and Innes, 2013).

In addition to R proteins, other immune-regulators proteins require to shuttle between cytoplasm and nucleus. The general immune regulator of *A. thaliana* ENHANCED DISEASE SUSCEPTIBILITY 1 (EDS1) is one component of various R complexes, able to physically interact with R proteins such as RSP4 and with defense co-regulators PHYTOALEXIN DEFICIENT 4 (PAD4) or Senescence Associated Gene101 (SAG101) to form complexes that localize to the nucleus, necessary for the transcriptional reprogramming of genes and induction of TIR-NB-LRR mediated resistance (García et al., 2010; Heidrich et al., 2011). Another crucial immune component, NPR1 (transcriptional regulator of SA immune signaling) is relocalized from the cytoplasm to the nucleus upon pathogen challenge, where it interacts with TFs of the TGA family (Shearer et al., 2012).

Another aspect of defense transcriptional programs is the involvement of TFs. R proteins can directly bind TFs to mediate gene expression regulations. For instance, MLA10 interacts with TFs of the WARKY (WRK1 and WRK2) and MYB (MYB6) families. Both WRKs are repressors of defense genes while MYB6 was demonstrated to be a positive regulator (Chang et al., 2013). In addition, the rice Pb1 interacts with the WRK45, a positive defense regulator of the SA signaling (Inoue et al., 2013). Moreover, the nuclear-localized N protein of tobacco has recently been shown to directly interact with SPL6, a positive regulator of defense gene expression which has also been suggested to be involved in the nuclear RPS4-mediated defense response (Padmanabhan et al., 2013). As a last example, the TIR-NB-LRR, SNC1 protein delocalizes to the nucleus where it interacts with TPR1 (Zhu et al., 2010). The characterization of one particular R protein, RRS1, has indicated that R proteins may be directly involved in regulation of defense gene expression. RRS1, which participates in AvrRPS4-mediated resistance to *P.syringae* and other pathogens, presents TF properties as it displays, in addition to TIR-NB-LRR domains, a Cterminal WRK domain (Deslandes et al., 2002).

Gene accessibility by the transcriptional machinery is also necessary for the proper induction of disease resistance. Chromatin configuration determines the accessibility of proteins to specific genomic loci. Post-translational modifications (acetylation, deacetylation, methylation ...) of DNA-associated histones proteins, by histone-modifying enzymes (i.e, histone acetyltransferases HAT, histone deacetylases HDA or histone methyltransferase HMT...), mediate chromatin dynamics and are associated to transcription regulation, DNA replication and DNA repair (Kouzarides, 2007). Their involvement in plant developmental processes like seed development and flowering are well documented (Ma et al., 2013) and their implication in plant immunity is beginning to be reported (Berr et al., 2012). For example, the loss of activity of Arabidopsis HDA19 conducts to an increase of SA defense-related genes and enhanced resistance to *P. syringae*. HDA19 interacts with two TFs WRKs that act as transcriptional activators of negative immune-regulator genes. Thus, HDA19 is proposed to regulate negatively plant immunity by impeding the transcriptional activation of negative regulator genes by both WRKs (Berr et al., 2012). In addition, the Arabidopsis HAT, ELP2, influences the expression kinetics of immune regulators EDS1, PAD4, and defense gene PR1 (Wang et al., 2013). Moreover, the HMT SDG8 has been shown to be induced upon infection of necrotrophic fungi *Botrytis cinerea* and *Alternaria brassicicola* and *sdg8* mutants display enhanced sensitivity to these pathogens which correlates with a decrease expression of hormones ET/JA –responsive genes (Berr et

al., 2012).

Consistent with the importance of the nuclear-cytoplasmic shuttling of these complexes for the correct immune gene activation, components of the nuclear trafficking machinery mediating their nuclear entering and accumulation have been identified. The transport of macromolecules across the Nuclear Envelope (NE) is ensured by Nuclear Pore Complexes (NPCs). NPCs are selective molecular “gates” of the NE formed by nucleoporines proteins (Nups). The passage of cargo molecules is ensured by Nuclear Transport Receptors (NTRs) referred to as importins α/β and exportins. NTRs recognize transport signals present in cargo proteins and direct directionality of the transport: importins α/β recognize Nuclear Localization Signals (NLS) while exportins recognize Nuclear Export Signals (NES) (Wirthmueller et al., 2013). Mutation of the *A. thaliana* nucleoporin MOS7 (also known as Nup88) causes an impairment of immunity responses controlled by SNC1 and EDS1 signaling complexes. EDS1 exhibits predicted NLS and NES sequences although their NTRs partners remain unknown. For SNC1 (carrying one predicted NLS and two predicted NES motifs) importin- $\alpha 3$ has been suggested as mediating its import since its loss impairs SNC1 nuclear accumulation and mediated resistance (Wirthmueller et al., 2013). Thus, an orchestrated nucleo-cytoplasmic traffic accompanying signaling of immune integrators is required to the proper activation of immunity during pathogen infection.

Nuclear localized effectors and their activities

Microbial effectors that target nuclear components and associated processes have been identified. Sequence inspection of effector candidates identified via several approaches (transcriptomics, proteomic and genomics) indicates that an important number of effectors are potentially addressed to host nuclei as evidenced by the presence of predicted NLS sequences or nuclear-related putative functions. In the nematode *M. incognita*, 13.5% of the infection secretome (66 proteins over 486) exhibits NLS and putative DNA/RNA binding domains (Bellafiore et al., 2008) and 10% of CSEPs of *B. graminis* are putative ribonuclease-like proteins (Pedersen et al., 2012). In addition, 14 NLS containing proteins (over 441 putative secreted effectors) of *U. maydis* display similarities to domains typical of transcription factors (Mueller et al., 2008).

Nuclear-associated functions and their dynamics during infection are important to support the plant immunity on set. Owing this, it is likely that nuclear functions related to plant defense or to other physiological processes (cell-growth, nutrition...) controlled in the

nucleus, may be subverted by effectors to allow the proper infection and development of pathogens. The biochemical activities of nuclear effectors and their relevance for virulence is better understood for bacterial effectors (for review refer to Bhattacharjee et al., 2013; Rivas and Deslandes, 2013) and are only beginning to be documented for nematodes, phytoplasma, fungi and oomycetes.

Bacterial effectors

Bacterial proteins often present a modular organization in which each module/domain carries a biochemical activity and a function within the whole protein. The execution *in planta* of each activity promotes the virulence function of the effector and can implicate different host targets. Despite that little is known about the spatio-temporal execution of such activities during infection, the fragmentary information gained through studies has evidenced major host processes that bacteria nuclear effectors are able to manipulate. Among these are host transcription, host mRNA metabolism and host proteasome machinery whose modulation can imply different physiological outcomes for the host.

Direct manipulation of host gene transcription is best exemplified by the Transcription Activator-Like Effectors (TALEs) of *Xanthomas spp* and *Ralstonia spp*. This family of Type 3 secreted effectors can account for up to 28 effectors in one single strain (Scholze and Boch, 2011). TALEs are capable to bind promoters of host genes and to activate their transcription. They present a modular architecture comprising a DNA-binding domain (DBD) of 34/35 amino acids repeats (the number of repeats varying), a NLS, and an acidic activation domain at their C-terminus. Direct binding to host DNA is mediated through their DBD domain and the specificity of the targeted DNA sequence is governed by a DBD amino acid/nucleotide code. While DBD specifically binds DNA, the activation domain at the Cterminus acts as an eukaryotic TF recruiting host transcriptional machinery (Scholze & Boch, 2011). AvrBs3 from *Xanthomonas vesicatoria pv. vesicatoria* was the first TALE identified and is the best characterized. In susceptible pepper it induces the expression of UPA20 gene which codes for a TF that is a key regulator of cell enlargement, leading to hypertrophy of mesophyll cells when expressed in *N. benthamiana*, symptoms that are observed during infection (Kay et al., 2007). The identification of other targeted genes indicates that TALEs manipulate directly the sugar metabolism of hosts. Indeed, in rice, the TALE PthXo1 of *Xanthomonas oryzae pv oryza* activates the transcription of the rice gene

osSWEET11/Xa13 which encodes a plasma membrane sugar transporter. Oncoming results indicate that osSWEET genes are common TALE targets; hence, it is thought that TALEs manipulate plant sugar metabolism and cell growth by inducing the release of sugars as well as larger space niches needed for bacteria growth, proliferation and dispersal (Chen et al., 2010). In addition to the direct binding to promoters, TALEs have also been shown to interact with regulators of RNA polymerase II and III. Such plant regulators control the activities of these RNA polymerases and restrict the assembly of factors implicated in the expression of the targeted gene. Therefore, the interaction of TALEs to these regulators perturbs the synthesis small RNAs, tRNA and the ribosome biogenesis. For instance, the TALE PthA4 is able to interact with the citrus protein MAF1 (a negative regulator of RNA pol III). The presence of PthA4 in plant cells coincides with the reduction of MAF1 levels and the development of cell hypertrophy and hyperplasia, symptoms typical of canker disease caused by this bacterium (Soprano et al., 2013).

Besides direct DNA-binding, bacteria effectors control host transcription via direct interaction with host TFs and histones. It is the case of XopD, a modular Type 3 effector of *Xanthomonas campestris pv vesicatoria* shown to repress gene transcription, perturbing the onset of defenses and cell-death. XopD presents an N-terminal DNA-binding domain (DBD) characterized by helix-loop-helix motif, two repeated EAR motifs involved in the transcriptional repression, a C-terminal cysteine protease domain involved in the release of SUMO (small ubiquitin-like modifier) and a NLS motif. Consistent with its modularity, XopD presents various activities in plants. First, XopD interacts through its helix-loop-helix domain with AtMYB30, a positive TF regulator of plant defenses to suppress plant immunity and to promote bacteria growth (Canonne et al., 2011). In addition, its SUMO protease C-terminal domain targets sumoylated proteins of plants to deconjugate SUMO from their substrates (Hotson et al., 2003). Because SUMO substrates include histone-modifying enzymes and histone tails, XopD has been suggested to target chromatin regulators via its SUMO protease activity. One particular observation is that XopD displays a “pointed” localization in host nuclei (said to be related to the targeting of nuclear bodies) and its presence is accompanied by the reorganization of DNA material (Canonne et al., 2011). The capacity to interact with host histones has also been proposed for Pop2 effector from *Ralstonia solanacearum*, based on its acetyltransferase activity in plant nucleus (Tasset et al., 2010).

Another strategy resides on the manipulation of host mRNA status. In this context, the Type 3 secreted HopU1 from *P.syringae* interacts with different host RNA-binding proteins (RBPs). RBPs participate in RNA metabolism (ie, splicing, degradation, translation, export...) by directly binding mRNAs via their RNA recognition motifs (RRM) (Keene,

2007). Among HopU1 targets, the RBP GRP7 was reported to be necessary for PTI activation upon perception of PAMPs flg22 (flagellin) and elf18 (elongation factor) (Fu et al., 2007; Nicaise et al., 2013). GRP7 interacts with FLS2 transcripts and HopU1 interaction with GRP7 correlates with a reduction of FLS2 and EFR protein levels. Hence, by manipulating host RNA metabolism of PRR, HopU1 impedes the accumulation of PAMP receptors proteins necessary for the correct PTI input (Nicaise et al., 2013).

Subversion of host ubiquitin-26S proteasome degradation system (UPS) is another virulence strategy of bacteria. Plant UPS is a multisubunit protein complex present in cytoplasm and in the nucleus that selectively degrades proteins conjugated with ubiquitin (Ub). This process regulates several aspects of plant biology including hormone signaling, and immunity (Vierstra, 2009). Addition of Ub to targeted proteins is performed by three enzymes among, which E3-ligase, ensures target specificity of Ub tails. Different type 3 effectors localizing in host cytoplasm exhibit E3-ligase activities leading to the degradation of virulence targets and suppression of plant defense; for review refer to Duplan and Rivas, 2014. A particular polypeptide secreted by *P. syringae*, SyringolinA, necessary for virulence, localizes both in the nucleus and cytoplasm of host cells inhibiting the activity of the proteasome (Kolodziejek et al., 2011).

Nematode effectors

Endoparasitic root-knot nematodes (RKNs) and cyst nematodes (CNs) are obligate biotroph parasites that enter plant roots and migrate intracellularly to reach host vascular tissues where they become sedentary. In there, they induce tremendous physiological and morphological changes on host root cells that conduct to the formation of feeding cells (FCs): giant cells in the case of RKNs and syncytia in the case of CNs. In both cases, these FCs are physiologically hyperactive as seen by the proliferation of subcellular organelles and secondary vacuoles. FC differentiation and maintenance are triggered by gland-secreted effectors, implying the manipulation of cellular processes like plasma membrane and cell-wall formation (Mitchum et al., 2013). Significant changes occur in host nuclei suggesting important events of plant nuclear biology likely to be triggered by nematode effectors. These include repeated karyogenesis with aborted cell divisions and successive endoreduplication of DNA material that lead to biogenesis of a multitude of nuclei that can enclose several nucleoli (a sign of intensive transcriptional activity) (Mitchum et al., 2013). Several NLS-containing effectors (66 in RKNs and in 15 CNs) and/or presenting nuclear-

related activities (i.e: DNA/RNA binding, chromatin binding and histone domains) have been predicted (Bellafiore et al., 2008; Elling et al., 2007; Gao et al., 2003) and represent candidate effectors possibly controlling directly host-nuclear biology during infection. Important transcriptional changes have been documented to occur in host cells upon nematode infection and have been long time predicted to be controlled by effectors (Hewezi and Baum, 2013) but the exact effector and targeted genes remain unknown.

A recent report has begun to bring light on this, as a nuclear-localized effector 7H08 of *M. incognita* was demonstrated to carry a transcriptional activity in plants (Zhang et al., 2014). Two secreted proteins identified via EST mining on the RKNs infecting tomato *Meloidogyne incognita* (Mi) and *Meloidogyne javanica* (Mj) have been demonstrated to be produced in oesophageal cells, secreted and localized in giant cell nuclei during infection (Jaouannet et al., 2012; Lin et al., 2013). MiEFF1 presents a functional NLS and lacks any similarity to other known proteins. Its accumulation outside the nematode is seen in giant cell during the sedentary phase of infection where it accumulates in nuclei (nucleolus excluded). Like MiEFF1, the Mj-NULG1 harbors a NLS, lacks similarity to other proteins and is nuclear-localized in giant feeding cells of roots cells. Mj-NULG1 is required for complete virulence. Consistent with this, its overexpression in plants increases plant susceptibility to Mj (Lin et al., 2013). MiEFF1 and Mj-NULG1 effector proteins appear as RKN-specific as they are absent in free-living and animal nematodes and homologues are found in various *Meloidogyne spp.* It is suggested that they manipulate a host nuclear function specifically leading to giant cells formation. How exactly both proteins participate in this is still unknown as their biochemical activities and host targets remain to be characterized.

16D10 effector of *Meloidogyne incognita* has been shown to stimulate host root proliferation. Although showed to function in the cytoplasm, it manipulates a nuclear-associated function since it interacts with two SCARECROW-like (SCL) transcription factors (Huang et al., 2006) which are known to mediate cell fate in *Arabidopsis* and are members of the GRAS superfamily of TFs largely involved in plant development (Cui et al., 2014; Hirsch and Oldroyd, 2009).

In the case of CNs, *in planta* transient overexpression of several proteins has revealed that specific subnuclear compartments like nucleoli can be targeted as it is the case for 6E07 from *Heteroderea glycines* (Elling et al., 2007) and Hs-UBI1 from *Heterodera schachtii* (Tytgat et al., 2004). 6E07 lacks similarity to known proteins. In contrast, the Nterminal moiety of HS-UBI1 identifies to Ubiquitin Extension C-terminal Proteins (UBCEPs) while its Cterminal remains particular to this protein. In eukaryotes UBCEPs are hybrid proteins constituted by an N-terminal monomer of ubiquitin followed by a carboxyl-terminal

extension domain. Both are released separately after translational cleavage. Carboxyl-terminal Extension Proteins (CEPs) are constituents of ribosomes and necessary for their biogenesis in the nucleolus and the ubiquitin counterpart acts as a chaperone to mediate this ribosome-related activity (Finley et al., 1989). In the case of plant pathogenic CNs, such type of proteins define a particular class because they are secreted and because their C-terminal do not relate to CEPs (Gao et al., 2003; Tytgat et al., 2004). Because of this latter observation, Hs-UBI1 could intervene in other cellular processes that are regulated in the nucleolus as the cell cycle control (Boisvert et al., 2007). Another ubiquitin extension protein UBCEP12 from the CN *Globodera rostochiensis* has been shown to be cleaved in plant cells; its C-terminal domain is nuclear-cytoplasmic localized and acts as a suppressor of cell-death related to ETI (Chronis et al., 2013).

Phytoplasma effectors

Phytoplasma are obligate phytopathogens bacteria transmitted by insects. In contrast to other phytopathogen bacteria, they present the particularity of colonizing animals (insects from Hemiptera family) and plants. In plant cells, they develop inside the host cytoplasm. About 56 effector candidates have been identified through genome surveys and gene expression profiling indicates they are differentially expressed on hosts, with specific or common repertoires expressed in plants and/or insects (Sugio and Hogenhout, 2012). SAP54 and SAP11 from the Aster Yellow Witches Broom phytoplasma are upregulated during plant infection and are the best functionally characterized. Both effectors display the same mechanism of action by binding to host TFs and triggering their degradation.

SAP11 is a small protein of 90 aa that localizes in nuclei; interacts with and destabilizes class II TCP transcription factors activities. This results in an altered leaf morphogenesis and reduction of hormone levels (Sugio et al., 2014). TCPs are a family of TFs regulating developmental processes including leaf morphogenesis and JA synthesis through the regulation of biosynthetic genes as LOX2. Interestingly, TCPs pop out as common targets of different microbial effectors: the extensive work of Mukhtar and colleagues (2011) identified them as direct targets of RxLR oomycete and bacterial type 3 effectors as well (Mukhtar et al., 2011) and further studies on CRNs (see CRN section) confirm the idea that these TFs are important plant hubs whose corruption determines the outcome is important for host infection.

SAP54 targets several MFTs (MAD-domains transcription factors). Its degradation is

mediated by SAP54's capability to interact with RAD23, a proteasome component that mediates polyubiquitination of plant proteins. Thus, SAP54 induces MTFs degradation via the exploitation of host proteasome. In plants, MTFs are involved in flower determination and development and, consistent with their function, ectopic overexpression of SAP54 leads to leaf-like vegetative flowers which is a common symptom of phytoplasma-infected plants. Such plants were shown to be more attractive to insects, suggesting that SAP54 may contribute to dispersal of phytoplasma by increasing chances of transmission via its insect host (MacLean et al., 2011).

Fungal effectors

Despite the evidence of nuclear localized fungal effectors provided by *in silico* prediction of NLS in putative effectors from different fungal species or by their similarity to nuclear-related functions (i.e: ribonuclease-like effectors of *B. graminis* (Pedersen et al., 2012), very few effectors have been functionally characterized.

The best known nuclear effector is Uf-RTP1 from the obligate biotrophic fungi *Uromyces faba*, which belongs to a family of cysteine protease inhibitors widely present in related species (Pretsch et al., 2013). Uf-RTP1 is specifically expressed in haustoria and was the first effector protein shown to be translocated inside host cell nuclei during infection (Kemen et al., 2005). Electron microscopy has revealed that, secreted to the extra-haustorial matrix, Uf-RTP1 localizes in protuberances that emerge inside host cells to finally distribute in cytoplasm and nucleoplasm of the invaded cell. Its accumulation inside host cells correlates with the blocking of nucleus and chloroplast cyclosis (Kemen et al., 2013), thus, Uf-RTP1 triggers a steady state in infected host cells. It has been proposed that this could inhibit several physiological responses among which the cell-death involving particularly chloroplasts. Moreover, recombinant Uf-RTP1 proteins showed inhibition of proteolytic activity in *Pichia pastoris*, an activity that might serve as protection from secreted host proteases during and after its translocation into host cells. How this activity contributes exactly to virulence is still not known but RTP1 proteins protrude so far as fungal effectors stabilizing host cells during infection.

In addition to effectors from pathogenic fungi, two proteins of symbiotic fungi have been identified as nuclear-addressed in hosts. The secreted MiSSP7 from the ectomycorrhizal fungus *Laccaria bicolor* corresponds to a small protein of 68 aa with no homology to known proteins. Its gene is the most highly induced during early infection of roots of the tree

Populus trichocarpa and is crucial for the establishment of symbiosis. Binding phospholipid assays indicated that MiSSP7 interacts with PI3P requiring a RxLR-like motif (RALG) present within the protein sequence. Moreover, this motif was also necessary for cell entry. Thus it seems that host cell entry mechanisms of MiSSP7 falls into the model proposed by Kale and associates (2010). Its biochemical activity is still unknown, but transcriptome analyses showed that its presence in nuclei modulates expression of 225 host genes involved in root architecture (auxin- response genes, CLE genes) and cell wall remodelling (Plett et al., 2011).

SP7 is a protein of 270 aa secreted by the arbuscular mycorrhizal (AM) fungus *Rhizophagus irregularis*. Consistent with the presence of a NLS sequence, the protein enters plant cells and accumulates in nuclei where it interacts with the TF ER19. ER19 is a member of a TF family known to lead to resistance to pathogen attack that correlates with expression of defense- related genes. In *M. truncatula* gene induction of ER19 and defense-related gene was shown to be highly reduced upon expression of SP7. In addition, an enhancement of symbiosis was observed in *M. truncatula* roots over expressing SP7 and by the silencing of root ER19. Results indicate that SP7 contributes to the establishment of symbiosis by attenuating plant defenses, a common infection strategy of pathogen microbes (Kloppholz et al., 2011).

Oomycete effectors

RxLR effectors

RxLR proteins represent one of the two largest families of intracellular protein effectors of oomycetes together with CRNs. 563 RxLR genes have been identified in *P. infestans* (Haas et al., 2009), 396 in *P. sojae*, 374 in *P. ramorum* and 134 genes in the obligate pathogen *H. parasitica* (Hpa) (Baxter et al., 2010). RxLR are modular proteins, comprising conserved Nterminal domains harbouring a “RxLR” amino acid motif and divergent Cterminal domains. It has been generally accepted that, while Ntermini ensure protein translocation inside host cells (Whisson et al., 2007; Kale et al., 2010), Ctermini carry the virulence activity. As reported previously, this functional dichotomy between both domains seems now blurred as recent data indicate that Ctermini might contribute also to the translocation (Yaeno and Shirasu, 2013).

Transcriptional profiles indicate that RxLRs are mostly expressed during early stages

corresponding to biotrophic phases and decrease during the terminal necrotrophic phases of infection (Pais et al., 2013). Functional high-throughputs of RxLR repertoires based on their *in planta* ectopic transient expression point out for defense-suppressive or susceptibility-inducing activities in plants (Fabro et al., 2011; Wang et al., 2011). The exact molecular mechanisms behind these defense-suppressive functions are beginning to be unraveled for studied RxLRs, although, given their number in species RxLR functions and mode of action remain largely elusive.

A substantial number of RxLRs are targeted to the nucleus. Indeed, expression of 49 *HpaRxLR* effectors in *N. benthamiana* showed that 66% localized in plant nuclei (33% were exclusively nuclear and 33% displayed both cytoplasmic and nuclear localization). Among those exclusively accumulating in nuclei, the majority (68%) were nucleolar localized while others presented particular patterns in the nucleoplasm (i.e: fibre-like structures) (Caillaud et al., 2012). Consistent with their localization, the identification of host interactors of *HpaRxLR* via Y2H screens revealed an overrepresentation of host proteins related to transcriptional regulation (Caillaud et al., 2012). For most of RxLRs studied so far a defense suppression activity has been reported, reason why they stand as a large family of defense suppressor proteins. A recent report on the nuclear localized *HpaRxLR44* showed that, by interacting with the nuclear host MED19 protein (a positive regulator of plant immunity) *HpaRxLR44* induces MED19 degradation in a proteasome-dependent manner. MED19 regulates negatively JA/ET signaling and its degradation by *HpaRxLR44* promotes induction of genes associated with JA/ET signaling pathway (Caillaud et al., 2013). Therefore, *Hpa* attenuates SA-related defense by triggering the antagonistic JA/ET pathway. *HpaRxLR44* is an example of RxLR capability to manipulate plant hormone signaling related to defense.

In *P.infestans*, RxLRs that have been studied display other mechanisms of action. *Avr3a* is a nucleo-cytoplasmic localized effector necessary for virulence and capable to suppress cell death triggered by PAMPs like INF1 in susceptible plants by interacting with the host protein CMPG1 (Bos et al., 2006, 2010). CMPG1 is a E3 ubiquitin ligase whose degradation via the 26S proteasomal complex positively regulates cell-death activated by the perception of PAMPs (Gilroy et al., 2011). *Avr3a* suppress cell-death by stabilizing CMPG1 which is no longer degraded and as a consequence accumulates in the nucleolus (Bos et al., 2010) Transcriptional induction of *Avr3a* during infection correlates with CMPG1's at early stages of infection, indicating that *Avr3a* suppression of PTI via by CMPG1 is important for the proper establishment of biotrophy.

SNE1 RxLR effector also suppresses immune responses but, in contrast to *Avr3a*, SNE1 suppresses cell-death activated by Avr/R recognition of different pathosystems as well

as cell-death induced by necrosis inducing effectors such as (Nep1)-like proteins toxin-like of *P.infestans* and *P.sojae* associated with necrotrophy (Kelley et al., 2010). Thus, SNE1 seems to suppress a different cell-death pathway than that of Avr3a, but the mechanistic behind this suppressive activity are not known.

PITG_03192 (Pi03192) which is essential for virulence of *P.infestans* has been demonstrated to bind two host NAC transcription factors (NTP1 and NTP2). Both NACs are ER membrane bound and are released from ER endomembrane to become nuclear localized upon pathogen perception. PITG_03192 (Pi03192) impedes their nuclear addressing by interacting directly with them (McLellan et al., 2013).

As a last example, a recent *in planta* functional screen on various RxLR proteins, evidenced SFI1 as a suppressor of immunity activated by the PAMP flagellin. SFI1 was shown to contribute to *P. infestans* and to localize in plant nucleus with prevalence for the nucleolus (Zheng et al., 2014).

CRN effectors.

In oomycetes, a second family of intracellular effectors are Crinklers and Necrosis, CRNs, proteins which protrude as a vast nuclear localized effector class and are the object of this PhD study.

Discovery and distribution

CRN proteins were first identified through a large screen of cDNAs of *P. infestans* obtained during infection and coding for secreted proteins (Torto et al., 2003). The study aimed to identify pathogen-secreted proteins potentially implicated in the manipulation of host processes and, thus, presenting an effect in plants. For this purpose, cDNAs were expressed in *N. benthamiana* and tomato leaves to assess any perturbation of host physiology. Two cDNAs induced Crinkling and Necrosis of leaf tissues and defense gene expression and were named proteins CRN1 and CRN2, upon the obtained macroscopic phenotype. Sequence comparison between them and to others sequences available at the time, including EST databases of *Phytophthora spp* (only type of oomycete genomic resources available at the time) revealed that these proteins corresponded to an ample gene family (Torto et al., 2003). It also evidenced the lack of similarity to any other protein, and so, the impossibility to assign a putative function. As full genome data of various oomycetes have been and are currently being obtained, it has been possible to undertake

Table 3. CRN gene number and consensus CRN Nterminal motifs of oomycetes and true fungi.

Species	Gene number	First Nterminal motif	Infectious life style	Reference
<i>A. euteiches</i>	160	LQLYLAL K	Hemibiotroph	Gaulin et al ., in preparation
<i>P. infestans</i>	196	LxLFLAK	Hemibiotroph	Haas et al., 2009
<i>P. capsici</i>	84	LxLFLAK	Hemibiotroph	Stam et al.,2013
<i>P.sojae</i>	100	LxLFLAK	Hemibiotroph	Tyler et al., 2006
<i>P. ramorum</i>	19	LxLFLAK	Hemibiotroph	Tyler et al.,2006
<i>H. arabidopsidis</i>	20		Obligate biotroph	Baxter et al.,2010
<i>P.ultimum</i>	26	LxLYLAR / K	Necrotroph	Lévesque et al., 2010
<i>A.candida</i>	6	LYLAK	Obligate biotroph	Links et al.,2011
<i>A.laibachii</i>	3	ND	Obligate biotroph	Kemen et al.,2011
<i>B.dendrobatidis</i>	84	divergent *	-	Sun et al., 2011
<i>R. irregularis</i>	42	LFLAK	Mutualistic	Lin <i>et al.</i> , 2014

* Consensus motif for a subset of CRN-like sequences : FYIQYLxNQPV and/orLVAA

analyses to identify CRN repertoires and distribution among oomycete species.

CRN genes in oomycetes stand as plant pathogen-specific as they have been identified in all phytopathogens sequenced so far and are missing in zoopathogens species *Saprolegnia parasitica* and *Pythium insidiosum* (Jiang et al., 2013; Krajaejun et al., 2011). Their number varies between species, ranging from 196 in *P. infestans*, 100 in *P. sojae*, 84 in *P. capsici* to 26 in *P. ultimum* and only 3 in *Albugo laibachii* (table 3). In our research group, an EST mining of cDNA libraries evidenced the presence of CRN sequences in *A. euteiches* (Gaulin et al., 2008) and, currently, its genome annotation has revealed 160 CRN gene models (Gaulin et al., *in preparation*). Since *A. euteiches* is an early divergent species among “crown oomycetes”, CRN genes protrude as ancient genes acquired early in the oomycete phytopathogen lineage (Schornack et al., 2010).

Outside the oomycete lineage, CRN-like sequences have been observed in the fungal pathogen *Batrachochytrium dendrobatidis* (Bd) and in the fungal symbiont *Rhizophagus irregularis* (Ri) (Sun et al., 2011; Lin et al., 2014). Bd causes chytridiomycosis in a large array of amphibian species and is responsible for the declines of amphibian population worldwide (Fisher et al., 2012). It can infect over 350 amphibian species and has led to the decline of 200 of them with a mortality reaching 100% for some species (Fisher et al., 2009). It has been estimated that 34.5% of all amphibian species are directly threatened by Bd (Kilpatrick et al., 2010) reason why it has been catalogued as an emerging global ecological threat. The pathogen infects and proliferates in keratinized amphibian skin causing its hyperplasia and hyperkeratosis. Its development on skin tissues (which in amphibians is an important organ regulating water uptake, osmotic balance and respiration) leads to the impairment of neurological functions and heart arrest. Little is known about the genetic base of Bd pathogenesis, but in view of its dangerousness, efforts are being made to understand it. Genome of strains JAM81 and JEL423 have been sequenced and surveyed to propose putative virulence factors (Joneson et al., 2011; Sun et al., 2011). Surprisingly, 84 CRN-like sequences presenting up to 46.5 % of similarity to CRNs of *P. infestans* were identified, exhibiting also a modular architecture, a LxFLAK-derived signal and Cterminal resembling oomycete Cterminal organization. Interestingly, these CRN-like are absent in Bd closest relative, the non-pathogen *Homolaphlyctis polyrhiza*. In Bd they appear under positive selection and are transcriptionally induced when the pathogen is cultured on amphibian skin substrate, observations that sustain the idea of their plausible role in virulence (Sun et al., 2011; Rosenblum et al., 2012). In the case of the arbuscular endomycorrhizal (AM) fungus *R. irregularis*, 42 genes models were predicted with high sequence similarity and canonical amino acid motifs of CRNs (Lin et al., 2014). These latest findings pivot CRN

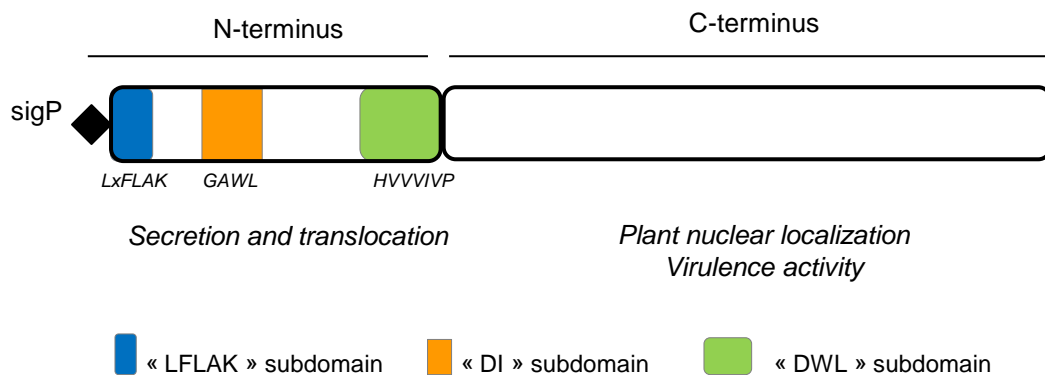


Figure 8 . Sequence and functional architecture of CRN proteins. The typical organization of CRN pre-protein comprises conserved Ntermini were a secretion signal (sigP) is followed the conserved subdomains “LFLAK”, “DI” and “DWL” harboring the conserved amino acid motifs LxFLAK, GAWL and HVVVIVP, respectively. Ntermini mediate secretion and delivery of CRNs to the cytoplasm of host cells. The motif LxFLAK has been shown to be required for this function. Ctermini are responsible for nuclear localization and effects in plant cells. These domains are variable and are composed of the combination of different types of subdomains for which a family categorization has been proposed (figure 8).

conception, which no longer stand as oomycetes-specific proteins nor specific to pathogenic microorganisms.

Protein architecture

At the level of the primary protein sequence, CRN display a modular architecture. A first degree of modularity is reflected by the contrasting degree of conservation between Nterminal and Cterminal moieties. While Nterminal domains are highly conserved among CRN proteins, Cterminal domains are very variable. Both domains are constituted by subdomains characterized by the presence of motifs, defining thus, a second degree of modularity within the protein. In *Phytophthora* CRNs, the conserved Ntermini (< 130aa) comprise the canonical LxFLAK motif (within the first 60aa). Although classical signal peptides (SP) can be predicted in the immature protein sequence, within the first 30 amino acids, around 40% of CRNs do not present a predictable SP for secretion (Haas et al., 2009). The “LxLFLAK” subdomain is followed by a called “DI” domain marked by the presence of conserved GAWL amino acids residues and followed itself by a “DWL” subdomain with a typical HVVVIVP motif denoting the end of the Nterminal moiety (figure 8). Some Ntermini can lack the DI in which case the LxFLAK subdomain is directly followed by the DWL subdomain. The LxFLAK motif (defined for *Phytophthora spp*) can diverge in other species as seen for *P. ultimum* and *A. euteiches* (i.e, LxLALR/K, LQLYLALK respectively) (table 3).

Cterminal domains consist on the juxtaposition of subdomains as well. Their characterization in *P. infestans* by sequence comparison led to propose 36 different conserved subdomains (figure 9) that can assemble in different combinations defining Cterminal subfamilies (Haas et al., 2009). In view of this organization, it has been proposed that the variability of Cterminal domains is the result of recombination events between subdomains. Very recently it was shown that 30 of these subfamilies are present in CRNs of *P.capsici* while 7 new subfamilies (formed by 6 new Cterminal subdomains) appear specific to this species (Stam et al., 2013a). Concerning *A. euteiches*, 160 CRN gene models have been described, among which 12 Cterminal domains are novel subdomains. Hence, *A. euteiches* harbors specific CRN proteins. The presence of CRN specific to certain phytopathogenic oomycete species hints they might manipulate physiological processes/targets specific to hosts and therefore they could define a set of CRNs at the basis of host adaptation. As different *Aphanomyces* species presenting different lifestyles have been sequenced in our research team, other CRN repertoires will be soon available (ANR JCJC APHANO-Effect

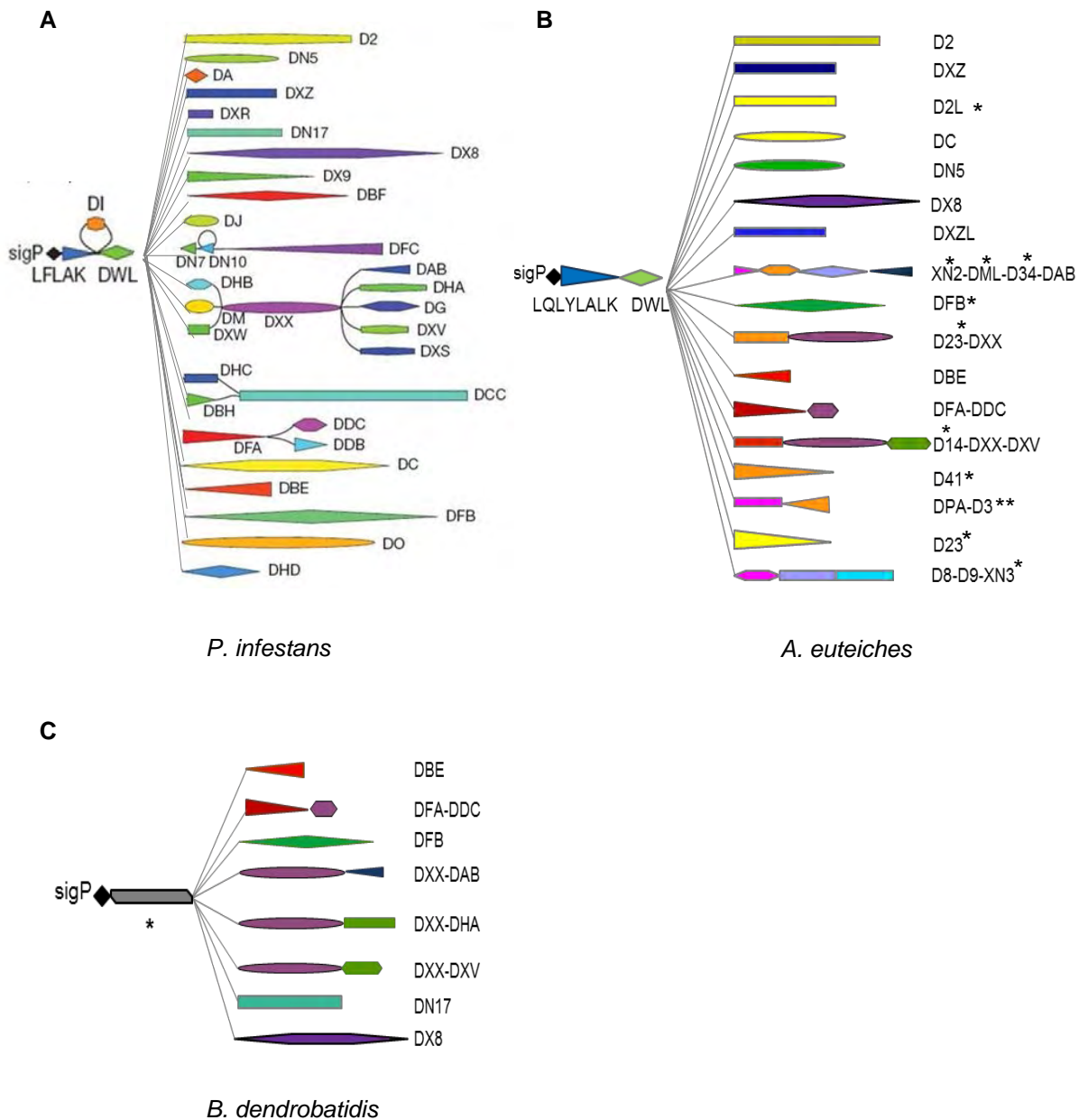


Figure 9. Schemes representing the modular protein architecture of CRNs and Cterminal combinations identified in CRNs of *P. infestans*, *A. euteiches* and *B. dendrobatidis*.

Scheme representation of CRNs of *P. infestans* (A) and *A. euteiches* (B) and *B. dendrobatidis* (C). Ntermini are highly conserved between both species with light variation of the conserved motifs. **A.** In *P. infestans*, 32 different Cterminal subdomains are present in 36 combinations defining 36 families (Haas *et al.*, 2009) **B.** In *A. euteiches*, 27 subdomains have been identified so far, whose combinations define 17 families (Gaulin *et al.*, in preparation). Specific domains to this species are indicated by an asterisk **C.** CRNs of *B. dendrobatidis* present divergent Ntermini compared to oomycete CRNs. Major similarity to oomycete CRNs is displayed in their Ctermini which fall into already identified oomycete CRN families: 12 subdomains ascribing to 8 families (Sun *et al.*, 2010).

2012-2015) and will permit to address CRN occurrence, diversity, evolution-and relevance to lifestyles of Saprolegniale species.

Concerning CRN-like proteins of *Bd*, their Nterminal domains diverge from the typical Nterminal domains of oomycete CRN. Some present a FLAK motif while others display more divergent (FYIQYLxNQPV or LVAA) motifs (Sun et al., 2011). Actually, major similarities to oomycetes CRNs reside on Ctermini which identify to 8 subfamilies (of the 36 subfamilies of CRN proposed for *P. infestans*) (Figure 9). CRN-like proteins of *R.irregularis* display also the canonical LFLAK motif and identify to 22 Cterminal CRN domains of *P. infestans* (Lin et al., 2014).

Translocation into plant cells

The overall sequence modularity of CRN is a featured shared with RxLR proteins and suggested that amino terminal regions in of CRN proteins could act as translocation signal. This hypothesis was tested via an infection-translocation assay (Schornack et al., 2010), summarized in figure 10.

The system was used to fuse full CRN Ntermini of *P. infestans* (CRN16, CRN2 and CRN8) and *A. euteiches* (AeCRN5) to Avr3a Cterminal domain. As chimera proteins induced depletion of *P. capsici* infection, it was concluded that CRN are cytoplasmic effectors whose Ntermini allow secretion and translocation of CRN proteins into host cells. In addition, mutation of conserved LxFLAK and LQLYLAK showed that, within Ntermini, these motifs are signals necessary for translocation function. Importantly, because AeCRN5 and CRN16 lack a predicted signal peptide in the first 30 amino acids, these results demonstrate that a discrete and still unpredictable secretion signal is present in this region and ensure secretion of CRNs in oomycetes (Schornack et al., 2010). Nevertheless, the mechanistics behind the translocation process are not known.

CRN subcellular localization

The use of fluorescent proteins to tag CRNs, followed by microscopy approaches have enabled to study their subcellular localization when ectopically overexpressed in plants, mostly in *N. benthamiana* leaves. Their heterologous expression in this system has shown that all CRN accumulate in nuclei of plant cells (Schornack et al., Stam et al., 2013b). While first localization studies of *P.infestans* CRNs revealed a homogenous nucleoplasm distribution of CRNs that excluded the nucleolus, very recently, CRNs of *P. capsici* were

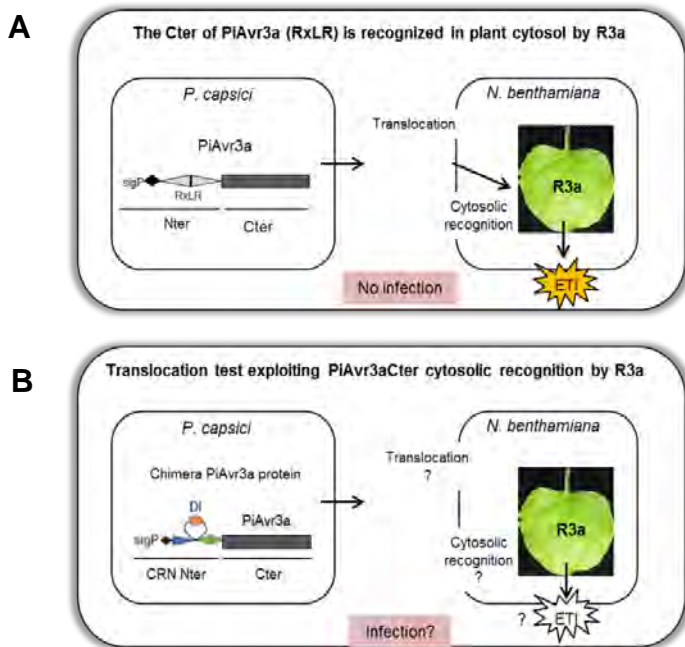


Figure 10. Principle of the Nterminal translocation assay.

The test is based on the recognition of the Cterminal domain of the RxLR Avr3a by the resistance protein R3a which takes place in the cytosol of plant cells and leads to ETI and full depletion of infection. **A.** *P. capsici* expressing PiAvr3a is inoculated on *N. benthamiana* leaves expressing R3a. Absence of infection indicates that PiAvr3a has been recognized by R3a in the cytosol and so that PiAvr3a has entered plant cells. **B.** A Nterminal CRN domain is fused to the Cterminus of Avr3a and expressed in *P. capsici*. After inoculation, the absence or presence of infection determines whether the chimera protein has been translocated into plant cytosol. For Nterminal CRN domains tested, *P.capsici* did not develop on leaves, indicating that there was ETI activation and so that the chimera protein was translocated inside plant cells. Mutation of LFLAK and LQLYLALK residues resulted in infection concluding that this motif is necessary for the translocation function of CRN Ntermini (Schornack et al., 2010). sigP: signal peptide

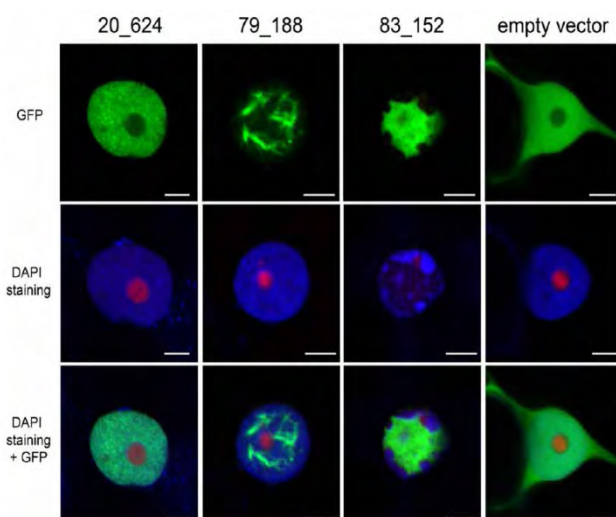


Figure 11. Diverse nuclear localization patterns of three Cterminal domains of CRN of *P. capsici* in epidermal cells of *N. benthamiana*.

Confocal imaging performed on epidermal cells of *N. benthamiana* expressing Cterminal domains of CRN 20_624 (DN17), 79_188 (D2) and 83_152 (DXZ) fused to GFP. GFP alone (empty vector) and CRN localizations are shown in the upper panels and are correlated to DNA by dapi staining (blue) and to the nucleolar marker fibrillin protein (red), in middle and lower panel. Adapted from Stam *et al.*, 2013a/b

seen also in the nucleolus as well as in yet undetermined regions of nuclei. These localizations are denoted by a constricted fluorescence accumulation in areas of the nucleus depicting particular pattern of fluorescence (i.e filament-like, patchy...) that have, in addition, been suggested to be accompanied of a rearrangement of DNA material (Stam et al., 2013a),(figure 11).

Expression of the full matured protein (lacking the signal peptide) or only the Cterminal domain of CRN of *P. capsici* (CRN20_624, categorized in the DN17 family) results in the accumulation of both protein versions in nuclei, indicating that the nuclear localization is ensured by Ctermini and that Ntermini only mediate translocation inside host cells (Schornack et al., 2010; Stam et al., 2013b). For some CRN proteins, their nuclear localization correlates with the presence of predictable NLS in the primary sequence of carboxyl termini. For this CRN-containing NLS, silencing of α -importin in *N. benthamiana* caused a decrease of CRN accumulation in nuclei (Schornack et al., 2010) proving that, by the presence of NLS, CRNs might exploit host routes of nuclear import.

CRN activities

P. infestans CRN are among the highly expressed genes during plant infection with 50% of CRNs corresponding to 10% of the most highly expressed genes (Haas et al., 2009). CRNs of *P. capsici* show differential expressions in tomato leaves and have been assigned into two classes. First class consists of very early up-regulated genes that are down regulated during biotrophic development and finally increasingly expressed during last stages of infection. A second class comprises CRNs whose expression is less variable showing a progressive increase as infection takes place (Stam et al., 2013a). The expression pattern of the first class suggests that CRNs may be required in very different, almost opposite, infection stages (biotrophic and necrotrophic stages) of *P. capsici* infection. Either CRN function is required on both phases or the same CRN could present more than one activity during infection. As mentioned above, most CRN proteins outstand by their scarcity of similarity to known proteins making difficult to assign putative functions.

Upon overexpression on leaves, some CRNs induce necrosis of epidermal cells while others do not. It is important to emphasize that the necrotic effect is not attributable to a specific subfamily of proteins as *in planta* expression of two CRNs of the same category can conduct or not to necrotic lesions. *P. sojae* PsCRN115 and PsCRN63 differ only by 4 amino acids on their carboxyl terminal domains. While PsCRN63 induces cell-death symptoms in *N. benthamiana*, PsCRN115 does not. In fact, PsCRN115 is able to suppress the

necrosis induced by PsCRN6 itself and by the cell-death inducer PsojNIP (Nep1-like protein). Therefore, these opposite activities are very fine tuned at the protein level. A protein deletion approach allowed to determine that the minimum peptide carrying such activities is contained in Ctermini and that the lack of the Nterminal domains does not abolish them (Liu et al., 2011). An immunity suppressive activity has also been reported for PsCRN70 (Rajput et al., 2014). Because it is able to suppress cell-death elicited by different cell-death pathogen-derived molecules as well as different defense responses as the induction of ROS, expression of PR genes and hormone signaling, PsCRN70 stands as a broad defense suppressor effector.

The only biochemical activity predicted is a phosphotransferase/kinase activity, based on the presence of serine/threonine kinases (RD kinases) sites for CRNs containing DBF, SN8 and D2 Cterminal domains. CRN8 (D2), from *P. infestans*, displays an autophosphorylation activity *in vitro* and is phosphorylated *in planta*, which has been shown as necessary to its cell-death activity, thus, relevant for its function (van Damme et al., 2012).

Finally, the transcription factor TCP14 of tomato has been proposed to be targeted by the *P. capsici* CRN12_997 containing Cterminal domains DHB-DXX-DHA (Stam Remco, personal communication). CRN12_997 promotes the degradation of TCP14 preventing its binding to DNA. TCP14 is a member of the TCP family of plant TFs found to be constituents of a plant hub network targeted by bacterial and oomycete effectors (Mukhtar et al., 2011). Because TCP14 seems to be a positive regulator of defenses, CRN12_997 is proposed to contribute to virulence as a suppressor of host gene defense output.

Scope of the thesis

Until today, functional studies have been addressed only on CRNs of *Phytophthora spp* for which elucidation of their function is beginning to be provided. Before the initiation of my PhD work, cDNA libraries of *A. euteiches*, generated in our group, provided first insights into the genetic basis of *A. euteiches* pathogenicity (Gaulin et al., 2008). Mining of ESTs corresponding to 8,000 unigenes from infected and uninfected conditions outlined the absence of RxLR proteins and the presence of CRNs, the first CRN proteins in an oomycete distinct from *Phytophthora spp*. The analysis of AeCRNs ESTs evidenced two major families of AeCRNs with similarities to *P. infestans* CRN13 and CRN5 known at the time (therefore, named AeCRN13 and AeCRN5) and physically represented by full length cDNA clones Ae_9AL5664 and Ae_1AL4462, respectively (Gaulin et al., 2008).

Before the beginning of my work, in September 2010, CRNs were supposed to be intracellular effectors. This was confirmed as the Nterminal domain of AeCRN5 and other *Phytophthora* CRNs were demonstrated to ensure secretion and translocation of these proteins inside plant cells (Schornack et al., 2010). In this context, my work aimed to functionally characterize AeCRN13 and AeCRN5 of the root pathogen *A. euteiches*. During my work, CRN-like proteins were evidenced in the fungal pathogen *B. dendrobatidis*, inferring possible functional commonalities to oomycetal CRNs. This encouraged us to undertake a comparative functional study of AeCRN13 and its putative ortholog BdCRN13, extending CRN functional characterization beyond oomycetes.

The functional study was mainly based on a heterologous ectopic expression of CRNs in order to phenotype the effects and localization of Ctermini expressed directly in host cells. We show that AeCRN5 and AeCRN13 and its ortholog from Bd are host nuclear-localized and cell-death inducing effectors. We demonstrate that AeCRNs target host nucleic acids to perturb host physiology, describing a new mode of action for eukaryotic effectors.

The first chapter of the manuscript presents the characterization of Cterminal activities of AeCRN13 and its ortholog BdCRN13, while the second chapter concerns AeCRN5 characterization.

In the last part of the manuscript, I discuss results that were obtained and contextualize them among latest related findings.

**Chapter 1: Functional
characterization of AeCRN13 of *A.
euteiches* and its ortholog BdCRN13
of *B. dendrobatidis*.**

Chapter 1: Functional characterization of AeCRN13 of *A. euteiches* and its ortholog BdCRN13 of *B. dendrobatidis*.

Since the initial identification of CRN proteins by Torto and associates (2003), CRN cataloguing has greatly been favoured by the arrival of several complete genome sequences of Peronosporales (*P. infestans*, *P. ramorum*, *P. sojae*...) and Saprolegniales (*S. parasitica*, Jiang et al., 2013 and *A. euteiches*, Gaulin et al., unpublished). In oomycetes, CRNs protrude as phytopathogen specific outstanding as a large and diversified protein family with more than 150 genes in one species and a total of 43 different subfamilies. All oomycete CRNs studied so far target host nuclei, but their biochemical activities remain poorly characterized. Today, CRN-like proteins have been described in the unrelated mycorrhizal fungus *Rhizophagus irregularis* (Lin et al., 2014) and the chytrid pathogen fungus *B. dendrobatidis* (Bd) for which experimental evidence suggests they might contribute to its interaction with amphibians (Sun et al., 2011). Still, no functional studies have been addressed for these CRN-like proteins. Intriguingly, these repertoires harbor Cterminal families also present in oomycetes, suggesting common activities in their respective hosts. Given the different nature of interactions and hosts (symbiotic vs pathogenic and animal vs plant) it is urgent to understand their mode of action and, by this, their contribution to each type of interaction. The work presented in this chapter ascribes to this problematic by addressing the functional study of AeCRN13 and BdCRN13, two CRN homologs of *A. euteiches* and *B. dendrobatidis*, respectively.

AeCRN13 (Ae_9AL5664) sequence represents one of the two CRN cDNA families identified through a transcriptomic approach on *A. euteiches* during infection of roots (*M. truncatula*) performed in the group (Gaulin et al 2008). Inspection of its protein sequence by comparison to other *Phytophthora* CRNs showed the presence of a canonical Nterminal domain with a LQLYLALK motif and a HLVVVP motif marking its end. Notably, no signal peptide in this region could be predicted, an observation that is consistent with observations made for other CRNs for which secretion and translocation has been shown (Schornack et al., 2010). The Nterminal of AeCRN13 is similar to the tested translocation signal of AeCRN5, suggesting its functionality. We assumed, then, that AeCRN13 may be translocated during the interaction and is a intracellular/cytoplasmic effector. In this context, we focused our work on the Cterminal region of AeCRN13. Since the *in silico* identification of AeCRN13, a protein family classification was proposed for the variable Cterminal domains of CRN of *P. infestans* by Haas and associates (2009). As a first part

of the functional characterization of AeCRN13 Cterminal domain, we compared it to other Ctermini of CRNs and found that it comprises a DFA domain followed by a DDC domain. Thus, AeCRN13 falls into the DFA-DCC CRN family.

AeCRN13 gene expression and protein accumulation during infection of *M. truncatula* roots (ecotype F83005.5) was studied by qRT-PCR and by the use of anti-AeCRN13 antibodies raised in rabbits against a recombinant Cterminal AeCRN13 protein produced in *E. coli*. We found that AeCRN13 gene is expressed during all times of infection tested (between 3, 6 and 9 days after root inoculation, dpi) (figure 1). Western blot analyses confirmed the presence and accumulation of AeCRN13 protein in infected roots (figure 1 C). Altogether, expression data revealed that AeCRN13 is expressed specifically during infection, that the protein is processed and possibly submitted to post-translational modifications. It remains to be elucidated whether these modifications are intrinsic to AeCRN13 regulation (controlled by the pathogen) or an artefact resulting from the action of plant proteases encountering AeCRN13. Nevertheless, because no supplementary products of degradation, we would tend to privilege the possibility of a processing linked to its function.

We tested the contribution of AeCRN13 to virulence. Because genetic transformation of *A. euteiches* is not possible, we made use of a foliar infection assay combined with agroinfiltration of AeCRN13 in *N. benthamiana*, an assay commonly used for the study of *Phytophthora* CRNs (van Damme et al., 2012; Stam et al., 2013a). For this, 24 hours after agroinfiltration of AeCRN13 in leaves, *P. capsici* zoospores were deposited on agroinfiltration zones and infection lesions were measured 3 and 4 days after inoculation.. These lesions were compared to infection lesions on zones agroinfiltrated with GFP. Results revealed greater size lesions for AeCRN13 zones, indicative of the greater colonization of tissues by *P. capsici*, and led to conclude that AeCRN13 contributes positively to virulence.

CRN-like proteins were identified in *B. dendrobatidis*. We searched for AeCRN13 ortholog (strain JEL423) and found a closest AeCRN13 homolog gene, named BdCRN13 (identified as BDGEG_03200.1) presenting 67 % similarity to AeCRN13. Further sequence inspection of both AeCRN13 and BdCRN13 showed a lack of predictable subcellular localization motifs (including NLS) as well as any similarity to functionally known proteins. Nevertheless, Pfam analysis on one particular region shared between both proteins at the end of the DFA domain, indicated the presence of a HNH-like motif, which is well represented in bacterial endonucleases and DNA binding/cutting factors. Despite the low significance detection via Pfam, we transferred its prediction within the DFA subdomain and hypothesized a possible DNA binding and cutting activities for AeCRN13 and BdCRN13. These putative shared activities encouraged us to undertake a comparative

functional study on both proteins.

The functional characterization of AeCRN13 and BdCRN13 was conducted via the use of heterologous expression systems either on plants (*N. benthamiana* and *M. truncatula*) and/or amphibian (*Xenopus laevis*). To express both proteins in amphibian cells, we used an embryo gene expression system, benefiting of the expertise of the team of Dr. Moreau (Centre de Biologie du Developpment, Toulouse). Both Ctermini were expressed fused to the GFP protein at their Nterminal moiety. In plants, both proteins localized in nuclei and inhibited root development of *M. truncatula* and induced necrotic lesions in leaves of *N. benthamiana* (figure 2 and figure 3). In amphibian cells, AeCRN13 and BdCRN13 conducted to bigger cells possibly caused by the disruption of cell cycle leading to the absence of cell division and to an abnormal development of embryos (figure 4). In plant and amphibian cells, while GFP:AeCRN13Cter presented an accumulation exclusively in the nucleus, GFP:BdCRN13Cter was nucleo-cytoplasmic localized. Mislocalization of GFP:AeCRN13Cter and GFP:BdCRN13Cter from nuclei was accompanied of the absence of cell-death, demonstrating that the nuclear accumulation of both proteins is necessary to the establishment of necrosis (figure 3). To further dissect the activities of CRN13 Cterminal subdomains DFA and DDC, we generated deleted version of AeCRN13 in *N. benthamiana* and tested their activities and localization (figure 5). Results indicated that the integrity of the protein is required for the activities characterized (cell-death and nuclear accumulation) and infer a synergistic implication of all domains.

The necessity of a nuclear presence to exert a necrotic activity, together with the presence a predicted HNH-like motif, led us to test whether AeCRN13 and BdCRN13 interact with nucleic acids. Because we observed that AeCRN13 and BdCRN13 recombinant proteins were able to bind *in vitro* dsDNA (figure 6), we developed a robust *in vivo* assay to test DNA binding activity based on FRET-FLIM technique in *N. benthamiana* epidermal cells. By this means, we demonstrated that AeCRN13 and BdCRN13 Ctermini bind DNA *in vivo* (table 1). Since the recombinant Δ HNH protein was unable to bind dsDNA *in vitro*, we revealed that this motif is functional in mediating DNA binding (figure 6).

As HNH bacterial endonucleases are known to bind and cleave DNA, we hypothesized that AeCRN13 and BdCRN13 might harbor a DNA cutting activity. We indirectly confirmed a DNA cutting activity for AeCRN13Cter and BdCRN13Cter by showing the accumulation of γ H2AX (a marker of DNA damage) on epidermal cells of *N. benthamiana* by western blotting (figure 7). Moreover, we also observed the accumulation of γ H2AX in roots of

M.truncatula infected by *A. euteiches*, which also correlates with the expression of plant DNA damage markers.

These results correspond to the first functional analysis of a CRN protein of *B. dendrobatidis* and of the saprolegniale *A. euteiches*. AeCRN13 and BdCRN13 proteins stand as the first eukaryotic effectors directly targeting host DNA. We showed that both CRN13s (DFA-DDC family) bind DNA and induce its damage, leading to host cell disruption (plant and animal cells). The work shows that sequence similarities support similar activities of homologs CRN proteins, sustaining the idea of shared functions of CRNs in distantly related organisms, and pointing the idea of the targeting of universal cellular functions as likely present in plant and animal cells.

This manuscript was submitted to Plos Pathogens the 10th march 2014. Reviewer's comments were received the 8th may 2014. These concerned (1) the secretion of AeCRN13 during infection: the Nterminal domain of AeCRN13 does not contain a predictable signal peptide for secretion and its function for host-delivery was not tested via the Nterminal translocation domain. Thus, reviewers argued that this must be proven in order for the protein to be considered as an effector and as playing a role during infection (2) the nuclease activity: we hypothesized a nuclease activity that we indirectly showed as happening *in planta* via the evidence of the phosphorylation of H2AX. Reviewers ask to provide the demonstration of a direct cutting activity on DNA. To provide answers to these aspects, at the end of the article manuscript, I present preliminary results concerning the immunolocalization of AeCRN13 in infected roots and results of the *in vitro* nuclease activity on DNA.

1
2
3
4
5
6
7
8
9
10
11
12
13
14
15
16
17
18
19
20
21
22
23
24
25
26
27
28
29
30
31
32
33
34
35
36
37
38
39
40
41
42
43
44
45

CRN13 effectors from plant and animal eukaryotic pathogens are DNA-binding proteins inducing host DNA damage

Diana Ramirez-Garcés, Laurent Camborde, Alain Jauneau, Yves Martinez , Isabelle Néant , Catherine Leclerc, Marc Moreau, Bernard Dumas, Elodie Gaulin

46 **CRN13 effectors from plant and animal eukaryotic pathogens are DNA-binding proteins**
47 **inducing host DNA damage**

48

49 Diana Ramirez-Garcés ^{1,2+}, Laurent Camborde ^{1,2+}, Alain Jauneau ³, Yves Martinez ³, Isabelle
50 Néant ^{4,5}, Catherine Leclerc ^{4,5}, Marc Moreau ^{4,5}, Bernard Dumas ^{1,2}, Elodie Gaulin ^{1,2*}

51

52 Affiliation :

53 ¹Université Toulouse 3, UPS, Laboratoire de Recherche en Sciences Végétales, 24 chemin de
54 Borde Rouge, BP42617, Auzeville, F-31326, Castanet-Tolosan, France

55 ²CNRS, Laboratoire de Recherche en Sciences Végétales, 24 chemin de Borde Rouge,
56 BP42617, Auzeville, F-31326, Castanet-Tolosan, France

57 ³CNRS, Plateforme Imagerie-Microscopie, Fédération de Recherche FR3450, F-31326
58 Castanet-Tolosan, France

59 ⁴Université Toulouse 3, Centre de Biologie du Développement, Toulouse, F31062, France

60 ⁵CNRS UMR5547, Toulouse, F31062, France

61

62 +: DRG and LC : participate equally to this work (co-authors)

63 *: Corresponding author: Dr Elodie Gaulin

64 UMR 5546 CNRS-UPS Pôle de Biotechnologie Végétale

65 24, chemin de Borde Rouge BP 42617 Auzeville

66 31326 Castanet-Tolosan, France

67 Tel.: +33 (0) 5 34 32 38 03 Fax: +33 (0) 5 34 32 38 01

68 e-mail: gaulin@lrsv.ups-tlse.fr

69

70 **Keywords:** CRN, CRN13, effector, Crinklers, Oomycetes, *Aphanomyces*, *Medicago*,
71 *Batrachochytrium*, translocation, DNA-binding, DNA-damage, nucleus, cell death, necrosis,
72 genotoxin, FRET-FLIM, *Xenopus*

73

74 **Short Title:** Genotoxic CRN13 effectors

75

76

77

78 **Abstract**

79

80 Filamentous plant pathogens deliver effectors proteins inside host cells to facilitate host
81 colonization, but the molecular mechanisms by which eukaryotic effectors promote such
82 effect remain largely unknown. One class of secreted oomycetes effectors comprises the
83 modular CRN (Crinkling and Necrosis) large family of proteins that contain a conserved N-
84 terminal domain specifying translocation into host cells and diverse C-terminal regions
85 harboring effector functions. CRNs were thought to be oomycete-specific until recently
86 identified in the genome of the fungus *Batrachochytrium dendrobatidis* (*Bd*), one of the major
87 contributors to the global amphibian decline. The presence of CRNs genes in phylogenetically
88 distant and unrelated eukaryotic pathogens suggested that eukaryotic effectors might display a
89 conserved mode of action during host infection. In the present study, we functionally
90 characterized the CRN13 from the oomycete pathogen of legume roots *Aphanomyces*
91 *euteiches* (*Ae*) and its ortholog from the chytrid pathogen *Bd*. By using model systems in a
92 cross-kingdom approach we detected that both proteins localize in nuclei of plant and
93 amphibian cells triggering cell-death and aberrant cell development. We identify by serial
94 deletion analysis, a conserved HNH-like motif initially found in bacterial endonucleases as
95 essential for this activity. By combining DNA-binding *in vitro* assays with Förster Resonance
96 Energy Transfer (FRET) experiments in tobacco cells we show that both CRN13s interact
97 with DNA. Overexpression of CRN13s induces a phosphorylation of histone H2AX
98 (γ H2AX), a marker of DNA double-strand breaks. Accordingly, we show that infection of *M.*
99 *truncatula* roots by *A. euteiches* induced host DNA damage responses. Overall our results
100 demonstrate for the first time that microbial eukaryotic effectors from phylogenetically distant
101 pathogens, alter host cell physiology through by targeting and cliving DNA.

102 **Author Summary**

103

104 During infection of their host, microbial pathogens deliver effectors proteins that act on plant
105 or animal cells to promote infection. Some of these effectors are translocated inside host cells
106 where they interact with molecular targets to modify host cell physiology to the benefit of the
107 parasite. Genomic surveys point out the existence of a large repertoire of hundreds of effector
108 genes in oomycetes, which are fungal-like microorganisms comprising devastating plant
109 pathogens. Here we focus on the CRN effector family which was firstly reported in
110 phytopathogenic oomycetes and recently identified in the pathogenic fungus of amphibians
111 *Batrachochytrium dendrobatidis*. We show that a CRN effector from both *Aphanomyces*
112 *euteiches*, an oomycete infecting plants and from Bd act inside the nucleus of either plant or
113 animal cells where they trigger abnormal cell development. We show that these CRN are able
114 to bind host DNA inducing DNA damage responses. This work shows that oomycete and
115 fungal pathogens infecting plant or animals are able to produce similar translocated effectors
116 which induce DNA damage responses in the host cells.

117

118 **Introduction**

119

120 In the pursuit of fungi and fungi-like oomycetes eradication, novel tools are in
121 constant demand due to the emergence of new diseases and resistant-parasites or to the lack of
122 effective molecules [1]. Deciphering the dialog between the host and the parasite at the
123 molecular level is a valid approach to provide reliable knowledge. It is well established that
124 upon microbe perception, thanks to the detection of specific molecular patterns exhibited by
125 the microorganism, plants like animals induce innate immune responses to provide a first type
126 of barrier against the intruder [2]. Adapted filamentous eukaryotic pathogens therefore secrete
127 effector molecules that modulate host physiology to benefit the microorganism [3]. Upon the
128 last few years ongoing sequencing of fungal and oomycetes genomes enable bioinformatic
129 prediction of whole effector repertoires of pathogens in ever-increasing numbers [4-8]
130 Intriguingly recent cellular studies show that a significant number of effector proteins from
131 prokaryote and eukaryote microorganisms are targeted to the nucleus of host cells [9].
132 Whereas it has been suggested that effectors may affect nuclear functions through for
133 example a direct activation of host transcription as reported for TAL-bacterial effector [10],
134 the mechanism by which intracellular effectors from filamentous eukaryotic microorganisms
135 interfere with host remains a largely open question.

136 In the field of phytopathology, eukaryotic intracellular effectors were firstly reported
137 in oomycetes. Oomycetes are fungal-like microorganisms, members of the Stramenopiles and
138 closely related to aquatic organisms such as diatoms and brown algae [11,12]. These
139 filamentous microorganisms are responsible for multi-billion dollar damages in agriculture
140 (e.g late blight of potato, *Phytophthora infestans*), in forestry (e.g sudden oak death,
141 *Phytophthora ramorum*) and aquaculture (e.g crayfish plague, *Aphanomyces astaci*) [13,14].
142 Two important groups of candidate host-translocated effector proteins, RxLR and CRN (for
143 crinkling and necrosis) have been revealed by analysis of oomycetes genome sequences. Both

144 RxLR and CRN effector proteins present a modular architecture and include conserved N-
145 termini functioning in host delivery and highly diverse C-terminal domains directing the
146 effector activity. While some *P. sojae* RxLRs are able to suppress cell-death triggered by
147 necrosis inducing factors [15], the precise mechanism behind this is still unknown. Similarly,
148 most of the RxLRs from *Hyaloperonospora arabidopsidis* enhance the growth of
149 *Pseudomonas* by suppressing *Arabidopsis* innate immune responses [16]. Subcellular
150 localization of 49 intracellular effectors candidates from *H. arabidopsidis* revealed that one-
151 third is localized strictly to the host nuclei [17]. Among them, the HaRxLR44 interact with
152 MED19a, a subunit of the *Arabidopsis* Mediator complex [18]. Although the mechanism by
153 which HaRxLR44 induces the degradation of MED19 to promote host susceptibility is still
154 unclear, these data strongly support the concept that nuclear host components manipulation
155 may be an effector mode of action.

156 The RxLRs family of effector is predicted for phytopathogenic species including
157 *Phytophthora* (> 350 genes) [4,19] and *Hyaloperonospora* species (>130 genes) [20], whereas
158 it is absent in *Pythium* [21] and *Aphanomyces* [22]. As one main function of the RxLR
159 effector is to suppress host defense responses [23,24], the lack of RxLR effectors in these
160 latter species indicates that modulation of host physiology may rely on other effector types.
161 The CRN family is ubiquitous in plant pathogenic oomycetes including *Aphanomyces* species
162 and their number ranges from 45 genes for *Pythium sp.* [21] to 200 genes for *P. infestans* [4].
163 All CRNs display a conserved LFLAK N-terminal motif, altered as LYLAK in *Albugo sp.*
164 [25], LxLYLAR/K in *Pythium sp.* [21] and LYLALK in *A. euteiches* [22]. The *Phytophthora*
165 and *Aphanomyces* N-terminal motif has been shown to act as a delivery signal into the
166 cytoplasm of plant cells [26]. Initially reported from *P. infestans* genome mining [4], the CRN
167 C-terminal region is highly diverse and fall into 36 families comprising numerous paralogues.
168 Few new CRNs families have been reported upon complete genome analysis of distinct
169 oomycete species (ie, *Phytophthora capsici*, *Pythium sp.*, *Aphanomyces euteiches*) [4,27,28]

170 suggesting that CRNs belong to an ancient effector family that arose early in oomycete
171 evolution [26]. To shed light on the function of CRNs, transient expression assays on plant
172 leaves using C-termini revealed that not all CRN cause cell death suggesting that the
173 perturbation of host processes may rely on different activities [4,26,27,29-31]. Indeed,
174 PsCRN63 and PsCRN115 from *P. sojae* sharing 95% identity at the amino acid level, display
175 contrasted activities since PsCRN63 triggers cell death *in planta* while PsCRN115 is able to
176 suppress this phenotype [30]. Although the subcellular localization of CRNs from *P. sojae*
177 was not investigated, it was proposed that both PsCRNs share the same plant targets required
178 for cell-death response and that their distinct activities depend on their subcellular localization
179 [32]. Subcellular localization studies of unrelated CRN C-termini from two divergent species
180 (CRN15, CRN8, CRN2 from *P. infestans* and CRN5 from *A. euteiches*) revealed the plant
181 nuclear accumulation of CRNs [31,33]. Similarly, CRN localization studies revealed that *P.*
182 *capsici* CRN C-termini target the plant nucleus and accumulate in specific sub-nuclear
183 compartments [27,29]. Little is known regarding the precise function of CRN, except that the
184 cell-death inducing CRN8 from *P. infestans* displays a functional S/T RD kinase domain at its
185 C-terminus [34] .

186 Up to recently, CRN proteins were reported exclusively in phytopathogenic
187 oomycetes. By looking for putative effectors in the arbuscular endomycorrhizal fungus
188 *Rhizophagus irregularis* genome, 42 LFLAK-containing proteins with *P. infestans* CRNs C-
189 termini similarity have been recently predicted [35], Thus, it is tempting to speculate that such
190 effectors play important roles in the AM symbiosis. The recent completion of the genome
191 sequence of the pathogenic chytrid *Batrachochytrium dendrobatidis* (*Bd*) led also to the
192 identification of a set of 84 CRN genes showing similarity with *P. infestans* CRNs [7,36]. *Bd*
193 is responsible of the recent emergence of an infectious disease on amphibians that is causing
194 the declines of hundreds of species worldwide, threatening the amphibian biodiversity
195 [1,37,38]. *Bd* CRNs presented an increased expression when the fungus is grown on host frog

196 tissues [36,39] and are absent in non-pathogenic chytrids suggesting a role in pathogenicity
197 [36]. Nevertheless, the role of CRNs in *Bd* pathogenicity is still unknown, but their presence
198 in the *Bd* genome is certainly intriguing raising the question of their origin and their role in
199 the emergence of chytridiomycosis.

200 In this study we report on the functional characterization of a CRN family detected in
201 oomycetes and in the fungus *Bd*. We focused our work on the CRN13s, from the root legume
202 pathogen *Aphanomyces euteiches* and its ortholog in *Bd*. We demonstrate that both effectors
203 target nuclei of plant and amphibian cells where they exert cytotoxic effect on plant and
204 animal tissue development. We show that both CRN13s target plant nuclear DNA thanks to
205 the presence of an HNH-like domain found in bacterial endonucleases. We combine *in vitro*
206 assays using recombinant proteins with an *in vivo* FRET-FLIM approach on tobacco cells
207 transiently expressing AeCRN13 or BdCNR13 to demonstrate that both CRN13s are able to
208 bind DNA. We finally show that both CRN13 induce plant DNA-damage responses that are
209 also observed in roots of legumes during infection by *A. euteiches*.

210

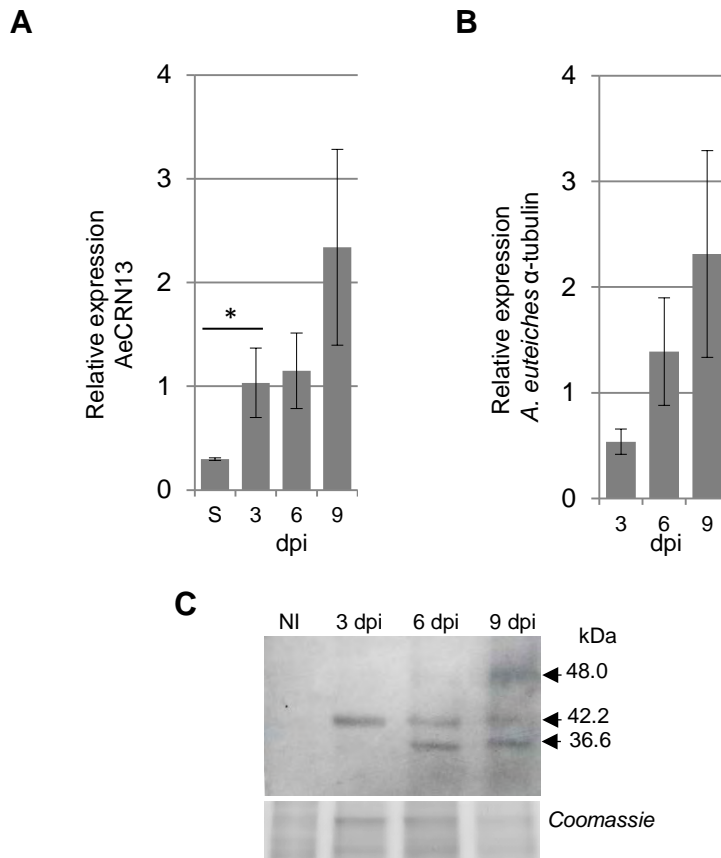


Figure 1. AeCRN13 is expressed during infection of *M. truncatula* roots. (A-B) Graphs show expression level of AeCRN13 (A) and *A. euteiches* α -tubulin (B) measured by qRT-PCR at 3, 6 and 9 days post-inoculation (dpi) in *M. truncatula* roots. S: mycelium grown as saprobe. Error bars are standard deviation errors. Asterisk indicate that the values are significantly different (p -value <0.05 , t-test). (C) Immunoblot using anti-CRN13 antibodies showing the proteolytic cleavage of AeCRN13 (42.2 kDa, 36.6 kDa) from 3 to 9 dpi and the presence of non-processed form (48 kDa) of AeCRN13 at 9 dpi. NI: non-infected.

211 **Results**

212

213 **AeCRN13 is expressed and proteolytically processed during infection of *Medicago***

214 ***truncatula* roots**

215 To investigate the expression of CRN13 from *Aphanomyces euteiches* (AeCRN13)
216 during host infection, we performed qRT-PCR analyses on total RNA extracted from growing
217 saprobe hyphae and infected-*Medicago truncatula* roots. AeCRN13 gene expression was
218 detected during saprophytic development and its expression was induced during infection. Its
219 expression level in roots was similar at early stages of the infection (3 to 6 dpi), whereas an
220 induction was detected from 6 to 9 days post infection (dpi) (Fig. 1A). Induction of
221 AeCRN13 at 9 dpi corresponds to an infection stage where the entire root cortex is colonized
222 by an actively growing mycelium [40,41] as observed by the expression of α -tubulin (Fig. 1B)
223 at 9 dpi.

224 To detect protein accumulation during root infection, specific AeCRN13 antibodies were
225 raised against the C-terminal domain of AeCRN13 (AeCRN13Cter) tagged with MBP
226 (maltose-binding protein) and expressed in *Escherichia coli*. The serum was purified by
227 negative adsorption using an unrelated MBP-tagged protein to remove anti-MBP antibodies.
228 At 3 dpi a 42 kDa band was detected while the predicted size of AeCRN13 is 50.1 kDa (Fig.
229 1C), suggesting a putative cleavage of a 8kDa fragment. At later stages (6 and 9 dpi) a
230 supplementary band of 36.6 kDa corresponding to the predicted size of the C-terminal domain
231 of AeCRN13 was observed, while a 48 kDa form corresponding to the predicted size of
232 AeCRN13 was detected at 9 dpi. These experiments revealed the existence of a putative two-
233 stage proteolytic processing of AeCRN13 during *M. truncatula* infection.

234

235

236

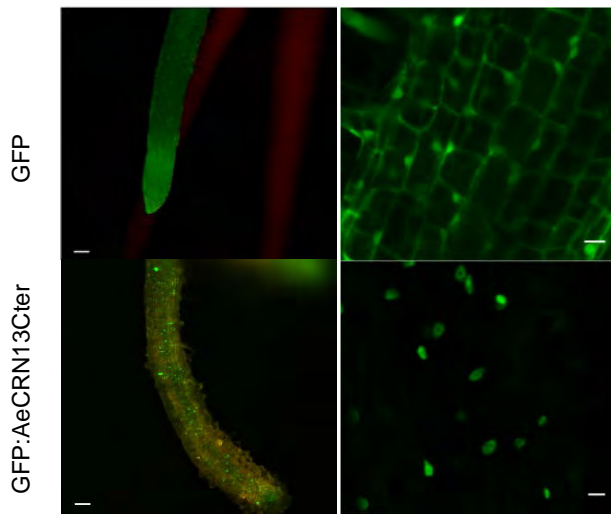
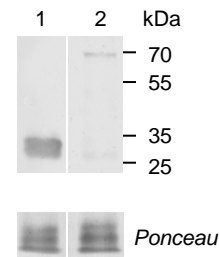
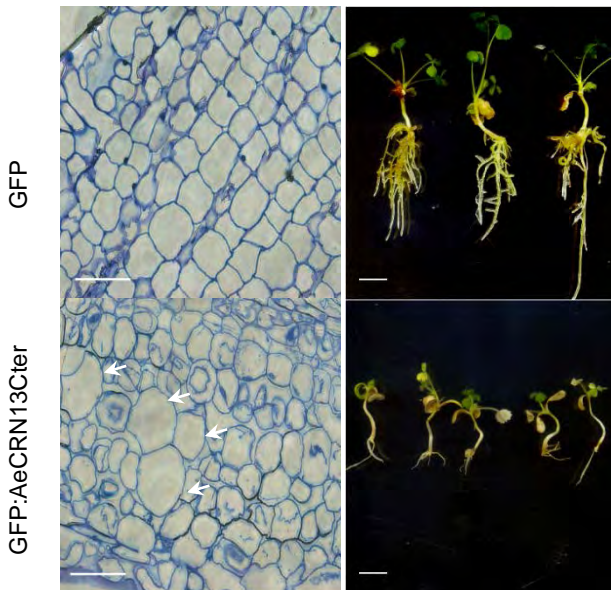
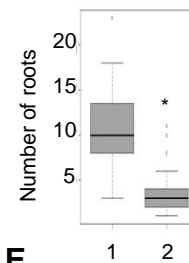
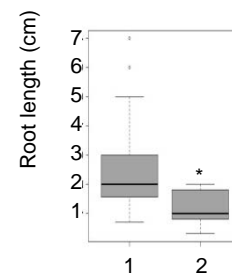
A**C****B****D****E**

Figure 2. AeCRN13 accumulates in host cell nuclei where it triggers cell size growth and inhibits root development.

(A) *M. truncatula* plantlets were transformed with *A. rhizogenes* to express in roots GFP and GFP:AeCRN13Cter constructs under the control of the cauliflower mosaic virus 35S promoter. At 13 days after *A. rhizogenes* transformation, epifluorescence large-field imaging of transformed roots (Left panel, scale bar: 100µm) and confocal images (Right panel, scale bar: 15 µm) reveal the preferential localization of AeCRN13Cter in host nuclei. (B). Micrographs of *M. truncatula* longitudinal cuts of 13 day-old transformed roots indicate that AeCRN13Cter causes a disorganization of root cells and the formation over-sized cells pointed by white arrows (Left panels, Scale bars: 20µm) as compared to GFP expressing roots. Entire 30 day-old composite plants expressing AeCRN13Cter presented a reduction in root and aerial development (Right panels, Scale bar: 1 cm) (C) Proteins extracts prepared from 30 day-old roots and used for immunoblot (anti-GFP antibody) showed the presence of the GFP (lane 1) and the GFP:AeCRN13Cter (lane 2) proteins as expected size (D-E) Box plot graphics depicting the decrease in the average number of roots per plant (D) and lengths of root systems (E) of 30 day-old composite plants expressing the GFP:AeCRN13Cter construct. 59 GFP-plants (1) and 29 GFP:AeCRN13Cter plants (2) were used for measurements and statistics (* p-value<0.05, t-test).

237 Nuclear localization of AeCRN13 worries legume and tobacco cells

238 To substantiate a role for AeCRN13 during host infection we transformed *M.*
239 *truncatula* roots with the C-terminal domain of the protein consisting of amino acid residues
240 from 106 to 423. *Agrobacterium rhizogenes* was used to express a GFP-tagged
241 *35S:AeCRN13Cter* construct into *M. truncatula* roots. Confocal imaging revealed dots of GFP
242 fluorescence in AeCRN13 expressing roots 13 days after transformation, while a
243 homogeneous fluorescence along the root tip was detected in the GFP-control samples (Fig.
244 2A). A higher magnification revealed that the AeCRN13Cter protein localized into the nuclei
245 of *M. truncatula* root cells as compared to the GFP-transformed roots in which fluorescence
246 was detected equally in cytoplasm and nuclei. Within two weeks, enlargement of *M.*
247 *truncatula* cell size was observed upon expression of AeCRN13 (Fig. 2B, left panel) and a
248 large number of the plantlets collapsed without generating new roots, in contrast to control
249 plants. Within three weeks, we noticed a reduction of the development of aerial and root
250 systems (Fig. 2B, right panel). The production of AeCRN13Cter in transformed roots was
251 confirmed by immunoblot and a ~69 kDa band was observed corresponding to the predicted
252 size of the GFP:AeCRN13Cter fusion protein (Fig. 2B). Quantification of the number and
253 length of new generated roots showed that about 10 roots were generated 30 days post-
254 transformation by control plants with a mean length of 2 cm (n=59), whereas less than 1 root
255 with a length lower than 1 cm is statistically observed in *35S:GFP-AeCRN13Cter* composite
256 plants (n=29) (Fig. 2C). Collectively, these results indicate that the C-terminal region of
257 AeCRN13, although devoid of a predicted Nuclear Localization Signal (NLS), is addressed to
258 the nuclei of *Medicago* root cells where it has an inhibitory effect on roots development.

259 When expressed in leaf tissues of *N. benthamiana*, AeCRN13 induced necrosis at 5
260 days post inoculation (Fig. 3A). Confocal imaging of infiltrated area at 24 hpi, revealed an
261 exclusive nuclear localization of GFP:AeCRN13Cter. The observed nuclear localization of the
262 protein contrasted with the GFP control, which was detected equally in the cytosol and the

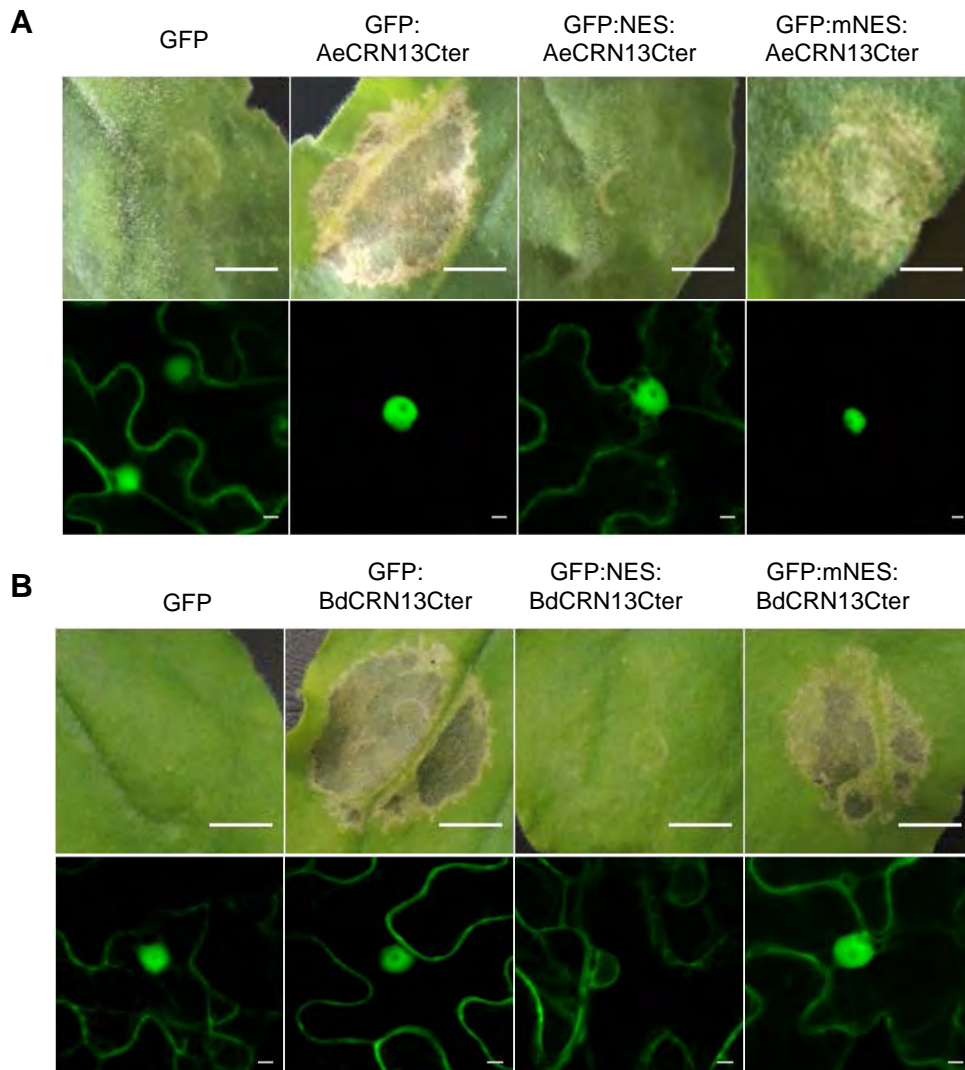


Figure 3. AeCRN13 and BdCRN13 have a cell-death nuclear-dependent activity in *N. benthamiana*

(A). Cell death symptoms are observed 5 days after *Agrobacterium*-transient expression of AeCRN13Cter in *N. benthamiana* leaves. Confocal imaging 24h after treatment show a nuclear-localization of AeCRN13Cter. The abolishment of necrosis was obtained by the addition of a Nuclear-Export Signal (NES) to the GFP:AeCRN13Cter construct and is correlated to the preferential localization of the fusion protein in the cytoplasm. Necrotic symptoms and nuclear localization of AeCRN13Cter were restored when a non-functional mutated version of NES (mNES) was used. Upper panels, scale bars: 0.5 cm. Lower panels, scale bars: 5µm. (B) Cell death symptoms are also observed 5 days after *Agrobacterium*-transient expression of BdCRN13Cter in *N. benthamiana*. Subcellular localization of the fusion protein at 24h by confocal imaging reveals a preferential nuclear localization of the effector. Macroscopic symptoms on tobacco leaves are abolished when the fusion protein is preferentially addressed to the cytoplasm thanks to the addition of a NES sequence. The GFP:mNES:BdCRN13Cter protein harboring a non-functional NES sequence, is preferentially located in the nucleus and trigger necrotic symptoms on leaves. Upper panels, scale bar: 0.5 cm. Lower panels, scale bar: 5µm.

263 nucleus (Fig. 3A). To go further and to estimate the importance of nuclear localization in
264 triggering necrosis, we fused the full C-terminal domain of AeCRN13 to a nuclear export
265 signal (NES) or its mutated (mNES) counterpart. The constructs were agroinfiltrated in *N.*
266 *benthamiana* leaves. No symptoms were observed on treated leaves even at longer time (>10
267 days) when a NES was fused to the construct. Confocal imaging revealed the enhancement of
268 nuclear export of AeCRN13Cter protein since the GFP signal was recovered mostly in the
269 cytoplasm (Fig. 3A). Immunoblot analysis confirmed the accumulation and stability of the
270 corresponding proteins from 1 to 3 days post inoculation (Fig. S1A). By contrast the addition
271 of a mutated (inactive) NES domain restored the nuclear accumulation of the C-terminus of
272 AeCRN13, as inferred by confocal observations, as well as its cell death effect. Taken
273 together, these results show that nuclear localization is required for AeCRN13 to trigger
274 necrosis in *N. benthamiana*.

275

276 **BdCRN13 is nuclear-localized and induces necrosis in tobacco cells**

277 Orthologous genes to AeCRN13 were recently reported in the amphibian pathogen *B.*
278 *dendrobatidis* raising the intriguing question of the origin of these sequences in a distantly
279 related fungus and their role in animal pathogenesis [7]. A *BdCRN13* sequence was amplified
280 from the *Bd* genome (strain JEL 423) and transiently expressed as a GFP fusion protein in *N.*
281 *benthamiana*. As observed with AeCRN13Cter, cell-death was detected 5 days after
282 agroinfiltration (Fig. 3B), indicating that cell-death inducing activity is conserved among
283 oomycete and chytrid CRN13 C-terminal domains. Subcellular localization assay shows that
284 GFP fluorescence of BdCRN13 is mostly detected in the nuclei of epidermal cells (Fig. 3B).
285 To correlate this preferential nuclear localization with BdCRN13 activity, we fused the full C-
286 terminal domain of the effector to a nuclear export signal (NES) or its mutated counterpart
287 (mNES). No symptoms were observed on agroinfiltrated leaves even at longer times (>10
288 days) with the NES construct, in contrast to areas treated with the mNES construct (Fig. 3B).

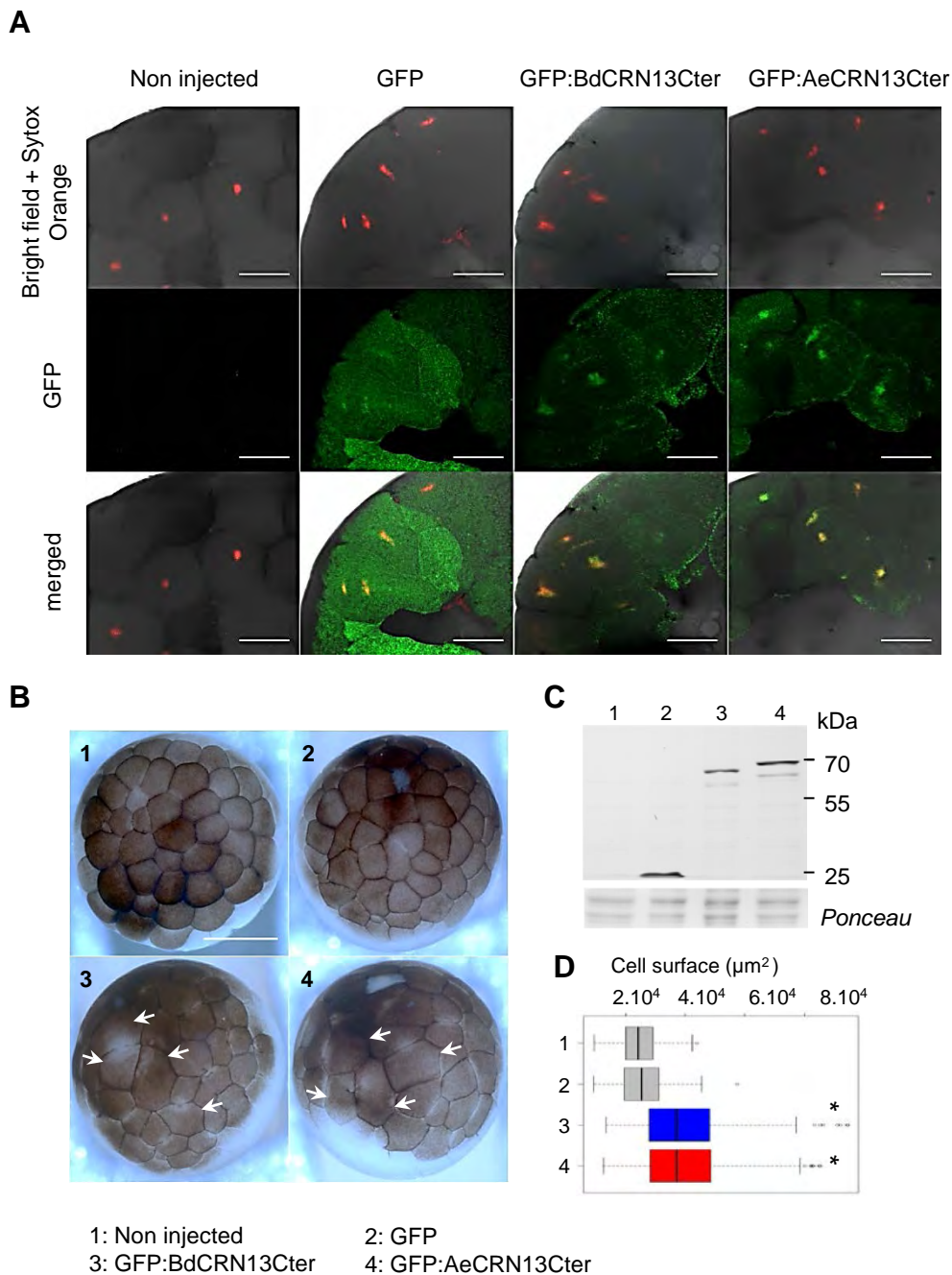


Figure 4. BdCRN13Cter and AeCRN13Cter are nuclear localized in *Xenopus laevis* and affect embryos development.

(A) Confocal images of hemisections of embryos fixed at stage 7 and stained with SytoxOrange, show nuclear localization of GFP:BdCRN13Cter and GFP:AeCRN13Cter fusion proteins. Upper panel: overlay of bright field and SytoxOrange fluorescence, middle panel: GFP fluorescence, lower panel: merged signals. Scale bar: 100µm. (B) Bright field images of stage 7 embryos. Delay in cell division evidenced by larger cell size (arrows) is observed in embryos injected with GFP:BdCRN13Cter or GFP:AeCRN13Cter mRNA. Scale bars: 500µm. (C) Immunoblot performed with anti-GFP antibodies show the stability of the different fusion proteins in *Xenopus* embryos. (D) Measurements of the cell surface of stage 7 embryo (n=30 embryos/condition). Statistical analyses reveal the larger size of the animal blastomeres from embryos injected with GFP:BdCRN13Cter or GFP:AeCRN13Cter mRNAs (* indicates a statistical difference between cell surface means of Non injected and GFP injected controls and either AeCRN13Cter or BdCRN13Cter injected embryos; p-value<0.05). 1: non injected, 2: GFP, 3: GFP:BdCRN13Cter, 4: GFP:AeCRN13Cter.

289 Immunoblots confirmed the accumulation of the corresponding fusion protein (Fig. S1B).
290 This suggests that necrotic activity of BdCRN13 is induced by its presence in the plant
291 nucleus, despite not having the same nuclear accumulation pattern as AeCRN13. Together
292 these data strongly support the view that C-termini domain of CRN13s from plant and animal
293 pathogens display a conserved mode of action.

294

295 **Expression of BdCRN13 and AeCRN13 in *Xenopus laevis* embryo triggers aberrant** 296 **development**

297 Based on the conserved effect of the C-ter domain of *Ae* and *Bd* CRN13 in plants, we
298 tested whether they both have the same activity in amphibian cells. We benefited from the
299 African clawed frog *Xenopus laevis* embryos expression assay. *Xenopus* embryos undergo
300 time-regulated synchronized cell divisions during the first 3 hours of development and
301 therefore are a useful *in vivo* model system for studying cell division. *GFP:BdCRN13Cter* and
302 *GFP:AeCRN13Cter* constructs were cloned into the pCS2 vector and *in vitro* transcribed.
303 GFP control mRNA was obtained from pCS2-GFP vector. To test the function of both CRNs,
304 one cell of a 2-cell stage embryos were microinjected with either *GFP*, *GFP:BdCRN13Cter* or
305 *GFP:AeCRN13Cter* mRNAs and effect on cell divisions observed at blastula stages.
306 Subcellular localization of the GFP-tagged proteins was conducted on hemisections of
307 injected embryos after staining of nucleic material with Sytox-Orange dye. Cells expressing
308 the GFP alone displayed fluorescence preferentially in the cytoplasm, whereas a green
309 fluorescent signal was also found to co-localized with the red fluorescence of Sytox-Orange
310 for the *GFP:BdCRN13Cter* or *GFP:AeCRN13Cter* constructs (Fig. 4A), showing that both
311 proteins were nuclear localized in *Xenopus* embryos. The pattern of cell division of GFP-
312 injected embryos behaved similarly to the uninjected embryos pattern, where blastomeres
313 dividing normally gave smaller blastomeres at each round of division, leading to a typical
314 stage 7 blastula (4 h post fertilization) as described in the normal table of *Xenopus laevis* [42]

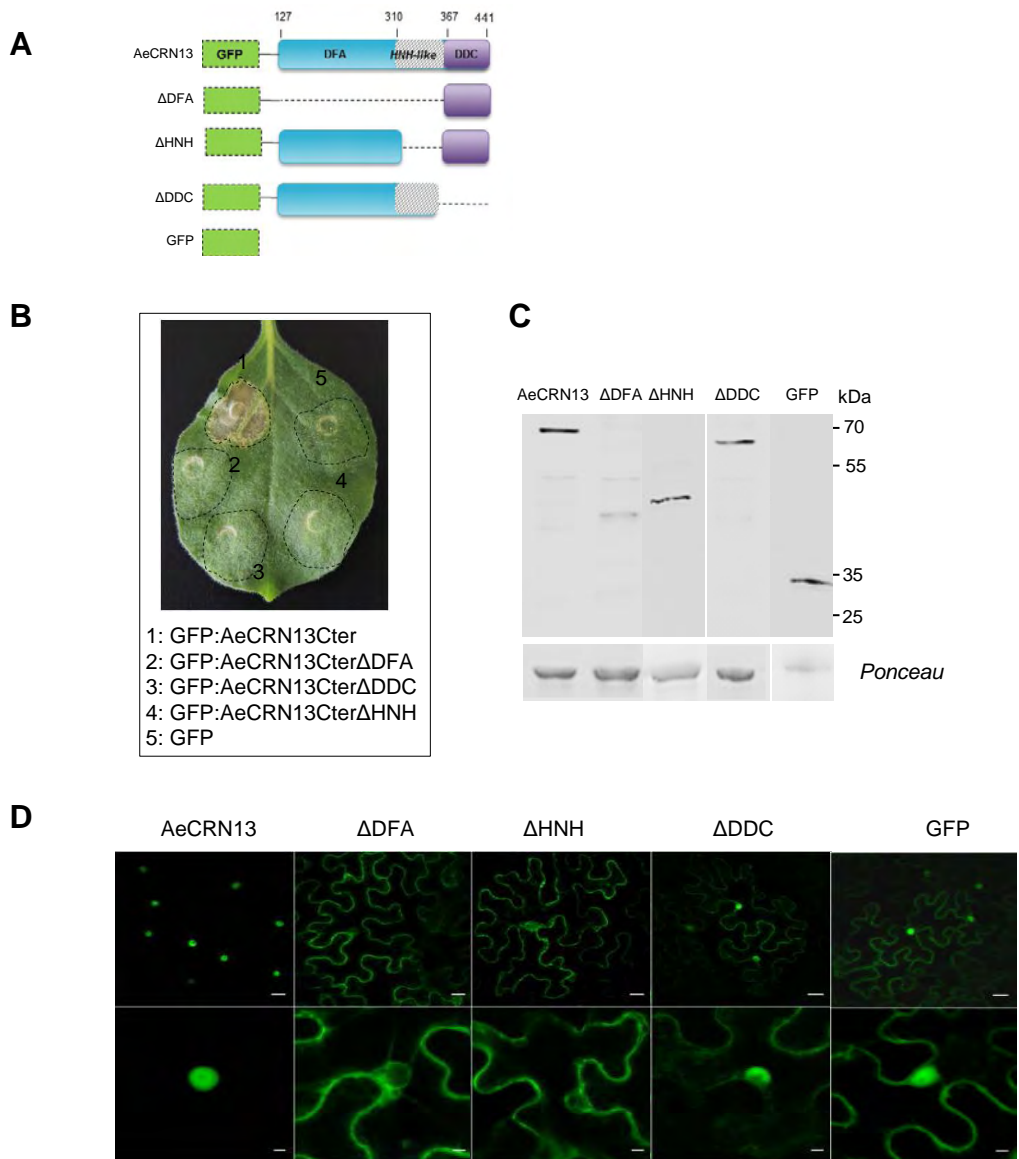


Figure 5. AeCRN13Cter nuclear localization requires a HNH-like motif in association with DFA and DDC subdomains.

(A) Schematic representation of GFP-tagged C-terminal deletions of AeCRN13 under the control of 35S promoter expressed with *A. tumefaciens* in *N. benthamiana* leaves. (B) A typical infiltrated leaf observed at 5 days post inoculation shows cell-death symptom only in the area treated with the full length version of AeCRN13Cter. (C) Western blot analysis using anti-GFP antibody reveals the accumulation of GFP:AeCRN13Cter (69,5kDa, lane 1), GFP:AeCRN13CterΔDFA (39,3kDa, lane 2), GFP:AeCRN13CterΔDDC (46,7 kDa, lane 3) and GFP:AeCRN13CterΔHNH (57,7kDa, lane4) fusion proteins 24 hours after agroinfiltration. (D) Confocal images of epidermal cells showing the exclusive nuclear localization of the full length version of AeCRN13Cter, while the DDC-mutated version presented a nucleocytoplasmic localization and the DFA-affected versions are preferentially detected in the cytoplasm (i.e deletion of DFA subdomain or deletion of the HNH-like motif). 1: AeCRN13Cter full length, 2: GFP:AeCRN13CterΔDFA, 3: GFP:AeCRN13CterΔDDC, 4: GFP:AeCRN13CterΔHNH. Upper panels: GFP fluorescence in several cells of a leaf zone. Scale bars: 20 μ m. Lower panels: focus on one representative cell. Scale bars: 5 μ m.

315 (Fig. 4B). In contrast, a cell division delay was observed in *GFP:BdCRN13Cter* or
316 *GFP:AeCRN13Cter* mRNA-injected embryos leading at stage 7 to an accumulation of
317 abnormally large blastomeres (Fig. 4B, lower panel). On later stages, most of these abnormal
318 blastomeres kept developmental delay where cell divisions were not achieved, leading to
319 larger or giant cells (Fig. S2). Evaluation of the average cell surface in injected embryos
320 (n=30 embryos) showed that for *GFP:BdCRN13Cter* or *GFP:AeCRN13Cter* mRNA-injected
321 embryos, cells were statistically larger than the non-injected or GFP-injected embryo cells
322 (Fig. 4D). This result suggests that CRN13 accumulation interfere with cell divisions leading
323 to a progressive accumulation of undivided and larger blastomeres.

324

325 **A conserved HNH-like motif is required for nuclear localization of AeCRN13**

326 A functional domain search on C-ter of BdCRN13 and AeCRN13 using the PFAM
327 database revealed a weak match with a HNH motif (PF13391), hereafter designed as HNH-
328 like motif. Initially found in bacterial proteins, this motif corresponds to a small nucleic acid
329 binding and cleavage module widespread in metal finger endonucleases in all life kingdoms
330 [43]. In CRN13s from *A. euteiches*, *Phytophthora* sp. and *Bd* the HNH-like motif is localized
331 in a highly conserved region at the C-ter of the DFA subdomain (Fig. S3). In order to define
332 whether this motif plays a role in CRN13 function, DFA, DDC and HNH-like deletion
333 mutants of AeCRN13Cter were generated (Fig. 5A) and tested by transient expression in *N.*
334 *benthamiana* leaves. None of the mutants were able to trigger cell death (10 dpi, Fig. 5B).
335 Specific bands corresponding to the expected protein sizes were detected in all samples
336 indicating the stability of the different fusion proteins, although we noticed a weaker
337 accumulation of the DFA deleted version of AeCRN13Cter (Fig. 5C, lane 2). Removal of the
338 DFA domain encompassing the HNH-like motif led to a GFP signal detected exclusively in
339 the cytoplasm indicating that nuclear import and retention of the protein in the nucleus was
340 impaired. In contrast GFP:AeCRN13Cter Δ DDC fusion protein, displayed a nucleo-

Table 1. FRET-FLIM measurements showing that AeCRN13Cter and BdCRN13Cter interact with nuclear DNA *in planta*

Donor	Acceptor	τ ^(a)	sem ^(b)	N ^(c)	E ^(d)	^(e) p-value
GFP	-	2.246	0.036	20	-	-
GFP	Sytox Orange	2.210	0.044	18	1.6	0,52
GFP-H2B	-	2.465	0,017	40	-	-
GFP-H2B	Sytox Orange	1.852	0.047	43	24.8	2,31E-19
GFP-AeCRN13Cter	-	2.154	0.024	36	-	-
GFP-AeCRN13Cter	Sytox Orange	1.655	0.048	35	23	9,58E-14
GFP-AeCRN13Cter	Sytox Orange (RNase treatment)	1.749	0.033	32	19	8,25E-15
GFP-BdCRN13Cter	-	2.196	0.048	37	-	-
GFP-BdCRN13Cter	Sytox Orange	1.915	0.037	30	12.8	3,26E-05
GFP-BdCRN13Cter	Sytox Orange (RNase treatment)	1.963	0.041	32	10.6	5,50E-04

τ : mean lifetime in nanoseconds (ns). For each nucleus, average fluorescence decay profiles were plotted and lifetimes were estimated by fitting data with exponential function using a non-linear least-squares estimation procedure. ^(b) s.e.m.: standard error of the mean. ^(c) N: total number of measured nuclei. ^(d) E: FRET efficiency in % : $E=1-(t_{DA}/t_D)$. ^(e) p-value (Student's *t* test) of the difference between the donor lifetimes in the presence or absence of acceptor.

341 cytoplasmic localization similar to the GFP control (Fig. 5D) thus, DFA full domain enters the
342 nucleus but does not maintained in it. The GFP-AeCRN13Cter Δ HNH was also localized
343 exclusively in the cytoplasm. These results suggest that the HNH-like motif and the DDC
344 domain are likely required for AeCRN13 nuclear localization.

345

346 **AeCRN13 and BdCRN13 bind DNA *in vitro* and *in planta***

347 The identification of the HNH-like motif and the requirement of this sequence for
348 CRN13s nuclear localization prompted us to check whether these proteins could interact with
349 DNA. Protein variants were produced in *E. coli* and purified to perform *in vitro* double-strand
350 DNA binding assays. The C-ter domains of AeCRN13 and BdCRN13, but not AeCRN13
351 deleted of the HNH-like motif, bound to dsDNA-beads (Fig. 6). To confirm that interaction
352 between CRN13 C-ter and dsDNA occurs *in vivo*, we set up a fluorescence resonance energy
353 transfer (FRET) assay coupled with fluorescence lifetime imaging microscopy (FLIM) in *N.*
354 *benthamiana* cells. GFP-tagged Cter domains of both CRN13s were transiently expressed in
355 *N. benthamiana* epidermal cells by agroinfiltration and plant nucleic acids were stained with
356 SytoxOrange. SytoxOrange in combination with GFP is suitable for FRET-FLIM due to
357 considerable overlap of the acceptor absorption and donor emission spectra [44]. The
358 occurrence of FRET, causing the fluorescence lifetime of the donor GFP to decrease in these
359 conditions, would only be due to the proximity (less than 10 nm) of GFP to SytoxOrange.
360 Energy transfer was detected by fluorescence lifetime imaging microscopy (FLIM). As a
361 positive DNA-binding and FRET control between GFP and Sytox Orange we used *N.*
362 *benthamiana* leaves expressing a GFP-tagged histone H2B (GFP-H2B) construct. As shown
363 in table 1 the average fluorescence lifetime of GFP and SytoxOrange was 2.20 nsec. In the
364 absence of SytoxOrange the lifetime of GFP:H2B is 2.4651 ± 0.017 nsec whereas its lifetime
365 decreased to 1.852 ± 0.047 4 nsec in the presence of the dye, indicating that FRET occurred as
366 expected from the binding of the histone H2B to nucleic acid. Regarding AeCRN13Cter

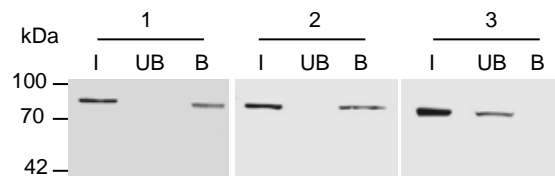


Figure 6. AeCRN13Cter and BdCRN13Cter bind DNA in vitro thanks to a HNH-like motif. Approximately 35 ng of purified recombinant proteins (1: MBP:AeCRN13Cter; 2: MBP:BdCRN13Cter, 3: MBP:AeCRN13CterDHNH) were incubated 20 minutes at room temperature with beads coupled to double strand DNA (dsDNA) before centrifugation. Immunoblot using anti-MBP antibodies showed the presence of AeCRN13Cter and BdCRN13Cter in the fraction in association with dsDNA. In the absence of the HNH-like motif, AeCRN13Cter does not bind to dsDNA. I: input protein fraction, UB: unbound, DNA protein fraction. B: bound-DNA protein fraction.

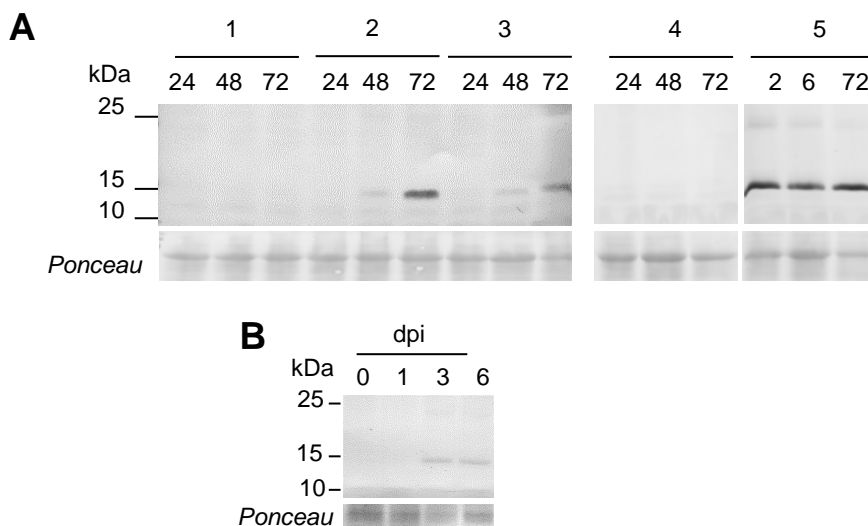


Figure 7. H2AX histone (gH2AX) phosphorylation is induced by AeCRN13Cter and during infection

(A) Tobacco leaves were agroinfiltrated with GFP (1) GFP:AeCRN13Cter (2) GFP:BdCRN13Cter (3) GFP:AeCRN13Cter Δ DDC (4) constructs and status of histone H2AX phosphorylation was compared using western blotting. Pronounced phosphorylation was observed in leaves cells expressing AeCRN13Cter or BdCRN13Cter two days after treatment with an emphasis at three days, while the deleted DDC version of AeCRN13Cter and the GFP control failed to induce phosphorylation modification. Bleomycin was used to induce DNA damage as a control and cells challenged with the chemical agent display H2AX phosphorylation within 2 hours after treatment. (B) H2AX phosphorylation is detected by western-blot in roots of *M. truncatula* infected by *A. euteiches* from 3 to 6 days post infection (dpi).

367 construct, the lifetime of GFP:AeCRN13Cter was 2.1542 ± 0.024 nsec in the absence of
368 SytoxOrange and decreased significantly to 1.655 ± 0.048 nsec in presence of the dye, a value
369 similar to the one observed with the GFP:H2B positive control. A similar decrease was
370 observed in the GFP life-time in samples expressing the BdCRN13Cter construct. These
371 results indicated an energy transfer and therefore the binding of CRN13s to nucleic acids.
372 While the Sytox Orange dye is not specific for either DNA or RNA [44,45] leaf samples were
373 treated with RNase A to digest RNA before performing the experiment. After RNase
374 treatment the lifetime of CRN13s GFP-tagged proteins remained unchanged as compared to
375 the GFP-H2B control (Table 1). Hence the decrease of the fluorescence lifetime of CRNs-
376 GFP-tagged proteins in the presence of SytoxOrange was only DNA-dependent and indicates
377 that both CRN13s bind nuclear DNA *in vivo*.

378

379 **CRN13s induce nuclear DNA damage**

380 Because of the observed phenotype on plant and animal cells upon CRN13 Cterminus
381 expression and DNA-binding capacity through a HNH-like motif, the putative DNA-damage
382 inducing activity of CRN13s was tested. A typical marker to examine DNA damage upon
383 genotoxic stress is the phosphorylation of the histone H2AX, namely γ H2AX [46]. Using a
384 monoclonal antibody specific for γ H2AX, we detected H2AX phosphorylation in
385 agroinfiltrated *N. benthamiana* leaves expressing AeCRN13Cter or BdCNR13Cter 24h after
386 treatment meaning before the apparition of cell-death symptoms (Fig. 7A). In contrast the
387 deleted version of AeCRN13 corresponding to the DFA subdomain and the GFP control are
388 not able to induce H2AX phosphorylation, suggesting that the full length of the C-terminus of
389 AeCRN13is required. When control leaves were treated with the DNA-damaging agent
390 bleomycin (BLM) a strong and early H2AX phosphorylation was detected. Since these results
391 suggest that *A. euteiches* can produce DNA damaging effectors during pathogenesis, the
392 phosphorylation status of H2AX was checked during infection of *M. truncatula* roots upon *A.*

393 *euteiches* infection. As shown by western-blot analysis H2AX phosphorylation is observed at
394 the early stage of *M. truncatula* roots infection (Fig. 7B) strongly suggesting that *A. euteiches*
395 triggers DNA damage during host colonization.

396

397

398

399

400

401

402 Discussion

403

404 In this study we concentrated on discovering the mode of action of eukaryotic
405 effectors by working on CRN13 intracellular effector from two unrelated filamentous
406 pathogenic microorganisms. Up to now, CRN13s were only predicted in the phytopathogenic
407 oomycetes *Phytophthora* sp. and *A. euteiches* and in the genome of the pathogen of
408 amphibians *B. dendrobatidis* (*Bd*). We show that AeCRN13 is expressed during infection of
409 roots of legumes by *A. euteiches*. AeCRN13 C-ter domain and its ortholog from *Bd* triggered
410 tobacco leaf cell death and restricted root development of *M. truncatula*. CRN13s cytotoxic
411 activity in plant cells relied on the nuclear localization of the effectors. Animal cells
412 expressing either AeCRN13 or BdCRN13 at the nuclear level from early *Xenopus* embryos
413 showed aberrant development with an enhancement of cell size. A putative HNH-like motif
414 reported in bacterial endonuclease was predicted in both effectors. This motif was required for
415 AeCRN13 retention in the nucleus of tobacco cells. Both CRN13s exhibited dsDNA-binding
416 affinity *in vitro* thanks to the HNH-like motif. The interaction of effectors with DNA was
417 unambiguously confirmed by FRET/FLIM assays on tobacco cells. Both CRN13s induced
418 phosphorylation of H2AX histone in tobacco leaves, indicating that the effectors trigger plant
419 DNA damage. Infection of host legumes roots by *A. euteiches* was accompanied by
420 phosphorylation of H2AX histone. Altogether these data reveal a new mode of action for
421 intracellular eukaryotic effectors in which host nuclear DNA is the central target. Indeed we
422 provide the first evidence that unrelated filamentous pathogens shared similar effector family
423 able to bind DNA and trigger host DNA damage.

424 Our first results showed that a CRN13 gene is expressed by *A. euteiches* during
425 infection of *M. truncatula* roots and the use of CRN13 antibodies revealed a partial processing
426 of the protein suggesting that the translocation signal of CRN is probably cleaved during the
427 translocation process. This result is reminiscent with the proteolytic cleavage occurring during

428 the translocation of *Plasmodium* effectors. The N-terminus export element (PEXEL;
429 RxLxE/Q/D) of effectors is cleaved at the parasite endoplasmic reticulum by protease
430 plasmepsin V and is required for export V [47]. However, translocation mechanism mediated
431 by the N-terminus targeting signal of CRN is still unknown.

432 Despite the absence of a predicted Nuclear Localization Signals (NLS), AeCRN13 and
433 BdCRN13 are addressed to the nucleus when heterogously expressed in plant or animal cells.
434 This data indicates that CRN13s C-terminus drives nuclear localization and contains an
435 atypical NLS not detected by available prediction programs, and/or are able to subvert
436 conserved nuclear translocation machinery to promote the efficient import of the effector into
437 nucleus. This result is consistent with previous analyses on CRNs from *P. infestans* and *P.*
438 *capsici* showing that all CRNs are nuclear localized when expressed in *N. benthamiana*
439 tissues, despite that only some CRNs harbor a predicted NLS [26,29]. The nuclear localization
440 of NLS-containing CRNs required host importin- α factor [26], however its function in the
441 transport of CRNs devoided of a NLS remains to be demonstrated.

442 CRN13s from *A. euteiches* and *Bd* induced similar phenotypes in plant and animal
443 tissues, and this activity is dependent of their nuclear localization. Overexpression of CRN13s
444 led to an inhibition of root development in *M. truncatula*, to cell-death symptoms on tobacco
445 leaves and to an enhancement of cell size due probably to an arrest of cell division in *Xenopus*
446 embryos. These results corroborate observations made during roots infection of legumes by *A.*
447 *euteiches*, where susceptible accessions harbor few days after infection a decrease of
448 secondary root development and necrosis of roots [40]. Similarly recent studies show that *Bd*
449 produced compounds that can impair amphibian lymphocyte proliferation to evade host
450 immunity [48]. While some data suggests that these compounds are not proteins, it should be
451 interesting to evaluate the contribution of BdCRNs in this process [48].

452 AeCRN13 and BdCRN13 show a divergent N-terminal targeting motif but conserved
453 C-terminus organization consisting of two subdomains association (DFA-DDC). *In silico*

454 analysis lead us to predict a putative HNH motif (PF13391) in the DFA subdomain of both
455 CRN13s. HNH stands for the three most conserved histidine and asparagine residues located
456 within the catalytic site [43]. These residues are found in all the CRN13 sequences analyzed.
457 Less common in eukaryotes, the motif allows DNA-binding and nuclease activities of a large
458 array of prokaryotic enzymes like the colicin E7 toxin from *E. coli* and play important role in
459 many cellular processes including immunity [49-51]. Deletion analysis shows that the HNH-
460 like motif in combination with the DDC domain contribute to CRNs nuclear localization in
461 *Nicotiana*. Thus, CRN13s appear to have a modular organization in which specific
462 subdomains are required for nuclear localization.

463 We discovered that AeCRN13 and BdCRN13 bind dsDNA *in vitro* and that this
464 capacity is linked to the presence of the HNH-like motif in the DFA subdomain. Although
465 preliminary experiments with recombinant proteins did not allow the detection of a nuclease
466 activity for CRN13 proteins in standard conditions, this possibility cannot be excluded. By
467 setting FRET/FLIM measurements to evaluate protein/DNA interactions in leaves samples,
468 we revealed DNA-binding capacity of CRN13s *in vivo*. These data show unambiguously for
469 the first time that filamentous eukaryotic effectors interact with nuclear DNA. While it is
470 known that the nucleus is a key cellular compartment for expression of immune responses and
471 is a target of many microbial effectors [9] [52], up to now direct interaction between effector
472 and host DNA has been reported only for transcriptional activator-like (TAL) bacterial
473 effectors of *Xanthomonas* sp. and *Ralstonia* sp. [33,53]. Only protein/protein interactions at
474 the nuclear level have been reported for eukaryotic filamentous organisms. In oomycetes, the
475 RxLR Pi03192 effector from *P. infestans* interact with two NAC transcription factors to
476 prevent them from being released from the ER to enter the nucleus where they limit disease
477 progression [16]. The interaction and stabilization of the U-box E3ligase CMPG1, required
478 for cell death, by Avr3a from *P. infestans* occurs in the nucleolus of plant cell [54]. In
479 addition, the RxLR44 from *H. arabidospis* interact with the mediator complex RD19a to

480 enhance its degradation and *Arabidopsis* susceptibility [18]. Rust transferred protein 1
481 (RTP1p) from the bean rust fungus *Uromyces fabae* is the only effector from a pathogenic
482 fungus for which a nuclear localization has been described to date but its plant target is still
483 unknown [55]. Here we propose that the CRN-DNA interaction occurs on unspecific nucleic
484 sequences or highly conserved in plant and animals cells, since BdCRN13 binding is effective
485 in *N. benthamiana*. Future work will aim to identify DNA regions targeted by both effectors.

486 Although nuclease activity of recombinant CRN13s effectors was not detected in
487 standard *in vitro* condition, the presence of a HNH-like motif leads us to hypothesize that
488 binding of CRN13s to host DNA may trigger nucleic damage. This effect was studied by
489 following the phosphorylation of H2AX histone (γ H2AX), which is recognized as a solid
490 marker of double strand DNA break (DSB) in plant and animal cells [46]. In *N. benthamiana*
491 cells expressing CRN13s and in *Medicago* roots infected with *A. euteiches*, γ H2AX
492 accumulation was observed revealing that CRN13s and *A. euteiches* infection induced DSB.
493 While DNA damage have been well characterized with regard to bacterial toxins upon
494 infection of animal tissues [56,57], this effect has not been reported in the case of plant
495 pathogen interactions. In plants, DSB due to environmental stresses or chemicals agent, have
496 extreme detrimental effects on plant growth with particularly severe effects on actively
497 dividing cells [58,59]. In animal systems, bacterial genotoxins leads to cell cycle arrest and
498 eventually apoptosis [60]. Due to the observed expansion of plant and *Xenopus* cells size and
499 cell-death symptoms upon CRN13 expression, we propose that genotoxic activity of CRNs
500 impacts host cell cycle. Therefore the presence of effectors capable of causing DNA damage
501 may constitute a predisposing factor for host colonization.

502

503 Taken together, this work provides first evidences that eukaryotic filamentous
504 pathogens express similar DNA-binding proteins able to trigger host DNA damage.
505 Additionally, our data show that unrelated plant and animal pathogens deployed a common

506 repertoire of effector with conserved mode of action. This raises the question of the origin and
507 evolution of these genes and their implication on the emergence of new pathogenic species.

508

509 **Materials and Methods**

510

511 **Plant material, microbial strains, and growth conditions**

512 *M. truncatula* F83005.5 seeds were scarified, sterilized and *in vitro*-cultured and transformed
513 as previously described [40,61]. Roots infection using *A. euteiches* (ATCC 201684) zoospore
514 inoculum was performed as [41]. *N. benthamiana* plants were grown from seeds in growth
515 chambers at 70% of humidity with a 16h/8h dark at 24/ 20°C regime. All *E.coli* strains
516 (DH5 α , DB3.5 and BL21AI), *A. tumefaciens* (GV310::pMP90RK) and *A. rhizogenes* (Arqual)
517 strains were grown on LB medium with the appropriate antibiotics.

518

519 **RNA extraction and qRT-PCR**

520 Samples were ground on liquid nitrogen and total RNA extracted using the RNAeasy kit
521 (Qiagen). Reverse transcription was performed on 1 μ g of total RNA using the
522 AppliedBiosystems kit (Life Technologies-Invitrogen). cDNAs were diluted 50- fold for
523 qPCR reaction. Each qPCR reaction was performed on a final volume of 10 μ l corresponding
524 to 8 μ l of PCR mix (0.5 μ M of each primer and 5 μ l SYBRGreen, Applied Biosystems) and
525 2 μ l of the diluted cDNA and was conducted on a ABI Prims SDS 7900 HT (Applied
526 Biosystems, Foster City, CA, USA) device using the following conditions: 5min at 95°C,
527 followed by 45 cycles of 15 s at 95°C and 1min at 60°C. Dissociation curves were obtained by
528 applying a 15s 95°C, 15s 95°C and 15s 95°C cycle. Each reaction was conducted on
529 triplicates for cDNAs of four biological replicates. Primers F: 5'-
530 TTATTGCTGTGCCAAATCAG-3' and R: 5'- GATATTGTATCTTGCGGTGAC-3' were
531 used for the detection of AeCRN13 (Ae_9AL5664, <http://www.polebio.scsv.ups->

532 tlse.fr/aphano/, [62]). Primers F: 5'-TGTCGACCCACTCCTTGTTG-3' and R: 5'-
533 TCGTGAGGGACGAGATGACT-3' were used to assess the expression of *A. euteiches*'s α -
534 tubulin coding gene (Ae_22AL7226) and normalize AeCRN13 expression. The histone 3-like
535 of *M. truncatula*, previously described [63], was used to normalize microorganism abundance
536 during infection. Relative expression of AeCRN13 and α -tubulin genes were calculated using
537 the $2^{-\Delta\Delta Cq}$ method described in [64].

538

539 **Construction of plasmid vectors and *Agrobacterium*-mediated transformation**

540 All primers used for the generation of the CRN constructs are listed in Supplementary Tab.
541 T1. *BdCRN13Cter* was generated by PCR from genomic DNA of *B. dendrobatidis* JAM81
542 (kindly provided by Jason Stajich, University of California, Riverside, USA) using primers
543 attB1_BdCRN13-F and attB2_BdCRN13-R. Unless noticed otherwise, cDNA clone
544 corresponding to the unigene Ae_9AL5664 (vector pSport_AeCRN13 [62]) was used as
545 template for the generation of C-terminal domain versions of AeCRN13. Gateway technology
546 in combination with pDONR-Zeo (Invitrogen) and pK7WGF2 vectors
547 (<http://gateway.psb.ugent.be/>) were used for cloning steps. AeCRN13Cter carrying Gateway
548 adaptators was generated by PCR using primers attB1_AeCRN13-F and attB2_AeCRN13-R.
549 AeCRN13Cter Δ DDC and AeCRN13Cter Δ DFA carrying the Gateway sequences were
550 amplified with primers set attB1_AeCRN13-F and attB2_DFAend-R and with primers set
551 attB1_AeCRN13_DDC-F and AttB2_AeCRN13-R, respectively. A three-step PCR strategy
552 was used to generate the *GFP:AeCRN13Cter Δ HNH* construct. Briefly, the amplicon
553 corresponding to the DFA subdomain deleted of the HNH-like motif (106aa-281aa) was
554 mixed with the amplicon corresponding to the DDC subdomain (338aa-423aa) and used as a
555 template for PCR with attB1_AeCRN13-F and attB2_AeCRN13-R primers. Amplicons were
556 BP recombined (Invitrogen) into pDONR-Zeo vector. NES sequence (LQLPPLERLTL) and
557 non-functional mutated NES sequence (mNES: LQAPPAERATL) were added to the

558 Nterminal moiety of AeCRN13Cter and BdCRN13Cter by PCR [26]. Amplicons were
559 introduced in pENTR/ D-TOPO vector by means of TOPO cloning (Invitrogen) and then
560 transferred to pK7GWF2 vector. Vector *pBII21:H2B:YFP* [65] was used as template to
561 amplify the histone2B from *A.thaliana* and the amplicon was clone into pENTR/ D-TOPO
562 vector and transferred into pK7WGF2 to obtain *GFP:H2B* fusion construct. Generation of *M.*
563 *truncatula* composite plants was performed as described by [61] using ARQUA-1 *A.*
564 *rhizogenes* strain. For leaves infiltration, GV3101 *A. tumefaciens* transformed strains were
565 syringe-infiltrated at OD₆₀₀ = 0.3 on 3-4 week-old *N. benthamiana* as described by [66].

566

567 **MBP-tagged CRN recombinant proteins**

568 AeCRN13Cter, AeCRN13Cter Δ HNH and BdCRN13Cter inserts cloned in pDONR-Zeo
569 entry vector were transferred in pHMWGA [67] expression vector by LR recombination
570 (Invitrogen).

571 Constructs carrying *the MBP:AeCRN13Cter*, *MBP:AeCRN13Cter Δ HNH* and fusions were
572 introduced in *E.coli* BL21-AI (Invitrogen) for protein production as recommended by the
573 provider. Purification of the proteins was performed by affinity chromatography using
574 amylose resin (BioLabs England).

575

576 **Anti-AeCRN13 antibodies generation and purification**

577 Polyclonal antibodies against the C-terminal domain of AeCRN13 were raised in rabbits
578 (ProteoGenix, France) by injecting the purified recombinant protein MBP:AeCRN13Cter.

579 Sera were purified by negative adsorption against recombinant MBP:AeCRN5Cter protein

580 (Gaulin, data unpublished) adsorbed onto an amylose column resin and used at a dilution of

581 1:1000 relative to initial sera for western-blot.

582

583

584 **Immunoblot analysis**

585 Infected *M. truncatula* roots or roots from *M. truncatula* composite plants were frozen in
586 liquid nitrogen and ground in 50mM NaP, 0.1% (v/v) triton, 10mM β -mercaptoethanol and 1x
587 complete protease inhibitor cocktail (Roche). Supernatants were separated by SDS-PAGE and
588 electroblotted to nitrocellulose membranes (Amersham BioSciences). AeCRN13 was detected
589 using anti-AeCRN13 purified antibodies and anti-rabbit secondary antibodies coupled to
590 alkaline phosphatase (Sigma-Aldrich) and revealed using CDPstar chemiluminescence kit
591 (Roche). *N. benthamiana* protein analyses were performed as described by ⁶ using a primary
592 rabbit anti-GFP polyclonal antibodies (1:2000, Clontech).

593 For γ H2AX experiments, *N.benthamiana* agroinfiltrated leaves and *M. truncatula* infected
594 roots were harvested at different time in liquid nitrogen and grounded in modified Rippa
595 buffer v/v (TrisHCl 50mM, NP-40 1%, NaCl 250mM, SDS 0.1%, EDTA 2mM, DOC 1%,
596 Protease inhibitors 1X (Complete Protease Inhibitors, Roche), orthovanadate 10mM, PMSF
597 1mM (Sigma-aldrich) using 23G needles (0.6mm diameter). Samples were then treated with
598 1 μ l of Benzonase (Sigma-aldrich, 250U/ μ l) for 30 min on ice, centrifuged for 20 min at 13000
599 rpm at 4 °C and supernatants were dosed and used for western blot. Approximately 30 μ g of
600 total protein extracts were loaded on 12% polyacrylamide gels, transferred on nitrocellulose
601 membrane, blocked in TBS Tween 0.1% BSA 2% for 2 hours and incubated overnight at 4°C
602 with monoclonal antibody γ H2AX (ser139) (Cell Signaling Technology) diluted at 1/1000 in
603 TBS-T-BSA2%. After washing steps in TBS Tween 0.05%, blots were incubated with anti-
604 rabbit secondary antibodies coupled to alkaline phosphatase (Sigma-Aldrich) diluted in TBS-
605 T-BSA2% at 1/2000 for 1 hour, washed and then revealed with NBT/BCIP substrate.

606

607 ***In vitro* DNA-binding assays**

608 Beads coupled to calf thymus double-stranded (ds) DNA (Sigma-Aldrich) were suspended in
609 KHN buffer [68] (whose pH was modified and fixed at 7). 35ng of MBP:AeCRN13Cter,

610 MBP:AeCRN13Cter Δ HNH and MBP:BdCRN13Cter recombinant proteins were incubated in
611 400 μ L of dsDNA beads for 20 min at room temperature (23°C-25°C) under moderate
612 rotation. Beads were centrifuged at 10000xg during 10 min. The first supernatant was retained
613 as the not bound fraction. This fraction (\approx 400 μ L) was concentrated using Vivaspin 500
614 column (cut-off 10kDa) for analysis. Beads were washed 4 times with 800 μ L of KHN buffer.
615 Proteins bound to DNA were eluted by adding 50 μ l of 2X Laemmli buffer and heating at
616 95°C for 10 min. Proteins were analysed by immunoblotting using monoclonal anti-MBP
617 antibodies.

618

619 **Preparation of *N. benthamiana* epidermal leaves for FRET / FLIM experiments**

620 Discs of agroinfiltrated *N. benthamiana* leaves were fixed 24 hours after treatment by vacuum
621 infiltrating a TBS (TRIS 25mM, NaCl 140 mM, KCl 3 mM) 4 % (w/v) paraformaldehyde
622 solution before incubation 20 min at 4°C. Samples were permeabilize 10 min at 37°C using a
623 TBS buffer supplemented with 20 μ g/ml of proteinase K (Invitrogen). Nucleic acid staining
624 was performed by vaccum-infiltrating a 5 μ M of Sytox Orange (Invitrogen) solution and
625 before incubating samples 30 min at room temperature. When RNase treatment was
626 performed, foliar discs were incubated 15 min at room temperature with 0.5 μ g/ml of RNase
627 A (Roche) before nucleic acid staining. Foliar discs were washed with and mounted on TBS
628 before observations on an inverted microscope (Eclipse TE2000E, Nikon, Japan).

629

630 **Confocal microscopy**

631 Scanning was performed on a Leica TCS SP2 DMRXA2 confocal microscope. Excitation
632 wavelengths were 488 nm (GFP) and 543nm (SytoxOrange). Images were acquired with a
633 40x water immersion lens, or a 20x water immersion lens for embryo *X. laevis* hemisections,
634 and correspond to Z projections of scanned tissues. All confocal images were analyzed and
635 treated using the Image J software.

636

637 **Cytological observations of transformed roots**

638 Roots of composite plants expressing transgene constructs were sampled 30 days after
639 transformation and fixed in 2% (v/v) paraformaldehyde in 50mM sodium cacodylate buffer,
640 pH 7. Fixed roots were dehydrated in a graded ethanol series and embedded in LRW resin
641 (London Resin Company Limited) also in a graded manner. Polymerisation was performed
642 over-night at 60°C. Longitudinal sections (1µm) were performed with an Ultracut microtom
643 (Reichert-Jung), placed on multi-well slide and stained with 0.05% (w/v) toluidine bleu in
644 2.5% (w/v) CaCO₃ buffer, pH 11, during 2 minutes at 60°C followed by a water wash.

645

646 **FRET / FLIM measurements**

647 Fluorescence lifetime measurements were performed in time domain using a streak camera
648 [69]. The light source is a mode-locked Ti:sapphire laser (Tsunami, model 3941, Spectra-
649 Physics, USA) pumped by a 10W diode laser (Millennia Pro, Spectra-Physics) and delivering
650 ultrafast femtosecond pulses of light with a fundamental frequency of 80MHz. A pulse picker
651 (model 3980, Spectra-Physics) is used to reduce the repetition rate to 2MHz to satisfy the
652 requirements of the triggering unit (working at 2MHz). The experiments were carried out at λ
653 = 820 nm (multiphoton excitation mode). All images were acquired with a 60x oil immersion
654 lens (plan APO 1.4 N.A., IR) mounted on an inverted microscope (Eclipse TE2000E, Nikon,
655 Japan). The fluorescence emission is directed back into the detection unit through a short pass
656 filter ($\lambda < 750$ nm) and a band pass filter (515/30 nm). The detector is a streak camera
657 (Streakscope C4334, Hamamatsu Photonics, Japan) coupled to a fast and high-sensitivity
658 CCD camera (model C8800-53C, Hamamatsu). For each nucleus, average fluorescence decay
659 profiles were plotted and lifetimes were estimated by fitting data with exponential function
660 using a non-linear least-squares estimation procedure. Fluorescence lifetime of the donor
661 (GFP) was experimentally measured in the presence and absence of the acceptor (Sytox

662 Orange). FRET efficiency (E) was calculated by comparing the lifetime of the donor in the
663 presence (τ_{DA}) or absence (τ_D) of the acceptor: $E=1-(\tau_{DA}) / (\tau_D)$. Statistical comparisons
664 between control (donor) and assay (donor + acceptor) lifetime values were performed by
665 Student *t-test*. For each experiment, four leaf discs removed from two agroinfiltrated leaves
666 were used to collect data.

667

668 **Vector constructions and *Xenopus laevis* embryos microinjection**

669 All primers used for cloning are listed in Supplementary Tab. S1. Briefly, GFP C-ter
670 constructs cloned into pK7WGF2 were subcloned into pGEMT (Promega) and inserted into
671 BamHI and XbaI restrictions site of pCS2⁺ plasmid [70]. *In vitro* transcription was performed
672 using SP6 mMessage mMachine kit (Ambion). Two-stage embryos were obtained by in vitro
673 fertilization [71] and 20 nl of transcripts (6 ng) were pressure-injected in one blastomere at the
674 animal pole in order to target the animal micromeres at later stages. Embryos were allowed to
675 develop at 22 °C and followed by live macro-imaging (Axiozoom). Embryos were fixed in
676 MEMFA buffer (100mM MOPS, pH7.4, 2mM EGTA, 1mM MgSO₄, 3.7%(v/v)
677 formaldehyde). Injections and assessment of development was performed on 3 independent
678 experiments where at least 20 embryos were used for each condition. Total proteins of 5
679 nitrogen frozen embryos were extracted in lysis buffer (50mM Tris pH 7.5, 150mM NaCl,
680 1mM EDTA, 1% NP40, 1x complete protease inhibitors (Roche) and analysed by immunoblot
681 using anti-GFP antibodies.

682

683 **Acknowledgments**

684 We would like to thank the French Ministry of Education and Research for the PhD
685 fellowship to Diana Ramirez-Garcés. We are grateful to Aurélie Le Ru (TRI-Imagery
686 Platform of Toulouse, France) for helpful assistance on confocal microscopes, Miguel Vega-
687 Sanchez (JBEI, USA) for discussion on DNA-binding *in vitro* assays, Christophe Lachaud

688 (University of Dundee, UK) for helpful discussions on DNA damage, Maxime Bonhomme
689 (LRSV, France) for useful comments on statistical analysis. The research was carried out in
690 the LRSV, part of the French Laboratory of Excellence "TULIP" (ANR-10-LABX-41; ANR-
691 11-IDEX-0002-02). This work was funded by the French Centre National de la Recherche
692 Scientifique (CNRS) and the Université Paul Sabatier, Toulouse and by the French Agence
693 Nationale pour la Recherche (ANR-12-JSV6-0004-01, APHANO-Effect to EG).

694

695 **Author Contributions**

696 Conceived and designed the experiments: EG, LC, BD. Performed the experiments: DRG,
697 LC, AJ, YM, BD, IN, CL, MM. Analyzed the data: DRGC, LC, IN, CL, MM, BD, EG.

698 Contributed reagents/materials/analysis tools: DRG, LC, YM, IN, CL. Wrote the paper: DRG,
699 LC, BD, EG. Conceived, directed and coordinated the project: EG.

700

701

702

703

704

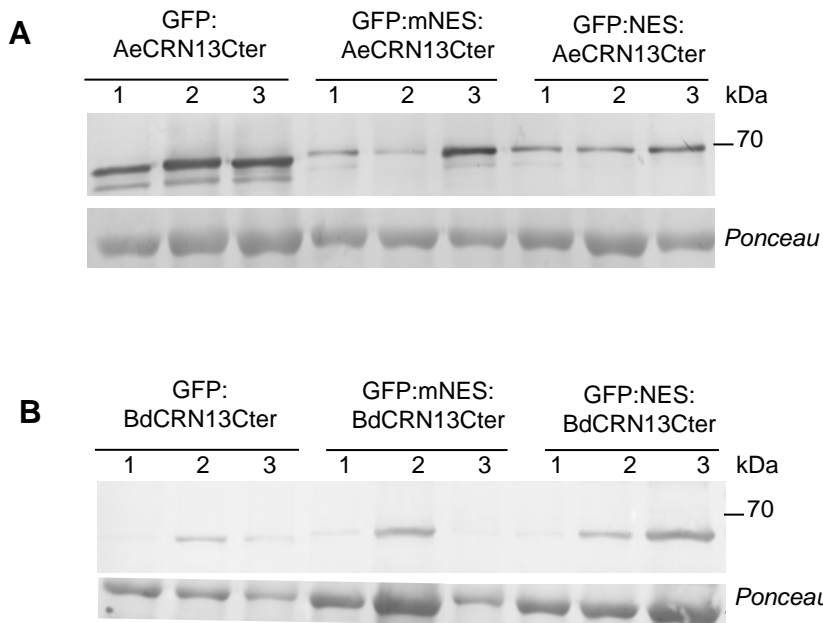
705

706

707

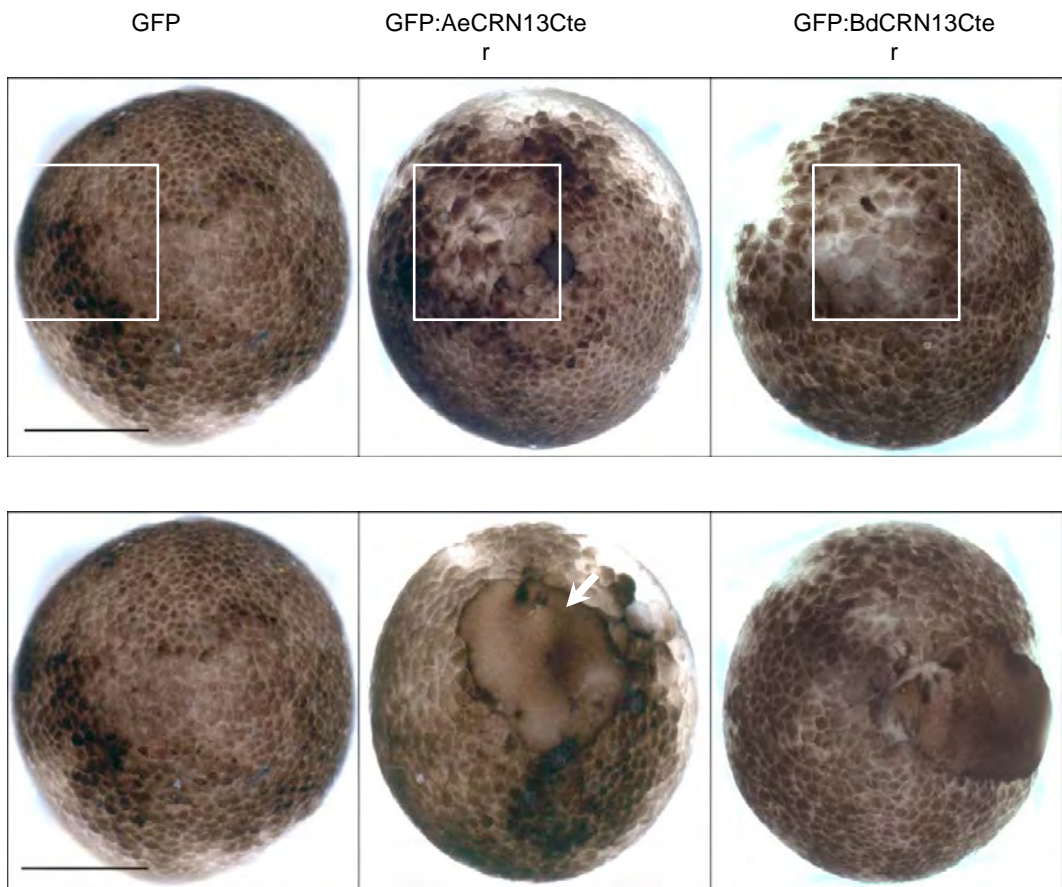
708

709



Supplemental Figure S1

Detection of AeCRN13Cter and BdCNR13Cter proteins in *N. benthamiana* leaves upon transient-expression assay. (A) Immunoblot of GFP:AeCRN13Cter, GFP:mNES:AeCRN13Cter and GFP:NES:AeCRN13Cter showing the accumulation of the fusion proteins in agroinfiltrated leaves 1, 2 and 3 days after treatment when probed with a GFP antibody. (B) Immunoblot using a GFP-antibody shows the accumulation of BdCRN13Cter fusion protein and its derivatives in *Nicotiana* leaves from 1 to 3 days post inoculation.



Supplemental Figure S2

AeCRN13 and BdCRN13 cause delay in cell division and aberrant phenotype in *Xenopus laevis*. Embryos injected with *GFP:AeCRN13Cter* or *GFP:BdCRN13Cter* mRNA presented delay in cell division leading to larger blastomeres (white square). Giant blastomeres (white arrows) are sometimes observed with both CRN13Cter constructs at stage 9 (7 hours post fertilization). Scale bar : 500 μ m.

		HNH motif																																																											
		*					*					*																																																	
BDEG_05578.1	260	M	G	K	A	E	S	C	H	L	I	S	D	S	H	C	R	N	Y	---	P	S	Y	E	K	Y	D	K	D	P	N	N	R	L	A	M	S	M	D	L	H	G	W	F	I	N	L	S	T	E	I	P	L	F	Y	L	K	I	V		
BDEG_03863	260	M	G	K	A	E	S	C	H	L	I	S	D	S	H	C	R	N	Y	---	P	S	Y	E	K	Y	D	K	D	P	N	N	R	L	A	M	S	M	D	L	H	G	W	F	I	N	L	S	T	E	I	P	L	F	Y	L	K	I	V		
BDEG_3200.1	258	M	G	K	A	E	S	C	H	L	I	S	A	S	H	C	R	N	Y	---	P	S	Y	E	K	Y	D	K	N	P	N	N	R	L	A	M	S	R	D	L	H	G	W	F	D	L	S	T	E	I	P	L	F	Y	L	K	I	V			
BDEG_07221	236	M	G	K	A	E	S	C	H	L	I	S	A	S	H	C	R	N	Y	---	S	F	Y	S	Q	Y	D	K	N	P	N	N	R	L	A	M	S	M	D	L	H	G	W	F	I	N	L	S	T	E	I	P	L	F	Y	L	K	I	V		
BDEG_03197	236	M	G	K	A	E	S	C	H	L	I	S	A	S	H	C	R	N	Y	---	S	F	Y	S	Q	Y	D	K	N	P	N	N	R	L	A	M	S	M	D	L	H	G	W	F	I	N	L	S	T	E	I	P	L	F	Y	L	K	I	V		
Ps_143535T0	274	V	G	K	A	Q	S	C	H	V	M	S	R	E	H	C	L	K	Y	---	P	S	Y	K	K	Y	D	N	D	P	S	N	R	L	A	L	S	A	E	M	H	E	W	F	D	A	R	S	Y	A	V	P	T	K	I	S	V	E			
PPTG_05866T0	280	Y	G	K	A	E	S	C	H	L	V	S	R	K	Q	---	S	R	D	H	K	R	E	F	A	K	Y	D	R	D	P	N	N	R	L	A	L	S	R	D	M	H	G	W	F	D	G	M	S	I	E	V	P	I	V	N	M	L	P	G	
PPTG_08911T0	279	Y	G	K	A	E	S	C	H	L	V	S	R	K	Q	---	S	R	D	H	K	R	E	F	A	K	Y	D	R	D	S	N	N	R	L	A	L	S	R	D	M	H	G	W	F	D	G	M	S	I	E	V	P	I	V	N	M	L	P	G	
Ps_159015T0	301	Y	G	K	A	E	S	C	H	L	V	S	R	K	Q	---	S	R	D	H	K	R	E	F	A	K	Y	D	R	D	S	N	N	R	L	A	L	S	R	E	M	H	G	W	F	D	G	M	S	I	E	V	P	I	V	N	M	L	P	G	
Ps_137003T0	300	Y	G	K	A	E	S	C	H	L	V	S	R	K	Q	---	S	R	D	H	K	R	E	F	A	K	Y	D	R	D	S	N	N	R	L	A	L	S	R	E	M	H	G	W	F	D	G	M	S	I	E	V	P	I	V	N	M	L	P	G	
Ps_158998T0	300	Y	G	K	A	E	S	C	H	L	V	S	R	K	Q	---	S	R	D	H	K	R	E	F	A	K	Y	D	R	D	S	N	N	R	L	A	L	S	R	E	M	H	G	W	F	D	G	M	S	I	E	V	P	I	V	N	M	L	P	G	
Ps_144118T0	301	Y	G	K	A	E	S	C	H	L	V	S	R	K	Q	---	S	R	D	H	K	R	E	F	A	K	Y	D	R	D	S	N	N	R	L	A	L	S	R	E	M	H	G	W	F	D	G	M	S	I	E	V	P	I	V	N	M	L	P	G	
Ps_159147T0	302	Y	G	K	A	E	S	C	H	L	V	S	R	K	Q	---	S	R	D	H	K	R	E	F	A	K	Y	D	R	D	S	N	N	R	L	A	L	S	R	E	M	H	G	W	F	D	G	M	S	I	E	V	P	I	V	N	M	L	P	G	
Ps_141914T0	305	Y	G	K	A	E	S	C	H	L	V	S	R	K	Q	---	S	R	D	H	K	R	E	F	A	K	Y	D	R	D	S	N	N	R	L	A	L	S	R	E	M	H	G	W	F	D	G	M	S	I	E	V	P	I	V	N	M	L	P	G	
Ps_139425T0	307	Y	G	K	A	E	S	C	H	L	V	S	R	K	Q	---	S	R	D	H	K	R	E	F	A	K	Y	D	R	D	S	N	N	R	L	A	L	S	R	E	M	H	G	W	F	D	G	M	S	I	E	V	P	I	V	N	M	L	P	G	
Ps_142770T0	308	Y	G	K	A	E	S	C	H	L	V	S	R	K	Q	---	S	R	D	H	K	R	E	F	A	K	Y	D	R	D	S	N	N	R	L	A	L	S	R	E	M	H	G	W	F	D	G	M	S	I	E	V	P	I	V	N	M	L	P	G	
Ps_134584T0	312	Y	G	K	A	E	S	C	H	L	V	S	R	K	Q	---	S	R	D	H	K	R	E	F	A	K	Y	D	R	D	S	N	N	R	L	A	L	S	R	E	M	H	G	W	F	D	G	M	S	I	E	V	P	I	V	N	M	L	P	G	
Ps_132308T0	313	Y	G	K	A	E	S	C	H	L	V	S	R	K	Q	---	S	R	D	H	K	R	E	F	A	K	Y	D	R	D	S	N	N	R	L	A	L	S	R	E	M	H	G	W	F	D	G	M	S	I	E	V	P	I	V	N	M	L	P	G	
Ae_9AL5664_1	279	Y	G	K	A	E	S	C	H	L	I	S	R	K	E	---	S	R	D	H	K	R	E	F	A	K	Y	D	R	D	P	N	N	R	L	A	L	S	R	E	M	H	G	Y	D	L	S	Y	E	V	P	I	V	N	M	L	P	G			
PPTG_14697T0	244	Y	G	N	A	E	S	C	H	L	V	S	R	K	Q	---	S	R	D	H	K	R	E	F	A	K	Y	D	R	D	I	N	N	R	L	A	L	S	R	E	M	H	G	F	Y	D	A	L	S	Y	D	V	P	I	V	N	M	V	P	V	
PITG_12609T0	320	Y	G	K	A	E	S	C	H	L	V	S	K	K	K	C	T	D	R	D	F	---	K	R	E	F	A	K	Y	D	R	D	A	N	N	R	L	A	L	S	R	E	M	H	G	F	Y	D	L	S	M	E	V	P	I	V	N	M	F	P	G
PITG_18826T0	319	Y	G	K	A	E	S	C	H	L	V	S	K	K	K	C	T	D	R	D	F	---	K	R	E	F	A	K	Y	D	R	D	A	N	N	R	L	A	L	S	R	E	M	H	G	F	Y	D	L	S	M	E	V	P	I	V	N	M	F	P	G

Supplemental Figure S3

The DFA subdomain of CRN13 proteins contains a HNH-like motif. The C-terminal part of AeCRN13 (Ae_9AL5664-1) amino acid sequence was used to BlastP *Phytophthora infestans* (PITG), *Phytophthora sojae* (Ps), *Phytophthora parasitica* (PPTG) and *Batrachochytrium dendrobatidis* (BDEG) using the corresponding databases at the Broad Institute. Box shade analysis was done with amino acid region encompassing the HNH-like motif and located at the C-terminus of the DFA subdomain. This motif first identified in bacterial endonucleases is the second most common motif in Type II restriction endonucleases, and is distributed in all life kingdoms. Asterisks indicated the three most conserved (histidine and asparagine) residues standing for the HNH motif (PFAM: PF13391).

710 References

- 711 1. Fisher MC, Henk DA, Briggs CJ, Brownstein JS, Madoff LC, et al. (2012) Emerging fungal threats to
712 animal, plant and ecosystem health. *Nature* 484: 186-194.
- 713 2. Dodds PN, Rathjen JP (2010) Plant immunity: towards an integrated view of plant-pathogen
714 interactions. *Nat Rev Genet* 11: 539-548.
- 715 3. Hogenhout SA, Van der Hoorn RA, Terauchi R, Kamoun S (2009) Emerging concepts in effector
716 biology of plant-associated organisms. *Mol Plant Microbe Interact* 22: 115-122.
- 717 4. Haas B, Kamoun S, Zody MC, Jiang RH, Handsaker RE, et al. (2009) Genome sequence and analysis
718 of the Irish potato famine pathogen *Phytophthora infestans*. *Nature* 461: 393-398.
- 719 5. Duplessis S, Cuomo CA, Lin YC, Aerts A, Tisserant E, et al. (2011) Obligate biotrophy features
720 unraveled by the genomic analysis of rust fungi. *Proc Natl Acad Sci U S A* 108: 9166-9171.
- 721 6. O'Connell RJ, Thon MR, Hacquard S, Amyotte SG, Kleemann J, et al. (2012) Lifestyle transitions in
722 plant pathogenic *Colletotrichum* fungi deciphered by genome and transcriptome analyses.
723 *Nat Genet* 44: 1060-1065.
- 724 7. Joneson S, Stajich JE, Shiu SH, Rosenblum EB (2011) Genomic transition to pathogenicity in chytrid
725 fungi. *PLoS Pathog* 7: e1002338.
- 726 8. Cock PJ, Grüning BA, Paszkiewicz K, Pritchard L (2013) Galaxy tools and workflows for sequence
727 analysis with applications in molecular plant pathology. *PeerJ* 1: e167.
- 728 9. Rivas S, Genin S (2011) A plethora of virulence strategies hidden behind nuclear targeting of
729 microbial effectors. *Front Plant Sci* 2: 104.
- 730 10. Mak AN, Bradley P, Bogdanove AJ, Stoddard BL (2013) TAL effectors: function, structure,
731 engineering and applications. *Curr Opin Struct Biol* 23: 93-99.
- 732 11. Baldauf SL, Roger AJ, Wenk-Siefert I, Doolittle WF (2000) A kingdom-level phylogeny of
733 eukaryotes based on combined protein data. *Science* 290: 972-977.
- 734 12. Beakes GW, Glockling SL, Sekimoto S (2011) The evolutionary phylogeny of the oomycete "fungi".
735 *Protoplasma* 249: 3-19.
- 736 13. Phillips AJ, Anderson VL, Robertson EJ, Secombes CJ, van West P (2008) New insights into animal
737 pathogenic oomycetes. *Trends Microbiol* 16: 13-19.
- 738 14. Fry W (2008) *Phytophthora infestans*: the plant (and R gene) destroyer. *Mol Plant Pathol* 9: 385-
739 402.
- 740 15. Yin W, Dong S, Zhai L, Lin Y, Zheng X, et al. (2013) The *Phytophthora sojae* Avr1d gene encodes an
741 RxLR-dEER effector with presence and absence polymorphisms among pathogen strains. *Mol*
742 *Plant Microbe Interact* 26: 958-968.
- 743 16. McLellan H, Boevink PC, Armstrong MR, Pritchard L, Gomez S, et al. (2013) An RxLR effector from
744 *Phytophthora infestans* prevents re-localisation of two Plant NAC transcription factors from
745 the endoplasmic reticulum to the nucleus. *PLoS Pathog* 9: e1003670.
- 746 17. Fabro G, Steinbrenner J, Coates M, Ishaque N, Baxter L, et al. (2011) Multiple candidate effectors
747 from the oomycete pathogen *Hyaloperonospora arabidopsidis* suppress host plant immunity.
748 *PLoS Pathog* 7: e1002348.
- 749 18. Caillaud MC, Asai S, Rallapalli G, Piquerez S, Fabro G, et al. (2013) A downy mildew effector
750 attenuates salicylic acid-triggered immunity in *Arabidopsis* by interacting with the host
751 mediator complex. *PLoS Biol* 11: e1001732.
- 752 19. Tyler B, Tripathy S, Zhang X, Dehal P, Jiang R, et al. (2006) *Phytophthora* genome sequences
753 uncover evolutionary origins and mechanisms of pathogenesis. *Science* 313: 1261-1266.
- 754 20. Baxter L, Tripathy S, Ishaque N, Boot N, Cabral A, et al. (2010) Signatures of adaptation to obligate
755 biotrophy in the *Hyaloperonospora arabidopsidis* genome. *Science* 330: 1549-1551.
- 756 21. Adhikari BN, Hamilton JP, Zerillo MM, Tisserat N, Lévesque CA, et al. (2013) Comparative
757 genomics reveals insight into virulence strategies of plant pathogenic Oomycetes. *PLoS One*
758 8: e75072.
- 759 22. Gaulin E, Madoui MA, Bottin A, Jacquet C, Mathé C, et al. (2008) Transcriptome of *Aphanomyces*
760 *euteiches*: new oomycete putative pathogenicity factors and metabolic pathways. *Plos One* 3:
761 e1723.

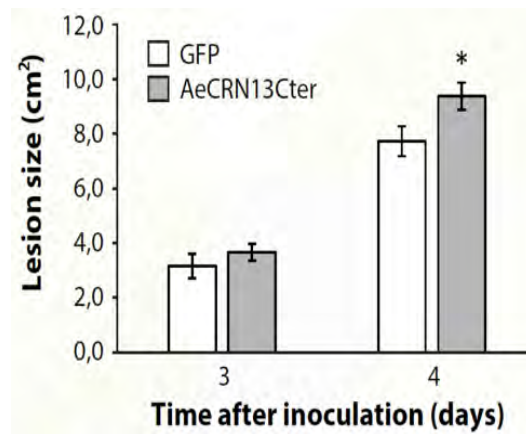
- 762 23. Stassen JH, Van den Ackerveken G (2011) How do oomycete effectors interfere with plant life?
763 Curr Opin Plant Biol 14: 407-414.
- 764 24. Caillaud MC, Wirthmueller L, Fabro G, Piquerez SJ, Asai S, et al. (2012) Mechanisms of nuclear
765 suppression of host immunity by effectors from the *Arabidopsis* downy mildew pathogen
766 *Hyaloperonospora arabidopsidis* (Hpa). Cold Spring Harb Symp Quant Biol 77: 285-293.
- 767 25. Kemen E, Gardiner A, Schultz-Larsen T, Kemen AC, Balmuth AL, et al. (2011) Gene gain and loss
768 during evolution of obligate parasitism in the white rust pathogen of *Arabidopsis thaliana*.
769 PLoS Biol. United States. pp. e1001094.
- 770 26. Schornack S, van Damme M, Bozkurt TO, Cano LM, Smoker M, et al. (2010) Ancient class of
771 translocated oomycete effectors targets the host nucleus. Proc Natl Acad Sci U S A 107:
772 17421-17426.
- 773 27. Stam R, Jupe J, Howden AJ, Morris JA, Boevink PC, et al. (2013) Identification and characterisation
774 CRN effectors in *Phytophthora capsici* shows modularity and functional diversity. PLoS One 8:
775 e59517.
- 776 28. Lévesque CA, Brouwer H, Cano L, Hamilton JP, Holt C, et al. (2010) Genome sequence of the
777 necrotrophic plant pathogen *Pythium ultimum* reveals original pathogenicity mechanisms
778 and effector repertoire. Genome Biol 11: R73.
- 779 29. Stam R, Howden AJ, Delgado-Cerezo M, M M Amaro TM, Motion GB, et al. (2013)
780 Characterization of cell death inducing *Phytophthora capsici* CRN effectors suggests diverse
781 activities in the host nucleus. Front Plant Sci 4: 387.
- 782 30. Liu T, Ye W, Ru Y, Yang X, Gu B, et al. (2010) Two host cytoplasmic effectors are required for
783 pathogenesis of *Phytophthora sojae* by suppression of host defenses. Plant Physiol 110: 490-
784 501.
- 785 31. Torto T, Li S, Styer A, Huitema E, Testa A, et al. (2003) EST mining and functional expression assays
786 identify extracellular effector proteins from the plant pathogen *Phytophthora*. Genome Res
787 13: 1675-1685.
- 788 32. Dong S, Yin W, Kong G, Yang X, Qutob D, et al. (2011) *Phytophthora sojae* avirulence effector
789 Avr3b is a secreted NADH and ADP-ribose pyrophosphorylase that modulates plant
790 immunity. PLoS Pathog 7: e1002353.
- 791 33. Boch J, Scholze H, Schornack S, Landgraf A, Hahn S, et al. (2009) Breaking the code of DNA binding
792 specificity of TAL-type III effectors. Science 326: 1509-1512.
- 793 34. van Damme M, Bozkurt TO, Cakir C, Schornack S, Sklenar J, et al. (2012) The Irish potato famine
794 pathogen *Phytophthora infestans* translocates the CRN8 kinase into host plant cells. PLoS
795 Pathog 8: e1002875.
- 796 35. Lin K, Limpens E, Zhang Z, Ivanov S, Saunders DG, et al. (2014) Single nucleus genome sequencing
797 reveals high similarity among nuclei of an endomycorrhizal fungus. PLoS Genet 10: e1004078.
- 798 36. Sun G, Yang Z, Kosch T, Summers K, Huang J (2011) Evidence for acquisition of virulence effectors
799 in pathogenic chytrids. BMC Evol Biol 11: 195.
- 800 37. Fisher MC (2008) Molecular toolkit unlocks life cycle of the panzootic amphibian pathogen
801 *Batrachochytrium dendrobatidis*. Proc Natl Acad Sci U S A 105: 17209-17210.
- 802 38. Rosenblum EB, James TY, Zamudio KR, Poorten TJ, Ilut D, et al. (2013) Complex history of the
803 amphibian-killing chytrid fungus revealed with genome resequencing data. Proc Natl Acad Sci
804 U S A 110: 9385-9390.
- 805 39. Rosenblum EB, Poorten TJ, Joneson S, Settles M (2012) Substrate-specific gene expression in
806 *Batrachochytrium dendrobatidis*, the chytrid pathogen of amphibians. PLoS One 7: e49924.
- 807 40. Djebali N, Jauneau A, Ameline-Torregrosa C, Chardon F, Jaulneau V, et al. (2009) Partial resistance
808 of *Medicago truncatula* to *Aphanomyces euteiches* is associated with protection of the root
809 stele and is controlled by a major QTL rich in proteasome-related genes. Mol Plant Microbe
810 Interact 22: 1043-1055.
- 811 41. Badreddine I, Lafitte C, Heux L, Skandalis N, Spanou Z, et al. (2008) Cell wall chitosaccharides are
812 essential components and exposed patterns of the phytopathogenic oomycete *Aphanomyces*
813 *euteiches*. Eukaryot Cell 7: 1980-1993.

- 814 42. Nieuwkoop PD, Faber, J (1967) Normal table of *Xenopus laevis* (Daudin) : a systematical and
815 chronological survey of the development from the fertilized egg till the end of
816 metamorphosis; Amsterdam N-HPC, editor.
- 817 43. Huang H, Yuan HS (2007) The conserved asparagine in the HNH motif serves an important
818 structural role in metal finger endonucleases. *J Mol Biol* 368: 812-821.
- 819 44. Cremazy FG, Manders EM, Bastiaens PI, Kramer G, Hager GL, et al. (2005) Imaging in situ protein-
820 DNA interactions in the cell nucleus using FRET-FLIM. *Exp Cell Res* 309: 390-396.
- 821 45. Haugland R.P. SMTZ, Johnson I.D., Basey A. (2005) The handbook: A guide to fluorescent probes
822 and labeling technologies.: Eugene, OR: Molecular Probes; 2005.
- 823 46. Friesner JD, Liu B, Culligan K, Britt AB (2005) Ionizing radiation-dependent gamma-H2AX focus
824 formation requires ataxia telangiectasia mutated and ataxia telangiectasia mutated and
825 Rad3-related. *Mol Biol Cell* 16: 2566-2576.
- 826 47. Russo I, Babbitt S, Muralidharan V, Butler T, Oksman A, et al. (2010) Plasmeprin V licenses
827 *Plasmodium* proteins for export into the host erythrocyte. *Nature* 463: 632-636.
- 828 48. Fites JS, Ramsey JP, Holden WM, Collier SP, Sutherland DM, et al. (2013) The invasive chytrid
829 fungus of amphibians paralyzes lymphocyte responses. *Science* 342: 366-369.
- 830 49. Yusufzai T, Kadonaga JT (2010) Annealing helicase 2 (AH2), a DNA-rewinding motor with an HNH
831 motif. *Proc Natl Acad Sci U S A* 107: 20970-20973.
- 832 50. Zhang D, Iyer LM, Aravind L (2011) A novel immunity system for bacterial nucleic acid degrading
833 toxins and its recruitment in various eukaryotic and DNA viral systems. *Nucleic Acids Res* 39:
834 4532-4552.
- 835 51. Sapranaukas R, Gasiunas G, Fremaux C, Barrangou R, Horvath P, et al. (2011) The *Streptococcus*
836 *thermophilus* CRISPR/Cas system provides immunity in *Escherichia coli*. *Nucleic Acids Res* 39:
837 9275-9282.
- 838 52. Bhattacharjee S, Garner CM, Gassmann W (2013) New clues in the nucleus: transcriptional
839 reprogramming in effector-triggered immunity. *Front Plant Sci* 4: 364.
- 840 53. de Lange O, Schreiber T, Schandry N, Radeck J, Braun KH, et al. (2013) Breaking the DNA-binding
841 code of *Ralstonia solanacearum* TAL effectors provides new possibilities to generate plant
842 resistance genes against bacterial wilt disease. *New Phytol* 199: 773-786.
- 843 54. Gilroy EM, Taylor RM, Hein I, Boevink P, Sadanandom A, et al. (2011) CMPG1-dependent cell
844 death follows perception of diverse pathogen elicitors at the host plasma membrane and is
845 suppressed by *Phytophthora infestans* RXLR effector AVR3a. *New Phytol* 190: 653-666.
- 846 55. Kemen E, Kemen AC, Rafiqi M, Hempel U, Mendgen K, et al. (2005) Identification of a protein
847 from rust fungi transferred from haustoria into infected plant cells. *Mol Plant Microbe*
848 *Interact* 18: 1130-1139.
- 849 56. Nougayrède JP, Homburg S, Taieb F, Boury M, Brzuszkiewicz E, et al. (2006) *Escherichia coli*
850 induces DNA double-strand breaks in eukaryotic cells. *Science* 313: 848-851.
- 851 57. Song J, Gao X, Galán JE (2013) Structure and function of the *Salmonella typhi* chimaeric A(2)B(5)
852 typhoid toxin. *Nature* 499: 350-354.
- 853 58. Ricaud L, Proux C, Renou JP, Pichon O, Fochesato S, et al. (2007) ATM-mediated transcriptional
854 and developmental responses to gamma-rays in *Arabidopsis*. *PLoS One* 2: e430.
- 855 59. Fulcher N, Sablowski R (2009) Hypersensitivity to DNA damage in plant stem cell niches. *Proc Natl*
856 *Acad Sci U S A* 106: 20984-20988.
- 857 60. Lara-Tejero M, Galán JE (2000) A bacterial toxin that controls cell cycle progression as a
858 deoxyribonuclease I-like protein. *Science* 290: 354-357.
- 859 61. Boisson-Dernier A, Chabaud M, Garcia F, Becard G, Rosenberg C, et al. (2001) *Agrobacterium*
860 *rhizogenes*-transformed roots of *Medicago truncatula* for the study of nitrogen-fixing and
861 endomycorrhizal symbiotic associations. *Mol Plant Microbe Interact* 14: 695-700.
- 862 62. Madoui M, Gaulin E, Mathe C, Clemente H, Couloux A, et al. (2007) AphanoDB: a genomic
863 resource for *Aphanomyces* pathogens. *BMC Genomics* 8: -.
- 864 63. Rey T, Nars A, Bonhomme M, Bottin A, Huguet S, et al. (2013) NFP, a LysM protein controlling
865 Nod factor perception, also intervenes in *Medicago truncatula* resistance to pathogens. *New*
866 *Phytol* 198: 875-886.

- 867 64. Livak KJ, Schmittgen TD (2001) Analysis of relative gene expression data using real-time
868 quantitative PCR and the 2(-Delta Delta C(T)) Method. *Methods* 25: 402-408.
- 869 65. Boissard-Lorig C, Colon-Carmona A, Bauch M, Hodge S, Doerner P, et al. (2001) Dynamic analyses
870 of the expression of the HISTONE::YFP fusion protein in arabidopsis show that syncytial
871 endosperm is divided in mitotic domains. *Plant Cell* 13: 495-509.
- 872 66. Gaulin E, Jauneau A, Villalba F, Rickauer M, Esquerre-Tugaye M, et al. (2002) The CBEL
873 glycoprotein of *Phytophthora parasitica var. nicotianae* is involved in cell wall deposition and
874 adhesion to cellulosic substrates. *J Cell Sci* 115: 4565-4575.
- 875 67. Busso D, Delagoutte-Busso B, Moras D (2005) Construction of a set Gateway-based destination
876 vectors for high-throughput cloning and expression screening in *Escherichia coli*. *Anal*
877 *Biochem* 343: 313-321.
- 878 68. Vega-Sánchez ME, Zeng L, Chen S, Leung H, Wang GL (2008) SPIN1, a K homology domain protein
879 negatively regulated and ubiquitinated by the E3 ubiquitin ligase SPL11, is involved in
880 flowering time control in rice. *Plant Cell* 20: 1456-1469.
- 881 69. Krishnan RV, Masuda A, Centonze VE, Herman B (2003) Quantitative imaging of protein-protein
882 interactions by multiphoton fluorescence lifetime imaging microscopy using a streak camera.
883 *J Biomed Opt* 8: 362-367.
- 884 70. Turner DL, Weintraub H (1994) Expression of achaete-scute homolog 3 in *Xenopus* embryos
885 converts ectodermal cells to a neural fate. *Genes Dev* 8: 1434-1447.
- 886 71. Leclerc C, Webb SE, Daguzan C, Moreau M, Miller AL (2000) Imaging patterns of calcium
887 transients during neural induction in *Xenopus laevis* embryos. *J Cell Sci* 113 Pt 19: 3519-3529.

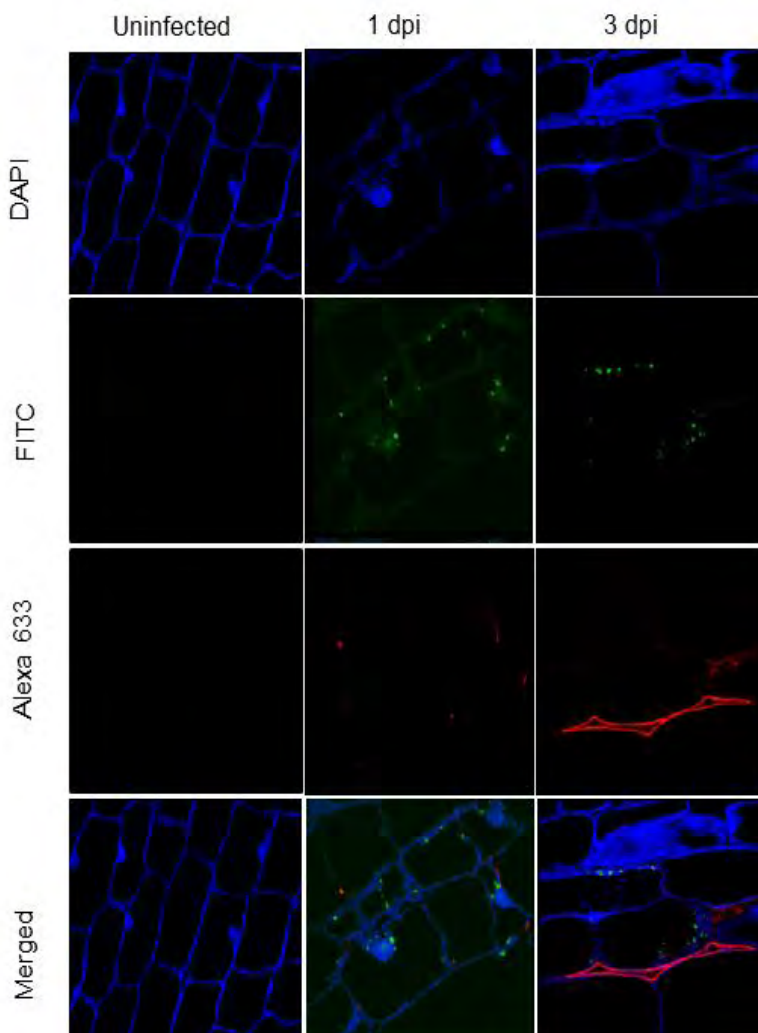
888

Chapter 1: Complementary results

A**B**

Complementary figure 1. AeCRN13 presence in plant cells enhances *P. capsici* growth

A. Photograph showing necrotic lesions caused by *P. capsici* 3 days post-inoculation (dpi) on *N. benthamiana* leaves in zones agroinfiltrated with GFP (left side) and GFP:AeCRN13 (right side) constructs. **B.** Graphic showing the average of lesion size (cm²) measured on GFP and AeCRN13 agroinfiltrated zones 3 and 4 dpi.



Complementary figure 2. Secretion and localization of AeCRN13 during infection of roots of *M. truncatula*.

Micrographs acquired by confocal microscopy on root sections (1µm thick) of *M. truncatula* infected by *A. euteiches* at 1 and 3 days post-infection (dpi). Anti-AeCRN13 rabbit antibodies were incubated and AeCRN13 signal revealed with anti-rabbit antibodies coupled to FITC (green) while *A. euteiches*'s mycelium was labelled with WGA-Alexa633 (red signal). Roots were treated with DAPI (bleu) to stain nuclei. Images show each signal separately (DAPI, FITC, Alexa633) and merged.

Complementary results

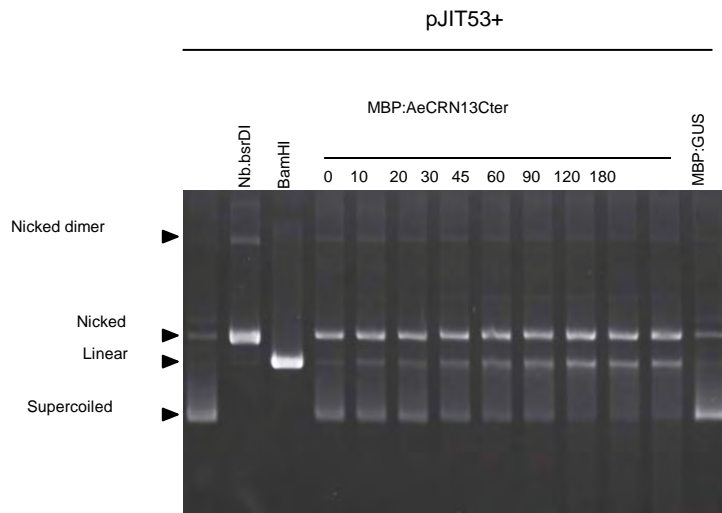
In view of the major points commented by reviewers, we performed complementary experiments to provide answers regarding AeCRN13 contribution to virulence, secretion and localization during infection and nuclease activity.

AeCRN13 enhances *P. capsici* in planta growth

To test the contribution of AeCRN13 to virulence we performed a virulence assay using *P. capsici*. For this, GFP protein alone and GFP:AeCRN13Cter were transiently expressed side by side on *N. benthamiana* by means of agroinfiltration and detached leaves were challenged on the agroinfiltrated zones by *P. capsici* zoospores 1 day after agroinfiltration. Progression of *P. capsici* on both agroinfiltrated zones was monitored during time and established by the size of necrotic lesions. As shown in complementary figure 1A, 3 days after zoospore inoculation, necrotic lesions were visible on both GFP and AeCRN13Cter agroinfiltrated zones leaves, indicative of *P. capsici* development. Size lesion measures (complementary figure 1B) indicated that lesions were greater for AeCRN13Cter than for GFP zones at 3 dpi and this differential was greater 4 days after. As lesion size depicts *P. capsici*'s growth on epidermal tissues, we conclude that the presence of AeCRN13Cer in plant cells contributes positively to the pathogen virulence.

AeCRN13 is secreted during infection into root tissues and addressed to host nuclei.

During our work, we developed anti-AeCRN13 rabbit antibodies raised against the recombinant fusion protein MBP:AeCRN13Cter produced in *E. coli*. We used these antibodies to address the localization of AeCRN13 in roots of *M. truncatula* during infection. Longitudinal sections of infected roots, corresponding to 1 and 3 days of infection were incubated with purified AeCRN13 antibodies and were revealed with secondary anti-rabbit antibodies coupled to FITC. In addition, *A. euteiches* mycelium (cell wall) was labelled using WGA lectin coupled to Alexa 633 fluorochrome and nuclei were stained with DAPI. Same treatments were performed on uninfected roots and used as a biological negative control. Internal negative controls (sections not incubated with ACRN13 and/or secondary anti-rabbit antibodies) were used to parameter confocal settings and ensure signal specificity during imaging acquisition. As shown in complementary figure 2, neither FITC nor Alexa 633 signals were detected on uninfected root sections. In infected roots at 1 dpi, *A. euteiches* was



Complementary figure 3. AeCRN13Cter displays a double-stranded nuclease activity *in vitro*

Plasmid DNA (vector pJIT53+) was incubated alone (first lane) during 180 minutes at 37°C with the nicking enzyme Nb.dsrDr, the double stranded cutting enzyme BamHI, with 1µg of recombinant proteins MBP:AeCRN13 and MBP:GUS. The picture corresponds to the electrophoretic analysis of pJIT53+ at the final point reaction (180 min) for the vector alone and controls Nb.bsrDR, BamHI and MBP:GUS and at different time point for MBP:AeCRN13Cter. The different conformations of pJIT53+ DNA molecule are indicated in the left side.

detected intercellularly around root cells. A strong AeCRN13 signal was detected outside *A. euteiches* in circled structures, vesicle-liked, on the apoplasm, and next to host cell nuclei. A faint AeCRN13 signal was detected also inside nuclei. At 3 dpi, these vesicles were still visible and the signal corresponding to *A. euteiches* cell-wall became more apparent confirming with its development in host roots. From these observations, we conclude that AeCRN13 is indeed secreted in roots during infection regardless the presence of a predicted classical signal peptide which suggests that a yet unknown secretion leader might ensure this function. We evidenced that the release of extracellular vesicles might be at the basis of AeCRN13 secretion. We postulate that AeCRN13 might be released from vesicles neighboring host nuclei as weak signal was recovered also inside nuclei and we explain this weak signal as a consequence of AeCRN13 protein diffusion.

While specificity of AeCRN13 antibodies on whole infected root proteins extracts is still under verification, the signal specificity of imaging acquisition revealed for the first time that an oomycetal effector is secreted and addressed into host cells during infection.

AeCRN13Cter displays a double-stranded nuclease activity *in vitro*

AeCRN13 harbors a HNH-like motif within the end of its DFA Cterminal domain. Because HNH motifs occur commonly in proteins with endonuclease activity we hypothesized that AeCRN13 might display such enzymatic activity. We showed that AeCRN13 binds dsDNA *in vitro* and that it induces double-stranded DNA damage *in vivo*. To further sustain its nuclease activity, we set up an *in vitro* assay using the purified recombinant protein MBP:AeCRN13Cter. For this 1 µg of MBP:AeCRN13 were incubated in presence of 1mM of MgCl₂ as a metal ion co-factor and 1µg of pJIT53+ plasmid DNA. The reaction was performed during three hours at 37°C. As a negative control we used the fusion protein MBP:GUS produced and purified using the same conditions as MBP:AeCRN13Cter. To further characterize the different forms of pJIT53+ and a possible activity of AeCRN13Cter on DNA, pJIT53+ was also incubated with commercial enzymes Nb.bsrDr and BamHI, which display a nicking and double stranded cutting activities on DNA, respectively.

As shown in complementary figure 3, pJIT53+ DNA was predominantly in a supercoiled and nicked circular form, presenting low amounts of the linear form before reactions. As expected, control reactions with Nb.bsrDr and BamHI led to the appearance of nicked and linear conformations respectively. Incubation with MBP:AeCRN13Cter resulted in the progressive decrease of the supercoiled form and the increase of the linear form. In latter times (90 min-180 min), a faint smear could be detected, indicative of a total DNA

degradation. No changes of conformation were detected with MBP:GUS protein. Thus, AeCRN13Cter displays a double-stranded nuclease activity on DNA *in vitro*. These results demonstrates that the DNA damage induced *in planta* by agroinfiltration of GFP:AeCRN13Cter is indeed a result of AeCRN13Cter activity on plant DNA.

Having set up this *in vitro* assay, our future experiments will be focused on characterizing AeCRN13 domains implicated in this nuclease activity, notably, the implication of the HNH motif by working with Cterminal deleted versions and point mutated version of the HNH domain.

Materials and methods of complementary experiments.

***P. capsici* growth assays**

GFP:AeCRN13 fusion protein and GFP protein alone were expressed in *N. benthamiana* leaves by agroinfiltration. One day after infiltration, infiltrated leaves were detached, placed on plastic dishes and agroinfiltrated zones were drop-inoculated with 5 μ L of *P. capsici* (strain LT312) zoospore solution corresponding to 100 zoospores. *P. capsici* growth was monitored over time. Photographs and leave lesions were assessed 3 and 4 days after inoculation. Lesion areas were measured using Image J software.

Antibody purification.

Polyclonal antibodies against the C-terminal domain of AeCRN13Cter were purified by negative adsorption against proteins from uninfected roots. For this, proteins extracted from uninfected roots of *M.truncatula* were spotted on 25x25 mm nitrocellulose membranes (Protan BA83, GE Healthcare Life Sciences), stained with Ponceau S and washed 3 times with PBS, 0.01% (v/v) Tween20 (PBS-T). Membranes were blocked with PBS-T, 1% (v/v) BSA during 2h at room temperature and incubated with diluted (1:10) sera overnight at 4°C. The obtained sera were used for cytological immunolocalization studies.

Preparation of roots sections and labeling of AeCRN13 and *A.euteiches* cell wall.

Infected and non-infected roots were sampled at 1, 3 and 6 days post inoculation and fixed with 2% (v/v) paraformaldehyde in 50mM of sodium cacodylate buffer, pH 7. Fixed roots were dehydrated in a graded ethanol series and embedded gradually in LR white (LRW) resin (London Resin Company Limited). Resin polymerisation was performed over-

night at 60°C. Roots were sectioned (1µm thick) using an Ultracut microtom (Reichert-Jung) and placed on multi-well slides for immunostaining steps. For this, sections were blocked for 2h30min in PBS, 2 % (v/v) Tween 20, 2 % (w/v) BSA buffer. Sections were then coincubated with purified anti-AeCRN13 rabbit antibodies and with the WGA lectin (Wheat Germ Agglutinin, W21404 Life technologies) conjugated to Alexa633 in blocking solution overnight at 4°C. Slides were washed 3x15 min with PBS, 2% (v/v) Tween 20 and incubated with goat anti-rabbit antibodies conjugated to fluorescein isothiocyanate (FITC) for 2h at room temperature. Slices were then rinsed and stained with 3µg/ml 4',6-diamidino-2-phenylindole (DAPI) for 5 min and rinsed again before confocal microscopy observation.

Confocal microscopy

Root sections were mounted on oil and scanned with a SP2 AOBS confocal microscope with the following excitation wavelengths: 405nm (DAPI), 488nm (FITC) and 688nm (Alexa688). To avoid signal interference, scanning was performed in a sequential mode. Parameters were set by analyzing all conditions and were the same for all images shown, which were treated using the Image J software.

Nuclease *in vitro* assay activity

1µg of purified proteins MBP: AeCRN13Cter or MBP: GUS (negative control) and restriction enzymes Nb.bsrDI and BamHI (10 units) were incubated in presence of 1µg of plasmid DNA pJIT53+, MgCl₂ (10 mM) in a MES (10mM), pH 7 buffer, at 37°C during 180 minutes. The state of DNA was monitored during time by sampling 10µl (≈100 ng) of reaction suspension and adding EDTA (0.2mM) to stop reactions, followed by electrophoresis analysis on an agarose gel (1%) and ethium bromide staining.

**Chapter 2: Functional
characterization of AeCRN5 of *A.
euteiches*.**

Chapter 2: Functional characterization of AeCRN5 of *A. euteiches*

Manipulation of plant nuclear biology is emerging as a crucial infection strategy deployed by prokaryotic and eukaryotic microbial pathogens through the secretion of intracellular effectors that target the host nucleus and/or nuclear-related processes (Bhattacharjee et al., 2013). Bacteria nuclear effectors have been shown to suppress plant defenses and manipulate host cellular metabolism by interacting with nuclear host proteins like histones, transcription factors, mRNA regulators as well as host nucleic acids (DNA) (Deslandes & Rivas, 2012). While host-delivery mechanisms, targets and nuclear activities are well characterized for nuclear effectors of bacteria, eukaryotic pathogen effectors are far less characterized.

The study presented in this chapter concerns the characterization of the Cterminal domain of AeCRN5 from the soil borne pathogen *A. euteiches*. AeCRN5 (379 aa) presents Nterminal harboring a LQLYALK (50-55aa) motif ended by a HVVVIVPEVPL (123-130aa) (figure 1 a) that ensures secretion and translocation into plant cells and presents a Cterminus of the DN17 oomycete subfamily containing a nuclear localization signal NLS (149-176aa). Its Cterminus was previously shown to trigger necrosis and to localize in nuclei of epidermal cells of *N. benthamiana* (Schornack et al., 2010). As CRN DN17-like subfamilies have been predicted in fungi *B. dendrobatidis* and *R. irregularis* (Sun et al., 2011; Li et al., 2014), we searched for homolog proteins on proteomes of oomycetes and both fungal species. BlastP resulted on the identification of homolog oomycete CRN ascribed to the DN17 subfamily with which it shares less than 38% identity (supplementary figure 1). The closest CRN sequence was identified in *B. dendrobatidis* with up to 48% identity, while the sequence found in *R. irregularis* only displayed 20% identity.

AeCRN5 was identified in a cDNA library generated from *A. euteiches* grown in close proximity to roots of *M. truncatula*. (Gaulin et al., 2008). The studied of AeCRN5 gene expression during infection showed that AeCRN5 is induced upon interaction with host root with a sustained expression during invasion of cortical root tissues (3-6 dpi) by *A. euteiches* (figure 1b/c). This suggests that AeCRN5 protein is implicated during infection and, thus, likely to be translocated to root cells. To address AeCRN5 effects in *M. truncatula* root cells, we expressed AeCRN5 in roots via *Agrobacterium rhizogenes* -transformation. Composite plants displayed modified root systems with reduced root length and an increased number of roots

(figure 2). Hence, AeCRN5 affects host root architecture, likely by inhibiting root elongation and stimulating root formation.

To rapidly dissect AeCRN5 activity in plant cells, we opted to use *N. benthamiana* ectopic expression system. Exclusion of AeCRN5 from the nucleus prevented its cytotoxic activity (figure 3), indicating that AeCRN5 activity is the result of a perturbation of a plant nuclear-related process.

Localization studies performed on CRNs of *P. capsici* have evidenced distinct nuclear localizations, and since CRN20_624 from *P. capsici*, the only CRN DN17 protein studied so far, was shown to present a punctuated pattern of nuclear localization 2 days after its accumulation in plant cells (Stam et al., 2013), we followed GFP:AeCRN5 nuclear localization over time. We evidenced that AeCRN5 shuttled from the nucleoplasm to unknown nuclear bodies characterized by the absence of DNA material (figure 4). The dynamism of AeCRN5 localization pattern and the absence of DNA led us to hypothesize the possibility of AeCRN5 to be addressed to Speckles, which are highly dynamic nuclear molecular complexes that participate in RNA metabolism and harbor protein factors associated with RNA splicing, RNA capping... . We hypothesize, then, that AeCRN5 could be associated or in close vicinity to RNA.

To first test this, we treated *N. benthamiana* leaves with RNase and assessed AeCRN5 localization. The treatment resulted in the depletion of the localization to nuclear bodies (figure 4). By FRET-FLIM *in vivo* assay on *N. benthamiana*, we showed that AeCRN5 interacts or is in close vicinity to plant nuclear RNA.

Through this work, we demonstrated that AeCRN5 (DN17) effector interferes with host root development. We showed that it targets plant RNA in the nucleus where it exhibits a dynamic subnuclear localization that depends on RNA. To our knowledge, AeCRN5 is the first eukaryotic effector shown to target RNA. The work provides new insights into the mode of action of eukaryotic effector where the targeting of host RNA seems central.

The corresponding results will be submitted on Molecular Plant Pathology.

AeCRN5 effector from *A. euteiches* targets plant nuclear RNA and worries host root architecture

Diana Ramirez-Garcés Laurent Camborde, Alain Jauneau, Yves Martinez, Bernard Dumas, Elodie Gaulin

38 **SUMMARY**

39
40
41
42

43 The Crincklers (or CRN) are a class of translocated effectors produced by oomycete
44 phytopathogens and little is known about their function. Here we report on the function
45 of AeCRN5 from the legume root pathogen *Aphanomyces euteiches*, belonging to a CRN
46 family which is ubiquitous in oomycetes and display orthologs in fungi. AeCRN5 is
47 a modular protein of the CRN effector family containing a functional translocation signal
48 at its N- terminus and a cell-death inducing nuclear C-terminus DN17 domain. The effector
49 expression is induced during colonization of the host root cortex of the legume *Medicago*
50 *truncatula*. Stable expression of AeCRN5 in *M. truncatula* trigger death of the root
51 system or restricts it drastically. Addition of a nuclear export signal abolished AeCRN5
52 cell-death inducing activity in *N. benthamiana* leaves. Confocal imaging show that
53 AeCRN5 shuttles in a RNA-dependent manner from plant nuclei to unknown nuclear
54 bodies. FRET-FLIM measurements on *N. benthamiana* leaves demonstrate the close
55 vicinity of AeCRN5 and plant RNA at the nuclear level. These results, combined with the
56 first demonstration that an eukaryotic effector targets plant RNA, reveals a new mode of
action of effector where nucleic acid from the host is a central target.

INTRODUCTION

Plant-associated microorganisms rely on the secretion of a particular class of molecules, termed “effectors” to successfully establish infection. These molecules interact with plant targets to modify plant defense responses and to reprogram host physiology, contributing in rendering host niche profitable to sustain growth and spreading of pathogens (Okmen and Doehlemann, 2014). Effectors can be secreted to the apoplastic interfaces (apoplastic effectors) or can be delivered into host cells (intracellular effectors) where they are addressed to different subcellular compartments. A substantial number of microbial effectors are addressed to plant nuclei and their function, assessed mainly through the identification of their plant target, are best characterized in bacteria (Rivas and Genin, 2011). These effectors target different nature of host nuclear factors including proteins, RNA and DNA to perturb plant physiology by, for example, reprogramming host transcription (Deslandes and Rivas, 2012; Bhattacharjee et al., 2013; Canonne and Rivas, 2012). In contrast, the mode of action of nuclear targeted eukaryotic effectors is still elusive.

Oomycetes (Stramenopiles) are eukaryotic filamentous microorganisms comprising several of the most devastating plant pathogens with tremendous impacts on natural and agricultural ecosystems (Thines and Kamoun, 2010). In oomycetes, two main classes of intracellular effectors have been described: the RXLR effectors and Crinklers (CRN), harboring distinct translocation signals. Crinklers (Crinkling and Necrosis, CRN), firstly reported on the potato late blight agent *Phytophthora infestans* (Torto et al., 2003; Haas et al., 2009), are ubiquitous in plant pathogenic oomycetes, with numbers ranging from 45 genes in *Pythium sp* (Lévesque et al., 2010) to 200 genes in *P. infestans* (Haas et al., 2009). All CRNs display a conserved LFLAK N-terminal motif, altered as LYLAK in *Albugo sp* (Kemen et al., 2011), LxLYLAR/K in *Pythium sp* (Lévesque et al., 2010) and LYLALK in *A. euteiches* (Gaulin et al., 2008). *Phytophthora* and *Aphanomyces* N-

85 terminal motifs have been shown to act as host cytoplasm-delivery signals (Schornack et al.,
86 2010). Not all CRNs harbor a predicted signal peptide, although detected by mass
87 spectrometry in culture medium of *P.infestans* (Meijer et al., 2014). CRN Ctermini diversity
88 contrasts to the conservation of Ntermini and is thought be the result of recombinations of
89 different subdomains occurring after a HVLVXXP Nterminal motif that occurs prior to the
90 C-terminus. First reported through a genome mining in *P. infestans*, these subdomains
91 associate, in different combination that define 27 CRN families (Haas et al., 2009), and do
92 not display any significant similarity to known functional domains, except few cases (ie,
93 serine/threonine kinase D2 domain of PiCRN8, (van Damme et al., 2012). Few new
94 CRNs families have been reported upon complete genome analysis of distinct oomycete
95 species (ie, *Phytophthora capsici*, *Pythium sp.*, *A. euteiches*) suggesting that CRNs belong
96 to an ancient effector family that arose early in oomycete evolution. CRN-like sequences
97 presenting similarities to *Phytophthora* Ctermini were recently evidenced in the genome of
98 the amphibian pathogen fungus *Batrachochytrium dendrobatidis* and the arbuscular
99 mycorrhizal fungus *Rhizophagus irregularis* (Sun et al., 2011; Lin et al., 2014).

100 Oomycetal CRNs Ctermini localize in plant nuclei where they display distinct
101 subcellular localisations including nuclei, nucleoli and unidentified nuclear bodies (Stam
102 et al., 2013a), depicting different nuclear activities and targets. Although initially
103 reported as necrosis-inducing proteins when expressed *in planta*, it has been shown that this
104 is only the case for few CRN as a large number do not cause cell-death (Haas et al.,
105 2009; Shen et al., 2013). *Phytophthora* CRNs have distinct pattern of expression during
106 various life stages and colonization of host plants (Stam et al., 2013c). Several *Phytophthora*
107 CRN can suppress cell death triggered by cell-death inducers or other CRNs (Liu et al.,
108 2011b; Shen et al., 2013), reduce plant defense gene expression or accumulation of reactive
109 oxygen species (ROS) in *N. benthamiana* (Rajput et al., 2014) sustaining the view that CRN
110 might act as suppressors of plant immunity, although not all promote infection (Stam et al.,

111 2013c). Up to now the precise function of CRN is still elusive, only biochemical activity
112 identified is a kinase activity of CRN8 of *P. infestans* (van Damme et al., 2012).

113 This work gives first insights into a new mode of action of an eukaryotic effector by
114 deciphering a nuclear activity of AeCRN5 C-terminal region of *A. euteiches*. The soil
115 born pathogen *Aphanomyces euteiches* causes root rot disease on various legumes including
116 alfalfa, clover, snap bean and stands as the most notorious disease agent of pea causing 20 to
117 100% yield losses and infects the model legume *M. truncatula* (Gaulin et al., 2007).
118 AeCRN5 was firstly identified in a cDNA library from *M. truncatula* roots in contact
119 with *A. euteiches* (Gaulin et al., 2008). It presents a modular architecture with a N-terminal
120 functional LYLALK ensuring host delivery (Schornack et al., 2010) and a DN17 family
121 domain at its Cterminus that triggers cell-death *in planta*. Here we showed that AeCRN5 is
122 induced during the cortex colonization of *Medicago truncatula* roots and that its
123 overexpression in host affects drastically *M. truncatula* root development. Confocal
124 studies on *N. benthamiana* leaves showed that the cell-death inducing activity of AeCRN5
125 required its nuclear localization. Moreover the observed dynamic relocalization of
126 AeCRN5 from nucleoplasm to unknown nuclear bodies required plant RNA. Finally
127 FRET-FLIM measurements revealed the close vicinity of AeCRN5 Cterminus and RNA at
128 the plant nuclear level. These results indicate that CRN DN17 family function by targeting
129 host plant nucleic acid.

130

131 **RESULTS**

132 **AeCRN5 is a CRN DN17 family protein and is expressed during *M. truncatula*** 133 **roots infection**

134

135 Oomycete CRNs proteins display a modular architecture, with conserved N-terminal
136 translocation regions (containing highly conserved LFLAK and HVLVXXP motifs)

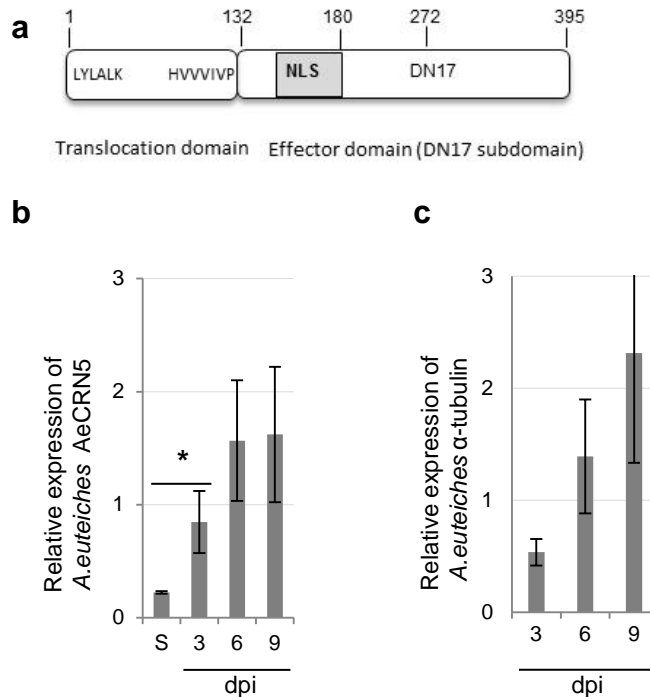


Fig 1. AeCRN5 from the oomycete *Aphanomyces euteiches* is a CRN DN17 effector family expressed during infection of *Medicago truncatula* roots. (a) Schematic representation depicting AeCRN5 protein architecture from the root rot pathogen of legumes *A. euteiches*. At the Nterminus a translocation domain characterized by a LYLALK and HVVVIVP conserved sequence that precedes the putative DN17_like effector domain (Cterminus) in which a NLS is predicted. Number indicates amino acid positions (b) Graphs show expression level of AeCRN5 (left) and *A. euteiches* α -tubulin (right) measured by qRT-PCR at 3, 6 and 9 days post-inoculation (dpi) in *M. truncatula* roots. S: free-living mycelium. Values are the mean of three independent biological replicates. Error bars are standard deviation errors. Asterisk indicate that the values are significantly different (p -value <0.05 , t -test).

137 followed by variable C-terminal regions organized in subdomain combinations that specify
138 effector function (Haas et al., 2009). The AeCRN5 (Ae_1AL4462,
139 [http://www.polebio.scsv.ups-
140 LQLYALK \(50-55aa\) motif and a HVVVIVPEVPL \(123-130aa\) motif marking its end
141 \(Figure 1a\). Although it lacks a predicted signal peptide, the AeCRN5 Nterminus is a
142 functional secretion domain mediating translocation of oomycetal effectors to plant cell
143 \(Schornack et al.2010\). The Cterminal region shows a sequence identity of 38% with the
144 CRN DN17 family domain of *P. infestans* \(Haas et al.2010\) and harbors a nuclear
145 localisation signal \(NLS 149-176aa\) consistent with its plant nuclear localization when
146 expressed in *Nicotiana benthamiana* leaves \(Schornack et al., 2010\). CRN- like sequences
147 including DN17 family have been recently reported in the fungus *Batrachochytrium*
148 *dendrobatidis* \(Bd\), a pathogen of amphibians, and the arbuscular mycorrhizal fungus
149 *Rhizophagus irregularis* \(Ri\) \(Sun et al., 2011; Lin et al., 2014\). The homology of CRN
150 proteins from the DN17 subfamily is most obvious in the C-terminal region. Sequence
151 comparison showed that AeCRN5 is closest to the *Bd* homolog \(45% identity\) than to
152 oomycetes CRN \(less than 38% identity\) \(Supplemental Figure 1\). The DN17 homolog in *R.*
153 *irregularis* displayed less than 20% identity with AeCRN5 at its Cterminal region and
154 harbored an extension of about 20 amino acid residues, suggesting distinct function and/or
155 localization for this candidate effector.](http://www.polebio.scsv.ups-tlse.fr/aphano/)

156 AeCRN5 was firstly identified in a cDNA library from *A. euteiches* mycelium grown
157 in close vicinity of *Medicago truncatula* roots (Gaulin et al., 2007). To characterize its
158 expression during infection, we conducted qRT-PCR analyses on saprophytic mycelium and
159 on infected roots of *M. truncatula*. AeCRN5 is expressed in saprophytic mycelium and
160 induced at the early stage of the infection of *M. truncatula* (3-6 dpi) (Figure 1b). This
161 expression is correlated to a sustained development of the infectious mycelium as shown by
162 *A. euteiches* quantification in roots (Figure 1c) and corresponds to an infection stage where

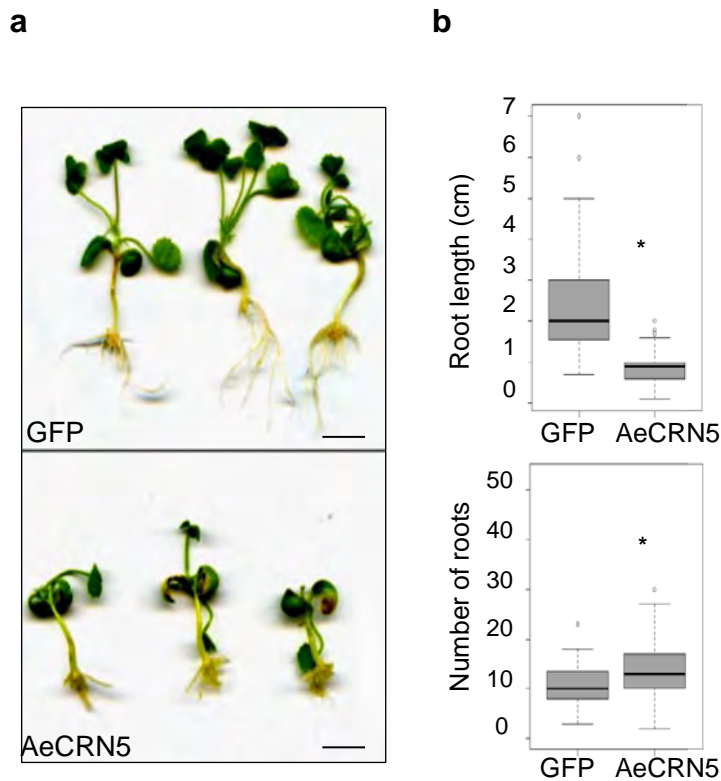


Fig 2. AeCRN5 modifies host root architecture. *M. truncatula* plantlets were transformed with *A. rhizogenes* to express GFP (control) and GFP-tagged AeCRN5 Cterminal domain (AeCRN5) constructs. (a) Photographs of 30 day-old composite plants showing representative phenotypes of composite plants and their effects on overall development and on root system architecture. Scale bars: 1 cm. (b) Box-plot graphics presenting the average of length and root number per root system. Measures and statistical analyses were performed on n=60 (GFP), n=145 (AeCRN5). * (*t*-test, p-value<0.05).

163 most of the cortical root tissues are colonized (Djéballi et al., 2009).

164

165 **AeCRN5 perturbs root architecture of the host plant *M. truncatula***

166

167 AeCRN5 Ctermini (DN17) induces cell death symptoms when overexpress in
168 *Nicotiana benthamiana* leaves (Schornack et al. 2010). To characterize AeCRN5 activity
169 in host cells, we transformed *M. truncatula* roots with a GFP-tagged AeCRN5 Ctermini
170 (130-370) using *Agrobacterium rhizogenes*-mediated transformation system (Boisson-
171 Dernier et al., 2001). Within two weeks after transformation, a large number of the
172 plantlets collapsed without generating new roots, in contrast to control plants
173 suggesting a cytotoxic activity for AeCRN5 in *M. truncatula*. Within three weeks, plants
174 that developed presented a reduction of development of aerial and root systems (Figure 2a).
175 Quantification of root length and number (Figure 2b) indicated that AeCRN5
176 transformed roots presented a decrease of root length and a higher number of roots as
177 compare to GFP- control plants. These observations indicate that AeCRN5 worries the
178 root architecture of the host plant *M. truncatula* by an unknown mechanism.

179

180 **AeCRN5 cell-death inducing activity requires nuclear localization**

181

182 To go further we assessed whether the observed cytotoxic effect of AeCRN5
183 Cterminus on *Nicotiana* and *Medicago* plants is the result of a nuclear-related localization.
184 For this purpose a Nuclear Export Signal (NES) or its mutated (mNES) counterpart was
185 fused Nterminally AeCRN5 Cterminus. The resultant fusion proteins were Nterm GFP
186 tagged and the constructs were expressed in *N. benthamiana* leaves by agroinfiltration.
187 Necrotic lesions were observed within 5 days with AeCRN5 construct, whereas no
188 symptoms were detected on leaves treated with NES:AeCRN5, even at longer times (>8

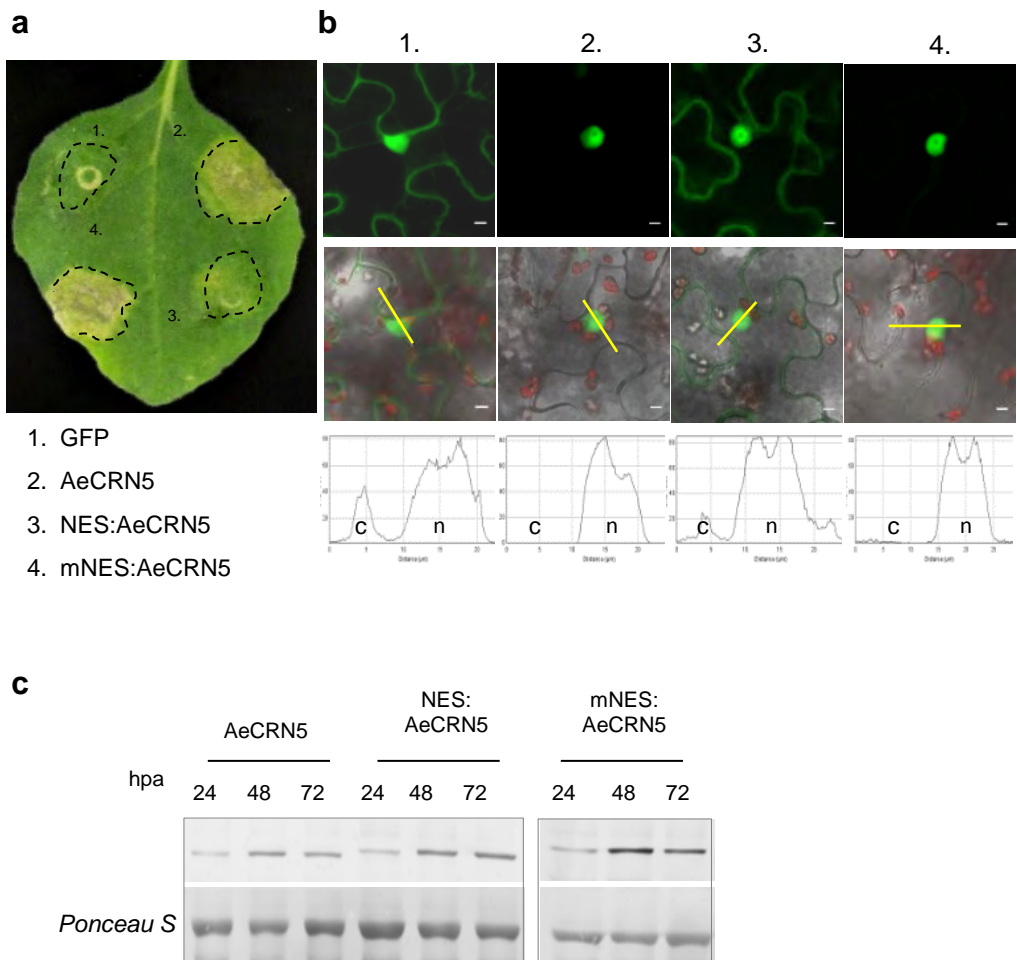


Fig 3. AeCRN5 nuclear localization is required for cell-death inducing activity. (a) Representative symptoms on *N. benthamiana* leaves expressing the indicated constructs (scale bar: 1 cm). Photographs were taken 5 days after agroinfection. (b) Micrographs of epidermal cells acquired 24h after agroinfiltration by confocal imaging. Upper panels shown the localization of GFP and GFP-tagged fusion proteins in *N. benthamiana* while middle panels show merged channels in which chloroplasts's autofluorescence appears in red while yellow lines indicate sections measured for GFP signal intensity whoan in lower panels (Scale bars : 5 μ m). (c) Western-blot analysis of expression of the indicated GFP-tagged fusion proteins in leaves of *N. benthamiana* 24, 48, and 72 hours post-agroinfiltration (hpa). Blots were probed with GFP antibodies.

189 days) (Figure 3a). The addition of a mNES, restored the cytotoxic activity of AeCRN5.
190 Confocal microscopy imaging carried 24h after agroinfiltration confirmed that GFP-
191 AeCRN5 fusion protein was restricted to the nucleus (Figure 3b). An enhancement of
192 nuclear export of AeCRN5 protein was detected with NES:AeCRN5 construct, since the
193 GFP signal was recovered also in the cytoplasm. Fluorescence intensity, measured in cells,
194 corroborated NES:AeCRN5 partial mislocalization from the nucleus (Figure 3b, lower
195 panels). A reestablishment of green fluorescence at the nuclear level was obtained for the
196 mNES:AeCRN5 construct. Immunoblot analysis confirmed the accumulation of the fusion
197 proteins from 1 to 3 days after agroinfection (Figure 3c). Altogether the results
198 showed that the cell death phenotype requires AeCRN5 to localize and accumulate in the
199 nucleus.

200

201 **AeCRN5 accumulates in subnuclear structures and does not co-localize with nuclear** 202 **DNA**

203

204 Recent evidences on *P. caspici* CRNs suggested a link between *N. benthamiana*
205 subnuclear localization and PcCRN activity (Stam et al., 2013b). We thus precised GFP-
206 AeCRN5 Cterminus localization using agrobacterium-mediated transient expression assay
207 on *N. benthamiana* leaves. Two distinct subnuclear localizations of AeCRN5 were
208 observed (Figure 4a-b). As reported above, the fluorescence was either dispersed
209 throughout the nucleoplasm with the exception of the nucleolus or sequestered in patches in
210 unknown nuclear bodies (Figure 4a-c). Both distributions were observed during time. This
211 dynamics and localization pattern in unknown nuclear bodies evokes 'nuclear speckles pattern.
212 Nuclear speckles are small subnuclear membraneless organelles which appear as irregular and
213 transient punctuate structures at the microscopic level located in interchromatin regions of the
214 nucleoplasm (Lorković et al., 2008; Spector and Lamond, 2011). Speckles act as a reservoir of
215 factors that participate in transcription and pre-mRNA processing. Thereby we evaluated

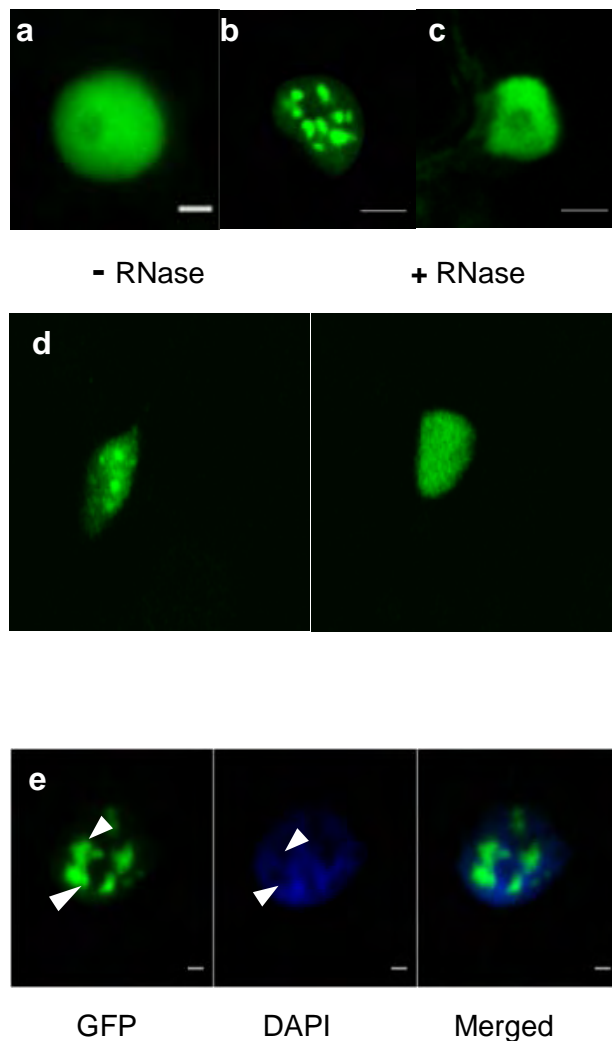


Fig 4. AeCRN5 shuttle from nucleoplasm to unknown nuclear bodies in a RNA-dependent manner. Confocal images of *N. benthamiana* leaves expressing GFP-tagged AeCRN5 effector at 1 day post-agroinfiltration. (a-c) Representative micrographs of AeCRN5 subnuclear localisation in which close-up images revealed either an homogeneous (a) or a ‘patched’ (b) distribution of fluorescence. This pattern is reminiscent with ‘nuclear speckle pattern’ (white arrows) (Scale bar 5 μ m). (d) Confocal micrographs depicting AeCRN5 subnuclear localisation after RNase treatment on cells, where the fluorescence is recovered only in the nucleoplasm with the exception of the nucleolus. (e) Representative images of a “patched” AeCRN5 localization where AeCRN5 distribution (white arrows) is shown in the GFP channel and chromatin distribution is revealed by DAPI labelling (DAPI). Merged signal indicates absence of DNA material in zones where AeCRN5 localizes (Scale bar 5 μ m).

216 whether subcellular localization of AeCRN5 is a RNA-dependent mechanisms. As shown
217 on Figure 4d, RNase treatment on *N. benthamiana* epidermal cells expressing
218 GFP:AeCRN5 abolished the ‘speckle pattern’ of AeCRN5. Moreover a counterstaining
219 with the nucleic acid stain 4',6-diamidino-2- phenylindole (DAPI), revealed an absence of
220 complementary fluorescence pattern in which nuclear DNA and GFP fluorescence do not
221 colocalized (Figure 4e). These data suggest a dynamic RNA-dependent process for
222 AeCRN5 nuclear localization and therefore activity, where plant DNA might not be a
223 central player.

224

225 **AeCRN5 targets nuclear RNA in planta**

226

227 We reasoned that AeCRN5 perturbs a plant nuclear-related process leading
228 to cytotoxic activity, probably by targeting plant nuclear components. We firstly assessed
229 the possibility that AeCRN5, like numerous nuclear-targeting bacterial effectors, may be
230 able to bind plant nucleic acids. We thus set up a fluorescence resonance energy
231 transfer (FRET) assay coupled with fluorescence lifetime imaging microscopy (FLIM)
232 in *N. benthamiana* cells. GFP:AeCRN5 and GFP alone were expressed in *N.*
233 *benthamiana* epidermal cells by agroinfiltration and plant nucleic acids were stained with
234 SytoxOrange. In these conditions, the occurrence of FRET, causing the fluorescence
235 lifetime of the donor GFP to decrease, would only be due to the proximity (less than 10
236 nm) of GFP to SytoxOrange. Energy transfer was detected by fluorescence lifetime
237 imaging microscopy (FLIM). Additionally to GFP alone, we used cells expressing the
238 DNA-binding protein H2B in fusion to GFP (GFP:H2B).

239 As reported in Table 1, in presence of Sytox Orange, GFP presented a mean life-time of
240 2.210 +/- 0.041 ns. Coupled to H2B, its life-time was reduced to 1.852 +/-0.047 nsec
241 attesting that, by interacting to DNA, H2B places GFP close to the a protein energy
242 acceptor. In the case of AeCRN5 construct, the lifetime of GFP:AeCRN5 was 2.128+/-

Table 1. Summary of FRET-FLIM conditions and values obtained on foliar discs of *N. benthamiana* expressing the different fluorescent donor proteins.

Donor	Acceptor	τ (a)	s.e.m (b)	N (c)	E (d)	p-value (e)
GFP	-	2.246	0.036	20	-	-
	Sytox Orange	2.210	0.0417	18	1.6	0.52
GFP:H2B	-	2.465	0,0167	40	-	-
	Sytox Orange	1.852	0,0472	43	24.8	2.31E-19
GFP:AeCRN5	-	2.128	0,0692	27	-	-
	Sytox Orange	1.899	0,0698	10	10.7	5.56E-07
	Sytox Orange (RNAse treatment)	2.228	0,1057	17	0	0.55

τ : mean GFP lifetime in nanoseconds (ns). For each nucleus, average fluorescence decay profiles were plotted and lifetimes were estimated by fitting data with exponential function using a non-linear least-squares estimation procedure. (b) s.e.m.: standard error of the mean. (c) N: total number of measured nuclei. (d) E: FRET efficiency in % : $E=1- \tau(DA)/ \tau(D)$. (e) p-value (Student's t test) of the difference between the donor lifetimes in the presence or absence of acceptor

243 0.069 nsec in the absence of SytoxOrange and decreased significantly to 1.899 +/-0.069
244 nsec in presence of the dye, indicating an energy transfer and thereby the binding of DN17
245 domain to nucleic acids. To go further, and since Sytox Orange dye is not specific for
246 either DNA or RNA, samples were treated with RNase A to digest RNA before
247 performing the experiment. After RNase treatment, the 2.228 +/-0.105 nsec lifetime of
248 GFP:AeCRN5 was similar than those observed without Sytox Orange (2.128 2.228 +/-0.069
249 nsec) (Table 1). Hence in these conditions FRET phenomenon was only RNA-dependent
250 and indicated that DN17 domain of AeCRN5 targets nuclear RNA *in vivo*.

251

252

253 **DISCUSSION**

254

255 To favor the establishment of disease, microorganisms have gained the ability
256 to deliver effector molecules inside host cells. The important number of effectors targeting
257 host nuclei places this organelle, and functions related to it, as important hubs whose
258 perturbations might be of crucial importance for the outcome of infection (Bhattacharjee et
259 al., 2013; Deslandes & Rivas, 2012). CRNs proteins are ubiquitous in plant pathogenic
260 oomycetes and are reported as a wide class of translocated effectors (Schornack et al.,
261 2010). Previously, we showed that the cell-death inducing AeCRN5 effector from the root
262 rot pathogen *A. euteiches* is a plant nuclear localized effector with a functional Nterminus
263 translocation signal (Schornack et al., 2010). In this work we showed that AeCRN5
264 perturbs root development of the host plant *Medicago truncatula* and targets plant RNA at
265 the nuclear level.

266 Oomycetal CRN proteins present a modular architecture and include a conserved
267 Ntermini functioning in plant delivery and diverse Cterminal domains thought to direct
268 the activity (Haas et al., 2009). AeCRN5 is a modular CRN DN17 protein family

269 with orthologous sequences in *Phytophthora* sp. and true fungal species including the
270 chytrid *B. dendrobatidis* and the ectomycorrhiza *R. irregularis*. The functional translocation
271 signal of AeCRN5 is characterized by a LYLALK and a HVVVIP motifs and the absence of
272 an obvious signal peptide (Schornack et al., 2010, Gaulin et al., 2007). The C-terminus
273 corresponds to a CRN DN17 domain family with a NLS (Haas et al., 2009, Schornack et al.,
274 2010) which have no significant similarity to functional domain. The closest ortholog of
275 AeCRN5 is found in the *Bd* fungus rather than *Phytophthora* species, suggesting a
276 conserved function for this orthologous gene. In contrast the sequences features of DN17
277 from *R. irregularis* may indicate distinct cellular localization and function for this candidate
278 effector.

279 *Phytophthora* CRNs were originally identified as activators of plant cell death
280 upon their *in planta* expression (Torto et al., 2003), although not all CRNs promote infection
281 including the AeCRN5 ortholog from *P. capsici* (Stam et al., 2013b). CRN5 sequences
282 from *A. euteiches* were firstly reported in a cDNA library from mycelium grown in close
283 vicinity of *M. truncatula* roots (Gaulin et al., 2008) and the corresponding gene models are
284 present in the complete genome sequence of ATTC201684 *A. euteiches* strain (Gaulin et
285 al., unpublished results). Here we showed by qRT-PCR analysis, that AeCRN5 is expressed
286 during vegetative growth and expression goes up from 3-6 days after infection of roots, a
287 stage where browning of roots is observed in combination to an entire colonization of the
288 root cortex of *M. truncatula*, and the initiation of propagation to vascular tissues (Djéballi et
289 al., 2009). Recently two classes of *P. capsici* CRN expression were defined based on
290 contrasted expression pattern during host leaves infection (Stam et al., 2013b) . *P. capsici*
291 DN17 ortholog felt in class 2 with genes expressed in the latest stages of *Solanum*
292 *lyopersicum* infection, suggesting an important role of PcCRN5 at the later stages of
293 colonization. However another similar study on *P.phaseoli* CRN showed that CRNs were
294 mostly repressed in leaves of lima bean (Kunjjeti et al., 2012). Thus for conclusive

295 statements, large gene expression studies of AeCRNs repertoire (> 100 genes models,
296 Gaulin et al., unpublished) are required to precise the putative contribution of AeCRN5 and
297 each AeCRN class during the different stages of *M. truncatula* infection.

298 We further explored the function of AeCRN5 by using a GFP-DN17 tagged version
299 of the domain. Overexpression of AeCRN5 in *M. truncatula* roots displayed a cytotoxic
300 effect leading in few days to death of transformed plants. The surviving plants were dwarf
301 and harbored reduced root systems with a higher number of roots. These results corroborate
302 observations made during *M. truncatula* roots infection, where susceptible accessions
303 present, within few days after *A. euteiches* infection, a decrease of secondary root
304 development and necrosis of roots (Djéballi et al., 2009).

305 Confocal studies on transiently transformed *N. benthamiana* leaves showed that DN17
306 cytotoxic effect of AeCRN5 required a plant nuclear accumulation. It is in accordance
307 with the observed reduction of cell death on *N. benthamiana* leaves, upon nuclear exclusion
308 of CRN8 (D2 domain) from *P. infestans* (Schornack et al., 2010). We can therefore suggest
309 that nuclear localization is an important requirement for the cell-death inducing
310 activity of necrotic CRN effectors. Previous study on *P. capsici* DN17 CRN domain has
311 shown its nucleoplasmic localization in *N. benthamiana* leaves upon its expression.

312 Interestingly, we observed here that DN17 shuttles between nucleoplasm and unknown
313 plant nuclear bodies where DNA is excluded. This subnuclear relocation of AeCRN5 is
314 RNA dependent. In addition FRET-FLIM measurements revealed the close vicinity of
315 DN17 with plant RNA at the nuclear level. The dynamics and punctuate localization of
316 DN17 in combination with its proximity to plant RNA, strongly suggest a 'nuclear speckled
317 pattern'. Nuclear speckles are nuclear granules of variable size and irregular shape, which
318 do not contain DNA and often observed close to highly active transcription site. Nuclear
319 speckles are best known to accumulate spliceosome subunit, splicing factor and many
320 factors involved in mRNA production (Spector and Lamond, 2011). Our results support the

321 idea that AeCRN5 might be recruited to speckles and, thus, suggests that AeCRN5
322 could affect directly or indirectly splicing activities on RNA molecules. Future studies
323 will aim to precise the subnuclear localization of AeCRN5 and its effect on host
324 transcriptional activity.

325 To our knowledge AeCRN5 is the first effector from eukaryotic plant pathogenic
326 microbes known to interfere with nuclear RNA, probably leading to host cytotoxic effect.
327 We are aware that *M. truncatula* root growth inhibition or cell-death inducing symptoms on
328 *N. benthamiana* leaves may be the result of AeCRN5 overexpression. Nonetheless,
329 perturbation of plant development caused by pathogens to facilitate microbial establishment
330 through an indirect manipulation of host RNA machinery have been documented for
331 prokaryotic effector. For instance, TAL effectors (ie, PthA4) from *Xanthomonas citri* target
332 negative regulators of RNA Pol II and Pol III to coordinately increase the transcription
333 activity of host cells thought to enhance bacterial installation (de Souza et al., 2012; Soprano
334 et al., 2013). Microbial manipulation of RNA machinery to subvert host immunity may be
335 another mode of action of effector. Recently two RXLR nuclear-localized effectors from
336 *Phytophthora sojae* were shown to inhibit the biogenesis of small RNA probably by
337 targeting plant DICER-like protein or cofactors, to promote infection (Qiao et al., 2013). In
338 fungi, 72 of the 492 candidate effectors of the fungus *Blumeria graminis* show structural
339 similarity to ribonucleases (Pedersen et al., 2012a). Some of them contribute to infection
340 (BEC1054) and their activity is supposed to be related to host RNA binding (Pliego et al.,
341 2013). Targeting of host RNA has also been proposed for effectors of the nematode *M.*
342 *incognita* as they present putative RNA binding domains (Bellafiore et al., 2008).

343 This study shows that the ancestral oomycete *A. euteiches* has evolved plant nuclear
344 CRN effectors that interfere with plant RNA and gives first insights into a new mode of
345 action of eukaryotic effectors. The nature of RNA targeted by DN17 domain as well as
346 interactors that could be involved in such process will provide further understanding on

347 CRN function and further elucidation of mechanisms by which pathogens may manipulate
348 host RNA machinery and related functions.

349
350

351 **EXPERIMENTAL PROCEDURES**

352

353 **Plant material, microbial strains, and growth conditions**

354

355 *M. truncatula* F83005.5 seeds were scarified, sterilized, and cultured *in vitro* for root
356 transformation of and infection as previously described (Boisson-Dernier et al.,2001;
357 Djébali et al., 2009). Infection of roots with zoospores of *A. euteiches* (strain ATCC
358 201684) was performed as Djébali et al., 2009. *N. benthamiana* plants were grown from
359 seeds in growth chambers at 70% of humidity with a 16h/8h dark at 24/ 20°C
360 temperature regime. *A. euteiches* (ATCC 201684) was grown on saprophytic conditions as
361 previously reported (Badreddine et al., 2008). All *E.coli* strains (DH5 α , DB3.5, BL21AI).
362 *A. tumefaciens* (GV3101:: pMP90RK) and *A. rhizogenes* (ArquaI) used were grown in LB
363 medium with the appropriate antibiotics.

364

365 **Sequence analyses**

366

367 Oomycetal and fungal orthologs of AeCRN5 (Ae_1AL4462,
368 <http://www.polebio.scsv.ups-tlse.fr/aphano/>) was retrieved by BlastP searches using Broad
369 Institute Database Search tools (<http://www.broadinstitute.org>) on the corresponding *P.*
370 *sojae* (Ps_132663) and *P. ramorum* (pRg882635), *P. capsici* (Pc_CRN20_624) and
371 *Batrachochytrium dendrobatidis* (BD_07009.1) genome database. The *Rhizophagus*
372 *irregularis* ortholog sequence ((Ri, gm1.18625_g) was collected from (Lin et al., 2014);
373 CRN DN17 consensus sequence was retrieved from supplementary data of Haas et al.,
374 2009. All sequences alignments were performed using ClustalW2.

375

376 **RNA extraction and qRT-PCR**

377

378 Samples were ground on liquid nitrogen and total RNA extracted using the RNAeasy kit
379 (Qiagen). Reverse transcription was performed on 1µg of total RNA using the
380 AppliedBiosystems kit (Life Technologies-Invitrogen). cDNAs were diluted 50- fold
381 for qPCR reaction. Each qPCR reaction was performed on a final volume of 10µl
382 corresponding to 8 µl of PCR mix (0.5µM of each primer and 5µl SYBRGreen, Applied
383 Biosystems) and 2µl of the diluted cDNA and was conducted on a ABI Prims SDS
384 7900 HT (AppliedBiosystems, Foster City, CA, USA) device using the following
385 conditions: 5min at 95°C, followed by 45 cycles of 15 s at 95°C and 1min at 60°C.
386 Dissociation curves were obtained by applying a 15s 95°C, 15s 95°C and 15s 95°C cycle.
387 Each reaction was conducted on triplicates for cDNAs of four biological replicates. Primers
388 F:5'- GAAATTCTGCAAGAAGACTCCA-3' and R:5'- CAATAAAGATGTTGAGAGTGGC-
389 3' were used for the detection of AeCRN5. Primers F: 5'-
390 TGTCGACCCACTCCTTGTTG-3' and R: 5'-TCGTGAGGGACGAGATGACT-3' were
391 used to assess the expression of *A. euteiches*'s α -tubulin gene (Ae_22AL7226) and
392 normalized AeCRN5 expression. Histone 3-like of *M. truncatula*, previously described
393 (Rey et al., 2013) was used to normalize *A. euteiches* abundance during infection. Relative
394 expression of AeCRN5 and α -tubulin genes were calculated using the $2^{-\Delta\Delta Cq}$ method
395 described by (Livak and Schmittgen, 2001).

396

397

398 **Construction of plasmid vectors**

399

400 Sequences and names of primers used in this study are listed in the supplementary Table 1.

401 AeCRN5 Cterminal version carrying Gateway adaptors were generated by PCR on a

402 template corresponding to the unigene Ae_1AL4462 (vector pSport_Ae_1AL4462). Full
403 length Cterminus AeCRN5 (132aa-370aa) was generated using primer AttB1AeCRN5-F
404 and AttB2AeCRN5-R. Amplicon was BP recombined in pDONR-Zéo vector (Invitrogen)
405 and subsequently introduced in vector pK7GWF2 by means of LR recombination
406 (Invitrogen). *GFP:NES:AeCRN5* and *GFP:mNES:AeCRN5* constructs were generated by
407 adding NES sequence (LQLPPLERLTL) and non-functional mutated NES sequence
408 (mNES: LQAPPAERATL) to the Nterminal moiety of AeCRN5. Amplicons NES:AeCRN5
409 and mNES:AeCRN5 were obtained using primers NES:AeCRN5-F and AeCRN5_end-R
410 and mNES_AeCRN5-F and AeCRN5_end-R respectively and introduced in pENTR/ D-
411 TOPO vector by means of TOPO cloning (Invitrogen) before insertion on vector
412 pK7GWF2. Amplification of the histone 2B of *A. thaliana* was performed on vector
413 pBI121:H2B:YFP REF with primers cacH2B-F and H2B-R. Amplicons were cloned in
414 pENTR/ D-TOPO and subsequently introduced in vector pK7GWF2 to obtain *GFP:H2B*
415 fusion construct. The obtained pK7GWF2 recombined vectors were introduced in
416 *Agrobacterium* strains for *N. benthamiana* agroinfiltration assays and/or *M. truncatula* roots
417 transformation.

418

419 **Immunoblot analyses**

420

421 Samples corresponding to agroinfiltrated *N. benthamiana* leaves were frozen in liquid
422 nitrogen. Protein extraction was performed as previously reported (Schornack et al., 2010).
423 Proteins were separated by SDS-PAGE and electroblotted on nitrocellulose
424 membranes (Amersham BioSciences). AeCRN5 and the respective mutant versions were
425 revealed using anti-GFP polyclonal antibodies 1:2000, Clontech) and anti-rabbit secondary
426 antibodies coupled to alkaline phosphatase (Sigma-Aldrich).

427

428

429

430 ***Agrobacterium*-mediated transformation**

431

432 Generation of *M. truncatula* composite plants was performed as described by Boisson-
433 d'arnier et al, 2001 using ARQUA-1 (*A. rhizogenes*) strain. Leaf infiltration were
434 performed with *A. tumefaciens* (GV3101:: pMP90RK) as previously reported (Schornack et
435 al., 2010).

436

437 **Confocal microscopy**

438

439 Foliar discs (5-8 mm of diameter) of infiltrated leaves of *N. benthamiana* were sampled
440 at different time points after agroinfiltration and fixed in a PBS, 4% (v/v) paraformaldehyde
441 solution and then stained with DAPI (3 μ g/ μ L). Scans were performed on a Leica TCS
442 SP2 AOBS device using wavelengths 488nm (GFP) and 350 nm (DAPI) and with a 40x
443 water immersion lens. Acquisitions were done in a sequential mode to avoid overlapping
444 fluorescence signals. Images were treated with Image J software and correspond to Z
445 projections of scanned tissues.

446

447 **Preparation of *N. benthamiana* epidermal leaves for FRET / FLIM**

448 **experiments**

449

450 Discs of agroinfiltrated *N. benthamiana* leaves were fixed 24 hours after treatment by
451 vacuum infiltrating a TBS (TRIS 25mM, NaCl 140 mM, KCl 3 mM) 4 % (w/v)
452 paraformaldehyde solution before incubation 20 min at 4°C. Samples were permeabilized 10
453 min at 37°C using a TBS buffer supplemented with 20 μ g/ml of proteinase K (Invitrogen).
454 Nucleic acid staining was performed by vacuum-infiltration of a 5 μ M of Sytox Orange
455 (Invitrogen) solution, before incubation of the samples 30 min at room temperature.
456 When RNase treatment was performed, foliar discs were incubated 15 min at room

457 temperature with 0.5 μ g/ml of RNase A (Roche) before acid nucleic staining. Foliar discs
458 were washed with and mounted on TBS before observations on an inverted microscope
459 (Eclipse TE2000E, Nikon, Japan).

460

461 **FRET/FLIM measurements**

462

463 Fluorescence lifetime measurements were performed in time domain using a streak
464 camera REF53. The light source is a mode-locked Ti:sapphire laser (Tsunami, model 3941,
465 Spectra- Physics, USA) pumped by a 10W diode laser (Millennia Pro, Spectra-Physics) and
466 delivering ultrafast femtosecond pulses of light with a fundamental frequency of 80MHz. A
467 pulse picker (model 3980, Spectra-Physics) is used to reduce the repetition rate to 2MHz to
468 satisfy the requirements of the triggering unit (working at 2MHz). The experiments were
469 carried out at $\lambda = 820$ nm (multiphoton excitation mode). All images were acquired with a
470 60x oil immersion lens (plan APO 1.4 N.A., IR) mounted on an inverted microscope
471 (Eclipse TE2000E, Nikon, Japan). The fluorescence emission is directed back into the
472 detection unit through a short pass filter ($\lambda < 750$ nm) and a band pass filter (515/30 nm). The
473 detector is a streak camera (Streakscope C4334, Hamamatsu Photonics, Japan) coupled
474 to a fast and high-sensitivity CCD camera (model C8800-53C, Hamamatsu). For each
475 nucleus, average fluorescence decay profiles were plotted and lifetimes were estimated by
476 fitting data with exponential function using a non-linear least-squares estimation procedure.
477 Fluorescence lifetime of the donor (GFP) was experimentally measured in the presence and
478 absence of the acceptor (Sytox Orange). FRET efficiency (E) was calculated by comparing
479 the lifetime of the donor in the presence (τ_{DA}) or absence (τ_D) of the acceptor: $E = 1 -$
480 $(\tau_{DA}) / (\tau_D)$. Statistical comparisons between control (donor) and assay (donor + acceptor)
481 lifetime values were performed by Student t-test. For each experiment, four leaf discs
482 removed from two agroinfiltrated leaves were used to collect data.

483

484 **ACKNOWLEDGEMENTS**

485

486 The authors would like to thank the French Ministry of Education and Research for the
487 PhD fellowship to Diana Ramirez-Garcés. We are grateful to Aurélie Le Ru (TRI-Imagery
488 Platform of Toulouse, France) for helpful assistance on confocal microscopes. The
489 research was carried out in the LRSV, part of the French Laboratory of Excellence
490 "TULIP" (ANR-10- LABX-41; ANR-11-IDEX-0002-02). This work was funded by the
491 French Centre National de la Recherche Scientifique (CNRS) and the Université Paul
492 Sabatier, Toulouse and by the French Agence Nationale pour la Recherche (ANR-12-
493 JSV6-0004-01, APHANO-Effect to EG).

References

- Badreddine, I., Lafitte, C., Heux, L., Skandalis, N., Spanou, Z., Martinez, Y., Esquerré-Tugayé, M.-T., Bulone, V., Dumas, B., and Bottin, A.** (2008). Cell wall chitosaccharides are essential components and exposed patterns of the phytopathogenic oomycete *Aphanomyces euteiches*. *Eukaryot Cell* **7**: 1980–93.
- Bellafiore, S., Shen, Z., Rosso, M.-N., Abad, P., Shih, P., and Briggs, S.P.** (2008). Direct identification of the *Meloidogyne incognita* secretome reveals proteins with host cell reprogramming potential. *PLoS Pathog* **4**: e1000192.
- Bhattacharjee, S., Garner, C.M., and Gassmann, W.** (2013). New clues in the nucleus: transcriptional reprogramming in effector-triggered immunity. *Front Plant Sci* **4**: 364.
- Boisson-Dernier, a, Chabaud, M., Garcia, F., Bécard, G., Rosenberg, C., and Barker, D.G.** (2001). *Agrobacterium rhizogenes*-transformed roots of *Medicago truncatula* for the study of nitrogen-fixing and endomycorrhizal symbiotic associations. *Mol Plant Microbe Interact* **14**: 695–700.
- Canonne, J. and Rivas, S.** (2012). Bacterial effectors target the plant cell nucleus to subvert host transcription © 2012 Landes Bioscience . © 2012 Landes Bioscience . 217–221.
- Van Damme, M., Bozkurt, T.O., Cakir, C., Schornack, S., Sklenar, J., Jones, A.M.E., and Kamoun, S.** (2012). The Irish potato famine pathogen *Phytophthora infestans* translocates the CRN8 kinase into host plant cells. *PLoS Pathog* **8**: e1002875.
- Deslandes, L. and Rivas, S.** (2012). Catch me if you can: bacterial effectors and plant targets. *Trends Plant Sci* **17**: 644–55.
- Djéballi, N. et al.** (2009). Partial resistance of *Medicago truncatula* to *Aphanomyces euteiches* is associated with protection of the root stele and is controlled by a major QTL rich in proteasome-related genes. *Mol Plant Microbe Interact* **22**: 1043–55.
- Gaulin, E., Jacquet, C., Bottin, A., and Dumas, B.** (2007). Root rot disease of legumes caused by *Aphanomyces euteiches*. *Mol plant ...* **8**: 539–548.
- Gaulin, E., Madoui, M.-A., Bottin, A., Jacquet, C., Mathé, C., Couloux, A., Wincker, P., and Dumas, B.** (2008). Transcriptome of *Aphanomyces euteiches*: new oomycete putative pathogenicity factors and metabolic pathways. *PLoS One* **3**: e1723.
- Haas, B.J. et al.** (2009). Genome sequence and analysis of the Irish potato famine pathogen *Phytophthora infestans*. *Nature* **461**: 393–8.
- Kemen, E., Gardiner, A., Schultz-Larsen, T., Kemen, A.C., Balmuth, A.L., Robert-Seilaniantz, A., Bailey, K., Holub, E., Studholme, D.J., Maclean, D., and Jones, J.D.G.** (2011). Gene gain and loss during evolution of obligate parasitism in the white rust pathogen of *Arabidopsis thaliana*. *PLoS Biol* **9**: e1001094.

- Lévesque, C.A. et al.** (2010). Genome sequence of the necrotrophic plant pathogen *Pythium ultimum* reveals original pathogenicity mechanisms and effector repertoire. *Genome Biol* **11**: R73.
- Lin, K. et al.** (2014). Single Nucleus Genome Sequencing Reveals High Similarity among Nuclei of an Endomycorrhizal Fungus. *PLoS Genet* **10**: 1–13.
- Liu, T., Ye, W., Ru, Y., Yang, X., Gu, B., Tao, K., Lu, S., Dong, S., Zheng, X., Shan, W., Wang, Y., and Dou, D.** (2011). Two host cytoplasmic effectors are required for pathogenesis of *Phytophthora sojae* by suppression of host defenses. *Plant Physiol* **155**: 490–501.
- Livak, K.J. and Schmittgen, T.D.** (2001). Analysis of relative gene expression data using real-time quantitative PCR and the 2(-Delta Delta C(T)) Method. *Methods* **25**: 402–8.
- Lorković, Z.J., Hilscher, J., and Barta, A.** (2008). Co-localisation studies of *Arabidopsis* SR splicing factors reveal different types of speckles in plant cell nuclei. *Exp Cell Res* **314**: 3175–3186.
- Meijer, H.J.G., Mancuso, F.M., Espadas, G., Seidl, M.F., Govers, F., and Sabidó, E.** (2014). Profiling the secretome and extracellular proteome of the potato late blight pathogen *Phytophthora infestans*. *Mol Cell Proteomics*: 1–33.
- Okmen, B. and Doehlemann, G.** (2014). Inside plant: biotrophic strategies to modulate host immunity and metabolism. *Curr Opin Plant Biol* **20C**: 19–25.
- Pedersen, C. et al.** (2012). Structure and evolution of barley powdery mildew effector candidates. *BMC Genomics* **13**: 2–20.
- Pliego, C. et al.** (2013). Host-induced gene silencing in barley powdery mildew reveals a class of ribonuclease-like effectors. *Mol Plant Microbe Interact* **26**: 633–42.
- Qiao, Y. et al.** (2013). Oomycete pathogens encode RNA silencing suppressors. *Nat Genet* **45**: 330–3.
- Rajput, N.A., Zhang, M., Ru, Y., Liu, T., Xu, J., Liu, L., Mafurah, J.J., and Dou, D.** (2014). *Phytophthora sojae* Effector PsCRN70 Suppresses Plant Defenses in *Nicotiana benthamiana*. *PLoS One* **9**: e98114.
- Rey, T., Nars, A., Bonhomme, M., Bottin, A., Huguet, S., Balzergue, S., Jardinaud, M.-F., Bono, J.-J., Cullimore, J., Dumas, B., Gough, C., and Jacquet, C.** (2013). NFP, a LysM protein controlling Nod factor perception, also intervenes in *Medicago truncatula* resistance to pathogens. *New Phytol* **198**: 875–86.
- Schornack, S., van Damme, M., Bozkurt, T.O., Cano, L.M., Smoker, M., Thines, M., Gaulin, E., Kamoun, S., and Huitema, E.** (2010). Ancient class of translocated oomycete effectors targets the host nucleus. *Proc Natl Acad Sci U S A* **107**: 17421–6.

- Shen, D., Liu, T., Ye, W., Liu, L., Liu, P., Wu, Y., Wang, Y., and Dou, D.** (2013). Gene duplication and fragment recombination drive functional diversification of a superfamily of cytoplasmic effectors in *Phytophthora sojae*. *PLoS One* **8**: e70036.
- Soprano, A.S., Abe, V.Y., Smetana, J.H.C., and Benedetti, C.E.** (2013). Citrus MAF1, a repressor of RNA polymerase III, binds the *Xanthomonas citri* canker elicitor PthA4 and suppresses citrus canker development. *Plant Physiol* **163**: 232–242.
- De Souza, T.A., Soprano, A.S., de Lira, N.P.V., Quaresma, A.J.C., Pauletti, B.A., Paes Leme, A.F., and Benedetti, C.E.** (2012). The TAL effector PthA4 interacts with nuclear factors involved in RNA-dependent processes including a HMG protein that selectively binds poly(U) RNA. *PLoS One* **7**: e32305.
- Spector, D.L. and Lamond, A.I.** (2011). Nuclear speckles. *Cold Spring Harb Perspect Biol* **3**:a000646.
- Stam, R., Howden, A.J.M., Delgado-Cerezo, M., M. M. Amaro, T.M., Motion, G.B., Pham, J., and Huitema, E.** (2013a). Characterization of cell death inducing *Phytophthora capsici* CRN effectors suggests diverse activities in the host nucleus. *Front Plant Sci* **4**: 1–11.
- Stam, R., Howden, A.J.M., Delgado-Cerezo, M., M. M. Amaro, T.M., Motion, G.B., Pham, J., and Huitema, E.** (2013b). Characterization of cell death inducing *Phytophthora capsici* CRN effectors suggests diverse activities in the host nucleus. *Front Plant Sci* **4**: 1–11.
- Stam, R., Jupe, J., Howden, A.J.M., Morris, J. a., Boevink, P.C., Hedley, P.E., and Huitema, E.** (2013c). Identification and Characterisation CRN Effectors in *Phytophthora capsici* Shows Modularity and Functional Diversity. *PLoS One* **8**: e59517.
- Sun, G., Yang, Z., Kosch, T., Summers, K., and Huang, J.** (2011). Evidence for acquisition of virulence effectors in pathogenic chytrids. *BMC Evol Biol* **11**: 195.
- Thines, M. and Kamoun, S.** (2010). Oomycete-plant coevolution: recent advances and future prospects. *Curr Opin Plant Biol* **13**: 427–33.
- Torto, T. a, Li, S., Styer, A., Huitema, E., Testa, A., Gow, N. a R., van West, P., and Kamoun, S.** (2003). EST mining and functional expression assays identify extracellular effector proteins from the plant pathogen *Phytophthora*. *Genome Res* **13**: 1675–85.

Table 1. Summary of FRET-FLIM conditions and values obtained on foliar discs of *N. benthamiana* expressing the different fluorescent donor proteins.

Donor	Acceptor	τ (a)	s.e.m (b)	N (c)	E (d)	p-value (e)
GFP	-	2.246	0.036	20	-	-
	Sytox Orange	2.210	0.0417	18	1.6	0.52
GFP:H2B	-	2.465	0,0167	40	-	-
	Sytox Orange	1.852	0,0472	43	24.8	2.31E-19
GFP:AeCRN5	-	2.128	0,0692	27	-	-
	Sytox Orange	1.899	0,0698	10	10.7	5.56E-07
	Sytox Orange (RNAse treatment)	2.228	0,1057	17	0	0.55

τ : mean GFP lifetime in nanoseconds (ns). For each nucleus, average fluorescence decay profiles were plotted and lifetimes were estimated by fitting data with exponential function using a non-linear least-squares estimation procedure. (b) s.e.m.: standard error of the mean. (c) N: total number of measured nuclei. (d) E: FRET efficiency in % : $E=1- \tau(DA/ \tau D)$. (e) p-value (Student's t test) of the difference between the donor lifetimes in the presence or absence of acceptor

Supplementary Table 1. Primers used for the generation of the different constructs.

Name	Sequence 5'-3'
attB1_AeCRN5-F	GGGGACAAGTTTGTACAAAAAAGCAGGCTTCTTGAAGGTG ACCGCTCTAGAACCC
attB2_AeCRN5-R	GGGGACCACTTTGTACAAGAAAGCTGGGTGTTGTTATTCA AAAAGTATGGCG
AeCRN5_end-R	TTGTTATTCAAAAAGTATGGCGTAAATTTTGGC
NESAeCRN5-F	CACCCTTCAACTCCTCCTCTTGAAGACTTACTCTTTTGA AGGTTGACCGCTCTAGAACCC
mNESAeCRN5-F	CACCCTTCAAGCTCCTCCTGCTGAAAGAGCTACTCTTTTGA AAGGTGACCGCTCTAGAACCC
AttB1_NLSDN17-F	GGGGACCACTTTGTACAAGAAAGCTGGGTGTTGTTATGCC TTCACATATTTCCC
caccH2B-F	CACCATGGCGAAGGCAGATAAGAAACCAGC
H2B-R	TTAAGAACTCGTAACTTCGTAACCGCC

```

AeCRN5_DN17      1  -VHPSVLRKRRREELN---QILSCAEIDAS-----NDSNRK-PKKSINFSSK
BDEG_07099      1  -SHHSEERKRWEEELN---PILIQAEIDAA-----AKSGKKNLESSAYSSIN
Ps_132663      1  -TAPHPSRKRWRWELN---EVLID-----KMKAKKAAGSGFGFSYVS
DN17_consensus  1  -IHRHPERLKRWAELN---EVLID-----KMKAKKADGSGFGFSYVS
Pc_CRN20_624    1  TIHRHPERLKRWAELN---AHLRCKNQANQKTTSEDTKKTSKKNHDKIVGSSIC
RiRT220960     1  SHKHEICRMEKQPAPVNDGAVLKIIVNDSK-----YTPLNDKLELEVLQLFVSN

AeCRN5_DN17      44 WELTAPLESR-VMSAYEQEKKATPREILQELQDYSAR-AFTCF-ELSSCSEATLNIPIAP
BDEG_07099      45 WSLTSEPELH-IHQYTPQVKEVPCETMELLENYIVT-LPRLSSVTGKESQRLHFIAP
Ps_132663      38 FPELDSIM---PAKVRPSSKFIPEDEKLALHRYFPI-LTKAFGDIIGKEAKRLHFIVE
DN17_consensus  38 FPELDSIM---PAKVRPSS--IPDEKLALLHAYTPI-LRKLFQDIIDG---KRLHFIVE
Pc_CRN20_624    58 WEDTRFPI-NFDDSFDPSS--IPDADPELLARIRD-LRELQCIIDGKEAKRLEFIAP
RiRT220960     50 KNLKFTVTDVYQIFSCGSAVLSSESKVVKELMAEINLRKKTTPIDVYEAATITVFC

AeCRN5_DN17      101 VLQVCALEN--GD-LKIFGKETKGGKVKANGRFEFVLKRGKLSFIVEAKRDFDQGA
BDEG_07099      103 ILVYVSDLRGPEDS--QILVEEDLVNGVNVKANGHEFFLKRNNKRVCIVEAKKDDMEQGM
Ps_132663      94 VLVVCALEFDG---GVQILAEETVIGKRVVGDGAFEFVLKRGKRVCIVEAKRDFDQGM
DN17_consensus  89 VLEIVCALEFGG---VQILVEETVIGKRVVGRGRFEFVLKRGKRVCIVEAKRDMQGM
Pc_CRN20_624    115 VLEIVSRLLKN---VRILVEEDLVGKNVLLKGRFEFVLKRGKRVCIVEAKRDMQGM
RiRT220960     110 YLVGVSFVEEN---FKLILEKFTVGRNGQGNLDLATECSTNIVGIVKVKKDFKQGF

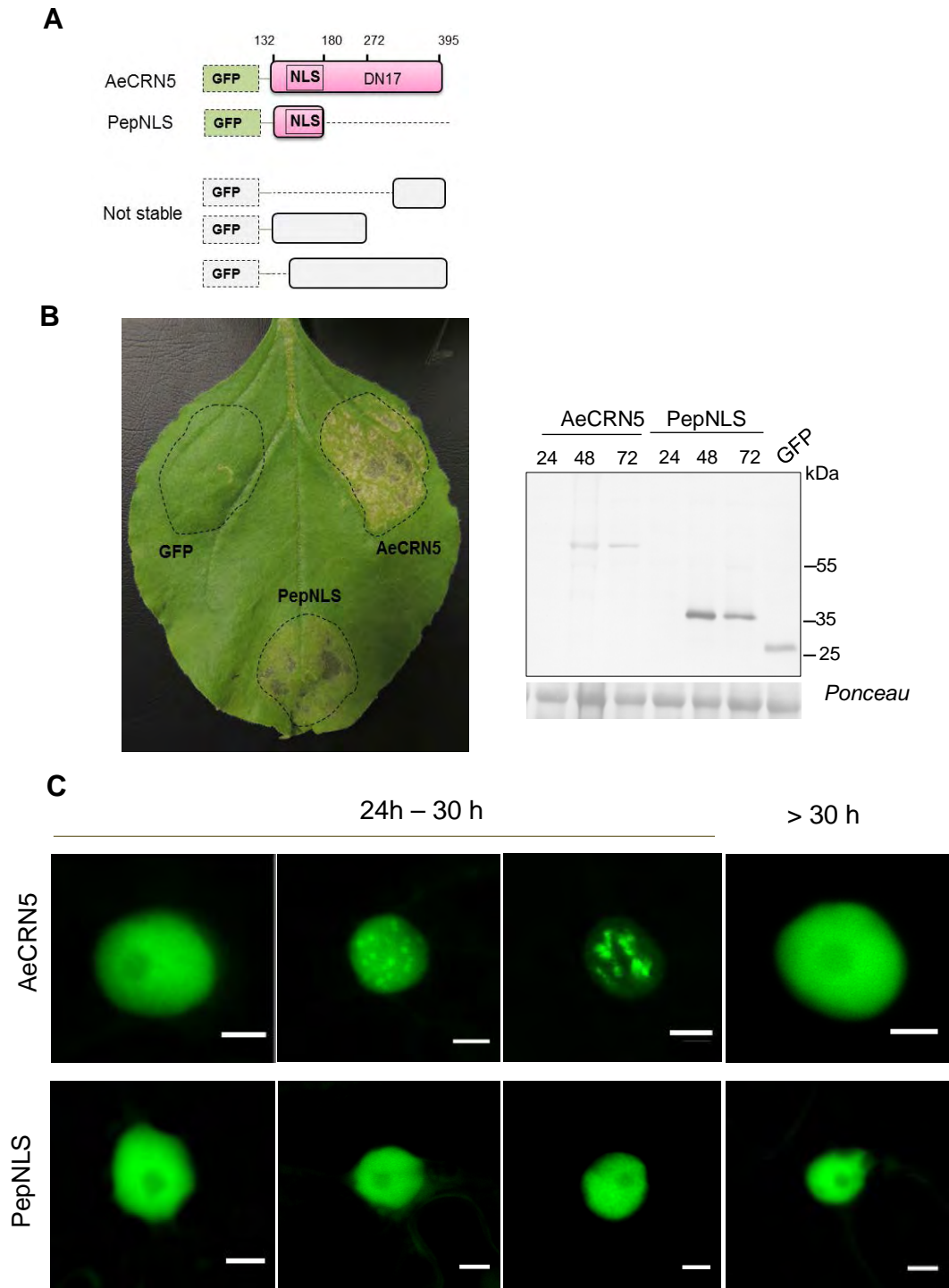
AeCRN5_DN17      158 AQEIVGAEVAAEIGSNVNVYIVTNFKEWVFRKSSNTKIEKD---ASFVYHPPKPYSE
BDEG_07099      162 VQDIVGMEVASDLGLDITVYGIVTNYVEWVFLKSNQKIEKN---MDTTFELEVATIE
Ps_132663      151 AQAYVGSALADVEGLEKQVYSIVTNFLEWVFSRSLDEIERA---TPVMMVMENDVEAP
DN17_consensus  145 AQAYVGLEALADVEGL-KVYSIVTNFLEWVFSRSLDEKIR---VMMVENDVE--
Pc_CRN20_624    171 VQNVIGLEALADVEDLLETYGIVTNFLEWKFVLSGDEKVR-E---HETVLPQANTPESE
RiRT220960     167 AQATVQVEID-DEHGLDKVIVGIVTDAERTYFVECLLNEGKLSFKLSKPVVYVDADAE

AeCRN5_DN17      214 TMDAATKTIYALFE-----
BDEG_07099      218 S-RKIAGKIYALLSE-----
Ps_132663      207 ESKVCIAGMIYSLSEDN-----
DN17_consensus  193 ESKV-IAG-IYSLSE-----
Pc_CRN20_624    226 EGRKEIVGKIYALIQ-----
RiRT220960     226 TKKRVLSHIVVLLDEAQKPDSDNS

```

Supplemental Fig 1: AeCRN5 is a CRN DN17 family. Alignment of Cterminus of AeCRN5 with the DN17 consensus sequence of *P. infestans* and its closest orthologs from *P. ramorum* (pRg882635), *P. sojae* (Ps_132663), *P. capsici* (Pc_CRN20_624), the chytrid fungus *Batrachochytrium dendrobatidis* (Bd) (BD_07009.1), the arbuscular mycorrhizal fungus *Rhizophagus irregularis* (Ri, gm1.18625_g) and the DN17 consensus sequence from *P. infestans*.

Chapter 2: Complementary results



Complementary Figure 1. Identification of a AeCRN5 Cterminal bioactive derivative (PepNLS) in *N. benthamiana*. **A.** Cartoons describe Cterminal AeCRN5 derivatives assayed for cell death activity and nuclear localization on *N. benthamiana* leaves. **B** Photograph of a *N. benthamiana* leaf agroinfiltrated with constructs GFP, AeCRN5 and PepNLS showing representative necrotic symptoms observed 5 days after agroinfiltration and western blot results showing the accumulation of both proteins in plant cells 24, 48, and 72 hours after agroinfiltration. Blots were probed with GFP antibodies. **C.** Panels correspond to micrographs acquired by confocal imaging showing the localization of both GFP fusion proteins AeCRN5 and PepNLS in epidermal cells at 24h-30h and after 30h after infiltration (Scale bars : 5 μ m).

Complementary results

Additional experiments were conducted attempting to precise the mechanisms of AeCRN5 nuclear activities.

PepNLS defines a minimal peptide of AeCRN5 presenting necrosis-inducing activity

As previously reported, we showed that AeCRN5 Cterminus domain (DN17) is a cell-death inducing domain which targets plant nuclear RNA with a dynamic localization within the plant nucleus. To identify the regions of DN17 required for these activities, we produced different Cterminal derivatives Nterminally fused to GFP, schematized in complementary figure 1. All constructs were agroinfiltrated in *N. benthamiana* leaves. Only the PepNLS version corresponding to the first 11 aa peptides coupled to the NLS (133aa-179aa) was stably expressed (complementary figure 1 C). Notably, PepNLS accumulation was greater than AeCRN5 and was accompanied of cell-death, similarly to the full DN17 domain (complementary figure 1 C). Confocal microscopy studies revealed a nuclear localization of the GFP:PepNLS fusion protein homogenously distributed in the nucleoplasm over time. Thus, in contrast to the full DN17, it did not display a shuttling to any obvious subnuclear bodies.

PepNLS also displays a RNA binding capacity

We tested whether PepNLS could target plant RNA by FRET-FLIM. Analyses were performed on three independent agroinfiltrations and on a minimum of 10 nuclei per construct and results were compared to GFP and GFP-H2B measurements. For PepNLS, we registered a GFP life- time decrease from 1.995 +/-0.032 to 1.692+/-0.020 in presence of Sytox Orange, indicative of FRET phenomenon (complementary table 1). Since Sytox Orange labels DNA and RNA, to discriminate the nature of nucleic acid targeted by PepNLS, samples were treated with RNase which resulted in the loss of FRET. Hence, PepNLS targets plant RNA. These preliminary results suggested that this first Nterminal region of DN17 domain may be a minimal peptide ensuring AeCRN RNA binding. Yet, it is not likely to contribute to AeCRN5 localization to nuclear bodies.

Complementary Table 1. Summary of FRET-FLIM conditions and values obtained on foliar discs of *N. benthamiana* expressing the different fluorescent donor proteins.

Donor	Acceptor	τ ^(a)	sem ^(b)	N ^(c)	E ^(d)
GFP	-	2.246	0.036	20	-
GFP	Sytox Orange	2.210	0.044	18	1.6
GFP-H2B	-	2.465	0,017	40	-
GFP-H2B	Sytox Orange	1.852	0.047	43	24.8
GFP-AeCRN5	-	2.128	0.069	27	-
GFP-AeCRN5	Sytox Orange	1.899	0.069	10	10.5
GFP-AeCRN5	Sytox Orange + RNAse treatment	2.228	0.105	17	0
GFP-PepNLS	-	1.995	0.032	23	-
GFP-PepNLS	Sytox Orange	1.692	0.020	32	15.2
GFP-PepNLS	Sytox Orange + RNAse treatment	1.969	0.042	31	1.3

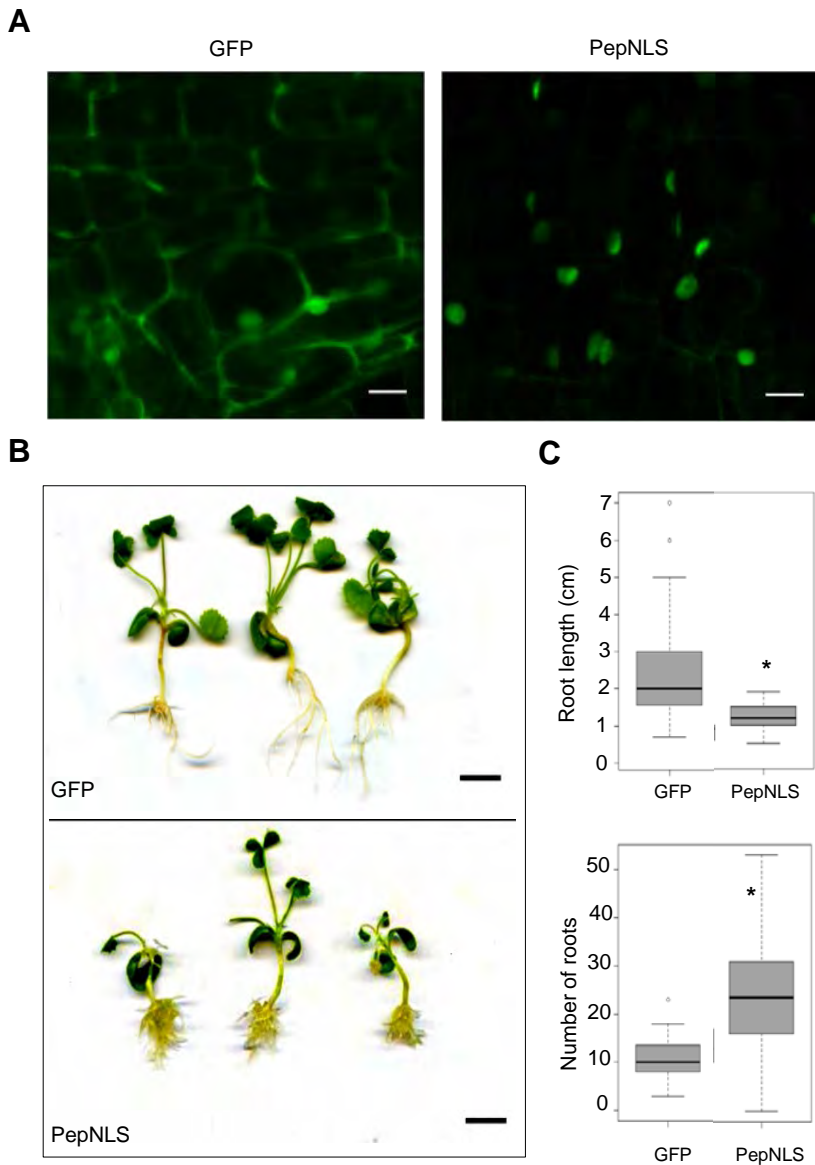
τ : mean GFP lifetime in nanoseconds (ns). For each nucleus, average fluorescence decay profiles were plotted and lifetimes were estimated by fitting data with exponential function using a non-linear least-squares estimation procedure. (b) s.e.m.: standard error of the mean. (c) N: total number of measured nuclei. (d) E: FRET efficiency in % : $E=1-(\tau_{DA}/\tau_D)$. (e) p-value (Student's t test) of the difference between the donor lifetimes in the presence or absence of acceptor

PepNLS worries host roots similarly to full AeCRN5

We showed that AeCRN5 (complete DN17 domain) affects host root development when overexpressed in *M. truncatula* roots. We further tested whether PepNLS could present similar AeCRN5 in roots of *M. truncatula*. For this, we transiently expressed constructs GFP:PepNLS (PepNLS) and control GFP in roots via a *A. rhizogenes*-mediated transformation. Composite plants were let to develop over time and fluorescent roots were used to study GFP localization by confocal microscopy. GFP corresponding to PepNLS was detected exclusively on nuclei in contrast to GFP alone, which presented its typical nucleo-cytoplasmic localization (complementary figure 3 A). Plants transformed with PepNLS presented an overall size reduction with major changes in root morphology compared to plants transformed with GFP alone (complementary figure 3 B). Quantification of root length and number indicated that roots transformed with PepNLS presented a decrease of root length and a higher number of roots (complementary figure 3 C), similar to effects triggered by AeCRN5. It is worth to note that PepNLS induced stronger effects on root architecture than AeCRN5

As a first approach to further characterize DN17 domain we generated AeCRN5 Cterminal truncated peptide. Only the 11-aa amino terminal peptide coupled to the NLS was stable, accumulating over time in plant cells. This peptide localizes in nuclei, binds RNA, triggers a cell-death but does not transiently localize in nuclear bodies. These results suggest that, within AeCRN5 Cterminal domain, distinct subdomains ensure the nuclear-body localization and that induction of cell-death may be nuclear-body independent. Our preliminary analyses on PepNLS and full DN17 by putative orthologs sequence analysis and 2D modeling did not show any obvious sequence characteristic leading to a particular known activity. In the future, similar experiments will be performed to generate viable Cterminal derivatives, mainly a DN17 version deleted of its first 11 amino acid to validate the importance of this region for DN17 activities, notably nuclear-body addressing.

In host roots, PepNLS accumulates in nuclei and leads to similar effects on root morphology that AeCRN5. In contrast to AeCRN5, PepNLS fluorescence accumulated sufficiently to be visualized in host roots. This is consistent with a greater protein accumulation observed for PepNLS in foliar leaves (*N. benthamiana*), and might explain the stronger effects seen for this version compared to those triggered by AeCRN5.



Complementary Figure 2. PepNLS modifies root morphology. *M. truncatula* plantlets were transformed with *A. rhizogenes* to express constructs GFP and PepNLS. **A.** Micrographs showing a nucleocytoplasmic localization of GFP and a nuclear accumulation of PepNLS. Fluorescent transformed roots were studied by confocal microscopy (scale bar: 20 μ m). **B.** Photographs of 30 day-old composite plants depict the effects of PepNLS on plant development and on root system morphology (scale bars: 1 cm). **C.** Quantification of length and root number per composite plant is presented in box-plot graphics which represent the average of both parameters and further confirms the impact of PepNLS on root development. Measures and statistical analyses were performed on n=60 (GFP) and n=140 (PepNLS) plants. * (*t*-test, p-value<0.05).

Overall, these preliminary results indicate that within the DN17 of AeCRN5 there could be a functional modularity that could explain AeCRN5 localization dynamism within the plant nucleus. Interestingly this dynamism does not seem to be required for cell-death activity. Why is AeCRN5 addressed to this constricted RNA-containing nuclear zones and how this contributes to its whole protein activity? Whether this functional modularity supposes different nature of RNA targets and/or interaction to other plant factors needs to be further investigated. Experiments to identify the nature of RNA targets associated to PepNLS (nucleocytoplasmic distributed) and to nuclear-bodies are in view to be performed on full DN17 and other protein versions that will be generated.

Materials and methods of complementary experiments

Construction of AeCRN5 Cterminal derivative vectors

Sequences of primers used are listed in complementary table 1. PepNLS, version 2 version 3 and version 4 carrying Gateway adaptors were generated by PCR using the cDNA template Ae_1AL4462 (vector pSport_Ae_1AL4462). PepNLS (132aa-180aa) was amplified using primers AttB1_AeCRN5-F and AttB1_PepNLS-R, version 2 (143aa-370aa) using AttB1_NLSDN17-F and AttB2_AeCRN5-R, version 3 (132aa-272aa) using AttB1_AeCRN5-F and AttB1_DN17dis-R and version 4 (273aa-370aa) using AttB1_Minus-F and AttB1_AeCRN5-R. Amplicons were BP recombined in pDONR-Zéo vector (Invitrogen) and subsequently introduced in vector pK7GWF2 by means of LR recombination (Invitrogen). The obtained pK7GWF2 vectors were introduced in *Agrobacterium* strains for *N. benthamiana* agroinfiltration assays and/or *M. truncatula* roots transformation.

Name	Sequence 5'-3'
attB1_AeCRN5-F	GGGGACAAGTTTGTACAAAAAAGCAGGCTTCTTGAAGG TGACCGCTCTAGAACCC
attB2_AeCRN5-R	GGGGACCACTTTGTACAAGAAAGCTGGGTGTTGTTATTC AAAAAGTATGGCG
AttB1_PepNLS-R	GGGGACCACTTTGTACAAGAAAGCTGGGTGTTGTTATTT CTTTGGCTTCTT GTT
AttB1_NLSDN17-F	GGGGACCACTTTGTACAAGAAAGCTGGGTGTTGTTATGC CTTCACATATTTCCC
AttB1_DN17dis-R	GGGG AC CAC TTT GTA CAA GAA AGC TGG GTG TTG TTA TGC CTT CAC ATA TTT CCC
AttB1_Minus-F	GGGG ACA AGT TTG TAC AAA AAA GCA GGC TTC AAT GGT CGT TTT GAA TTT GTA

General discussion and perspectives

General discussion and perspectives

Throughout this work, we performed the functional analysis of two putative cytoplasmic effectors from the root rot pathogen *A. euteiches*, AeCRN5 and AeCRN13. Their corresponding genes were detected in a cDNA library generated from infected roots of *M. truncatula*, before my arrival in the research team. In this section I will discuss the main results obtained during my PhD work and the immediate perspectives of our findings.

CRN proteins, more than just phytopathogenic oomycete proteins.

In the oomycete lineage, CRNs are ancestral proteins described in all phytopathogenic species including the early divergent species *A. euteiches* and latest results of RNA sequencing data indicate that they might be also present in the zoopathogenic species like *A. astaci* (Gaulin et al., in preparation). One characteristic of the CRN protein family is its extensive expansion and diversity, typically found in *Phytophthora* species (*P. infestans*, *P. ramorum*, *P. sojae*...) and also in *A. euteiches*. In *Phytophthora* species, this gene number expansion and sequence variability is attributed to gene duplication events and fragment recombination mechanisms between CRN sequences (Haas et al., 2009; Shen et al., 2013) that are thought to give rise to novel CRN proteins and, by this, contribute to host adaptation. In *P. sojae* almost 50% of CRNs have been found to issue from gene duplication and are under diversifying selection, denoting likely a neo-functionalization of the resultant CRNs.

At the beginning of this project, CRN proteins were thought to be restricted to the oomycete lineage, but during my PhD work, CRN-like proteins were reported in the chytrid fungus species *B. dendrobatidis*, an amphibian pathogen and in the plant mycorrhizal fungus *R. irregularis*. Thus, CRN are no longer oomycetes specific nor linked to a pathogenic lifestyle but might also contribute to a mutualistic lifestyle. Because CRN-like proteins are limited only to these two fungal species, their occurrence in Bd and Ri is proposed to be the result of Horizontal Gene Transfer (HGT) events from oomycetes (Sun et al., 2011). HGT is very common between bacteria and from bacteria to eukaryotes (Gilbert and Cordaux, 2013) and is becoming evident also between plant parasitic nematodes, oomycetes and fungi for which it has been proposed as a mechanism shaping parasitism (Gardiner, Kazan, & Manners, 2013; Haegeman, Jones, &

Danchin, 2011; Richards et al., 2011). Fixation of new genes supposes then that novel functions somehow fit in functional networks already present in the receiver organism and that these functions add an advantage to the network (Richards et al., 2006). Therefore, the presence in fungi implies that CRN functions fit in the biochemical networks and confer a benefit to the biology of these two organisms.

Several gene transfers have been evidenced between fungi and oomycetes (Richards et al., 2011). 33 fungi-to-*Phytophthora* oomycete species genes have been identified accounting for up to 7.6% of the predicted secretome (*P. ramorum*). Among the transferred genes, some code for secreted proteins with functions in the degradation of cell wall structural polysaccharides specific to plants and therefore putatively involved in the degradation of plant cell wall for tissue colonization and/or nutrient acquisition. Notably, among transferred genes are LysM protein-coding genes which have been demonstrated in phytopathogen fungi as effectors allowing plant defense suppression (Richards et al., 2011).

B. dendrobatidis and *R. irregularis* share a repertoire of oomycete CRNs that include DFA-DDC, DN17, DXX, DX8 Cterminal families with up to 46.5 % of sequence similarity (Sun et al., 2011; Lin et al., 2014). It is expected that fungal CRN could have undergone sequence divergence linked to a specialization and functional adaptation to the recipient's biology since their actual transfer from oomycetes. Nevertheless, this shared core of CRNs could imply similar protein activities and likely similar functions. In the case of *B. dendrobatidis*, the observation that CRN proteins display signs of diversifying selection and are induced upon infection (Rosenblum et al., 2012) supports their possible involvement during host infection. The results obtained on AeCRN13 and BdCRN13 support the idea that sequence similarities can correlate to similar activities and open the question of the exact contribution of similar CRN activities in microorganisms that present different lifestyles and develop in different nature of hosts. If this shared core of CRNs presents indeed similar activities, it would be logic to assume that such activities are necessary for common infectious processes. Then, it is likely that common CRNs target universal functions and/or processes present in both plants and animals. The elucidation of oomycetes and fungal CRN activities together with the identification of targeted processes is of current need to understand the CRN protein family.

AeCRN secretion and translocation

The *in silico* characterization of CRN proteins in oomycetes and fungi has denoted the lack of predictable signal peptides (SPs) in their Nterminal moieties. In fact, 40% of CRNs of *P. infestans* do not contain a SP (Haas et al., 2009) and only 11% of Bd and 12% of Ri CRNs exhibit a SP (Sun et al., 2011; Lin et al., 2014). The lack of SP is also the case for both AeCRN studied in this work. CRN Ntermini lacking predictable SP, including AeCRN5, were shown to allow the secretion and host-delivery of proteins (Schornack et al., 2010). Hence, it is possible that some CRN possess particular unknown secretion leaders that cannot be accurately predicted by available algorithms (i.e SignalP). Another possibility is that some CRN fall into the category of the so-called leaderless secretory proteins (LSPs) that undergo unconventional protein secretion. The latter idea is sustained by a recent study of *P. infestans*'s *in vivo* proteome that evidenced the presence of proteins devoid of SP in the extracellular space, among which CRNs (Meijer et al., 2014). Unconventional secretion refers to secretion mechanisms other than the classical ER-Golgi trans-membrane route to which canonical SP-containing proteins are addressed, that allow secretion of SP-lacking proteins. Unconventional protein secretion has been described mainly in mammal and fungal systems and in plants (Ding et al., 2012; Oliveira et al., 2013) and its experimental evidence lies on the identification in the extracellular space of proteins that are typically intracellular (cytoplasmic/nuclear) and/or that lack SPs and on the observation that secretion of some proteins is Brefeldin A (BFA) independent. BFA is a potent inhibitor of membrane recruitment of factors that mediate the formation of coated vesicles from Golgi membrane to the plasma membrane. Models for unconventional secretion suppose the direct translocation of the protein across the plasma membrane or a vesicle-dependent secretion, but the exact factors controlling the biogenesis of such vesicles, the shedding and sorting of secreted proteins is not well understood (Nickel and Rabouille, 2009). Studies in various fungal systems, mainly carried in animal pathogenic species (like *Cryptococcus neoformans* and *Paracoccidioides brasiliensis*) have described the release of vesicles to the extracellular space during infection. Isolation and analysis of extracellular vesicles or “exosomes” has denoted a variety of cargo molecules (lipids, proteins, polysaccharides...) that have been associated with virulence (Oliveira et al., 2013).

The demonstration that effectors undergo differential secretion pathways has been recently brought thought studies on the phytopathogenic fungus *Magnaporthe oryzae*. Localization studies of effector proteins tagged with fluorescent proteins expressed in this fungus, have shown

that apoplastic effectors are found dispersed and retained in the EIHM compartment (a close-up apoplastic space delimited by the invasive hyphae and the plasma membrane of the invaded host cell) while intracellular effectors accumulate in the BIC (a plant derived structure developed adjacent to the infectious hyphae). Secretion of apoplastic effectors such as Bas4, Bas113 and Slp1 was blocked by BFA, indicating that these effectors undergo an ER-to-Golgi secretion. In contrast BFA treatment did not affect the secretion of the intracellular effectors Pwl2, Bas1 and Avr-Pita (Giraldo et al., 2013).

Our preliminary immunolocalization results on AeCRN13 during *M. truncatula* root infection provided, for the first time, the visualization of an oomycetal intracellular/cytoplasmic effector secretion and translocation during the natural infection conditions. AeCRN13 was detected in particular cup-shaped structures outside *A. euteiches* infectious mycelium that we denoted as “vesicle-like” or “exosomes”. This localization pattern contrasts to what has been observed in haustoria-forming fungi and oomycetes in which intracellular effectors have been seen to accumulate in located zones of haustoria and other particular biotrophic structures as the above mentioned BIC (Kemen et al., 2005, Whisson et al. 2007, Giraldo et al., 2013). In *A. euteiches* such structures have never been detected and AeCRN13 was not detected in any particular zone of the infectious hyphae.

AeCRN13 signal was detected in vesicle-like structures near host nuclei and a faint AeCRN13 signal was reported in nuclei. We postulate that once in the vicinity of host nuclei, AeCRN13 is released from these structures and addressed into nuclei to exert its function. Future work will be directed to precise the nature of these “vesicles”. Immuno-electron microscopy techniques will be used to precise their size, morphology and the exact localization of AeCRN13 within these structures. To further characterize their molecular composition, these vesicles will be isolated from infected tissues and analysed for protein and lipid composition. Different methods for isolation and analysis have been described in the literature based on ultracentrifugation, filtration and immunoaffinity (Witwer et al., 2013). This latter strategy could be contemplated by using AeCRN13 antibodies. Such studies will be also directed on AeCRN5 and other *Phytophthora* CRNs to see whether secretion is conserved in oomycetes (Saprolegniales and Peronosporales). In addition it will be interesting to direct similar approaches on CRN displaying canonical SP leaders in order to see whether CRN secretion and translocation differ between SP-containing/lacking CRNs.

We followed AeCRN13 protein accumulation during *M. truncatula* infection with AeCRN13 antibodies. The results pointed out the possibility for AeCRN13 to be processed since different specific AeCRN13 signals were detected upon western blot analyses of infected roots. Our interpretation of AeCRN13 processing is based on predicted sizes and on speculations brought by other studies and we are aware of the necessity to sustain our hypotheses with mass spectrometry analyses of the products that were identified to be conclusive.

Nterminal processing of intracellular effectors has been described. For instance, a mass spectrometry analysis of SIX2 (Avr2) protein of *F. oxysporum* isolated from infected tissues revealed that only its Cterminal domain is present in infected xylem tissues (Houtemann et al., 2007; Ma et al., 2013). In addition, it has been demonstrated that the Ntermini of intracellular “Pexel” effectors of *P. falciparum* are processed during its transit on the ER (Osborne et al., 2010) and it is also the case for the Nterminal domain of the RxLR effector Avr3a from *P. infestans* (Warva S, OMGN meeting July 2014).

Post-translational modifications could also constitute a regulation of CRN proteins. So far, phosphorylation has been shown as one type of post-translational decoration of CRN proteins. The recent “phospho-proteome” study on *P. infestans* showed that Cterminal domains belonging to the DBF, DO, DXZ, DXX families are targets of phosphorylation (Resjö et al., 2014) and a previous study indicated that CRN8 (carrying a D2 Cterminal domain) is phosphorylated when expressed *in planta*, a modification necessary to its cell-death activity (van Damme et al., 2012). These observations point to a functionally relevant regulation of CRN at the post-translational level which is in agreement to latest finding on the fungal LysM (Slp1) effector of *M. oryzae* for which its N-glycosylation during its Golgi-dependent secretion is necessary for its chitin binding and virulence activity (Chen et al., 2014).

Nuclear and subnuclear localization of AeCRNs

Nuclear import of proteins larger than 40kDa is an active process mediated by protein complexes associated at the nuclear pores, that solicits import receptors (importins) recognizing NLS motifs in imported cargo proteins (Tamura and Hara-Nishimura, 2014). All CRN proteins studied so far localize in plant nuclei but their nuclear localization not always correlates to the presence of predicted NLS in their Cterminal domains. For instance, only 26% of *P. capsici* CRNs present NLS (Stam et al., 2013). AeCRN13, BdCRN13 and AeCRN5 exemplify this since only AeCRN5 contains a predictable NLS. Their presence in some CRNs infers that CRNs

subvert directly the nuclear transport machinery of host cells by interacting with α/β -importins. This was actually shown for *Phytophthora* NLS-containing CRNs and for AeCRN5 for which silencing of plant α -1- importin partially impairs their nuclear accumulation (Schornack et al.2010). The direct subversion of the host nuclear traffic machinery by bacteria and oomycetal effectors has also been reported (Deslandes and Rivas 2011; Caillaud et al., 2012). How exactly, non-containing NLS CRNs localize in nuclei is still not clear. A possible explanation is that these proteins may harbor discrete NLS, still not characterized, and therefore unpredicted with algorithms at disposition. Other possibility is that they could co-opt host factors that mediate direct interaction with importins as it has been shown for the *Agrobacterium* effector VirE2 that subverts the plant NLS-containing VIP1 protein to mediate its entry (Liu et al., 2010).

AeCRN13 and AeCRN5 localize entirely to nuclei. Confocal imaging performed on GFP-tagged AeCRN5 over time revealed a dynamic subnuclear localization for this protein. AeCRN5, which is a DN17 CRN, first displays an even nucleoplasm distribution then exhibits a punctuated localization that results in its location to uncharacterized nuclear bodies characterized by the lack of DNA material. Another DN17 CRN protein, CRN12_624 (from *P. capsici*) exhibits similar punctuated concentrations of fluorescence all over the nucleus, but the possible dynamism of its localization was not examined.

The dynamics of AeCRN5 localization together with the fact that nuclear bodies do not contain DNA material and required plant RNA integrity to form, suggest that AeCRN5 localization might be linked speckles. Among the different membrane-free nuclear compartments evidenced in plant and animal cells (ie Cajal bodies, nucleoli...), speckles are interchromatin molecular complexes that form throughout the nucleoplasm in regions containing little or no DNA and that exhibit a granular shape. Major components of speckles are proteins involved in pre-mRNA splicing (SR proteins, snRNP protein splicing factors) but transcription factors as well as subunits of RNA poly II and RNA have also been identified (Reddy et al., 2012; Spector and Lamond, 2011). The function of speckles is not clear, but because of their molecular composition together with the fact that their localization often correlates to active transcriptional sites, they have been proposed as splicing centres (spliceosomes) and as domains devoted to the storage and regulation of splicing factors. Speckles are highly dynamics structures, changing in size, shape and number with individual components able to shuttle in and out (Reddy et al., 2012). Future work on AeCNR5 will be devoted to further characterize its subnuclear localization by the use of protein markers of different nuclear compartments.

AeCRNs nuclear targets

An increasing number of experimental data places the nucleus and/or nuclear-related functions as important hubs targeted by microbial effectors. While the nature of nuclear targets are best known for prokaryotic effectors, only few have been identified for eukaryotic effectors which have been shown to be proteins. These include transcription factors of the NAC family (NTP 1 and NTP2) and TCP (TCP14) targeted by RxLR of *P. infestans* and CRN of *P. capsici*, respectively, that have been proposed be positive regulators of plant defense. Other targeted plant defense regulators include the proteasomal protein CMPG1 and MED19 which are targeted by RxLRs (McLellan et al., 2013; Bos et al., 2010; Caillaud et al., 2013; Stam et al., personal communication). This study reveals, for the first time, that filamentous eukaryotic effectors can target nucleic acids. By setting FRET-FLIM measurements *in planta*, we demonstrate the close vicinity of AeCRN13 and AeCRN5 with plant DNA and RNA, respectively. In addition, by working with BdCRN13, we show that this targeting is a conserved CRN activity, suggesting that the targeting host nucleic acids may be a common infection strategy of eukaryotic pathogens. TAL effectors from bacteria illustrate the concept of plant physiology modulation through a direct interaction with nucleic acid. Their binding is DNA sequence specific and has a direct repercussion on host gene transcription.

Next work will aim to decipher the interaction (direct or not) between AeCRNs and plant nucleic acid by developing cutting-edge technology including ChipSeq approach on *M. truncatula*. This approach will also provide answer to a possible specificity of the targeted nucleic sequence. Transcriptional modifications caused by CRNs in host plant will be also evaluated to precise their mode of action. Finally, Y2H on infected *M. truncatula* root is underway in the group in order to identify putative co-interactors of AeCRNs.

Cell death activity and contribution to virulence

At the beginning of the work, all *Phytophthora* CRNs studied were described as cell-death inducing proteins when expressed directly in plant tissues but works have shown that a large number do not carry a cytotoxic activity and/or can even suppress cell-death induced by other CRNs and other microbial-derived cell-death inducers (Stam et al., 2013; Shen et al., 2013; Li et al., 2011). As *Phytophthora* species present hemibiotrophic lifestyles, it has been generally

assumed that CRNs with necrotic activities could be required during necrotrophic stages of infection. Nevertheless, gene expression profiles of CRN in *Phytophthora* species indicate that this might not be generally the case as some necrotic CRN are expressed during the biotrophic development of the pathogen (Stam et al., 2013; Li et al., 2011). In addition, CRN proteins of the obligate biotrophic oomycete *Albugo candida* have been shown to trigger cell-death which is in direct contradiction to its infection behaviour (Links et al., 2011). Thus, the cell-death activity observed for some CRNs *in planta* might not be the intrinsic virulence function but rather the consequence of their overexpression and thus “over-activity” in host tissues. Giving the high number of CRN genes, high-through put systems to assess the contribution to virulence of CRN have been based on pathogen challenging of plant tissues expressing ectopically the effectors and measure of pathogen spreading. These studies indicate that not all CRN display an obvious contribution and have suggested that some CRN may present more discrete virulence activities during infection (Stam et al., 2013).

Our work shows that overexpression of both AeCRNs and BdCRN13 has important effects in plant and amphibian cells manifested by tissue necrotic symptoms or host developmental defects, all of which attest for the perturbation of host cellular processes by these AeCRNs. AeCRN13 contributes to *P. capsici* virulence, since AeCRN13 overexpression enhanced *N. benthamiana* leaves colonization. One way to better understand AeCRN13 contribution to infection is to contextualize their expression during infection in regards to the whole CRNs. *A. euteiches* genome contains 160 CRN gene models and currently their expression is being characterized by high-through put qPCR system (Fluidigm Biomark) on various life stages of the pathogen.

Nuclease activity and DNA damage

During this work we provided first insights into the function of CRN13 by identifying a putative HNH-like endonuclease motif in the Cterminal DFA subdomains of Ae and Bd effectors. *In vitro* assays demonstrated the AeCRN13 binds and cleaves DNA. This is suspected to be mediated by the HNH-like motif. HNH motifs are phylogenetically wide spread functional protein domains associated to DNA-binding factors of prokaryotic and eukaryotic organisms and they occur commonly in homing endonucleases (HNH endonucleases) (Belfort and Roberts, 1997). Studies of bacteria HNH endonucleases place this domain as an important structural domain necessary for the hydrolytic activity on DNA ensuring DNA and cutting activities

(Huang and Yuan, 2007; Shen et al., 2004). Interestingly, some bacterial HNH-containing proteins act like toxins and play ecological roles in bacteria populations. For instance, bacterial colicins have been shown to be secreted and translocated inside other bacteria cells where their nuclease activity leads to cell-death and is HNH-dependent (Hsia et al., 2004; Pommer et al., 2001 ; Braun and Patzer, 2013) . Future studies will evaluate the functionality of the HNH-like motif of AeCRN13 and its requirement in the cell-death inducing phenotype. For this, different versions of the protein will be made (punctual mutation and HNH-deleted version...) and, for them, DNA-binding affinity as well as nuclease activity will be evaluated.

Lastly, we reported the induction of plant DNA double-strand breaks (DSB) upon overexpression of AeCRN13 in *N. benthamiana* and interestingly during *M. truncatula* infection by *A. euteiches*, using phosphorylated-H2AX detection. This finding identifies CRN effector as inducer of DSB probably through its nuclease activity. Song and Bent (2014) recently demonstrated the occurrence of DSB in plants during infection by phytophagogens *P. syringae* and *P. infestans*. The authors speculate that DSB may be due to a direct effect of microbial effector, toxins or cytotoxic microbial molecules since it was observed only with pathogenic species and in the absence of ROS accumulation (Song and Bent, 2014). In animals and plants, DNA breakage initiates a phosphorylation mediated signal transduction cascade leading to cell cycle arrest, cell-death or repair of DSB. Orthologous genes of the *A. thaliana* or animal signaling cascade have been detected in the *M. truncatula* genomes (i.e . *wee1*, *rad51*, *brca1*...). Future work will aim to evaluate their involvement in the observed mechanism DNA damage.

Concluding remarks

During my PhD work I deciphered a new mode of action of an exciting class of nuclear effectors from the root pathogen *A. euteiches*. I have showed that CRN oomycetal effectors are translocated into the cytoplasm of the host plant during interaction. I identified host nucleic acids as a novel target of AeCRNs that impact plant physiology. Finally I've revealed that eukaryotic effectors induce host DNA damage during infection probably through the secretion of cytoplasmic effector like the CRN DFA-DCC family. Altogether this PhD opens intriguing avenues for future studies.

References

References

- Adhikari, B.N., Hamilton, J.P., Zerillo, M.M., Tisserat, N., Lévesque, C.A., and Buell, R.** (2013). Comparative genomics reveals insight into virulence strategies of plant pathogenic oomycetes. *PLoS One* **8**: e75072.
- Akai, S.** (1974). History of Plant Pathology in Japan. *Annu Rev Phytopathol* **12**: 13–26.
- Allen, R.L., Bittner-Eddy, P.D., Grenville-Briggs, L.J., Meitz, J.C., Rehmany, A.P., Rose, L.E., and Beynon, J.L.** (2004). Host-parasite coevolutionary conflict between *Arabidopsis* and downy mildew. *Science* **306**: 1957–1960.
- Armstrong, M.R. et al.** (2005). An ancestral oomycete locus contains late blight avirulence gene *Avr3a*, encoding a protein that is recognized in the host cytoplasm. *Proc Natl Acad Sci U S A* **102**: 7766–7771.
- Badreddine, I., Lafitte, C., Heux, L., Skandalis, N., Spanou, Z., Martinez, Y., Esquerré-Tugayé, M.-T., Bulone, V., Dumas, B., and Bottin, A.** (2008). Cell wall chitosaccharides are essential components and exposed patterns of the phytopathogenic oomycete *Aphanomyces euteiches*. *Eukaryot Cell* **7**: 1980–1993.
- Baltrus, D. a, Nishimura, M.T., Romanchuk, A., Chang, J.H., Mukhtar, M.S., Cherkis, K., Roach, J., Grant, S.R., Jones, C.D., and Dangl, J.L.** (2011). Dynamic evolution of pathogenicity revealed by sequencing and comparative genomics of 19 *Pseudomonas syringae* isolates. *PLoS Pathog* **7**: e1002132.
- Baxter, L. et al.** (2010). Signatures of adaptation to obligate biotrophy in the *Hyaloperonospora arabidopsidis* genome. *Science* **330**: 1549–1551.
- Beakes, G and Sekimoto, S.** (2009). The evolutionary phylogeny of oomycetes—insights gained from studies of holocarpic parasites of algae and invertebrates. In *Oomycete genetics and genomics: diversity, interactions and research tools*, K. Lamour and S. Kamoun, eds (Annual Reviews), pp. 1–24.
- Beakes, G., Glockling, S., and Sekimoto, S.** (2012). The evolutionary phylogeny of the oomycetes “fungi”. *Protoplasma* **249**: 3–19.
- Bellaifiore, S., Shen, Z., Rosso, M.-N., Abad, P., Shih, P., and Briggs, S.P.** (2008). Direct identification of the *Meloidogyne incognita* secretome reveals proteins with host cell reprogramming potential. *PLoS Pathog* **4**: e1000192.
- Bendtsen, J.D., Nielsen, H., von Heijne, G., and Brunak, S.** (2004). Improved prediction of signal peptides: SignalP 3.0. *J Mol Biol* **340**: 783–795.
- Berr, A., Ménard, R., Heitz, T., and Shen, W.-H.** (2012). Chromatin modification and remodelling: a regulatory landscape for the control of *Arabidopsis* defense responses upon pathogen attack. *Cell Microbiol* **14**: 829–839.
- Bhattacharjee, S., Garner, C.M., and Gassmann, W.** (2013). New clues in the nucleus: transcriptional reprogramming in effector-triggered immunity. *Front Plant Sci* **4**: 364.
- Bhattacharjee, S., Hiller, N.L., Liolios, K., Win, J., Kanneganti, T.-D., Young, C., Kamoun, S., and Haldar, K.** (2006). The malarial host-targeting signal is conserved in the Irish potato famine pathogen. *PLoS Pathog* **2**: e50.
- Blum, M., Waldner, M., and Gisi, U.** (2010). A single point mutation in the novel *PvCesA3* gene confers resistance to the carboxylic acid amide fungicide mandipropamid in *Plasmopara viticola*. *Fungal Genet Biol FG Biol* **47**: 499–510.

- Bohlmann, H. and Sobczak, M. (2014).** The plant cell wall in the feeding sites of cyst nematodes. *Front Plant Sci* **5**: 89.
- Boisson-Dernier, a, Chabaud, M., Garcia, F., Bécard, G., Rosenberg, C., and Barker, D.G. (2001).** *Agrobacterium rhizogenes*-transformed roots of *Medicago truncatula* for the study of nitrogen-fixing and endomycorrhizal symbiotic associations. *Mol Plant Microbe Interact* **14**: 695–700.
- Boisvert, F.-M., van Koningsbruggen, S., Navascués, J., and Lamond, A.I. (2007).** The multifunctional nucleolus. *Nat Rev Mol Cell Biol* **8**: 574–585.
- Boller, T. and Felix, G. (2009).** A renaissance of elicitors: perception of microbe-associated molecular patterns and danger signals by pattern-recognition receptors. *Annu Rev Plant Biol* **60**: 379–406.
- Bonhomme, M. et al. (2014).** High-density genome-wide association mapping implicates an F-box encoding gene in *Medicago truncatula* resistance to *Aphanomyces euteiches*. *New Phytol* **201**: 1328–1342.
- Bos, J.I.B. et al. (2010).** *Phytophthora infestans* effector AVR3a is essential for virulence and manipulates plant immunity by stabilizing host E3 ligase CMPG1. *Proc Natl Acad Sci U S A* **107**: 9909–9914.
- Bos, J.I.B., Kanneganti, T.-D., Young, C., Cakir, C., Huitema, E., Win, J., Armstrong, M.R., Birch, P.R.J., and Kamoun, S. (2006).** The C-terminal half of *Phytophthora infestans* RXLR effector AVR3a is sufficient to trigger R3a-mediated hypersensitivity and suppress INF1-induced cell death in *Nicotiana benthamiana*. *Plant J* **48**: 165–176.
- Boys, C. a, Rowland, S.J., Gabor, M., Gabor, L., Marsh, I.B., Hum, S., and Callinan, R.B. (2012).** Emergence of epizootic ulcerative syndrome in native fish of the Murray-Darling River System, Australia: hosts, distribution and possible vectors. *PLoS One* **7**: e35568.
- Brinkmann, H. and Philippe, H. (2007).** The diversity of eukaryotes and the root of the eukaryotic tree. *Adv Exp Med Biol* **607**: 20–37.
- Brunner, Â., Rosahl, S., Lee, J., Rudd, J.J., Geiler, C., Scheel, D., and Nu, T. (2002).** Pep-13, a plant defense-inducible pathogen-associated pattern from *Phytophthora* transglutaminases. *EMBO J* **21**: 6681–6688.
- Büttner, D. and Bonas, U. (2006).** Who comes first? How plant pathogenic bacteria orchestrate type III secretion. *Curr Opin Microbiol* **9**: 193–200.
- Caillaud, M.-C., Asai, S., Rallapalli, G., Piquerez, S., Fabro, G., and Jones, J.D.G. (2013).** A downy mildew effector attenuates salicylic Acid-triggered immunity in *Arabidopsis* by interacting with the host mediator complex. *PLoS Biol* **11**: e1001732.
- Caillaud, M.-C., Piquerez, S.J.M., Fabro, G., Steinbrenner, J., Ishaque, N., Beynon, J., and Jones, J.D.G. (2012).** Subcellular localization of the Hpa RxLR effector repertoire identifies a tonoplast-associated protein HaRxL17 that confers enhanced plant susceptibility. *Plant J* **69**:252–265.
- Canonne, J. and Rivas, S. (2012).** Bacterial effectors target the plant cell nucleus to subvert host transcription . *Plant Signal Behav* **7**:2: 217–221.
- Canonne, J., Marino, D., Jauneau, A., Pouzet, C., Brière, C., Roby, D., and Rivas, S. (2011).** The *Xanthomonas* type III effector XopD targets the *Arabidopsis* transcription factor MYB30 to suppress plant defense. *Plant Cell* **23**: 3498–3511.
- Cantu, D., Vicente, A.R., Labavitch, J.M., Bennett, A.B., and Powell, A.L.T. (2008).** Strangers in the matrix: plant cell walls and pathogen susceptibility. *Trends Plant Sci* **13**: 610–617.
- Caplan, J.L., Mamillapalli, P., Burch-Smith, T.M., Czymmek, K., and Dinesh-Kumar, S.P. (2008).** Chloroplastic protein NRIP1 mediates innate immune receptor recognition of a viral effector. *Cell* **132**: 449–462.
- Chang, C., Zhang, L., and Shen, Q.-H. (2013).** Partitioning, repressing and derepressing: dynamic regulations in MLA immune receptor triggered defense signaling. *Front Plant Sci* **4**: 396.
- Chen, L.-Q. et al. (2010).** Sugar transporters for intercellular exchange and nutrition of pathogens.
- Chen, S., Songkumarn, P., Venu, R.C., Gowda, M., Bellizzi, M., Hu, J., Liu, W., Ebbolle, D., Meyers,**

- B., Mitchell, T., and Wang, G.-L.** (2013). Identification and characterization of in planta-expressed secreted effector proteins from *Magnaporthe oryzae* that induce cell death in rice. *Mol Plant Microbe Interact* **26**: 191–202.
- Chen, S., Tao, L.I.Z.E.N., Zeng, L., Vega-Sanchez, M.E., Umemura, K., and WANG, G.-L.** (2006). A highly efficient transient protoplast system for analyzing defense gene expression and protein–protein interactions in rice. *Mol Plant Pathol* **7**: 417–427.
- Chen, X.-L., Shi, T., Yang, J., Shi, W., Gao, X., Chen, D., Xu, X., Xu, J.-R., Talbot, N.J., and Peng, Y.-L.** (2014). N-glycosylation of effector proteins by an α -1,3-mannosyltransferase is required for the rice blast fungus to evade host innate immunity. *Plant Cell* **26**: 1360–1376.
- Chronis, D., Chen, S., Lu, S., Hewezi, T., Carpenter, S.C.D., Loria, R., Baum, T.J., and Wang, X.** (2013). A ubiquitin carboxyl extension protein secreted from a plant-parasitic nematode *Globodera rostochiensis* is cleaved in planta to promote plant parasitism. *Plant J* **74**: 185–196.
- Cobb, R.C., Eviner, V.T., and Rizzo, D.M.** (2013). Mortality and community changes drive sudden oak death impacts on litterfall and soil nitrogen cycling. *New Phytol* **200**: 422–431.
- Cook, D.** (1999). *Medicago truncatula*: a model in the making! *Curr Opin Plant Biol* **2**:301–304.
- Cui, H., Kong, D., Liu, X., and Hao, Y.** (2014). SCARECROW, SCR-like 23 and SHORT-ROOT control bundle sheath cell fate and function in *Arabidopsis thaliana*. *Plant J.* **78**:319-327
- De Souza, T.A., Soprano, A.S., de Lira, N.P.V., Quaresma, A.J.C., Pauletti, B.A., Paes Leme, A.F., and Benedetti, C.E.** (2012). The TAL effector PthA4 interacts with nuclear factors involved in RNA-dependent processes including a HMG protein that selectively binds poly(U) RNA. *PLoS One* **7**: e32305.
- Deslandes, L. and Rivas, S.** (2012). Catch me if you can: bacterial effectors and plant targets. *Trends Plant Sci* **17**: 644–655.
- Deslandes, L., Olivier, J., Frédéric, T., Hirsch, J., Feng, D.X., Bittner-Eddy, P., Beynon, J., and Marco, Y.** (2002). Resistance to *Ralstonia solanacearum* in *Arabidopsis thaliana* is conferred by the recessive RRS1-R gene, a member of a novel family of resistance genes. *Proc Natl Acad Sci* **99**: 2104–2409.
- Diéguez-Uribeondo, J., García, M. a, Cerenius, L., Kozubíková, E., Ballesteros, I., Windels, C., Weiland, J., Kator, H., Söderhäll, K., and Martín, M.P.** (2009). Phylogenetic relationships among plant and animal parasites, and saprotrophs in *Aphanomyces* (Oomycetes). *Fungal Genet Biol* **46**: 365–376.
- Ding, Y., Wang, J., Wang, J., Stierhof, Y.-D., Robinson, D.G., and Jiang, L.** (2012). Unconventional protein secretion. *Trends Plant Sci.* **17**: 606–615.
- Djébali, N. et al.** (2009). Partial resistance of *Medicago truncatula* to *Aphanomyces euteiches* is associated with protection of the root stele and is controlled by a major QTL rich in proteasome-related genes. *Mol Plant Microbe Interact* **22**: 1043–1055.
- Dodds, P.N. and Rathjen, J.P.** (2010). Plant immunity: towards an integrated view of plant-pathogen interactions. *Nat Rev Genet* **11**: 539–548.
- Dou, D., Kale, S.D., Wang, X., Jiang, R.H.Y., Bruce, N. a, Arredondo, F.D., Zhang, X., and Tyler, B.M.** (2008). RXLR-mediated entry of *Phytophthora sojae* effector Avr1b into soybean cells does not require pathogen-encoded machinery. *Plant Cell* **20**: 1930–1947.
- Duplan, V. and Rivas, S.** (2014). E3 ubiquitin-ligases and their target proteins during the regulation of plant innate immunity. *Front Plant Sci* **5**: 42.
- Duplessis, S. et al.** (2011). Obligate biotrophy features unraveled by the genomic analysis of rust fungi. *Proc Natl Acad Sci* **108**: 9166–9171.
- Elling, A. a, Davis, E.L., Hussey, R.S., and Baum, T.J.** (2007). Active uptake of cyst nematode

- parasitism proteins into the plant cell nucleus. *Int J Parasitol* **37**: 1269–1279.
- Engelhardt, S., Boevink, P.C., Armstrong, M.R., Ramos, M.B., Hein, I., and Birch, P.R.J.** (2012). Relocalization of late blight resistance protein R3a to endosomal compartments is associated with effector recognition and required for the immune response. *Plant Cell* **24**: 5142–5158.
- Erbs, G., Silipo, A., Aslam, S., De Castro, C., Liparoti, V., Flagiello, A., Pucci, P., Lanzetta, R., Parrilli, M., Molinaro, A., Newman, M.-A., and Cooper, R.M.** (2008). Peptidoglycan and muropeptides from pathogens *Agrobacterium* and *Xanthomonas* elicit plant innate immunity: structure and activity. *Chem Biol* **15**: 438–448.
- Fabro, G. et al.** (2011). Multiple candidate effectors from the oomycete pathogen *Hyaloperonospora arabidopsidis* suppress host plant immunity. *PLoS Pathog* **7**: e1002348.
- Felix, G., Duran, J.D., Volko, S., and Boller, T.** (1999). Plants have a sensitive perception system for the most conserved domain of bacterial flagellin. *Plant J* **18**: 265–276.
- Feng, B.Z. and Li, P.Q.** (2013). Molecular characterization and functional analysis of the Nep1-like protein-encoding gene from *Phytophthora capsici*. *Genet Mol Res* **12**: 1468–1478.
- Feng, J., Zhang, H., Strelkov, S.E., and Hwang, S.-F.** (2014). The LmSNF1 Gene Is Required for Pathogenicity in the Canola Blackleg Pathogen *Leptosphaeria maculans*. *PLoS One* **9**: e92503.
- Filipova, L., 1, 2, Adam Petrussek1, Kla ́ra Matasova ́1, Carine Delaunay2, Fre ́de ́ric Grandjean2Filipová, L., Petrussek, A., Matasová, K., Delaunay, C., and Grandjean, F.** (2013). Prevalence of the crayfish plague pathogen *Aphanomyces astaci* in populations of the signal crayfish *Pacifastacus leniusculus* in France: evaluating the threat to native crayfish. *PLoS One* **8**: e70157.
- Finley, D., Bartel, B., and Varshavsky, A.** (1989). The tails of ubiquitin precursors are ribosomal proteins whose fusion to ubiquitin facilitates ribosome biogenesis. *Nature* **338**: 394–401.
- Fisher, M.C., Garner, T.W.J., and Walker, S.F.** (2009). Global emergence of *Batrachochytrium dendrobatidis* and amphibian chytridiomycosis in space, time, and host. *Annu Rev Microbiol* **63**: 291–310.
- Fisher, M.C., Henk, D. a, Briggs, C.J., Brownstein, J.S., Madoff, L.C., McCraw, S.L., and Gurr, S.J.** (2012). Emerging fungal threats to animal, plant and ecosystem health. *Nature* **484**: 186–94.
- Flood, J.** (2010). The importance of plant health to food security. *Food Secur* **2**: 215–231.
- Flor, H.H.** (1971). Current Status of the Gene-For-Gene Concept. *Annu Rev Phytopathol* **9**: 275–296.
- Fraiture, M., Zheng, X., and Brunner, F.** (2014). An Arabidopsis and Tomato Mesophyll Protoplast System for Fast Identification of Early MAMP-Triggered Immunity-Suppressing Effectors. In *Plant-Pathogen Interactions*, P. Birch, J.T. Jones, and J.I.B. Bos, eds, *Methods in Molecular Biology*. (Humana Press), pp. 213–230.
- Fu, H., Feng, J., Aboukhaddour, R., Cao, T., Hwang, S.-F., and Strelkov, S.E.** (2013). An *exo*-1,3 β -glucanase *GLU1* contributes to the virulence of the wheat tan spot pathogen *Pyrenophora tritici-repentis*. *Fungal Biol* **117**: 673–681.-
- Fu, Z.Q., Guo, M., Jeong, B., Tian, F., Elthon, T.E., Cerny, R.L., Staiger, D., and Alfano, J.R.** (2007). A type III effector ADP-ribosylates RNA-binding proteins and quells plant immunity. *Nature* **447**: 284–288.
- Gan, P.H.P., Rafiqi, M., Ellis, J.G., Jones, D. a., Hardham, A.R., and Dodds, P.N.** (2010). Lipid binding activities of flax rust *AvrM* and *AvrL567* effectors. *Plant Signal Behav* **5**: 1272–1275.
- Gao, B., Allen, R., Maier, T., Davis, E.L., Baum, T.J., and Hussey, R.S.** (2003). The Parasitome of the Phytonematode *Heterodera glycines*. **16**: 720–726.
- Gao, L., Kelliher, T., Nguyen, L., and Walbot, V.** (2013). *Ustilago maydis* reprograms cell proliferation in maize anthers. *Plant J* **75**: 903–914.
- García, A. V, Blanvillain-Baufumé, S., Huibers, R.P., Wiermer, M., Li, G., Gobbato, E., Rietz, S., and**

- Parker, J.E.** (2010). Balanced nuclear and cytoplasmic activities of EDS1 are required for a complete plant innate immune response. *PLoS Pathog* **6**: e1000970.
- Gardiner, D.M., Kazan, K., and Manners, J.M.** (2013). Cross-kingdom gene transfer facilitates the evolution of virulence in fungal pathogens. *Plant Sci* **210**: 151–158.
- Gaulin, E. et al.** (2006). Cellulose Binding Domains of a Phytophthora Cell Wall Protein Are Novel Pathogen-Associated Molecular Patterns. *Plant Cell* **18**: 1766–1777.
- Gaulin, E., Bottin, A., and Dumas, B.** (2010). Sterol biosynthesis in oomycete pathogens. *Plant Signal Behav* **5**: 258–260.
- Gaulin, E., Jacquet, C., Bottin, A., and Duamas, B.** (2007). Root rot disease of legumes caused by *Aphanomyces euteiches*. *Mol Plant Pathol* **8**: 539–548.
- Gaulin, E., Madoui, M.-A., Bottin, A., Jacquet, C., Mathé, C., Couloux, A., Wincker, P., and Dumas, B.** (2008). Transcriptome of *Aphanomyces euteiches*: new oomycete putative pathogenicity factors and metabolic pathways. *PLoS One* **3**: e1723.
- Gessler, C., Pertot, I., and Perazzolli, M.** (2011). *Plasmopara viticola*: a review of knowledge on downy mildew of grapevine and effective disease management. *Phytopathol Mediter* **50**: 3–44.
- Gijzen, M. and Nürnberger, T.** (2006). Nep1-like proteins from plant pathogens: recruitment and diversification of the NPP1 domain across taxa. *Phytochemistry* **67**: 1800–7.
- Gilbert, C. and Cordaux, R.** (2013). Horizontal transfer and evolution of prokaryote transposable elements in eukaryotes. *Genome Biol Evol* **5**: 822–832.
- Gilroy, E.M., Taylor, R.M., Hein, I., Boevink, P., Sadanandom, A., and Birch, P.R.J.** (2011). CMPG1-dependent cell death follows perception of diverse pathogen elicitors at the host plasma membrane and is suppressed by *Phytophthora infestans* RXLR effector AVR3a. *New Phytol* **190**: 653–666.
- Giraldo, M.C., Dagdas, Y.F., Gupta, Y.K., Mentlak, T. a, Yi, M., Martinez-Rocha, A.L., Saitoh, H., Terauchi, R., Talbot, N.J., and Valent, B.** (2013). Two distinct secretion systems facilitate tissue invasion by the rice blast fungus *Magnaporthe oryzae*. *Nat Commun* **4**: 1996.
- Godfrey, D., Böhlenius, H., Pedersen, C., Zhang, Z., Emmersen, J., and Thordal-Christensen, H.** (2010). Powdery mildew fungal effector candidates share N-terminal Y/F/WxC-motif. *BMC Genomics* **11**: 317.
- Gómez-Gómez, L., Felix, G., and Boller, T.** (1999). A single locus determines sensitivity to bacterial flagellin in *Arabidopsis thaliana*. *Plant J* **18**: 277–284.
- Goodin, M.M., Zaitlin, D., Naidu, R. a, and Lommel, S.** (2008). *Nicotiana benthamiana*: its history and future as a model for plant-pathogen interactions. *Mol Plant Microbe Interact* **21**: 1015–1026.
- Grenville-Briggs, L., Gachon, C.M.M., Strittmatter, M., Sterck, L., Küpper, F.C., and van West, P.** (2011). A molecular insight into algal-oomycete warfare: cDNA analysis of *Ectocarpus siliculosus* infected with the basal oomycete *Eurychasma dicksonii*. *PLoS One* **6**: e24500.
- Grünwald, N.J., Garbelotto, M., Goss, E.M., Heungens, K., and Prospero, S.** (2012). Emergence of the sudden oak death pathogen *Phytophthora ramorum*. *Trends Microbiol* **20**: 131–138.
- Guerriero, G., Avino, M., Zhou, Q., Fugelstad, J., Clergeot, P.-H., and Bulone, V.** (2010). Chitin synthases from *Saprolegnia* are involved in tip growth and represent a potential target for anti-oomycete drugs. *PLoS Pathog* **6**: e1001070.
- Haas, B.J. et al.** (2009). Genome sequence and analysis of the Irish potato famine pathogen *Phytophthora infestans*. *Nature* **461**: 393–398.
- Haegeman, A., Jones, J.T., and Danchin, E.G.J.** (2011). Horizontal gene transfer in nematodes: a catalyst for plant parasitism? *Mol Plant Microbe Interact* **24**: 879–887.
- Hahn, M. and Mendgen, K.** (1997). Characterization of in planta-induced rust genes isolated from a haustorium-specific cDNA library. *Mol Plant Microbe Interact* **10**: 427–37.

- Hamon, C. et al.** (2013). QTL meta-analysis provides a comprehensive view of loci controlling partial resistance to *Aphanomyces euteiches* in four sources of resistance in pea. *BMC Plant Biol* **13**: 45.
- Heidrich, K., Wirthmueller, L., Tasset, C., Pouzet, C., Deslandes, L., and Parker, J.E.** (2011). *Arabidopsis* EDS1 connects pathogen effector recognition to cell compartment-specific immune responses. *Science* **334**: 1401–4.
- Heidrich, K., Wirthmueller, L., Tasset, C., Pouzet, C., Deslandes, L., and Parker, J.E.** (2011).
- Hématy, K., Cherk, C., and Somerville, S.** (2009). Host-pathogen warfare at the plant cell wall. *Curr Opin Plant Biol* **12**: 406–413.
- Hemetsberger, C., Herrberger, C., Zechmann, B., Hillmer, M., and Doehlemann, G.** (2012). The *Ustilago maydis* effector Pep1 suppresses plant immunity by inhibition of host peroxidase activity. *PLoS Pathog* **8**: e1002684.
- Hewezi, T. and Baum, T.J.** (2013). Manipulation of plant cells by cyst and root-knot nematode effectors. *Mol Plant Microbe Interact* **26**: 9–16.
- Hiller, N.L., Bhattacharjee, S., van Ooij, C., Liolios, K., Harrison, T., Lopez-Estraño, C., and Haldar, K.** (2004). A host-targeting signal in virulence proteins reveals a secretome in malarial infection. *Science* **306**: 1934–1937.
- Hirsch, S. and Oldroyd, G.E.D.** (2009). GRAS-domain transcription factors that regulate plant development. *Plant Signal Behav* **4**: 698–700.
- Hobbelen, P.H.F., Paveley, N.D., and van den Bosch, F.** (2011). Delaying selection for fungicide insensitivity by mixing fungicides at a low and high risk of resistance development: a modeling analysis. *Phytopathology* **101**: 1224–1233.
- Hogenhout, S., Van der Hoorn, R., Terauchi, R., and Kamoun, S.** (2009). Emerging concepts in effector biology of plant-associated organisms. *Mol Plant Microbe Interact* **22**: 115–22.
- Hotson, A., Chosed, R., Shu, H., Orth, K., and Mudgett, M.B.** (2003). *Xanthomonas* type III effector XopD targets SUMO-conjugated proteins in planta. *Mol Microbiol* **50**: 377–389.
- Houterman, P.M., Ma, L., van Ooijen, G., de Vroomen, M.J., Cornelissen, B.J.C., Takken, F.L.W., Rep, M.** (2009). The effector protein Avr2 of the xylem-colonizing fungus *Fusarium oxysporum* activates the tomato resistance protein I-2 intracellularly. *Plant J* **58**: 970–978.
- Houterman, P.M., Speijer, D., Dekker, H.L., De Koster, C.G., Cornelissen, B.J., and Martijn, R.** (2007). The mixed xylem sap proteome of *Fusarium oxysporum* -infected tomato plants. *Mol Plant Pathol* **8**: 215–221.
- Huang, G., Dong, R., Allen, R., Davis, E.L., Baum, T.J., and Hussey, R.S.** (2006). A root-knot nematode secretory peptide functions as a ligand for a plant transcription factor. *Mol Plant Microbe Interact* **19**: 463–470.
- Huang, G., Dong, R., Maier, T., Allen, R., Davis, E., Baum, T.J., and Hussey, R.S.** (2004). Use of solid-phase subtractive hybridization for the identification of parasitism gene candidates from the root-knot nematode *Meloidogyne incognita*. *Mol Plant Pathol* **5**: 217–222.
- Inoue, H., Hayashi, N., Matsushita, A., Xinqiong, L., Nakayama, A., Sugano, S., Jiang, C.-J., and Takatsuji, H.** (2013). Blast resistance of CC-NB-LRR protein Pb1 is mediated by WRKY45 through protein-protein interaction. *Proc Natl Acad Sci U S A* **110**: 9577–9582.
- Jaouannet, M., Perfus-barbeoch, L., Deleury, E., Magliano, M., Engler, G., Vieira, P., Danchin, E.G.J., Rocha, M. Da, Coquillard, P., and Abad, P.** (2012). Rapid report A root-knot nematode-secreted protein is injected into giant cells and targeted to the nuclei. *New Phytol* **194**:924–931.
- Jelenska, J., Yao, N., Vinatzer, B. a, Wright, C.M., Brodsky, J.L., and Greenberg, J.T.** (2007). A J domain virulence effector of *Pseudomonas syringae* remodels host chloroplasts and suppresses defenses. *Curr Biol* **17**: 499–508.

- Jiang, R.H.Y. et al.** (2013). Distinctive Expansion of Potential Virulence Genes in the Genome of the Oomycete Fish Pathogen *Saprolegnia parasitica*. *PLoS Genet* **9**: e1003272.
- Joneson, S., Stajich, J.E., Shiu, S.-H., and Rosenblum, E.B.** (2011). Genomic transition to pathogenicity in chytrid fungi. *PLoS Pathog* **7**: e1002338.
- Judelson, H.S. and Senthil, G.** (2006). Investigating the role of ABC transporters in multifungicide insensitivity in *Phytophthora infestans*. *Mol Plant Pathol* **7**: 17–29.
- Kale, S.D. et al.** (2010). External lipid PI3P mediates entry of eukaryotic pathogen effectors into plant and animal host cells. *Cell* **142**: 284–295.
- Kamoun, S., van West P, Vleeshouwers, V., de Groot KE, and Govers, F.** (1998). Resistance of *Nicotiana benthamiana* to *Phytophthora infestans* is mediated by the recognition of the elicitor protein INF1. *Plant Cell* **10**: 1413–1426.
- Kankanala, P., Czymmek, K., and Valent, B.** (2007). Roles for rice membrane dynamics and plasmodesmata during biotrophic invasion by the blast fungus. *Plant Cell* **19**: 706–24.
- Kanneganti, T.-D., Bai, X., Tsai, C.-W., Win, J., Meulia, T., Goodin, M., Kamoun, S., and Hogenhout, S. a** (2007). A functional genetic assay for nuclear trafficking in plants. *Plant J* **50**: 149–158
- Kanzaki, H., Saitoh, H., Takahashi, Y., Berberich, T., Ito, A., Kamoun, S., and Terauchi, R.** (2008). NbLRK1, a lectin-like receptor kinase protein of *Nicotiana benthamiana*, interacts with *Phytophthora infestans* INF1 elicitor and mediates INF1-induced cell death. *Planta* **228**: 977–987.
- Kanzaki, H., Yoshida, K., Saitoh, H., Tamiru, M., and Terauchi, R.** (2014). Protoplast Cell Death Assay to Study *Magnaporthe oryzae* AVR Gene Function in Rice. In *Plant-Pathogen Interactions*, P. Birch, J.T. Jones, and J.I.B. Bos, eds, *Methods in Molecular Biology*. (Humana Press), pp. 269–275.
- Kay, S., Hahn, S., Marois, E., Hause, G., and Bonas, U.** (2007). A bacterial effector acts as a plant transcription factor and induces a cell size regulator. *Science* **318**: 648–651.
- Kelley, B.S., Lee, S.-J., Damasceno, C.M.B., Chakravarthy, S., Kim, B.-D., Martin, G.B., and Rose, J.K.C.** (2010). A secreted effector protein (SNE1) from *Phytophthora infestans* is a broadly acting suppressor of programmed cell death. *Plant J* **62**: 357–366.
- Kemen, E., Gardiner, A., Schultz-Larsen, T., Kemen, A.C., Balmuth, A.L., Robert-Seilaniantz, A., Bailey, K., Holub, E., Studholme, D.J., Maclean, D., and Jones, J.D.G.** (2011). Gene gain and loss during evolution of obligate parasitism in the white rust pathogen of *Arabidopsis thaliana*. *PLoS Biol* **9**: e1001094.
- Kemen, E., Kemen, A., Ehlers, A., Voegelé, R., and Mendgen, K.** (2013). A novel structural effector from rust fungi is capable of fibril formation. *Plant J* **75**: 767–780.
- Kemen, E., Kemen, A.C., Rafiqi, M., Hempel, U., Mendgen, K., Hahn, M., and Voegelé, R.T.** (2005). Identification of a protein from rust fungi transferred from haustoria into infected plant cells. *Mol Plant Microbe Interact* **18**: 1130–1139.
- Khang, C.H., Berruyer, R., Giraldo, M.C., Kankanala, P., Park, S.-Y., Czymmek, K., Kang, S., and Valent, B.** (2010). Translocation of *Magnaporthe oryzae* effectors into rice cells and their subsequent cell-to-cell movement. *Plant Cell* **22**: 1388–1403.
- Kilpatrick, a M., Briggs, C.J., and Daszak, P.** (2010). The ecology and impact of chytridiomycosis: an emerging disease of amphibians. *Trends Ecol Evol* **25**: 109–118.
- Kim, B.H., Kim, S.Y., and Nam, K.H.** (2013). Assessing the diverse functions of BAK1 and its homologs in *Arabidopsis*, beyond BR signaling and PTI responses. *Mol Cells* **35**: 7–16.
- King, B.C., Waxman, K.D., Nenni, N. V, Walker, L.P., Bergstrom, G.C., and Gibson, D.M.** (2011); Arsenal of plant cell wall degrading enzymes reflects host preference among plant pathogenic fungi. *Biotechnol Biofuels* **4**: 4.
- Kloppholz, S., Kuhn, H., and Requena, N.** (2011). A secreted fungal effector of *Glomus intraradices* promotes symbiotic biotrophy. *Curr Biol* **21**: 1204–1209.
- Kolodziejek, I., Misas-Villamil, J.C., Kaschani, F., Clerc, J., Gu, C., Krahn, D., Niessen, S., Verdoes, M., Willems, L.I., Overkleeft, H.S., Kaiser, M., and van der Hoorn, R. a L.** (2011). Proteasome

- activity imaging and profiling characterizes bacterial effector syringolin A. *Plant Physiol* **155**: 477–489.
- Kombrink, A. and Thomma, B.P.H.** (2013). LysM Effectors : Secreted Proteins Supporting Fungal Life. *Plos Pathog* **9**: 1–4.
- Kouzai, Y., Nakajima, K., Hayafune, M., Ozawa, K., Kaku, H., Shibuya, N., Minami, E., and Nishizawa, Y.** (2014). CEBiP is the major chitin oligomer-binding protein in rice and plays a main role in the perception of chitin oligomers. *Plant Mol Biol* **84**: 519–528.
- Kouzai, Y., Nakajima, K., Hayafune, M., Ozawa, K., Kaku, H., Shibuya, N., Minami, E., and Nishizawa, Y.** (2014). CEBiP is the major chitin oligomer-binding protein in rice and plays a main role in the perception of chitin oligomers. *Plant Mol. Biol.* **84**: 519–28.
- Kouzarides, T.** (2007). Chromatin modifications and their function. *Cell* **128**: 693–705.
- Krajaejun, T., Khositnithikul, R., Lerksuthirat, T., Lowhnoo, T., Rujirawat, T., Petchthong, T., Yingyong, W., Suriyaphol, P., Smittipat, N., Juthayothin, T., Phuntumart, V., and Sullivan, T.D.** (2011). Expressed sequence tags reveal genetic diversity and putative virulence factors of the pathogenic oomycete *Pythium insidiosum*. *Fungal Biol* **115**: 683–696.
- Kroon, L.P.N.M., Brouwer, H., de Cock, A.W. a M., and Govers, F.** (2012). The genus *Phytophthora* anno 2012. *Phytopathology* **102**: 348–364.
- Kunze, G., Zipfel, C., Robatzek, S., Niehaus, K., Boller, T., and Felix, G.** (2004). The N Terminus of Bacterial Elongation Factor Tu Elicits Innate Immunity in Arabidopsis Plants. *Plant Cell* **16**: 3496–3507.
- Larroque, M., Belmas, E., Martinez, T., Vergnes, S., Ladouce, N., Lafitte, C., Gaulin, E., and Dumas, B.** (2013). Pathogen-associated molecular pattern-triggered immunity and resistance to the root pathogen *Phytophthora parasitica* in Arabidopsis. *J Exp Bot* **64**: 3615–3625.
- Lee, L.-Y. et al.** (2012). Screening a cDNA library for protein-protein interactions directly in planta. *Plant Cell* **24**: 1746–1759
- Lévesque, C.A. et al.** (2010). Genome sequence of the necrotrophic plant pathogen *Pythium ultimum* reveals original pathogenicity mechanisms and effector repertoire. *Genome Biol* **11**: R73.
- Lin, B., Zhuo, K., Wu, P., Cui, R., Zhang, L.-H., and Liao, J.** (2013). A novel effector protein, MJ-NULG1a, targeted to giant cell nuclei plays a role in *Meloidogyne javanica* parasitism. *Mol Plant Microbe Interact* **26**: 55–66.
- Lin, K. et al.** (2014). Single Nucleus Genome Sequencing Reveals High Similarity among Nuclei of an Endomycorrhizal Fungus. *PLoS Genet* **10**: 1–13.
- Links, M.G., Holub, E., Jiang, R.H.Y., Sharpe, A.G., Hegedus, D., Beynon, E., Sillito, D., Clarke, W.E., Uzuhashi, S., and Borhan, M.H.** (2011). De novo sequence assembly of *Albugo candida* reveals a small genome relative to other biotrophic oomycetes. *BMC Genomics* **12**: 503.
- Liu, T., Ye, W., Ru, Y., Yang, X., Gu, B., Tao, K., Lu, S., Dong, S., Zheng, X., Shan, W., Wang, Y., and Dou, D.** (2011). Two host cytoplasmic effectors are required for pathogenesis of *Phytophthora sojae* by suppression of host defenses. *Plant Physiol* **155**: 490–501.
- Livak, K.J. and Schmittgen, T.D.** (2001). Analysis of relative gene expression data using real-time quantitative PCR and the 2^{(-Delta Delta C(T))} Method. *Methods* **25**: 402–408.
- Lorković, Z.J., Hilscher, J., and Barta, A.** (2008). Co-localisation studies of Arabidopsis SR splicing factors reveal different types of speckles in plant cell nuclei. *Exp Cell Res* **314**: 3175–3186.
- Lozano-Torres, J.L. et al.** (2012). Dual disease resistance mediated by the immune receptor Cf-2 in tomato requires a common virulence target of a fungus and a nematode. *Proc Natl Acad Sci U S A* **109**: 10119–10124.
- Ma, X., Lv, S., Zhang, C., and Yang, C.** (2013). Histone deacetylases and their functions in plants. *Plant*

- Cell Rep **32**: 465–478.
- MacLean, A.M., Sugio, A., Makarova, O. V, Findlay, K.C., Grieve, V.M., Tóth, R., Nicolaisen, M., and Hogenhout, S. a** (2011). Phytoplasma effector SAP54 induces indeterminate leaf-like flower development in Arabidopsis plants. *Plant Physiol* **157**: 831–841.
- Maleck, K., Levine, a, Eulgem, T., Morgan, a, Schmid, J., Lawton, K. a, Dangl, J.L., and Dietrich, R. a** (2000). The transcriptome of Arabidopsis thaliana during systemic acquired resistance. *Nat Genet* **26**: 403–410.
- Malvick, D.K. and Grau, C.R.** (2001). Characteristics and frequency of *Aphanomyces euteiches* races 1 and 2 associated with alfalfa in the Midwestern United States. *Plant Dis* **74**:716-718.
- Marti, M., Good, R.T., Rug, M., Knuepfer, E., and Cowman, A.F.** (2004). Targeting malaria virulence and remodeling proteins to the host erythrocyte. *Science* **306**: 1930–1933.
- Matari, N.H. and Blair, J.E.** (2014). A multilocus timescale for oomycete evolution estimated under three distinct molecular clock models. *BMC Evol Biol* **14**: 101.
- McLellan, H., Boevink, P.C., Armstrong, M.R., Pritchard, L., Gomez, S., Morales, J., Whisson, S.C., Beynon, J.L., and Birch, P.R.J.** (2013). An RxLR effector from *Phytophthora infestans* prevents re-localisation of two plant NAC transcription factors from the endoplasmic reticulum to the nucleus. *PLoS Pathog* **9**: e1003670.
- Meijer, H.J.G., Mancuso, F.M., Espadas, G., Seidl, M.F., Govers, F., and Sabidó, E.** (2014). Profiling the secretome and extracellular proteome of the potato late blight pathogen *Phytophthora infestans*. *Mol Cell Proteomics*: 1–33.
- Mélida, H., Sandoval-Sierra, J. V, Diéguez-Uribeondo, J., and Bulone, V.** (2013). Analyses of extracellular carbohydrates in oomycetes unveil the existence of three different cell wall types. *Eukaryot Cell* **12**: 194–203.
- Mikes, V., Milat, M.L., Ponchet, M., Panabières, F., Ricci, P., and Blein, J.P.** (1998). Elicitins, proteinaceous elicitors of plant defense, are a new class of sterol carrier proteins. *Biochem Biophys Res Commun* **245**: 133–139.
- Mingora, C., Ewer, J., and Ospina-Giraldo, M.** (2014). Comparative structural and functional analysis of genes encoding pectin methyl esterases in *Phytophthora* spp. *Gene* **538**: 74–83.
- Mitchum, M.G., Hussey, R.S., Baum, T.J., Wang, X., Elling, A.A., Wubben, M., and Davis, E.L.** (2013). Nematode effector proteins : an emerging paradigm of parasitism. *New Phytol* **199**: 879–894.
- Moussart, A., Even, M., and Tivoli, B.** (2008). Reaction of genotypes from several species of grain and forage legumes to infection with a French pea isolate of the oomycete *Aphanomyces euteiches*. *Eur. J. Plant Pathol.* **122**:321-333.
- Moussart, A., Onfroy, C., Lesne, A., Esquibet, M., Grenier, E., and Tivoli, B.** (2007). Host status and reaction of *Medicago truncatula* accessions to infection by three major pathogens of pea (*Pisum sativum*) and alfalfa (*Medicago sativa*). *Eur J Plant Pathol* **117**: 57–69.
- Mueller, A.N., Ziemann, S., Treitschke, S., Abmann, D., and Doehlemann, G.** (2013). Compatibility in the *Ustilago maydis*-maize interaction requires inhibition of host cysteine proteases by the fungal effector Pit2. *PLoS Pathog* **9**: e1003177.
- Mueller, O., Kahmann, R., Aguilar, G., Trejo-Aguilar, B., Wu, A., and de Vries, R.P.** (2008). The secretome of the maize pathogen *Ustilago maydis*. *Fungal Genet Biol* **45 Suppl 1**: S63–70.
- Mukhtar, M.S. et al.** (2011). Independently evolved virulence effectors converge onto hubs in a plant immune system network. *Science* **333**: 596–601.
- Nafisi, M., Stranne, M., Zhang, L., van Kan, J.A., and Sakuragi, Y.** (2014). The endo-arabinanase BcAra1 is a novel host-specific virulence factor of the necrotic fungal phytopathogen *Botrytis cinerea*. *Mol Plant Microbe Interact*: 1–56.
- Nars, A. et al.** (2013). *Aphanomyces euteiches* cell wall fractions containing novel glucan-

- chitosaccharides induce defense genes and nuclear calcium oscillations in the plant host *Medicago truncatula*. *PLoS One* **8**: e75039.
- Nature* **468**: 527–534.
- Nicaise, V., Joe, A., Jeong, B., Korneli, C., Boutrot, F., Westedt, I., Staiger, D., Alfano, J.R., and Zipfel, C.** (2013). *Pseudomonas* HopU1 modulates plant immune receptor levels by blocking the interaction of their mRNAs with GRP7. *EMBO J* **32**: 701–712.
- Nickel, W. and Rabouille, C.** (2009). Mechanisms of regulated unconventional protein secretion. *Nat. Rev. Mol. Cell Biol.* **10**: 148–155.
- Nivaskumar, M. and Francetic, O.** (2014). Type II secretion system: A magic beanstalk or a protein escalator. *Biochim Biophys Acta.* **1843**: 1568–1577
- Nomura, K., Mecey, C., Lee, Y.-N., Imbode, L.A., Chang, J.H., and He, S.Y.** (2011). Effector-triggered immunity blocks pathogen degradation of an immunity-associated vesicle traffic regulator in *Arabidopsis*. *Proc Natl Acad Sci U S A* **108**: 1077–10779.
- Nowicki, M., Foolad, M.R., Nowakowska, M., and Kozik, E.U.** (2012). Potato and tomato late blight caused by *Phytophthora infestans*: an overview of pathology and resistance breeding. *Plant Dis* **96**.
- Nürnbergger, T., Nennstiel, D., Jabs, T., Sacks, W.R., Hahlbrock, K., and Scheel, D.** (1994). High affinity binding of a fungal oligopeptide elicitor to parsley plasma membranes triggers multiple defense responses. *Cell* **78**: 449–60.
- O’Connell, R.J. et al.** (2012). Lifestyle transitions in plant pathogenic *Colletotrichum* fungi deciphered by genome and transcriptome analyses. *Nat Genet* **44**: 1060–1065.
- Okmen, B. and Doehlemann, G.** (2014). Inside plant: biotrophic strategies to modulate host immunity and metabolism. *Curr Opin Plant Biol* **20C**: 19–25.
- Oliveira, D.L., Rizzo, J., Joffe, L.S., Godinho, R.M.C., and Rodrigues, M.L.** (2013). Where do they come from and where do they go: candidates for regulating extracellular vesicle formation in fungi. *Int. J. Mol. Sci.* **14**: 9581–9603.
- Ospina-Giraldo, M.D., Griffith, J.G., Laird, E.W., and Mingora, C.** (2010). The CAZyome of *Phytophthora* spp.: a comprehensive analysis of the gene complement coding for carbohydrate-active enzymes in species of the genus *Phytophthora*. *BMC Genomics* **11**: 525.
- Padmanabhan, M.S., Ma, S., Burch-Smith, T.M., Czymmek, K., Huijser, P., and Dinesh-Kumar, S.P.** (2013). Novel positive regulatory role for the SPL6 transcription factor in the N TIR-NB- LRR receptor-mediated plant innate immunity. *PLoS Pathog* **9**: e1003235.
- Pais, M., Win, J., Yoshida, K., Etherington, G.J., Cano, L.M., Raffaele, S., Banfield, M.J., Jones, A., Kamoun, S., and Go Saunders, D.** (2013). From pathogen genomes to host plant processes: the power of plant parasitic oomycetes. *Genome Biol* **14**: 211.
- Pang, Z., Shao, J., Chen, L., Lu, X., Hu, J., Qin, Z., and Liu, X.** (2013). Resistance to the novel fungicide pyrimorph in *Phytophthora capsici*: risk assessment and detection of point mutations in *CesA3* that confer resistance. *PLoS One* **8**: e56513.
- Papavizas G, Davey C.** (1960). Some factors affecting growth of *Aphanomyces euteiches* in synthetic media. *Amer J Bot* **47**: 758–765.
- Pedersen, C. et al.** (2012). Structure and evolution of barley powdery mildew effector candidates
- Peeters, N., Carrère, S., Anisimova, M., Plener, L., and Cazalé, A.** (2013). Repertoire , unified nomenclature and evolution of the Type III effector gene set in the *Ralstonia solanacearum* species complex. *BMC Genomics* **14**: 2–18.
- Peng, H.-C. and Kaloshian, I.** (2014). The Tomato Leucine-Rich Repeat Receptor-Like Kinases *SISERK3A* and *SISERK3B* Have Overlapping Functions in Bacterial and Nematode Innate Immunity. *PLoS One* **9**: e93302.

- Pennisi, E.** (2010). Armed and dangerous. *Science* **327**: 804–805.
- Petersen, A.B. and Rosendahl, S.** (2000). Phylogeny of the Peronosporomycetes (Oomycota) based on partial sequences of the large ribosomal subunit (LSU rDNA). *Mycol Res* **104**: 1295–1303.
- Petutschnig, E.K., Jones, A.M.E., Serazetdinova, L., Lipka, U., and Lipka, V.** (2010). The lysin motif receptor-like kinase (LysM-RLK) CERK1 is a major chitin-binding protein in *Arabidopsis thaliana* and subject to chitin-induced phosphorylation. *J Biol Chem* **285**: 28902–20911.
- Phillips, A.J., Anderson, V.L., Robertson, E.J., Secombes, C.J., and van West, P.** (2008). New insights into animal pathogenic oomycetes. *Trends Microbiol* **16**: 13–29.
- Phytophthora sojae Effector PsCRN70 Suppresses Plant Defenses in *Nicotiana benthamiana*.** *PLoS One* **9**: e98114.
- Pitzschke, A., Schikora, A., and Hirt, H.** (2009). MAPK cascade signalling networks in plant defense. *Curr Opin Plant Biol* **12**: 421–426.
- Plett, J.M., Kemppainen, M., Kale, S.D., Kohler, A., Legué, V., Brun, A., Tyler, B.M., Pardo, A.G., and Martin, F.** (2011). A secreted effector protein of *Laccaria bicolor* is required for symbiosis development. *Curr Biol* **21**: 1197–1203.
- Pliego, C. et al.** (2013). Host-induced gene silencing in barley powdery mildew reveals a class of ribonuclease-like effectors. *Mol Plant Microbe Interact* **26**: 633–642.
- Pretsch, K., Kemen, A., Kemen, E., Geiger, M., Mendgen, K., and Voegele, R.** (2013). The rust transferred proteins: a new family of effector proteins exhibiting protease inhibitor function. *Mol Plant Pathol* **14**: 96–107.
- Pritchard, L. and Birch, P.** (2011). A systems biology perspective on plant-microbe interactions: biochemical and structural targets of pathogen effectors. *Plant Sci* **180**: 584–603.
- Purugganan, M.D. and Fuller, D.Q.** (2009). The nature of selection during plant domestication. *Nature* **457**: 843–848.
- Qi, D. and Innes, R.W.** (2013). Recent Advances in Plant NLR Structure, Function, Localization, and Signaling. *Front Immunol* **4**: 1–10.
- Qiao, Y. et al.** (2013). Oomycete pathogens encode RNA silencing suppressors. *Nat Genet* **45**: 330–333.
- Rafiqi, M., Gan, P.H.P., Ravensdale, M., Lawrence, G.J., Ellis, J.G., Jones, D. a, Hardham, A.R., and Dodds, P.N.** (2010). Internalization of flax rust avirulence proteins into flax and tobacco cells can occur in the absence of the pathogen. *Plant Cell* **22**: 2017–2022.
- Rajput, N.A., Zhang, M., Ru, Y., Liu, T., Xu, J., Liu, L., Mafurah, J.J., and Dou, D.** (2014).
- Rehmany, A.P., Gordon, A., Rose, L.E., Allen, R.L., Armstrong, M.R., Whisson, S.C., Kamoun, S., Tyler, B.M., Birch, P.R.J., and Beynon, J.L.** (2005). Differential Recognition of Highly Divergent Downy Mildew Avirulence Gene Alleles by RPP1 Resistance Genes from Two *Arabidopsis* Lines. *Plant Cell* **17**: 1839–1850.
- Rep, M., van der Does, H.C., Meijer, M., van Wijk, R., Houterman, P.M., Dekker, H.L., de Koster, C.G., and Cornelissen, B.J.C.** (2004). A small, cysteine-rich protein secreted by *Fusarium oxysporum* during colonization of xylem vessels is required for I-3-mediated resistance in tomato. *Mol Microbiol* **53**: 1373–1383.
- Rey, T., Nars, A., Bonhomme, M., Bottin, A., Huguet, S., Balzergue, S., Jardinaud, M.-F., Bono, J.-J., Cullimore, J., Dumas, B., Gough, C., and Jacquet, C.** (2013). NFP, a LysM protein controlling Nod factor perception, also intervenes in *Medicago truncatula* resistance to pathogens. *New Phytol* **198**: 875–886.
- Ribot, C., Césari, S., Abidi, I., Chalvon, V., Bournaud, C., Vallet, J., Lebrun, M.-H., Morel, J.-B., and**

- Kroj, T.** (2013). The Magnaporthe oryzae effector AVR1-CO39 is translocated into rice cells independently of a fungal-derived machinery. *Plant J* **74**: 1–12.
- Richards, T. a, Dacks, J.B., Jenkinson, J.M., Thornton, C.R., and Talbot, N.J.** (2006). Evolution of filamentous plant pathogens: gene exchange across eukaryotic kingdoms. *Curr Biol* **16**: 1857–1864.
- Richards, T.A., Soanes, D.M., Jones, M.D.M., Vasieva, O., Leonard, G., Paszkiewicz, K., Foster, P.G., Hall, N., and Talbot, N.J.** (2011). Horizontal gene transfer facilitated the evolution of plant parasitic mechanisms in the oomycetes. *Proc Natl Acad Sci* **108**: 15258–15263.
- Rivas, S. and Deslandes, L.** (2013). Nuclear components and dynamics during plant innate immunity. *Front Plant Sci* **4**: 481.
- Rosenblum, E.B., Poorten, T.J., Joneson, S., and Settles, M.** (2012). Substrate-specific gene expression in Batrachochytrium dendrobatidis, the chytrid pathogen of amphibians. *PLoS One* **7**: e49924.
- Rouxel, T. et al.** (2011). Effector diversification within compartments of the Leptosphaeria maculans genome affected by Repeat-Induced Point mutations. *Nat Commun* **2**: 202.
- Royo, F., Andersson, G., Bangyeekhun, E., Múzquiz, J.L., Söderhäll, K., and Cerenius, L.** (2004). Physiological and genetic characterisation of some new Aphanomyces strains isolated from freshwater crayfish. *Vet Microbiol* **104**: 103–112.
- Ryan, R.P., Vorhölter, F.-J., Potnis, N., Jones, J.B., Van Sluys, M.-A., Bogdanove, A.J., and Dow, J.M.** (2011). Pathogenomics of Xanthomonas: understanding bacterium-plant interactions. *Nat Rev Microbiol* **9**: 344–355.
- Sarowar, M.N., van den Berg, A.H., McLaggan, D., Young, M.R., and van West, P.** (2013). Saprolegnia strains isolated from river insects and amphipods are broad spectrum pathogens. *Fungal Biol* **117**: 752–763.
- Saunders, D.G.O., Win, J., Cano, L.M., Szabo, L.J., Kamoun, S., and Raffaele, S.** (2012). Using hierarchical clustering of secreted protein families to classify and rank candidate effectors of rust fungi. *PLoS One* **7**: e29847.
- Schirawski, J. et al.** (2010). Pathogenicity determinants in smut fungi revealed by genome comparison. *Science* **330**: 1546–1548.
- Scholze, H. and Boch, J.** (2011). TAL effectors are remote controls for gene activation. *Curr Opin Microbiol* **14**: 47–53.
- Schornack, S., van Damme, M., Bozkurt, T.O., Cano, L.M., Smoker, M., Thines, M., Gaulin, E., Kamoun, S., and Huitema, E.** (2010). Ancient class of translocated oomycete effectors targets the host nucleus. *Proc Natl Acad Sci U S A* **107**: 17421–17426.
- Sekizaki, H., Yokosawa, R., Chinen, C., Adachi, H. and Yamane, Y.** (1993). Studies on zoospore attracting activity: synthesis of isoflavones and their attractive activity to Aphanomyces euteiches zoospores *Bioll Pharm Bull* **16**:698-701
- Shearer, H.L., Cheng, Y.T., Wang, L., Liu, J., Boyle, P., Després, C., Zhang, Y., Li, X., and Fobert, P.R.** (2012). Arabidopsis clade I TGA transcription factors regulate plant defenses in an NPR1-independent fashion. *Mol Plant Microbe Interact* **25**: 1459–1468.
- Sheen, J.** (2001). Signal Transduction in Maize and Arabidopsis Mesophyll Protoplasts. *Plant Physiol* **127**: 1466–1475.
- Shen, D., Liu, T., Ye, W., Liu, L., Liu, P., Wu, Y., Wang, Y., and Dou, D.** (2013). Gene duplication and fragment recombination drive functional diversification of a superfamily of cytoplasmic effectors in Phytophthora sojae. *PLoS One* **8**: e70036.
- Song, J. and Bent, A.F.** (2014). Microbial pathogens trigger host DNA double-strand breaks whose abundance is reduced by plant defense responses. *PLoS Pathog.* **10**: e1004030.
- Song, J., Win, J., Tian, M., Schornack, S., Kaschani, F., Ilyas, M., van der Hoorn, R.A., and**

- Kamoun, S.** (2009). Apoplastic effectors secreted by two unrelated eukaryotic plant pathogens target the tomato defense protease Rcr3. *Proc Natl Acad Sci U S A* **106**: 1654–1659.
- Soprano, A.S., Abe, V.Y., Smetana, J.H.C., and Benedetti, C.E.** (2013). Citrus MAF1, a repressor of RNA polymerase III, binds the *Xanthomonas citri* canker elicitor PthA4 and suppresses citrus canker development. *Plant Physiol* **163**: 232–242.
- Spector, D.L. and Lamond, A.I.** (2011). Nuclear speckles. *Cold Spring Harb Perspect Biol* **3**:a000646
- Stam, R., Howden, A.J.M., Delgado-Cerezo, M., M. M. Amaro, T.M., Motion, G.B., Pham, J., and Huitema, E.** (2013b). Characterization of cell death inducing *Phytophthora capsici* CRN effectors suggests diverse activities in the host nucleus. *Front Plant Sci* **4**: 1–11.
- Stam, R., Jupe, J., Howden, A.J.M., Morris, J. a., Boevink, P.C., Hedley, P.E., and Huitema, E.** (2013a). Identification and Characterisation CRN Effectors in *Phytophthora capsici* Shows Modularity and Functional Diversity. *PLoS One* **8**: e59517.
- Stanton-Geddes, J. et al.** (2013). Candidate genes and genetic architecture of symbiotic and agronomic traits revealed by whole-genome, sequence-based association genetics in *Medicago truncatula*. *PLoS One* **8**: e65688.
- Staskawicz, B.J., Dahlbeck, D., and Keen, N.T.** (1984). Cloned avirulence gene of *Pseudomonas syringae* pv. *glycinea* determines race-specific incompatibility on *Glycine max* (L.) Merr. *Proc Natl Acad Sci U S A* **81**: 6024–6028.
- Strange, R.N. and Scott, P.R.** (2005). Plant disease: a threat to global food security. *Annu Rev Phytopathol* **43**: 83–116.
- Structure and evolution of barley powdery mildew effector candidates.
- Strullu-Derrien, C., Kenrick, P., Rioult, J.P., and Strullu, D.G.** (2011). Evidence of parasitic Oomycetes (Peronosporomycetes) infecting the stem cortex of the Carboniferous seed fern *Lyginopteris oldhamia*. *Proc Biol Sci* **278**: 675–680.
- Sugio, A. and Hogenhout, S.** (2012). The genome biology of phytoplasma: modulators of plants and insects. *Curr Opin Microbiol* **15**: 247–254.
- Sugio, A., Maclean, A.M., and Hogenhout, S. a** (2014). The small phytoplasma virulence effector SAP11 contains distinct domains required for nuclear targeting and CIN-TCP binding and destabilization. *New Phytol* **202**: 838–848.
- Sun, F., Kale, S.D., Azurmendi, H.F., Li, D., Tyler, B.M., and Capelluto, D.G.S.** (2013). Structural basis for interactions of the *Phytophthora sojae* RxLR effector Avh5 with phosphatidylinositol 3-phosphate and for host cell entry. *Mol Plant Microbe Interact* **26**: 330–344.
- Sun, G., Yang, Z., Kosch, T., Summers, K., and Huang, J.** (2011). Evidence for acquisition of virulence effectors in pathogenic chytrids. *BMC Evol Biol* **11**: 195.
- Tamura, K. and Hara-Nishimura, I.** (2014). Functional insights of nucleocytoplasmic transport in plants. *Front Plant Sci* **5**: 1–10.
- Tao, Y., Xie, Z., Chen, W., Glazebrook, J., Chang, H., Han, B., Zhu, T., Zou, G., and Katagiri, F.** (2003). Quantitative Nature of Arabidopsis Responses during Compatible and Incompatible Interactions with the Bacterial Pathogen *Pseudomonas syringae*. **15**: 317–330.
- Tasset, C., Bernoux, M., Jauneau, A., Pouzet, C., Brière, C., Kieffer-Jacquino, S., Rivas, S., Marco, Y., and Deslandes, L.** (2010). Autoacetylation of the *Ralstonia solanacearum* effector PopP2 targets a lysine residue essential for RRS1-R-mediated immunity in Arabidopsis. *PLoS Pathog* **6**: e1001202.
- Thines, M. and Kamoun, S.** (2010). Oomycete-plant coevolution: recent advances and future prospects. *Curr Opin Plant Biol* **13**: 427–33.
- Thines, M., Go, M., Telle, S., Ryley, M., Mathur, K., Narayana, Y.D., Spring, O., Thakur, R.P., and Voglmayr, H.** (2008). Phylogenetic relationships of gramicolous downy mildews based on cox 2 sequence data. **112**: 345–351.

- Tian, M., Benedetti, B., and Kamoun, S.** (2005). A Second Kazal-Like Protease Inhibitor from *Phytophthora infestans* Inhibits and Interacts with the Apoplastic Pathogenesis-Related Protease P69B of Tomato. *Plant Physiol* **138**: 1785–1793.
- Tian, M., Win, J., Song, J., van der Hoorn, R., van der Knaap, E., and Kamoun, S.** (2007). A *Phytophthora infestans* cystatin-like protein targets a novel tomato papain-like apoplastic protease. *Plant Physiol* **143**: 364–377.
- Tilsner, J., Linnik, O., Louveaux, M., Roberts, I.M., Chapman, S.N., and Oparka, K.J.** (2013). Replication and trafficking of a plant virus are coupled at the entrances of plasmodesmata. *J Cell Biol* **201**: 981–995.
- Torto, T. a, Li, S., Styer, A., Huitema, E., Testa, A., Gow, N. a R., van West, P., and Kamoun, S.** (2003). EST mining and functional expression assays identify extracellular effector proteins from the plant pathogen *Phytophthora*. *Genome Res* **13**: 1675–1685.
- Tsuda, K. and Katagiri, F.** (2010). Comparing signaling mechanisms engaged in pattern-triggered and effector-triggered immunity. *Curr Opin Plant Biol* **13**: 459–465.
- Tyler, B.** (2007). *Phytophthora sojae*: root rot pathogen of soybean and model oomycete. *Mol Plant Pathol* **8**: 1–8.
- Tytgat, T., Vanholme, B., De Meutter, J., Claeys, M., Couvreur, M., Vanhoutte, I., Gheysen, G., Van Criekinge, W., Borgonie, G., Coomans, A., and Gheysen, G.** (2004). A new class of ubiquitin extension proteins secreted by the dorsal pharyngeal gland in plant parasitic cyst nematodes. *Mol Plant Microbe Interact* **17**: 846–852.
- Umemoto, N., Kakitani, M., Iwamatsu, A., Yamaoka, N., and Ishida, I.** (1997). The structure and function of a soybean β -glucan-elicitor-binding protein. *Proc Natl Acad Sci U S A* **94**: 1029–1034.
- Uzuhashi, S., Kakishima, M., and Tojo, M.** (2010). Phylogeny of the genus *Pythium* and description of new genera. *Mycoscience* **51**: 337–365.
- Van Damme, M., Bozkurt, T.O., Cakir, C., Schornack, S., Sklenar, J., Jones, A.M.E., and Kamoun, S.** (2012). The Irish potato famine pathogen *Phytophthora infestans* translocates the CRN8 kinase into host plant cells. *PLoS Pathog* **8**: e1002875
- Van der Hoorn, R. a, Laurent, F., Roth, R., and De Wit, P.J.** (2000). Agroinfiltration is a versatile tool that facilitates comparative analyses of Avr9/Cf-9-induced and Avr4/Cf-4-induced necrosis. *Mol Plant Microbe Interact* **13**: 439–446.
- Van Kan, J.A., van den Ackerveken, Guido, F.J., and de Wit, P.J.G.** (1991). Cloning and Characterization of cDNA of Avirulence Gene *avr9* of the Fungal Pathogen *Cladosporium fulvum*, Causal Agent of Tomato Leaf Mold. *Mol Plant Microbe Interact* **4**: 52–59.
- Ve, T., Williams, S.J., Catanzariti, A.-M., Rafiqi, M., Rahman, M., Ellis, J.G., Hardham, A.R., Jones, D. a, Anderson, P. a, Dodds, P.N., and Kobe, B.** (2013). Structures of the flax-rust effector AvrM reveal insights into the molecular basis of plant-cell entry and effector-triggered immunity. *Proc Natl Acad Sci U S A* **110**: 17594–17599.
- Vierstra, R.D.** (2009). The ubiquitin-26S proteasome system at the nexus of plant biology. *Nat Rev Mol Cell Biol* **10**: 385–397.
- Voglmayr, H. and Riethmüller, A.** (2006). Phylogenetic relationships of *Albugo* species (white blister rusts) based on LSU rDNA sequence and oospore data. *Mycol Res* **110**: 75–85.
- Vrålstad1, T., Johnsen, S.I., Fristad, R.F., Edsman, L., and Strand, D.** (2011). Potent infection reservoir of crayfish plague now permanently established in Norway. *Dis Aquat Organ* **97**: 75–83.
- Walton, J.D.** (1994). Deconstructing the Cell Wall. *Plant Physiol* **104**: 1113–1118.
- Wang, Q. et al.** (2011). Transcriptional programming and functional interactions within the *Phytophthora sojae* RXLR effector repertoire. *Plant Cell* **23**: 2064–2086.
- Wang, Y., An, C., Zhang, X., Yao, J., Zhang, Y., Sun, Y., Yu, F., Amador, D.M., and Mou, Z.** (2013). The Arabidopsis elongator complex subunit2 epigenetically regulates plant immune responses.

Plant Cell **25**: 762–776.

- Wawra, S., Djamei, A., Albert, I., Nürnberger, T., Kahmann, R., and van West, P.** (2013). In vitro translocation experiments with RxLR-reporter fusion proteins of Avr1b from *Phytophthora sojae* and AVR3a from *Phytophthora infestans* fail to demonstrate specific autonomous uptake in plant and animal cells. *Mol Plant Microbe Interact* **26**: 528–536.
- Whisson, S.C. et al.** (2007). A translocation signal for delivery of oomycete effector proteins into host plant cells. *Nature* **450**: 115–118.
- Wicker E and Rouxel F.** (2001). Specific behaviour of French *Aphanomyces euteiches* Drechs. Populations for virulence and aggressiveness on pea, related to isolates from Europe, America and New Zealand. *Eur J Plant Pathol* **107**: 919–929.
- Willmann, R., Lajunen, H.M., Erbs, G., Newman, M., Kolb, D., and Tsuda, K.** (2011). Arabidopsis lysin-motif proteins LYM1 LYM3 CERK1 mediate bacterial peptidoglycan sensing and immunity to bacterial infection. *Proc Natl Acad Sci U S A* **108**: 19824–19829.
- Win, J., Morgan, W., Bos, J., Krasileva, K. V., Cano, L.M., Chaparro-Garcia, A., Ammar, J., Staskawicz, B.J., and Kamoun, S.** (2007). Adaptive evolution has targeted the C-terminal domain of the RXLR effectors of plant pathogenic oomycetes. *Plant Cell* **19**: 2349–2369.
- Wirthmueller, L., Roth, C., Banfield, M.J., and Wiermer, M.** (2013). Hop-on hop-off: importin- α -guided tours to the nucleus in innate immune signaling. *Front Plant Sci* **4**: 1–8.
- Yaeno, T. and Shirasu, K.** (2013). The RXLR motif of oomycete effectors is not a sufficient element for binding to phosphatidylinositol monophosphates. *Plant Signal Behav* **8**: e23865.
- Yaeno, T., Li, H., Chaparro-Garcia, A., Schornack, S., Koshiba, S., Watanabe, S., Kigawa, T., Kamoun, S., and Shirasu, K.** (2011). Phosphatidylinositol monophosphate-binding interface in the oomycete RXLR effector AVR3a is required for its stability in host cells to modulate plant immunity. *Proc Natl Acad Sci U S A* **108**: 14682–14687.
- Zerillo, M.M., Adhikari, B.N., Hamilton, J.P., Buell, C.R., Lévesque, C.A., and Tisserat, N.** (2013). Carbohydrate-active enzymes in *pythium* and their role in plant cell wall and storage polysaccharide degradation. *PLoS One* **8**: e72572.
- Zhang, L., Davies, L.J., and Elling, A.A.** (2014). A *Meloidogyne incognita* effector is imported into the nucleus and exhibits transcriptional activation activity in planta. *Mol Plant Pathol* (in press).
- Zheng, X., McLellan, H., Fraiture, M., Liu, X., Boevink, P.C., Gilroy, E.M., Chen, Y., Kandel, K., Sessa, G., Birch, P.R.J., and Brunner, F.** (2014). Functionally redundant RXLR effectors from *Phytophthora infestans* act at different steps to suppress early flg22-triggered immunity. *PLoS Pathog* **10**: e1004057.
- Zhu, Z., Xu, F., Zhang, Y., Ti, Y., Wiermer, M., Li, X., and Zhang, Y.** (2010). Arabidopsis resistance protein SNC1 activates immune responses through association with a transcriptional corepressor. *Proc Natl Acad Sci* **107**: 13960–13965.
- Zuluaga, A.P., Puigvert, M., and Valls, M.** (2013). Novel plant inputs influencing *Ralstonia solanacearum* during infection. *Front Microbiol* **4**: 349.

Author: Diana RAMIREZ-GARCES

Title: Analyses of CRN effectors (Crinkler and Necrosis) of the oomycete *Aphanomyces euteiches*

Discipline: Plant-Microorganism Interactions

Defence date and place: LSRV laboratory , the 29 October 2014

Summary: The oomycete *Aphanomyces euteiches* is an important pathogen infecting roots of legumes (pea, alfalfa...) and the model legume *Medicago truncatula*. Oomycetes and other microbial eukaryotic pathogens secrete and deliver effector molecules into host intracellular compartments (intracellular/cytoplasmic effectors) to manipulate plant functions and promote infection. CRN (Crinkling and Necrosis) proteins are a wide class of intracellular, nuclear-localized effectors commonly found in oomycetes and recently described in true fungi whose host targets, virulence roles, secretion and host-delivery mechanisms are poorly understood. We addressed the functional characterization of CRN proteins AeCRN5 and AeCRN13 of *A. euteiches* and AeCRN13's homolog of the chytrid fungal pathogen of amphibians *Batrachochytrium dendrobatidis*, BdCRN13. Gene and protein expression studies showed that AeCRN5 and AeCRN13 are expressed during infection of *M. truncatula*'s roots. Preliminary immunolocalization studies on AeCRN13 in infected roots indicated that the protein is secreted and translocated into root cells, depicting for the first time CRN secretion and translocation into the host during infection. The heterologous ectopic expression of AeCRNs and BdCRN13 in plant and amphibian cells indicated that these proteins target host nuclei and lead to the perturbation of host physiology. By developing an *in vivo* FRET-FLIM-based assay, we revealed that these CRNs target host nucleic acids: AeCRN5 targets plant RNA while AeCRN13 and BdCRN13 target DNA. Both CRN13 exhibit a HNH-like motif commonly found in endonucleases and we further demonstrated that both CRN13 display a nuclease activity *in vivo* inducing double-stranded DNA cleavage. This work reveals a new mode of action of intracellular eukaryotic effectors and brings new aspects for the comprehension of CRN's activities not only in oomycetes but, for the first time, also in true fungi.

Keywords: CRN, oomycetes, nucleus, effector, secretion, FRET-FLIM, *Aphanomyces euteiches*
